



*A Duke Energy Company*

McGuire Nuclear Station  
Catawba Nuclear Station

MULTIDIMENSIONAL REACTOR TRANSIENTS AND  
SAFETY ANALYSIS PHYSICS PARAMETERS METHODOLOGY

DPC-NE-3001-A

November 1991

Republished December 2000

Nuclear Engineering Division  
Nuclear Generation Department  
Duke Power Company



UNITED STATES  
NUCLEAR REGULATORY COMMISSION  
WASHINGTON, D. C. 20555  
November 15, 1991

Docket Nos. 50-369, 50-370  
50-413 and 50-414

Mr. H. B. Tucker, Senior Vice President  
Nuclear Generation  
Duke Power Company  
P. O. Box 1007  
Charlotte, North Carolina 28201-1007

Dear Mr. Tucker:

SUBJECT: SAFETY EVALUATION ON TOPICAL REPORT DPC-NE-3001, "MULTIDIMENSIONAL REACTOR TRANSIENTS AND SAFETY ANALYSIS PHYSICS PARAMETERS"  
(TAC NOs. 75954/75955/75956/75957)

The NRC staff has reviewed Duke Power Company Topical Report DPC-NE-3001, "Multidimensional Reactor Transients and Safety Analysis Physics Parameters," dated January 29, 1990, as supplemented by letters dated February 13 and June 3, 1991. The staff has found the topical report to be acceptable for referencing in licensing analyses for the McGuire and Catawba Nuclear Stations subject to the conditions in section 4.0 of the attached Safety Evaluation.

This concludes our review activities in response to your submittals regarding Topical Report DPC-NE-3001 addressed by TAC numbers 75954/75955/75956/75957.

Sincerely,

A handwritten signature in black ink, appearing to read "T. A. Reed", is written over a large, stylized circular flourish.

Timothy A. Reed, Project Manager  
Project Directorate II-3  
Division of Reactor Projects - I/II  
Office of Nuclear Reactor Regulation

Enclosure:  
Safety Evaluation

cc: See next page

Duke Power Company

Catawba Nuclear Station  
McGuire Nuclear Station

cc:

Mr. R. C. Futrell  
Regulatory Compliance Manager  
Duke Power Company  
Catawba Nuclear Site  
Clover, South Carolina 29710

Mr. A.V. Carr, Esq.  
Duke Power Company  
422 South Church Street  
Charlotte, North Carolina 28242-0001

J. Michael McGarry, III, Esq.  
Winston and Strawn  
1400 L Street, N.W.  
Washington, DC 20005

North Carolina MPA-1  
Suite 600  
P.O. Box 29513  
Raleigh, North Carolina 27626-513

Mr. Frank Modrak  
Project Manager, Mid-South Area  
ESSD Projects  
Westinghouse Electric Corporation  
MNC West Tower - Bay 241  
P.O. Box 355  
Pittsburgh, Pennsylvania 15230

County Manager of York County  
York County Courthouse  
York, South Carolina 29745

Richard P. Wilson, Esq.  
Assistant Attorney General  
S.C. Attorney General's Office  
P.O. Box 11549  
Columbia, South Carolina 29211

Piedmont Municipal Power Agency  
121 Village Drive  
Greer, South Carolina 29651

Mr. Alan R. Herdt, Chief  
Project Branch #3  
U.S. Nuclear Regulatory Commission  
101 Marietta Street, NW, Suite 2900  
Atlanta, Georgia 30323

North Carolina Electric Membership  
Corp.  
P.O. Box 27306  
Raleigh, North Carolina 27611

Saluda River Electric Cooperative,  
Inc.  
P.O. Box 929  
Laurens, South Carolina 29360

Senior Resident Inspector  
Route 2, Box 179N  
York, South Carolina 29745

Regional Administrator, Region II  
U.S. Nuclear Regulatory Commission  
101 Marietta Street, NW, Suite 2900  
Atlanta, Georgia 30323

Mr. Heyward G. Shealy, Chief  
Bureau of Radiological Health  
South Carolina Dept. of Health  
and Environmental Control  
2600 Eull Street  
Columbia, South Carolina 29201

Ms. Karen E. Long  
Assistant Attorney General  
North Carolina Dept. of Justice  
P.O. Box 629  
Raleigh, North Carolina 27602

Mr. R. L. Gill, Jr.  
Licensing  
Duke Power Company  
P.O. Box 1007  
Charlotte, North Carolina 28201-1007



Duke Power Company

County Manager of Mecklenburg County  
720 East Fourth Street  
Charlotte, North Carolina 28202

Mr. R. O. Sharpe  
Compliance  
Duke Power Company  
McGuire Nuclear Site  
12700 Hagers Ferry Road  
Huntersville, North Carolina 28078-8985

Senior Resident Inspector  
c/o U.S. Nuclear Regulatory Commission  
12700 Hagers Ferry Road  
Huntersville, North Carolina 28078

Mr. T. C. McMeekin  
Vice President, McGuire Site  
Duke Power Company  
12700 Hagers Ferry Road  
Huntersville, North Carolina 28078-8985

Catawba Nuclear Station  
McGuire Nuclear Station

Dr. John M. Barry  
Department of Environmental Health  
Mecklenburg County  
1200 Blythe Boulevard  
Charlotte, North Carolina 28203

Mr. Dayne H. Brown, Director  
Department of Environmental Health  
and Natural Resources  
Division of Radiation Protection  
P. O. Box 27687  
Raleigh, North Carolina 27611-7687

Mr. M. S. Tuckman  
Vice President, Catawba Site  
Duke Power Company  
P. O. Box 256  
Clover, South Carolina 29710



UNITED STATES  
NUCLEAR REGULATORY COMMISSION  
WASHINGTON, D. C. 20555

SAFETY EVALUATION FOR DPC-NE-3001-P

"MULTIDIMENSIONAL REACTOR TRANSIENTS AND SAFETY ANALYSIS

PHYSICS PARAMETERS METHODOLOGY"

1.0 INTRODUCTION

By letter dated January 29, 1990 (Ref. 1), Duke Power Company (DPC) submitted topical report DPC-NE-3001-P, "Multidimensional Reactor Transients and Safety Analysis Physics Parameters Methodology." The methodology described in this topical report expands on the currently approved reload design analyses of Reference 2 and is intended for application to the Catawba and McGuire Nuclear Power Stations. The report includes the overall methodology for using bounding reference analyses together with key safety parameters for analyzing the required Final Safety Analysis Report (FSAR) Chapter 15 events as well as the DPC reference analyses for selected transients involving multidimensional neutronics.

The bounding analysis methodology used by DPC to ensure that the accident analysis for the reference core conservatively bounds the reload core is described in the topical report. The important key safety parameters for each Chapter 15 event are identified, and the methods for calculating these parameters are described. New DPC bounding reference analyses are given for (1) the rod ejection accident (REA), (2) the steam line break accident (SLBA), and (3) the dropped rod accident (DRA). The new reference analysis for the REA is performed with three-dimensional spatial neutronics, and the analyses for SLBA and DRA are performed with a point kinetics model. The new reference analyses are analyzed in detail and shown to satisfy the appropriate 10 CFR Part 100 dose limits, the departure from nucleate boiling ratio (DNBR) safety limit, the fuel enthalpy limit, and the American Society of Mechanical Engineers reactor coolant system pressure limit. In reload applications, DPC will show that the reference analysis is bounding by demonstrating that the event-specific key safety parameters of the reload core are within the conservative envelope of the reference analysis.

The topical report is reviewed in Section 2, and the safety evaluation of the DPC methodology is summarized in Section 3. The limitations imposed concerning the licensing application of the DPC methods are given in Section 4.

The following summary and technical evaluation include the contribution of Brookhaven National Laboratory as staff consultant under FIN No. A-3686.

2.0 SUMMARY OF THE TOPICAL REPORT

DPC's topical report DPC-NE-3001-P (1) identifies the key safety parameters, (2) describes the methods for calculating these parameters, and (3) gives the new reference analyses for the rod ejection accident, steam line break accident and dropped rod accident. The DPC methods associated with these analyses are summarized in the following sections.

## 2.1 Key Safety Parameters

The key safety parameters play a crucial role in the DPC reload methodology. By comparing these parameters for a reload core to the values determined for the reference analysis, any nonconservatism in the reference analysis may be identified and the need for a new safety analysis may be established. The DPC methodology defines both generic and event-specific safety parameters.

The initial core power distribution, scram reactivity, effective delayed neutron fraction and decay constants, and prompt neutron lifetime are important for many transients and are considered to be generic. A conservative scram reactivity is determined using the minimum shutdown margin allowed by the technical specifications and the rod insertion limits, together with a minimum rate of reactivity insertion. This rate is determined using the measured rod speeds and a conservative correlation between rod insertion and fractional inserted reactivity. The core power distribution is assumed to provide the maximum peaking allowed (including perturbations) by the  $F_0$  and  $F_{4h}$  technical specification limits. For rapid transients a minimum delayed neutron fraction beta is used; for slow transients, which are insensitive to beta, a maximum value of beta is recommended. For conservatism the initial fuel temperature is taken to be the maximum.

The FSAR Chapter 15 accident analyses are reviewed in Chapter 2 of the topical report, and event-specific key safety parameters are identified for each event. The events analyzed include feedwater malfunctions, increased steam flow, turbine trip, loss of nonemergency ac power, loss of coolant flow, rod ejection, inadvertent actuation of the emergency core cooling system, and loss-of-coolant accidents. On the basis of the dynamics of the transient, the conservative direction for each key safety parameter is given for the events analyzed. The event-specific key safety parameters include the Doppler temperature coefficient (DTC), moderator temperature coefficient (MTC), shutdown margin (SDM), accident reactivity, and critical boron concentration.

## 2.2 Determination of the Key Safety Parameters

The key safety parameters are determined using physics codes and methods that the NRC staff has approved (Ref. 2) or is reviewing (Ref. 3). The three-dimensional static power distribution and depletion calculations are performed with NODE-P or SIMULATE-3P. The models used are based on accumulated operating history of previous reload cycles.

The static physics parameters include control rod worth, shutdown margin and trip reactivity. The calculated parameters depend on the three-dimensional power shape and, consequently, core loading, rod insertion, and time in life. The shutdown margin and rod worth calculations are performed at beginning-of-cycle (BOC) and at end-of-cycle (EOC). The shutdown margin calculations assume the highest worth rod is stuck in its fully withdrawn position and account for the power defect, rod insertion, and calculational uncertainties.

The transient parameters include the MTC, DTC, delayed neutron parameters, and boron worths. The temperature coefficients are calculated using a static model and account for power level and cycle exposure. The boron worths are determined using a set of perturbed static calculations, and the dependence on power level, moderator temperature, fuel exposure, and control rod insertion is included.

## 2.3 New Reference Analyses for the Rod Ejection, Steam Line Break and Dropped Rod Accidents

The topical report includes new reference analyses for the rod ejection, steam line break, and dropped rod accidents. The detailed methods for analyzing the events are presented together with the resulting consequences, margin to limits, and acceptance criteria. The cases analyzed are extreme and should bound most reload cores. In practice, whether these reference analyses actually bound the postulated events for the reload core will be determined by comparing the key safety parameters, which are given for each of the DPC reference analyses.

### 2.3.1 Rod Ejection Accident Reference Analysis

The rod ejection accident (REA) reference analysis consists of three distinct and coupled analyses: (1) a core neutronics analysis, (2) a core thermal-hydraulics analysis, and (3) a systems thermal-hydraulics analysis. The core neutronics response to the rod ejection reactivity insertion is calculated with the Electric Power Research Institute (EPRI) ARROTTA code (Ref. 4). ARROTTA calculates the three-dimensional power/flux solution in (x,y,z) geometry both for the static analyses required for determining the key parameters and for the core response during the transient. The ARROTTA core model uses one radial node per assembly and twelve axial nodes. The fuel and reflector two-group cross sections and nuclear input parameters were determined with CASMO-3 (Ref. 3). The local cross sections are a function of fuel and moderator temperature and relative water density. ARROTTA uses assembly discontinuity factors, calculated by CASMO-3, to account for the local heterogeneities within the fuel assembly. ARROTTA includes a core thermal-hydraulics model that is identical to the one included in the EPRI BEAGL program (Ref. 5).

The ARROTTA time-dependent core power/flux solution is used as input to the subchannel core thermal-hydraulics analysis performed with VIPRE-01 (Ref. 6). The NRC has approved VIPRE-01 for referencing in licensing analyses. VIPRE-01 calculates the core flow distribution and coolant conditions, fuel rod temperatures, and DNBR during the REA. VIPRE-01 uses a single-channel fuel conduction model together with the ARROTTA time-dependent peak pin power to calculate the peak fuel enthalpy. The transient pressure is calculated using a multichannel VIPRE-01 model and the ARROTTA time-dependent power/flux solution.

A RETRAN-02 (Ref. 7) system model is used to determine the reactor coolant system (RCS) response during the REA. The RETRAN model which is based on the McGuire/Catawba model (Ref. 8), uses the VIPRE-01 core coolant expansion rate to determine the limiting RCS transient pressure.

The REA reference analysis model is based on a Cycle 2 Catawba 1 core and is performed at hot-full-power (HFP) and hot-zero-power (HZP) conditions at BOC and EOC. The nuclear cross sections have been adjusted to increase the power peaking and ejected rod worth (at off-center location D-12) so that the reference analysis will bound expected core reloads. The D-12 rod is ejected in (a conservative) 0.1 second. The core inlet flow is reduced by 2.2 percent to account for measurement uncertainty in the HFP case. The core inlet flow is reduced an additional 54 percent for the (two-pump) HZP case. The reference analysis indicated that the REA results in a maximum fuel enthalpy of 133 cal/gm and a peak system pressure of 2699 psig which are lower than the corresponding limits. The number of rods in departure from nucleate boiling (DNB) was less than 37 percent, and the resulting offsite doses were well within the 10 CFR Part 100 limits.

The REA key safety parameters (which vary from cycle to cycle) are the moderator and Doppler temperature coefficients, the delayed neutron fraction, and the ejected rod worth.

### 2.3.2 Steam Line Break Accident Reference Analysis

The steam line break accident reference analysis consists of (1) a RETRAN-02 systems analysis of the RCS response to the steam line break, (2) a NODE-P (Ref. 2) or SIMULATE-3P (Ref. 3) neutronics calculation of the core power distribution at the time of minimum DNBR, and (3) a VIPRE-01 core thermal-hydraulics analysis of the minimum DNBR. The systems analysis model is based on the McGuire/Catawba model (Ref. 8). To model the thermal mixing, the RETRAN-02 model was modified to include parallel flowpaths, with one path connected to the faulted loop and the other path representing the intact loops. Special mixing junctions are included to allow for thermal mixing. The RETRAN-02 neutronics feedback is included, using a precalculated  $k_{eff}$  versus moderator temperature function and a Doppler temperature coefficient. A range of break sizes was evaluated to determine the limiting break size.

The three-dimensional power distribution is calculated for the asymmetric core conditions determined by RETRAN-02 at the time of minimum DNBR (MDNBR). This power distribution is then used in the VIPRE-01 multichannel steady-state calculation to determine the MDNBR. The VIPRE-01 calculation uses the calculated asymmetric core inlet temperature and flow as boundary conditions.

The initial conditions and boundary conditions used in the reference analysis are generally conservative. These include a low pressurizer level and RCS flow and a high RCS temperature and steam generator water inventory. The core is initially at hot-zero-power conditions to maximize the cooldown. The reference analysis is performed with and without offsite power for a limiting break size of 1.4 ft<sup>2</sup>. In both cases, the MDNBR is greater than 1.45, which is greater than the limiting MDNBR value.

### 2.3.3 Dropped Rod Accident Reference Analysis

The dropped rod transient is analyzed with a RETRAN-02 plant systems model. The input dropped rod worth and core moderator and fuel reactivity coefficients are determined with NODE-P. The RETRAN-02 model calculates the initial reduction in power, bank withdrawal and moderator cooldown, and the final minimum DNBR statepoint. The DNBR analysis is performed with a multichannel VIPRE-01 model using the RETRAN-02 systems input together with a detailed three-dimensional power distribution determined with either NODE-P or SIMULATE-3P.

For the reference analysis, a single-loop Catawba 1 RETRAN-02 model is used. The uncertainty in plant operating variables is accounted for by using either the statistical core design (SCD) methodology or conservative upper-limit input values. This includes a low pressurizer level and a maximum average fuel temperature. The reference analysis is performed at BOC, MOC and EOC for a range of dropped rod worths. The reference analysis calculations indicate that the MDNBR does not reach the SCD DNBR limit for the cases analyzed.

The key physics parameters for the dropped rod analysis that will be used to evaluate each DPC reload core are the initial radial peaking  $F_{0h}$ , axial flux shape, moderator and doppler temperature coefficients, dropped rod worth, and bank withdrawal worth.

## 3.0 EVALUATION

DPC's topical report DPC-NE-3001-P provides the physics methods that will be used to evaluate reload cores against precalculated reference analyses. The focus of this review was on the identification of the key safety parameters and on the reference analyses provided for the rod ejection, dropped rod, and steam line break accident. The initial review of the topical report resulted in a series of questions. This evaluation included the review of DPC-NE-3001-P and DPC's responses to these questions in References 9 and 10. The evaluation of the major issues raised during this review is summarized in the following sections.

### 3.1 Key Safety Parameters

Both generic and event-specific key safety parameters are used in the DPC methodology. The identified parameters are based on the dynamics of the transient, the sensitivity with respect to the safety parameter, and the approach to safety limits. The list of key safety parameters in Table 2-1 of the topical report does not include all the modeling input data used in the reference analysis that may change with a new reload core design. However, DPC intends to examine all of the thermal-hydraulic and mechanical parameters, as well as the physics key parameters, in validating the reference analysis for application to a reload core.

In Chapter 3 of the topical report and in Response 4 of Reference 9, DPC has indicated that the key safety parameters will be determined using approved codes and methods. However, the SIMULATE-P methods described in DPC topical report DPC-HE-1004 (Ref. 3) are being reviewed by the NRC staff and should not be used until they have been approved.

DPC intends to use the key safety parameters identified in Table 2-1 to evaluate the licensing events. The only issue raised was the prompt neutron lifetime which DPC does not consider as a key safety parameter for the uncontrolled withdrawal of the rod cluster control assembly. In Response 27 of Reference 10, DPC indicated that for the bank withdrawal at power, the prompt neutron lifetime affects the bank reactivity insertion rate. However, DPC has performed sensitivity calculations that indicate that the MDNBR is essentially unaffected by changes in the prompt neutron lifetime. For the withdrawal of a single rod, the limiting statepoint occurs well after the rod is completely withdrawn and there is only minimum sensitivity to the prompt neutron lifetime. DPC has also performed sensitivity calculations for the bank withdrawal from subcritical. These calculations indicate only a very weak sensitivity of the transient to the neutron lifetime.

On the basis of the above, the staff concludes that the determination and application of the key safety parameters in the DPC reload methodology are acceptable.

### 3.2 Rod Ejection Accident Analysis

The RETRAN-02 systems model and VIPRE-01 core thermal-hydraulics model used in the DPC rod ejection accident (REA) analysis are based on the Babcock & Wilcox Mark-BW fuel and the Westinghouse optimized fuel designs. The introduction of new fuel designs (involving changes in loss coefficients, dimensions, etc.) may invalidate the applicability of the reference analysis to the reload core. This is also a concern for the steam line break and dropped rod accident analyses. DPC has indicated in Responses 1, 18, and 24 of Reference 9 that when a new fuel design is included in a cycle reload core, the impact of the design changes on all analyses will be evaluated and a reanalysis will be performed if necessary.

The ARROTTA analysis neglects the change in the assembly-wise flow distribution and assembly crossflow during the REA. This is considered to be a good approximation, since no significant heating is transferred to the moderator until after the power transient has been reversed in both the hot-full-power (HFP) and hot-zero-power (HZIP) cases, and no bulk boiling occurs until after local departure from nucleate boiling (DNB) occurs.

The nuclear cross sections in ARROTTA are represented as functions of the local moderator density, control rod insertion, and fuel and moderator temperature. The ARROTTA REA model includes the local fuel exposure dependence by defining a set of about 75 distinct fuel compositions. However, a typical reload core consists of a continuous three-dimensional fuel exposure distribution and about 1000 unique fuel compositions. DPC collapses this set of fuel compositions from about 1000 down to about 75 using the SIGTRAN code. In response to question 9 Reference 9, DPC states that the ARROTTA sensitivity calculations in which the number of compositions was increased by about 50 percent indicated no significant change in the ARROTTA predictions.

In the DPC methodology, the REA safety parameters ( $\beta_0$ , moderator temperature coefficient, doppler temperature coefficient, beta, rod ejection worth, and the pin power census) are calculated for the reference core in which the cross sections in the neighborhood of the ejected rod have been adjusted to increase the rod worth and local peaking. This is an appropriate definition of the key safety parameters, since it ensures consistency between the REA reference results and the cycle reload core safety parameters. The temperature coefficient and rod reactivity safety parameters are calculated by standard static eigenvalue differencing. The temperature reactivity feedback is calculated using an isothermal analysis for the HZP case (Response 13, Ref. 9). At HFP the feedbacks are determined by an increase in uniform inlet temperature and an increase in core thermal power. The ejected rod worth is calculated without feedback (Response 13, Ref. 9).

The ARROTTA code uses the analytic nodal method of Reference 11 and the thermal-hydraulics model of Reference 5. The flux solution is calculated in two groups, and the use of discontinuity factors allows an accurate reconstruction of the local pin-wise power distribution.

In Reference 12, DPC has indicated that ARROTTA is only used for the REA and, because of the rapid nature of this event, the neutronics solution rather than the moderator feedback effects are most important for this application. As qualification of the ARROTTA neutronics solution, Combustion Engineering (CE) under contract to Electric Power Research Institute (EPRI) compared the ARROTTA code (Ref. 13) to the NRC-approved CE HERMITE code (Ref. 14). Comparisons were made for steady-state conditions and for an off-center REA in half-core geometry from HZP conditions. Good agreement was obtained for the REA transient core power, peak assembly power, core average fuel temperature and peak fuel temperature, and steady-state power distributions. In Reference 15, additional ARROTTA comparisons are given for four static calculations and two transient calculations, two of which included thermal-hydraulics feedback. These comparisons indicate good agreement in the static eigenvalues, transient core power, and both static and transient power distributions. In Response 5 of Reference 9 DPC stated that Version 1.02 of ARROTTA was used in the HERMITE benchmarking calculations, which is the same version as that used in the Reference 15 analyses and the DPC REA reference analysis. The EPRI/CE ARROTTA-HERMITE comparisons in Reference 13 and the ARROTTA comparisons of Reference 15 indicate that ARROTTA provides an accurate calculation of the rod ejection transient.



On the basis of the above and the responses in Reference 10, the staff concludes that the DPC analysis of the REA is acceptable.

### 3.3 Steam Line Break Accident Analysis

In the DPC steam line break accident (SLBA) analysis the stuck rod is located in the sector of the core associated with the faulted loop. This results in maximum core peaking, but also results in minimum inlet temperature. DPC has shown in Response 37 of Reference 10 that the location of the rod in the faulted loop sector results in an MDNBR and is conservative.

Two of the key factors affecting the DPC steam line break response are the steam generator inventory and the auxiliary feedwater flow to the faulted steam generator. The Catawba units have higher feedwater flow to the faulted steam generator than McGuire. In addition, of the two Catawba units, Catawba 2 has the highest initial steam generator inventory. In its Response 30 of Reference 10, DPC has indicated that Catawba 2 also has a higher steam generator inventory than both McGuire units at the SLBA initial conditions. DPC's selection of Catawba 2 as the bounding unit for the SLBA is therefore conservative.

On the basis of the above and the responses in Reference 10, the staff concludes that the DPC analysis of the SLBA is acceptable.

### 3.4 Dropped Rod Accident Analysis

The measured core power is a primary factor in determining the power overshoot in the response to the dropped rod in the dropped rod accident (DRA). The location of the dropped rod can produce a core power tilt and adversely affect the measured core thermal power. As indicated in Responses 42 and 43 of Reference 10, DPC assumes a control rod system failure that results in the limiting power tilt and a minimum measured core thermal power. This assumption maximizes the DRA power overshoot and minimizes the margin to DNB. In addition, DPC assumes the control withdrawal stops are inoperative allowing the power overshoot to proceed above 103 percent power (Response 43, Ref. 10).

In the dropped rod event the least negative temperature coefficient provides a conservative minimum feedback to the power transient, but also results in a nonconservative minimum positive reactivity insertion resulting from the cooldown. DPC has performed sensitivity calculations which indicated that the feedback reactivity dominates the core response and a least negative temperature coefficient provides the bounding conservative DRA analysis.

On the basis of the above and the responses in Reference 10, the staff concludes that the DPC analysis of the DRA is acceptable.

### 3.5 Applications of Codes and Methodology

The RETRAN-02 and VIPRE-01 codes are used in the DPC rod ejection, steam line break, and dropped rod accident analyses. In Response 29 of Reference 10, DPC has indicated that the application of these codes is outside the limitations of their present NRC approval in two instances: (1) RETRAN-02 MOD005 is used to determine the boron transport in the steamline break accident analysis and (2) the VIPRE-01 heat transfer correlations are used for post critical heat flux (CHF) analyses in the rod ejection accident (REA) analysis.

In response to the VIPRE-01 concerns, DPC has indicated that the application of the post-CHF heat transfer correlations in the REA analysis affects both the peak fuel enthalpy and reactor coolant system (RCS) peak pressure calculations. DPC has determined through sensitivity analysis that the available post-CHF correlations result in conservative fuel temperatures or have a negligible effect on the peak fuel temperatures or both. In view of the large (factor of about 2) margin between the calculated REA peak fuel enthalpy and the fuel enthalpy limit, this is acceptable. DPC has also evaluated the effect of the post-CHF heat transfer correlations on the peak RCS pressure and found they have less than a 14-psig effect, which is within the available margin to the RCS pressure limit. Consequently, DPC's application of the VIPRE-01 post-CHF heat transfer correlations in the REA analysis is acceptable. Since no additional information is provided on RETRAN-02, the approval of the DPC transient analysis methods is contingent on the approval of MOD005 of RETRAN-02 for boron transport calculations.

The thermal-hydraulics methodology described in the DPC topical report DPC-NE-3000 (Ref. 8) has been used in the DPC transient analyses. The limitations of the NRC approval of the DPC-NE-3000 thermal-hydraulics methodology will, therefore, also apply to the transient analysis methodology of DPC-NE-3001-P.

### 4.0 LIMITATIONS

The staff has reviewed in detail the DPC reactor transients and safety analysis physics parameters methodology topical report and the supporting documentation in References 9 and 10. The topical report documents the DPC reload key safety parameter methods and the reference analyses for the rod ejection, dropped rod, and steam line break accidents. On the basis of this review, the staff concludes that the DPC methodology is acceptable for performing licensing analyses under the conditions stated in Section 3 of this evaluation and summarized as follows:

- (1) The licensing application of the SIMULATE-3P static methods for determining the key safety parameters requires NRC approval of the reference topical report, DPC-NE-1004 (Section 3.1).

- (2) The licensing application of the DPC-NE-3001-P transient analysis methods requires NRC approval of MOD005 of RETRAN-02 for boron transport calculations (Section 3.5).
- (3) The licensing application of the DPC-NE-3001-P transient analysis methods requires NRC approval of the thermal-hydraulics topical report DPC-NE-3000 (Section 3.5).

## 5.0 REFERENCES

1. Letter, H. B. Tucker (DPC) to U.S. Nuclear Regulatory Commission, "Safety Analysis Physics Parameters and Multidimensional Reactor Transients Methodology," DPC-NE-3001-P, January 29, 1990.
2. Duke Power Company, "Nuclear Physics Methodology for Reload Design," DPC-NF-2010A, June 1985.
3. Duke Power Company, "Nuclear Design Methodology Using CASMO-3/SIMULATE-3P," DPC-NE-1004, January 1990.
4. L. D. Eisenhart, "ARROTTA-01 - An Advanced Rapid Reactor Operational Transient Analysis Computer Code," Computer Code Documentation Package, EPRI NP-7375-CCML, Volume 1, Electric Power Research Institute August 1991.
5. D. J. Diamond, H. S. Cheng, and L. D. Eisenhart, "BEAGL-01, A Computer Code for Calculating Rapid Core Transients," EPRI NP-3243-CCM, Volume I, Electric Power Research Institute, 1983.
6. Letter from C. E. Rossi (NRC) to J. A. Blaisdell (UGRA), "Acceptance for Referencing of Licensing Topical Report, VIPRE-01: A Thermal-Hydraulic Analysis Code for Reactor Cores," EPRI NP-2511-CCM, Vol. 1-5, May 1986.
7. Electric Power Research Institute, "RETRAN-02: A Program for Transient Thermal-Hydraulic Analysis of Complex Fluid Flow Systems," EPRI NP-1850-CCMA, Revision 4, November 1988.
8. Letter, H. B. Tucker (DPC) to NRC, "Thermal-Hydraulic Transient Analysis Methodology," DPC-NE-3000, September 29, 1987.
9. Letter, H. B. Tucker (DPC) to U.S. Nuclear Regulatory Commission, "Response to Request for Additional Information Relative to Topical Report DPC-NE-3001-P," February 13, 1991.
10. Letter, H. B. Tucker (DPC) to U.S. Nuclear Regulatory Commission, "Response to Request for Additional Information Relative to Topical Report DPC-NE-3001-P," June 3, 1991.
11. K. S. Smith, "An Analytic Nodal Method for Solving the 2-Group, Multi-Dimensional, Static and Transient Neutron Diffusion Equations," Nuclear Engineering Thesis, Department of Nuclear Engineering, Massachusetts Institute of Technology, Cambridge, Massachusetts, February 1979.

12. Letter, H. B. Tucker (DPC) to U.S. Nuclear Regulatory Commission, "Topical Report DPC-NE-3001-P," September 14, 1990.
13. Electric Power Research Institute, "ARROTTA-HERMITE Code Comparison," NP-6614, EPRI, December 1989.
14. P. E. Rohan, S. G. Wagner, S. E. Ritterbusch, "HERMITE: A Multidimensional Space-time Kinetics Code for PWR Transients," CENPD-188-A, Combustion Engineering, Inc., July 1976.
15. Electric Power Research Institute, "ARROTTA Validation and Verification - Standard Benchmarks Set," Project 1936-6, July 1989.

Date: November 15, 1991

McGuire Nuclear Station  
Catawba Nuclear Station

MULTIDIMENSIONAL REACTOR TRANSIENTS AND  
SAFETY ANALYSIS PHYSICS PARAMETERS METHODOLOGY

DPC-NE-3001-A

November 1991

Republished December 2000

Nuclear Engineering Division  
Nuclear Generation Department  
Duke Power Company

## Abstract

This report describes the Duke Power Company methodologies for: i) simulating the FSAR Chapter 15 events characterized by multidimensional reactor transients, and ii) systematically confirming that reload physics parameters important to Chapter 15 transients and accidents are bounded by values assumed in the licensing analyses. The multidimensional reactor transients described are the rod ejection accident, the main steam line break, and the dropped rod transient. The analytical approaches combine neutronics calculations with system and core thermal-hydraulics simulations. It is concluded that applications of the methodologies and physics parameters checks will result in conservative predictions of the consequences, and that the applicable acceptance criteria are met. This report is applicable to the McGuire and Catawba Nuclear Stations.

MULTIDIMENSIONAL REACTOR TRANSIENTS  
AND SAFETY ANALYSIS PHYSICS PARAMETERS

Table of Contents

|        |  |
|--------|--|
| 1.0    | INTRODUCTION   |
| 2.0    | DETERMINATION OF SAFETY ANALYSIS PHYSICS PARAMETERS  |
| 2.1    | <u>Overview</u>  |
| 2.2    | <u>Generic Parameters</u>  |
| 2.3    | <u>Discussion of FSAR Chapter 15 Transients and Accidents</u>                              |
| 2.3.1  | Feedwater System Malfunctions That Result in a Reduction in Feedwater Temperature (15.1.1) |
| 2.3.2  | Feedwater System Malfunction Causing an Increase in Feedwater Flow (15.1.2)                |
| 2.3.3  | Excessive Increase in Secondary Steam Flow (15.1.3)  |
| 2.3.4  | Inadvertent Opening of a Steam Generator Relief or Safety Valve (15.1.4)                   |
| 2.3.5  | Steam System Piping Failure (15.1.5)   |
| 2.3.6  | Loss of External Load (15.2.2)   |
| 2.3.7  | Turbine Trip (15.2.3)  |
| 2.3.8  | Inadvertent Closure of Main Steam Isolation Valves (15.2.4)                                |
| 2.3.9  | Loss of Condenser Vacuum (15.2.5)  |
| 2.3.10 | Loss of Non-Emergency AC Power (15.2.6)  |
| 2.3.11 | Loss of Normal Feedwater Flow (15.2.7)   |
| 2.3.12 | Feedwater System Pipe Break (15.2.8)   |
| 2.3.13 | Partial Loss of Forced Reactor Coolant Flow (15.3.1)                                       |
| 2.3.14 | Complete Loss of Forced Reactor Coolant Flow (15.3.2)                                      |
| 2.3.15 | Reactor Coolant Pump Locked Rotor (15.3.3)   |
| 2.3.16 | Reactor Coolant Pump Shaft Break (15.3.4)  |
| 2.3.17 | Uncontrolled Bank Withdrawal From Subcritical (15.4.1)                                     |
| 2.3.18 | Uncontrolled Bank Withdrawal at Power (15.4.2)   |
| 2.3.19 | Dropped Rod(s) and Dropped Bank (15.4.3)   |
| 2.3.20 | Statically Misaligned Control Rod (15.4.3)   |
| 2.3.21 | Single Control Rod Withdrawal (15.4.3)   |

## Table of Contents (cont.)

|         |  |
|---------|--|
| 2.3.22  | Improper Startup of the Fourth Reactor Coolant Pump (15.4.4)         |
| 2.3.23  | Moderator Dilution Accident (15.4.6)                                 |
| 2.3.24  | Rod Ejection Accident (15.4.8)                                       |
| 2.3.25  | Inadvertent ECCS Actuation (15.5.1)                                  |
| 2.3.26  | CVCS Malfunction Resulting in Increase in Primary Inventory (15.5.2) |
| 2.3.27  | Inadvertent Opening of a Pressurizer Relief or Safety Valve 15.6.1)  |
| 2.3.28  | Instrument Line Rupture (15.6.2)                                     |
| 2.3.29  | Steam Generator Tube Rupture (15.6.3)                                |
| 2.3.30  | Loss of Coolant Accidents (15.6.5)                                   |
| 2.4     | <u>Reload Cycle Evaluation</u>                                       |
| 3.0     | CALCULATION OF KEY SAFETY ANALYSIS PHYSICS PARAMETERS                |
| 3.1     | <u>Control Rod Worth Calculations</u>                                |
| 3.2     | <u>Reactivity Coefficients and Kinetics Parameters</u>               |
| 4.0     | ROD EJECTION ANALYSIS  |
| 4.1     | <u>Overview</u>  |
| 4.1.1   | Description of Rod Ejection Accident                                 |
| 4.1.2   | Acceptance Criteria  |
| 4.1.3   | Analytical Approach  |
| 4.2     | <u>Simulation Codes and Models</u>                                   |
| 4.2.1   | Nuclear Analysis   |
| 4.2.2   | Core Thermal-Hydraulic Analysis                                      |
| 4.2.2.1 | VIPRE-01 Code Description  |
| 4.2.2.2 | Fuel Temperature and Enthalpy Calculation                            |
| 4.2.2.3 | Coolant Expansion Rate Calculation                                   |
| 4.2.2.4 | DNBR Evaluation  |
| 4.2.3   | System Thermal-Hydraulic Analysis                                    |
| 4.3     | <u>ARROTTA Analysis</u>  |
| 4.3.1   | Initial Conditions   |
| 4.3.2   | Boundary Conditions  |



## Table of Contents (cont.)

|         |  |
|---------|--|
| 4.3.3   | Results                                  |
| 4.4     | <u>VIPRE Analysis</u>                    |
| 4.4.1   | Initial Conditions                       |
| 4.4.2   | Fuel Temperature and Enthalpy            |
| 4.4.3   | Coolant Expansion Rate                   |
| 4.4.4   | DNBR and Fuel Pin Census                 |
| 4.5     | <u>RETRAN Analysis</u>                   |
| 4.5.1   | Initial Conditions                       |
| 4.5.2   | Boundary Conditions                      |
| 4.5.3   | Results                                  |
| 4.6     | <u>Dose Consequences</u>                 |
| 4.7     | <u>Cycle Specific Evaluation</u>         |
| 5.0     | STEAM LINE BREAK ANALYSIS                |
| 5.1     | <u>Overview</u>                          |
| 5.1.1   | Description of Steam Line Break Accident |
| 5.1.2   | Acceptance Criteria                      |
| 5.1.3   | Analytical Approach                      |
| 5.2     | <u>Simulation Codes and Models</u>       |
| 5.2.1   | System Thermal-Hydraulic Analysis        |
| 5.2.1.1 | Selection of a Bounding Unit             |
| 5.2.1.2 | Modifications to Base Plant Model        |
| 5.2.1.3 | Break Modeling                           |
| 5.2.2   | Nuclear Analysis                         |
| 5.2.2.1 | Core Physics Parameters                  |
| 5.2.2.2 | Power Distributions                      |
| 5.2.3   | Core Thermal-Hydraulic Analysis          |
| 5.2.3.1 | VIPRE Code Description                   |
| 5.2.3.2 | Analysis Methodology                     |
| 5.3     | <u>Transient Analysis</u>                |
| 5.3.1   | Initial Conditions                       |

## Table of Contents (cont.)

|         |  |
|---------|--|
| 5.3.2   | Boundary Conditions                            |
| 5.3.2.1 | Availability of Systems and Components         |
| 5.3.2.2 | Response Times                                 |
| 5.3.2.3 | Flow From Interfacing Systems                  |
| 5.3.2.4 | Engineered Safety Features Actuation Setpoints |
| 5.3.2.5 | Boron Injection Modeling                       |
| 5.3.2.6 | Core Kinetics Modeling                         |
| 5.4     | <u>Results and Conclusions</u>                 |
| 5.4.1   | Primary and Secondary System Response          |
| 5.4.2   | Core Response                                  |
| 5.4.2.1 | Axial and Radial Power Distributions           |
| 5.4.2.2 | Minimum DNBR Results                           |
| 5.5     | <u>Cycle Specific Evaluation</u>               |
| 6.0     | DROPPED ROD ANALYSIS                           |
| 6.1     | <u>Overview</u>                                |
| 6.1.1   | Description of Dropped Rod Accident            |
| 6.1.2   | Acceptance Criteria                            |
| 6.1.3   | Analytical Approach                            |
| 6.2     | <u>Simulation Codes and Models</u>             |
| 6.2.1   | System Thermal-Hydraulic Analysis              |
| 6.2.2   | Nuclear Analysis                               |
| 6.2.3   | Core Thermal-Hydraulic Analysis                |
| 6.3     | <u>Transient Analysis</u>                      |
| 6.3.1   | Initial Conditions                             |
| 6.3.2   | Boundary Conditions                            |
| 6.3.2.1 | Physics Parameters                             |
| 6.3.2.2 | Reactor Protection System                      |
| 6.3.2.3 | Power Range Nuclear Instrumentation            |
| 6.3.2.4 | Rod Control System                             |
| 6.3.2.5 | Pressurizer Pressure and Level Control         |

## Table of Contents (cont.)

6.3.2.6 Main Feedwater and Turbine Control

### 6.4 Results and Conclusions

6.4.1 System Transient Results

6.4.1.1 Typical Beginning-of-Cycle Response

6.4.1.2 Typical End-of-Cycle Response

6.4.1.3 Limiting Statepoint Selection

6.4.2 Core Response


6.4.2.1 Statepoint Conditions

6.4.2.2 Thermal-Hydraulic Results for DNBR

### 6.5 Cycle Specific Evaluation

## Appendix A - REACTOR VESSEL THERMAL MIXING EVALUATION

## List of Figures

|      |   |
|------|---|
| 1-1  | Reload Core Safety Analysis Verification Process  |
| 4-1  | Catawba 1 Cycle 2 Assembly Enrichments and Fuel Exposures   |
| 4-2  | [  ] VIPRE Model |
| 4-3  |   |
| 4-4  | Rod Ejection Accident Control Rod Locations   |
| 4-5  | BOC, HFP ARO Power Distributions  |
| 4-6  | EOC, HFP ARO Power Distributions  |
| 4-7  | Trip Reactivity Curve   |
| 4-8  | BOC, HFP Core Power vs. Time  |
| 4-9  | BOC, HFP Power Distribution at 0.0 seconds  |
| 4-10 | BOC, HFP Power Distribution at 0.09 seconds   |
| 4-11 | BOC, HZP Core Power vs. Time  |
| 4-12 | BOC, HZP Power Distribution at 0.0 seconds  |
| 4-13 | BOC, HZP Power Distribution at 0.2 seconds  |
| 4-14 | BOC, HZP Power Distribution at 0.34 seconds   |
| 4-15 | EOC, HFP Core Power vs. Time  |
| 4-16 | EOC, HFP Power Distribution at 0.0 seconds  |
| 4-17 | EOC, HFP Power Distribution at 0.09 seconds   |
| 4-18 | EOC, HZP Core Power vs. Time  |
| 4-19 | EOC, HZP Power Distribution at 0.0 seconds  |
| 4-20 | EOC, HZP Power Distribution at 0.13 seconds   |
| 4-21 | EOC, HZP Power Distribution at 0.17 seconds   |
| 4-22 | BOC, HFP MARP Curves  |
| 4-23 | BOC, HZP MARP Curves  |
| 4-24 | EOC, HFP MARP Curves  |
| 4-25 | EOC, HZP MARP Curves  |
| 4-26 | BOC, HFP Number of Pins in DNB by Assembly  |
| 4-27 | BOC, HZP Number of Pins in DNB by Assembly  |
| 4-28 | EOC, HFP Number of Pins in DNB by Assembly  |
| 4-29 | EOC, HZP Number of Pins in DNB by Assembly  |

List of Figures (cont.)

|      |   |
|------|---|
| 4-30 | HFP BOC Case Core Coolant Volume Expansion Rate                     |
| 4-31 | HFP BOC Case RCS Pressure Response                                  |
| 5-1  | RETRAN Reactor Vessel Model   |
| 5-2  | K-effective vs Moderator Temperature                                |
| 5-3  | VIPRE [       ] Model   |
| 5-4  | Offsite Power Maintained Steam Line Pressure                        |
| 5-5  | Offsite Power Maintained Cold Leg Temperature                       |
| 5-6  | Offsite Power Maintained Hot Leg Temperature                        |
| 5-7  | Offsite Power Maintained Core Boron Concentration                   |
| 5-8  | Offsite Power Maintained Core Reactivity                            |
| 5-9  | Offsite Power Maintained Neutron Power                              |
| 5-10 | Offsite Power Maintained Core Heat Flux                             |
| 5-11 | Offsite Power Maintained Pressurizer Level                          |
| 5-12 | Offsite Power Maintained Pressurizer Pressure                       |
| 5-13 | Offsite Power Maintained Break Mass Flow Rate                       |
| 5-14 | Offsite Power Maintained Core Mass Flux                             |
| 5-15 | Offsite Power Lost Steam Line Pressure                              |
| 5-16 | Offsite Power Lost Cold Leg Temperature                             |
| 5-17 | Offsite Power Lost Hot Leg Temperature                              |
| 5-18 | Offsite Power Lost Core Boron Concentration                         |
| 5-19 | Offsite Power Lost Core Reactivity                                  |
| 5-20 | Offsite Power Lost Neutron Power                                    |
| 5-21 | Offsite Power Lost Core Heat Flux                                   |
| 5-22 | Offsite Power Lost Pressurizer Level                                |
| 5-23 | Offsite Power Lost Pressurizer Pressure                             |
| 5-24 | Offsite Power Lost Break Mass Flow Rate                             |
| 5-25 | Offsite Power Lost Core Mass Flux                                   |
| 5-26 | Offsite Power Maintained Typical Assembly Radial Power Distribution |
| 5-27 | Offsite Power Lost Typical Assembly Radial Power Distribution       |
| 6-1  | VIPRE [       ] Model   |
| 6-2  | BOC F-Delta-H vs. Dropped Rod Worth                                 |

List of Figures (cont.)

|      |   |
|------|---|
| 6-3  | MOC F-Delta-H vs. Dropped Rod Worth         |
| 6-4  | EOC F-Delta-H vs. Dropped Rod Worth         |
| 6-5  | Minimum Tilt vs. Dropped Rod Worth          |
| 6-6  | BOC Case Actual and Indicated Reactor Power |
| 6-7  | BOC Case Control Bank D Position            |
| 6-8  | BOC Case Reactor Coolant System T-ave       |
| 6-9  | BOC Case Pressurizer Level                  |
| 6-10 | BOC Case Pressurizer Pressure               |
| 6-11 | EOC Case Actual and Indicated Reactor Power |
| 6-12 | EOC Case Control Bank D Position            |
| 6-13 | EOC Case Reactor Coolant System T-ave       |
| 6-14 | EOC Case Pressurizer Level                  |
| 6-15 | EOC Case Pressurizer Pressure               |
| 6-16 | BOC Cases Reactor Power                     |
| 6-17 | BOC Cases Reactor Coolant System T-ave      |
| 6-18 | BOC Cases Pressurizer Pressure              |
| 6-19 | MOC Cases Reactor Power                     |
| 6-20 | MOC Cases Reactor Coolant System T-ave      |
| 6-21 | MOC Cases Pressurizer Pressure              |
| 6-22 | EOC Cases Reactor Power                     |
| 6-23 | EOC Cases Reactor Coolant System T-ave      |
| 6-24 | EOC Cases Pressurizer Pressure              |
| 6-25 | Limiting Cases Reactor Power                |
| 6-26 | Limiting Cases Reactor Coolant System T-ave |
| 6-27 | Limiting Cases Pressurizer Pressure         |
| 6-28 | Axial Power Shapes                          |
| A-1  |   |
| A-2  |   |
| A-3  |   |
| A-4  |   |
| A-5  |   |

### List of Figures (cont.)

A-6

A-7

[

]

### List of Tables

|     |  |
|-----|--|
| 2-1 | Summary of Safety Analysis Physics Parameters  |
| 4-1 | Rod Ejection Transient Kinetics Parameters   |
| 4-2 | Rod Ejection Transient Initial Conditions  |
| 4-3 | Rod Ejection ARROTTA Results   |
| 4-4 | Rod Ejection Reload Checklist  |
| 5-1 | Sequence of Events for 1.4 ft <sup>2</sup> Split Break with Offsite Power Maintained           |
| 5-2 | Sequence of Events for 1.4 ft <sup>2</sup> Split Break with Offsite Power Lost at SI Actuation |

## List of Abbreviations

|          |  |
|----------|--|
| ARO      | All rods out   |
| BOC      | Beginning of cycle   |
| CETC     | Core exit thermocouples  |
| CHF      | Critical heat flux   |
| CVCS     | Chemical and Volume Control System   |
| DEG      | Double-ended guillotine  |
| DNBR     | Departure from nucleate boiling ratio  |
| DTC      | Doppler temperature coefficient  |
| ECCS     | Emergency Core Cooling System  |
| EFPD     | Effective full power days  |
| EOC      | End of cycle   |
| $F_{DH}$ | Ratio of the integral of linear power along the rod to the average rod power |
| $F_Q$    | Maximum local heat flux/average fuel rod heat flux                           |
| FSAR     | Final Safety Analysis Report   |
| HFP      | Hot full power   |
| HZP      | Hot zero power   |
| kw/ft    | Kilowatts per foot   |
| LM       | Limiting mixing  |
| LOCA     | Loss-of-coolant-accident   |
| MARP     | Maximum allowable radial power   |
| MTC      | Moderator temperature coefficient  |
| NI       | Nuclear instrumentation  |
| OAC      | Operator aid computer  |
| PORV     | Power-operated relief valve  |
| PZR      | Pressurizer  |
| RCS      | Reactor Coolant System   |
| RIL      | Rod insertion limits   |
| RPS      | Reactor Protection System  |
| RTD      | Resistance temperature detector  |
| SCD      | Statistical core design  |
| SG       | Steam generator  |



List of Abbreviations (cont.)

|     |                  |
|-----|------------------|
| SI  | Safety injection |
| swd | Steps withdrawn  |
| TM  | Thermal mixing   |

## 1.0 INTRODUCTION

This report describes the methodologies to be used by Duke Power Company to simulate multidimensional reactor transients and to verify that the key physics parameters calculated for a reload core are bounded by values assumed in the licensing Chapter 15 analyses. This report is applicable to the McGuire and Catawba Nuclear Stations, which are 4-loop 3411 MWt Westinghouse units. These methodologies expand on the NRC-approved reload design methods of DPC-NF-2010A (Reference 1-1) and on the system and core transient thermal-hydraulic simulation methods of DPC-NE-3000 (Reference 1-2).

Chapter 15 accident analyses show that the design of a reactor and its associated systems will mitigate the events of various postulated accidents and ensure that the consequences of these accidents are acceptable. These analyses, hereafter referred to as the "reference safety analyses," along with the facility Technical Specifications, establish the bases and conditions for safe operation of the plant. Important parts of the reference analyses include values of parameters assumed in the analyses, performance characteristics of the mitigating systems, and the analytical models used. Values of parameters selected in the reference analyses are chosen to bound values expected during the life of the plant. Performance characteristics of the mitigating systems are modeled to give conservative performance characteristics and produce bounding consequences for each of the accidents.

For each fuel cycle design, each reference analysis is validated by examining all of the key physics, thermal-hydraulic, and mechanical parameters which are assumed in the reference analysis and which might be affected by a reload design. These values are compared to those calculated for the particular cycle. If all parameters are within the envelope of values assumed in the reference analysis, then the analysis is valid and no reanalysis is necessary. If, however, one or more of the plant parameters assumed in the reference analysis are found to be nonconservative for the reload cycle, those accident analyses which are affected by the nonconservative parameters must be reevaluated or the loading pattern must be revised. This validation process is shown schematically in Figure 1-1.

Input to these checks will come from various groups associated with the reload design and safety analysis of reload cores including nuclear design, safety analysis, mechanical, and thermal-hydraulic groups. This checklist concept applies only to changes in important parameters resulting from refueling of the reactor core. Other changes in plant systems or setpoints might necessitate the reanalysis of certain transients independently of the reload design process. In some cases, the effects of plant modifications might be incorporated into the reload analysis. The first two chapters of this report concentrate on the generation of key physics parameters and the methods for using these parameters to validate existing safety analyses.

Chapter 2 specifies those physics parameters determined to be important for each Chapter 15 event. The appropriateness of selecting a maximum, minimum, or nominal value for each parameter is justified. Future reanalyses of Chapter 15 transients would use the specifications of Chapter 2 to determine physics data required to perform a conservative analysis.

Chapter 3 describes the nuclear design methods employed to calculate values of the important safety analysis physics parameters. These parameters can be influenced by core composition, boron concentration, control rod position, power level, xenon distribution, and other considerations. The approach taken to determine a conservative value of a parameter is to utilize the results of Chapter 2, and then investigate combinations of the above factors as permitted by Technical Specifications.

Three FSAR Chapter 15 events involve significant asymmetric core power peaking and require evaluation of the core response from a multidimensional simulation perspective. These events are the steam line break (15.1.5), the dropped rod transient (15.4.3), and the rod ejection accident (15.4.8). In order to conservatively predict the transient response, a combination of neutronic, system thermal-hydraulic, and core thermal-hydraulic simulation codes is employed. Depending on the dynamics of the particular analysis, it is possible in some situations to adequately and conservatively model aspects of the transient with static methods. Otherwise, an explicit transient evaluation is performed. The analyses presented are intended to bound future reload core designs. As such, a cycle-specific check of important safety analysis physics

parameters and/or a limited scope analysis will be all that is necessary to confirm that the existing analysis results remain bounding.

The rod ejection accident analysis methodology is presented in Chapter 4. The rapid core transient response is simulated with the three-dimensional space-time transient neutronics nodal code ARROTTA (Reference 1-3). The rod ejection accident is analyzed at full power and zero power at both beginning and end-of-cycle. The core thermal response is modeled with the VIPRE-01 (Reference 1-4) code. Peak fuel enthalpy, a core-wide DNBR evaluation and transient core coolant expansion are calculated. The Reactor Coolant System pressure response is simulated with the RETRAN-02 (Reference 1-5) code. The results of the analysis are shown to meet all acceptance criteria.

The steam line break accident analysis methodology is presented in Chapter 5. The system thermal-hydraulic analysis is performed with RETRAN-02. The worst case scenario, which occurs at zero power at end-of-cycle, is presented. Cases both with and without offsite power are analyzed. The core power peaking at the return-to-power statepoint condition and including the worst stuck rod is determined. The approach to DNBR is then predicted with VIPRE-01. The results show that the DNBR limit is not exceeded for the limiting cases.

The dropped rod transient analysis methodology is presented in Chapter 6. The transient response to single and multiple dropped rods from within the same group are evaluated. A complete range of dropped rod worths at beginning, middle, and end-of-cycle are analyzed. The system thermal-hydraulic analysis is performed with RETRAN-02. The core power peaking at the limiting statepoints is evaluated with VIPRE-01 to demonstrate that the DNBR limit is not exceeded.

The analyses presented in Chapters 4-6 of this report are intended to replace the existing FSAR Chapter 15 analyses. Reanalysis of these accidents in the future by Duke Power Company will use the methods described in this report.

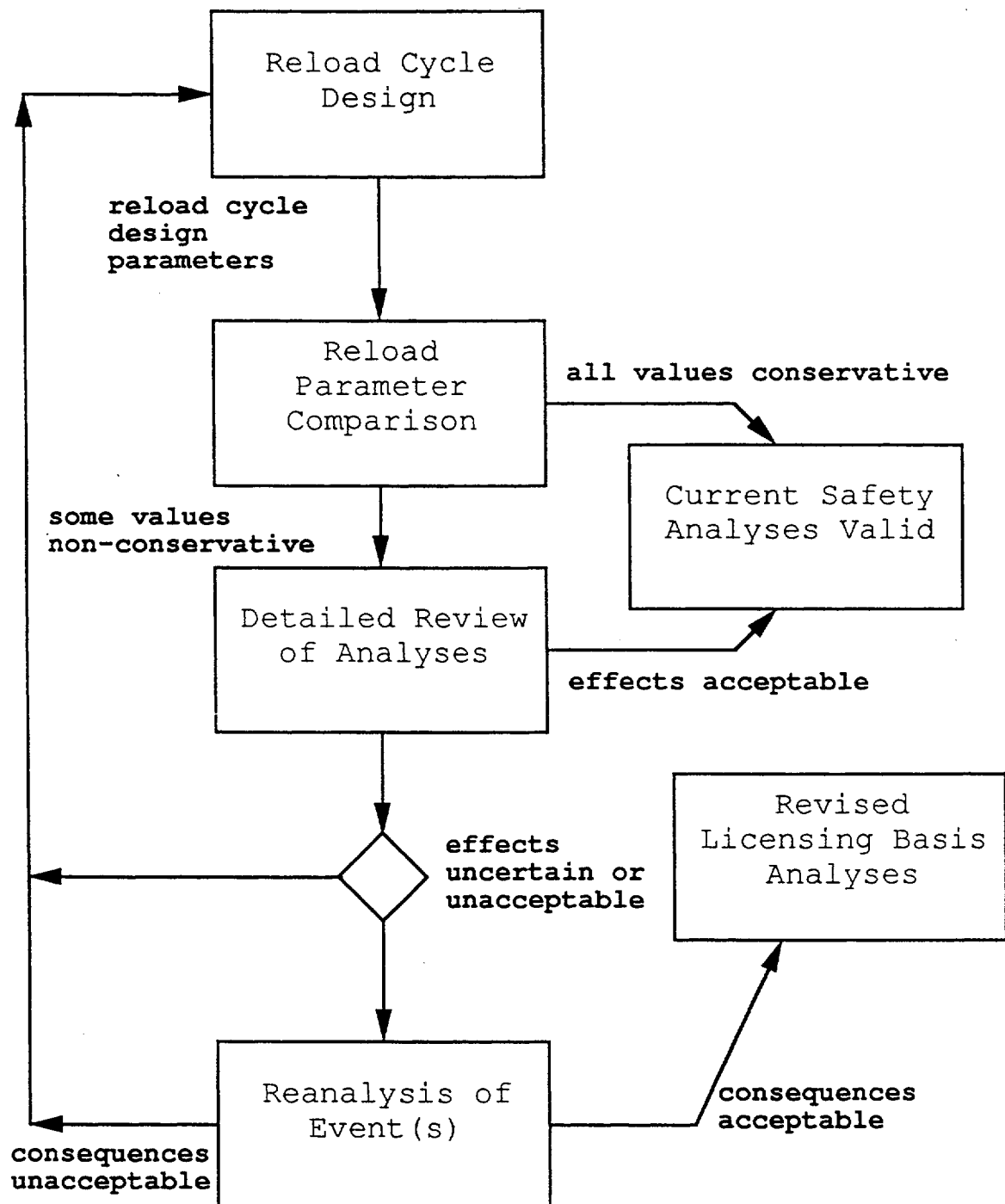
Topical report DPC-NE-2009P-A (Reference 1-6) included revisions to DPC-NE-3001-PA that are associated with the use of Westinghouse RFA fuel assemblies. Those revisions are not included in the December 2000 republication version.

## References

- 1-1 Nuclear Physics Methodology for Reload Design, DPC-NF-2010A, Duke Power Co., June 1985.
- 1-2 Thermal-Hydraulic Transient Analysis Methodology, DPC-NE-3000-PA, Revision 2, Duke Power Co., December 2000
- 1-3 ARROTTA: Advanced Rapid Reactor Operational Transient Analysis Computer Code, Computer Code Documentation Package, EPRI.
- 1-4 VIPRE-01: A Thermal-Hydraulic Code for Reactor Cores; EPRI NP-2511-CCMA Revision 3, EPRI, August 1989
- 1-5 RETRAN-02 - A Program for Transient Thermal-Hydraulic Analysis of Complex Fluid Flow Systems, EPRI NP-1850-CCMA Revision 4, EPRI, November 1988.
- 1-6 Duke Power Company Westinghouse Fuel Transition Report, DPC-NE-2009P-A, December 1999

Figure 1-1

Reload Core Safety Analysis Verification Process



## 2.0 DETERMINATION OF SAFETY ANALYSIS PHYSICS PARAMETERS

### 2.1 Overview

FSAR Chapter 15 transients and accidents must be conservatively analyzed to ensure that the applicable fuel design limits, system overpressure design limits, and dose consequences are not exceeded. Each transient and accident analysis incorporates a set of assumptions, which when combined in a consistent or conservative manner, produce conservative analysis results. These analyses bound the licensed operating conditions and modes for the current plant design and fuel cycle. An important subset of the analysis assumptions includes the core physics parameters necessary to characterize the initial conditions and transient response of the core. The relative importance of various physics parameters and the sensitivity to variations in the values of the parameters varies between transients. However, it is possible to identify, for each event, a set of physics parameters which are significant and directly affect the results of the analysis. Once these key parameters have been determined, then the impact of variation in the range of values due to a change in the core loading pattern and operating history can be assessed. A conservative or consistent value can then be selected for analysis, or several combinations can be analyzed to ensure the transient response is bounded.

The purpose of this chapter is to review and identify the key physics parameters for each FSAR Chapter 15 event. The conservative direction for each parameter (e.g., minimum/maximum) is identified where important. Table 2-1 summarizes the key parameters identified in this chapter. The actual analysis values are not provided but can be obtained by referencing the current valid licensing analysis for each event and plant.

### 2.2 Generic Parameters

Some of the important safety analysis physics parameters can be considered generic in that the value of the parameter is important for many transient analyses. The descriptions of the following generic parameters are not repeated for each specific transient in Section 2.3.

### Reactivity Insertion Following Reactor Trip

The reactivity insertion following reactor trip is a combination of a minimum available tripped rod worth and a normalized reactivity insertion rate. The minimum available tripped rod worth assumed in safety analyses must ensure, as a minimum, that the shutdown margin in Technical Specifications is preserved. This shutdown margin assumes that the most reactive rod remains in the fully withdrawn position and that the other control rods drop from their power dependent insertion limits. The normalized reactivity insertion rate is determined by bounding control rod drop times as determined by plant testing, and by developing a conservative relationship between rod position (%inserted) and normalized reactivity worth.

### Initial Core Power Distribution

Technical Specifications require that the core power distribution remains within prescribed limits during power operation. These power peaking limits are typically expressed as limits on total peak ( $F_Q$ ) and radial peak ( $F_{DH}$ ) limits are typically a function of elevation in the core and might also vary as a function of burnup and power level. The transient and accident analyses assume that any core power distribution permitted within normal operating limits is a valid initial condition. For those transients in which the initial power distribution has a significant impact on the course of the event, perturbed power distributions allowed by operating limits are considered. These events are discussed individually in Section 2.3.

### Effective Delayed Neutron Fractions and Decay Constants

The delayed neutron parameters are mainly important during rapid reactivity excursion transients. For an event such as the rod ejection accident, the minimum value of the effective delayed neutron fraction (beta-effective) is conservative. If the transient is not characterized by a rapid change in reactivity, then the value of beta-effective is not significant. The values of the fractions and decay constants for each delayed neutron precursor group are not key parameters, and typical values are sufficient.



### Prompt Neutron Lifetime

The prompt neutron lifetime is mainly important during rapid reactivity excursion transients. This parameter is not a key parameter, and so typically beginning and end-of-cycle values are used consistent with the limiting core condition for the transient.

### Initial Fuel Temperatures

Both the initial core average fuel temperature and the initial hot spot temperature are important to a conservative evaluation of the transient core response. These temperatures are determined using approved methods (References 2-1 and 2-2). The initial hot spot temperature is determined in a manner consistent with the initial power distribution and appropriate hot channel factors. Fuel temperatures are assumed to be conservative when taken at the maximum values.

## 2.3 Discussion of FSAR Chapter 15 Transients and Accidents

### 2.3.1 Feedwater System Malfunctions That Result in a Reduction in Feedwater Temperature (15.1.1)

This transient is bounded by 15.1.2 and 15.1.3, which are discussed in Sections 2.3.2 and 2.3.3.

### 2.3.2 Feedwater System Malfunction Causing an Increase in Feedwater Flow (15.1.2)

This transient is initiated by a failed-open main feedwater control valve which results in an increase in main feedwater flow. Due to the increase in the secondary heat sink, the primary coolant temperature decreases. The transient response is most conservative in the presence of a most negative moderator temperature coefficient (MTC) which will result in the maximum increase in reactor power. Similarly, a least negative Doppler temperature coefficient (DTC) is conservative since this maximizes the core power response. The MTC and DTC are the only key physics parameters for this event.

### 2.3.3 Excessive Increase in Secondary Steam Flow (15.1.3)

This transient is initiated by an increase in secondary steam flow, which can result from the turbine governor valves opening or from a spurious steam dump to condenser event. Due to the increase in the secondary heat sink, the primary coolant temperature decreases. Similar to the discussion in Section 2.3.2, a most negative MTC and a least negative DTC are conservative modeling assumptions.

### 2.3.4 Inadvertent Opening of a Steam Generator Relief or Safety Valve (15.1.4)

This transient is initiated by uncontrolled secondary depressurization resulting from a failure of a secondary steam dump valve, safety valve, or PORV. The worst case scenario begins from a no-load condition. The resulting primary system overcooling can cause a loss of core shutdown and a return-to-power can occur prior to boron injection from the actuation of safety injection. Since the steam system piping failure (15.1.5) is analyzed to the acceptance criteria that are applicable to the 15.1.4 transient, and since it bounds 15.1.4 in all aspects, there is no basis for analyzing 15.1.4. The 15.1.5 analysis can simply be referenced.

### 2.3.5 Steam System Piping Failure (15.1.5)

This transient is initiated by a rupture of a main steam line. The worst case scenario begins from a no-load condition. The resulting primary system overcooling causes a loss of core shutdown and a return-to-power condition occurs. This transient is analyzed by assuming a conservatively large reactivity insertion as the core cools down. The power increase is exacerbated by assuming a least negative Doppler coefficient. The boron concentration in the safety injection flowpath and the boron worth are both minimized. Due to the assumption of a stuck rod, the core power distribution at the limiting statepoint will be highly peaked. Consequently, the core power distribution must be evaluated to quantify the number of fuel pins exceeding the DNBR limit.

### 2.3.6 Loss of External Load (15.2.2)

This transient is bounded by 15.2.3, which is discussed in Section 2.3.7.

### 2.3.7 Turbine Trip (15.2.3)

This transient is initiated by a rapid closure of the turbine stop valves, resulting in a decrease in the secondary heat sink. As a result, primary coolant temperatures increase. The transient response is most conservative at beginning-of-cycle where the MTC and DTC are least negative. The least negative MTC and DTC maximize the pre-trip core power response. With this approach, the mismatch between heat source and heat sink is conservatively maximized.

### 2.3.8 Inadvertent Closure of Main Steam Isolation Valves (15.2.4)

This transient is bounded by 15.2.3, which is discussed in Section 2.3.7.

### 2.3.9 Loss of Condenser Vacuum (15.2.5)

This transient is bounded by 15.2.3, which is discussed in Section 2.3.7.

### 2.3.10 Loss of Non-Emergency AC Power (15.2.6)

This transient is initiated by a loss of non-emergency AC power. Similar to the turbine trip transient in Section 2.3.7, this transient is basically a loss of heat sink event. Since this event is determined mainly by decay heat, which is maximum at EOC, a most-negative MTC and a least-negative DTC are assumed.

### 2.3.11 Loss of Normal Feedwater Flow (15.2.7)

This transient is initiated by a loss of main feedwater flow. Similar to the turbine trip transient in Section 2.3.7, this transient is basically a loss of heat sink event. Therefore, the conservative physics parameters are least negative MTC and DTC.

### 2.3.12 Feedwater System Pipe Break (15.2.8)

This transient is initiated by a rupture of a main feedwater line. Similar to the turbine trip transient in Section 2.3.7, this transient is basically a loss of heat sink event. Therefore, the conservative physics parameters are least negative MTC and DTC.

#### 2.3.13 Partial Loss of Forced Reactor Coolant Flow (15.3.1)

This transient is initiated by a trip of one reactor coolant pump. Due to the decrease in core flow, the core average moderator temperature increases. In order to maximize the pre-trip core power response and conservatively predict the minimum DNBR, least negative MTC and DTC are appropriate.

#### 2.3.14 Complete Loss of Forced Reactor Coolant Flow (15.3.2)

This transient is initiated by a simultaneous trip of all four reactor coolant pumps. Similar to the single reactor coolant pump trip transient in Section 2.3.13, the conservative physics parameters are least negative MTC and DTC.

#### 2.3.15 Reactor Coolant Pump Locked Rotor (15.3.3)

This transient is initiated by an instantaneous seizure of a reactor coolant pump which results in a rapid decrease in loop and core flow. Similar to the single reactor coolant pump trip transient in Section 2.3.13, the conservative physics parameters are least negative MTC and DTC.

#### 2.3.16 Reactor Coolant Pump Shaft Break (15.3.4)

This transient is bounded by 15.3.3, which is discussed in Section 2.3.15.

#### 2.3.17 Uncontrolled Bank Withdrawal From Subcritical (15.4.1)

This transient is initiated by a malfunction in the Rod Control System which results in the withdrawal of two sequential control banks from a subcritical condition. In order to maximize the pre-trip core power response, a most positive MTC and a least negative DTC are conservative assumptions. The reactivity addition rate resulting from the rod withdrawal is taken to be the maximum credible value. This value is a combination of two sequential control banks moving at maximum speed in 100% overlap over the span of rod positions resulting in the maximum differential summed rod worth.

### 2.3.18 Uncontrolled Bank Withdrawal at Power (15.4.2)

This transient is initiated by a malfunction in the Rod Control System which results in the withdrawal of two sequential control banks at power. Unlike most other transients, the uncontrolled rod withdrawal at power analysis typically requires that a spectrum of cases be analyzed in order to confirm that the minimum DNBR limit is not exceeded. Due to the increase in core power peaking at reduced power levels, the analyses must consider all power levels as viable worst case initial conditions. The limiting reactivity addition rate is also not obvious and so all rates up to the maximum credible value (refer to Section 2.3.17) must be considered. A most positive MTC is combined with a least negative DTC. The impact of the rod withdrawal on the core power distribution is another parameter requiring evaluation.

### 2.3.19 Dropped Rod(s) and Dropped Bank (15.4.3)

This transient is initiated by a malfunction in the Rod Control System which results in one or more rods from the same group dropping into the core. Key physics parameters include the dropped rod worth, the total worth of the controlling rod groups which are available for withdrawal, the flux incident on the excore power range flux detectors, and the post-drop core power distribution. In order to bound the effect of thermal feedback, bounding values for MTC and DTC as a function of core burnup must be analyzed. The dropped bank transient generally results in a reactor trip on low pressurizer pressure. For those events which do not result in a reactor trip, the core power peaking is bounded by the dropped rod(s) transient due to the symmetric nature of a dropped rod bank. Therefore, the dropped rod bank is not analyzed.

### 2.3.20 Statically Misaligned Control Rod (15.4.3)

The statically misaligned control rod evaluation considers the situation where one Bank D control rod is mispositioned relative to the remaining Bank D rods. The single rod can be at any position while the bank is within its normal operating limits. The important physics parameter is the core power distribution resulting from the asymmetric condition.

#### 2.3.21 Single Control Rod Withdrawal (15.4.3)

This transient is initiated from full power by a spurious withdrawal of one Bank D rod. Key physics parameters include the integral worth of the Bank D rod beginning from the full power insertion limit, the flux incident on the excore power range flux detectors, and the core power distribution resulting from the asymmetric condition. In order to maximize the core power response, a least negative MTC and a least negative DTC are selected.

#### 2.3.22 Improper Startup of the Fourth Reactor Coolant Pump (15.4.4)

This transient is initiated by an improper manual restart of the fourth reactor coolant pump while at power. Due to the resulting increase in core flow, core average temperature decreases. Cold water originally in the idle loop is also transported towards the core by restarting the pump. In order to conservatively maximize the core power response, a most negative MTC and a least negative DTC are selected.

#### 2.3.23 Moderator Dilution Accident (15.4.6)

Moderator dilution events can result from malfunctions or misoperation of the makeup and letdown systems. These events can occur in various operating modes as detailed in the FSARs. The important physics parameters in each mode are the same. These are the critical boron concentration and the initial boron concentration. The initial boron concentration is determined by a prescribed initial value or by adding to the critical boron concentration the mode-specific shutdown margin converted to ppmb. In order to be conservative, the boron concentrations should be large, since the effect of a dilution will be greater. The boron worth used to convert the shutdown margin to ppmb should be conservatively large.

#### 2.3.24 Rod Ejection Accident (15.4.8)

The rod ejection accident is initiated by a mechanical failure of the control rod drive mechanism pressure housing. The event is evaluated at both hot full power and hot zero power conditions at both beginning and end-of-cycle. For each condition, the physics parameters are selected in a consistent manner to conservatively bound the transient response. A conservatively high ejected rod worth is evaluated. The MTC is specified as least negative to minimize negative reactivity addition via thermal feedback. The

DTC is specified as least negative to minimize thermal feedback and maximize core power response. Beta is also minimized to maximize the core power response. The resulting core power distribution including the maximum total peak are key parameters.

#### 2.3.25 Inadvertent ECCS Actuation (15.5.1)

This transient is initiated by a spurious actuation of the Emergency Core Cooling System, which results in boron injection into the primary system. Reactor power decreases slowly until a reactor trip occurs. All thermal margins increase during this transient, and there are no important physics parameters.

#### 2.3.26 CVCS Malfunction Resulting in Increase in Primary Inventory (15.5.2)

This transient is bounded by 15.5.1.

#### 2.3.27 Inadvertent Opening of a Pressurizer Relief or Safety Valve (15.6.1)

This transient is initiated by a spurious lifting of a pressurizer relief or safety valve and a failure to close. A loss of primary coolant results and primary pressure decreases until reaching the reactor trip setpoint. There are no important physics parameters associated with this event.

#### 2.3.28 Instrument Line Rupture (15.6.2)

This transient, similar to 15-6.1, does not involve any important physics parameters.

#### 2.3.29 Steam Generator Tube Rupture (15.6.3)

This transient, similar to 15.6.1, does not involve any important physics parameters.

#### 2.3.30 Loss of Coolant Accidents (15.6.5)

The only important physics parameter for LOCA is the initial power distribution. Linear heat flux (kw/ft) limits are established as a function of core elevation. These limits may also account for differences in fuel assembly design and burnup.

## 2.4 Reload Cycle Evaluation

The important physics parameters in Table 2-1 are evaluated each reload cycle to ensure that values assumed in the current licensing analyses bound the reload core. Accidents for which the physics parameters are not bounded would be reevaluated to ensure acceptable accident consequences or the core would be redesigned so the physics parameters fall within the limits assumed in the reference analysis.

### References

- 2-1 Y. H. Hsui, et al., TACO2: Fuel Pin Performance Analysis, Revision 1, BAW-10141P-A, June 1983.
- 2-2 D. A. Wesley and K. J. Firth, TACO3 - Fuel Pin Thermal Analysis Code, BAW-10162P-A, Babcock & Wilcox, November 1989



Table 2-1

Summary of Safety Analysis Physics Parameters

| Report Section | Transient Or Accident   | FSAR Section | Key Parameters   |  | Conservative Direction |
|----------------|-------------------------|--------------|--|--|------------------------|
| 2.2            | Generic                 | N/A          | <ul style="list-style-type: none"><li>• Reactivity insertion following reactor trip</li><li>• Initial core power distribution</li><li>• Effective delayed neutron fraction and decay constants</li><li>• Initial fuel temperatures</li></ul> | <ul style="list-style-type: none"><li>• Minimum worth</li><li>• Slowest insertion</li><li>• Maximum power peaking per Tech Spec</li><li>• Minimum for rapid reactivity transients</li><li>• Minimum for 15.1.2 and 15.1.3</li><li>• Maximum for all other transients</li><li>• Nominal precursor group fractions and decay constants</li><li>• Maximum</li></ul> |                        |
| 2.3.2          | Feedwater flow increase | 15.1.2       | <ul style="list-style-type: none"><li>• MTC</li></ul>  | <ul style="list-style-type: none"><li>• Most negative</li></ul>  |                        |
| 2.3.3          | Increase in steam flow  | 15.1.3       | <ul style="list-style-type: none"><li>• DTC</li></ul>  | <ul style="list-style-type: none"><li>• Least negative</li></ul>   |                        |
| 2.3.4          | SG safety valve failure | 15.1.4       | <ul style="list-style-type: none"><li>• MTC</li></ul>  | <ul style="list-style-type: none"><li>• Most negative</li></ul>  |                        |
| 2.3.5          | Steam line break        | 15.1.5       | <ul style="list-style-type: none"><li>• DTC</li><li>• SI boron concentration</li><li>• Boron worth</li><li>• Core power distribution with stuck rod</li></ul>  | <ul style="list-style-type: none"><li>• Least negative</li><li>• Minimum</li><li>• Minimum</li><li>• Maximum peaking</li></ul>   |                        |
| 2.3.7          | Turbine trip            | 15.2.3       | <ul style="list-style-type: none"><li>• MTC</li><li>• DTC</li></ul>  | <ul style="list-style-type: none"><li>• Least negative</li><li>• Least negative</li></ul>  |                        |

Table 2-1 (cont'd)

Summary of Safety Analysis Physics Parameters

| Report Section | Transient Or Accident                        | FSAR Section | Key Parameters   | Conservative Direction   |
|----------------|--|--------------|--|--|
| 2.3.10         | Loss of AC power                             | 15.2.6       | <ul style="list-style-type: none"> <li>• MTC</li> <li>• DTC</li> </ul>   | <ul style="list-style-type: none"> <li>• Most negative</li> <li>• Least negative</li> </ul>  |
| 2.3.11         | Loss of feedwater flow                       | 15.2.7       | <ul style="list-style-type: none"> <li>• MTC</li> <li>• DTC</li> </ul>   | <ul style="list-style-type: none"> <li>• Least negative</li> <li>• Least negative</li> </ul>   |
| 2.3.12         | Feedwater line break                         | 15.2.8       | <ul style="list-style-type: none"> <li>• MTC</li> </ul>  | <ul style="list-style-type: none"> <li>• Least negative</li> </ul>   |
| 2.3.13         | Partial loss of flow                         | 15.3.1       | <ul style="list-style-type: none"> <li>• DTC</li> </ul>  | <ul style="list-style-type: none"> <li>• Least negative</li> </ul>   |
| 2.3.14         | Complete loss of flow                        | 15.3.2       | <ul style="list-style-type: none"> <li>• Core power distribution</li> </ul>  | <ul style="list-style-type: none"> <li>• Maximize number of pins in DNB</li> </ul>   |
| 2.3.15         | Locked rotor                                 | 15.3.3       | <ul style="list-style-type: none"> <li>(locked rotor only)</li> </ul>  |  |
| 2.3.17         | Uncontrolled rod withdrawal from subcritical | 15.4.1       | <ul style="list-style-type: none"> <li>• MTC</li> <li>• DTC</li> <li>• Reactivity addition rate</li> </ul>                                   | <ul style="list-style-type: none"> <li>• Most positive</li> <li>• Least negative</li> <li>• Maximum</li> </ul>   |
| 2.3.18         | Uncontrolled rod withdrawal                  | 15.4.2       | <ul style="list-style-type: none"> <li>• MTC</li> <li>• DTC</li> <li>• Excore detector signal</li> <li>• Reactivity addition rate</li> </ul> | <ul style="list-style-type: none"> <li>• Most positive</li> <li>• Least negative</li> <li>• Minimum indicated power</li> <li>• Small to maximum</li> </ul> |

Table 2-1 (cont'd)

Summary of Safety Analysis Physics Parameters

| Report Section | Transient Or Accident              | FSAR Section | Key Parameters  |   | Conservative Direction |
|----------------|------------------------------------|--------------|---|---|------------------------|
| 2.3.19         | Dropped rod(s)<br>Dropped rod bank | 15.4.3       | <ul style="list-style-type: none"> <li>• MTC</li> <li>• DTC</li> <li>• Dropped rod worth</li> <li>• Available rod worth for withdrawal</li> <li>• Excore detector tilt</li> <li>• Core power distribution with dropped rod</li> </ul> | <ul style="list-style-type: none"> <li>• Bounding vs burnup</li> <li>• Bounding vs burnup</li> <li>• Small to maximum</li> <li>• Maximum</li> <li>• Minimum indicated power</li> <li>• Maximum peaking</li> </ul> |                        |
| 2.3.20         | Statically misaligned rod          | 15.4.3       | <ul style="list-style-type: none"> <li>• Core power distribution with misaligned rod</li> </ul>   | <ul style="list-style-type: none"> <li>• Maximum peaking</li> </ul>   |                        |
| 2.3.21         | Single rod withdrawal              | 15.4.3       | <ul style="list-style-type: none"> <li>• MTC</li> <li>• DTC</li> <li>• Worth of single rod</li> <li>• Core power distribution with rod withdrawn</li> <li>• Excore detector tilt</li> </ul>   | <ul style="list-style-type: none"> <li>• Least negative</li> <li>• Least negative</li> <li>• Maximum</li> <li>• Maximize number of pins in DNB .</li> <li>• Minimum indicated power</li> </ul>                    |                        |
| 2.3.22         | Fourth RCP startup                 | 15.4.4       | <ul style="list-style-type: none"> <li>• MTC</li> <li>• DTC</li> </ul>  | <ul style="list-style-type: none"> <li>• Most negative</li> <li>• Least negative</li> </ul>   |                        |
| 2.3.23         | Moderator dilution                 | 15.4.6       | <ul style="list-style-type: none"> <li>• Critical boron concentration</li> <li>• Initial boron concentration</li> </ul>   | <ul style="list-style-type: none"> <li>• Highest</li> <li>• Closest to critical concentration</li> </ul>  |                        |

Table 2-1 (cont'd)

Summary of Safety Analysis Physics Parameters

| Report<br>Section | Transient Or Accident    | FSAR<br>Section | Key Parameters  |   | Conservative<br>Direction |
|-------------------|--------------------------|-----------------|---|---|---------------------------|
| 2.3.24            | Rod ejection             | 15.4.8          | <ul style="list-style-type: none"> <li>• MTC</li> <li>• DTC</li> <li>• Ejected rod worth</li> <li>• Beta-effective</li> <li>• Core power distribution with ejected rod</li> </ul> | <ul style="list-style-type: none"> <li>• Most positive</li> <li>• Least negative</li> <li>• Maximum</li> <li>• Minimum</li> <li>• Maximum total peak</li> <li>• Maximize number of pins in DNB</li> </ul> |                           |
| 2.3.30            | Loss of coolant accident | 15.6.5          | <ul style="list-style-type: none"> <li>• Initial core power distribution</li> </ul>   | <ul style="list-style-type: none"> <li>• Maximum kw/ft vs. core elevation</li> </ul>  |                           |

### 3.0 CALCULATION OF KEY SAFETY ANALYSIS PHYSICS PARAMETERS

Three-dimensional core models such as EPRI-NODE-P (Reference 3-1) and SIMULATE-3P (Reference 3-2) are used to calculate core physics parameters and power distributions. In some cases, simpler two-dimensional calculations may be performed with PDQ (Reference 3-1) or SIMULATE-3P. In these cases, appropriate corrections for flux redistribution effects are made.

Core physics parameters are calculated as part of the safety analysis for each reload core using NRC-approved methodology to systematically confirm the physics parameters for a reload core are bounded by the licensing Chapter 15 analyses. The models used to perform these calculations are based on the available operating history of the previous reload cycle to ensure best estimate calculations. Determination of whether a nuclear-related physics parameter is within the bounding value assumed in the reference safety analysis must be made by performing explicit calculations of the parameter, or by comparison to values generated in previous reload core designs. Comparison to previously calculated physics parameters (to determine if the physics parameter is bounding) is only performed if the reload core being analyzed is similar to previously analyzed reload cores. These comparisons can be performed to determine the bounding nature of a physics parameter because of the predictable behavior of most physics parameters as a function of reactor power, moderator temperature, burnup, and soluble boron concentration. The calculation of control rod worths, reactivity coefficients, and kinetics parameters are described below.

#### 3.1 Control Rod Worth Calculations

The primary purpose of control rods is to provide adequate shutdown capability during normal plant operation and accident conditions. Control rods are also used to maintain criticality during rapid reactivity changes such as those that would occur during typical load follow maneuvers. They can also be used to offset reactivity changes produced from fuel depletion and changes in boron concentration, xenon concentration, and moderator temperature. However, control rods are maintained at or near their all rod out (ARO) position during nominal power operation and are normally only used to compensate for rapid reactivity changes.

Control rod integral and differential rod worths are sensitive to local and global power distribution changes. Since the placement of fresh and depleted fuel assemblies produces unique power distributions, it is necessary to analyze control rod worths for each reload core. Rod worth related calculations that are evaluated for each reload core are:

- Shutdown margin
- Trip reactivity
- Control rod insertion limits
- Maximum differential rod withdrawal at power
- Maximum differential rod withdrawal from subcritical
- Dropped rod worth
- Ejected rod worth

#### Shutdown Margin

Shutdown margin calculations are typically performed for each reload core at beginning of cycle (BOC) and end of cycle (EOC) at various power levels including hot full power (HFP) and hot zero power (HZP) conditions. These calculations are typically performed in three dimensions, taking into account the power defect, stuck rod worth, allowance for rods being at their power dependent insertion limits, xenon maldistribution, and rod worth uncertainty.

#### Trip Reactivity

The minimum trip reactivity and the trip reactivity shape are evaluated for each reload core. Trip reactivity is defined as the amount of negative reactivity inserted into the reactor core following a reactor trip. Allowances for the highest worth stuck rod and for the control banks at the rod insertion limits are taken into account. If the results from this calculation are not bounded by the trip reactivity assumed in the safety analysis, reanalyses of the affected accidents are performed with a new minimum trip reactivity. The minimum normalized trip reactivity shape is also analyzed for each reload core. This calculation is performed from HFP, and is structured to conservatively delay the amount of negative reactivity inserted into the reactor core versus rod position. The highest worth stuck rod is assumed stuck in its fully withdrawn position after trip. This conservatism is achieved by allowing for a bottom peaked power distribution.

### Control Rod Insertion Limits

Control rod insertion limits serve several functions and are dependent upon the acceptable results of power peaking analyses, shutdown margin calculations, ejected rod worth calculations, and inserted reactivity assumptions for safety analyses. Verification of the rod insertion limits from a peaking standpoint is performed in the operating limits and RPS setpoint analysis performed for each reload core design. The methodology used to perform this analysis is discussed in detail in Reference 3-3. Rod insertion limits also impact the available shutdown margin by influencing the magnitude of the rod insertion allowance. The rod insertion allowance is calculated at various burnups and includes allowances for top peaked power distributions. Rod insertion limits also impact the ejected rod worth and the amount of worth available for withdrawal for accidents sensitive to this parameter.

### Maximum Differential Rod Withdrawal from Power

The maximum differential rod worth at power is calculated for each reload core at BOC and EOC. This calculation is performed to ensure that inputs to the uncontrolled bank withdrawal at power accident are bounded. The maximum differential rod worth of any two control banks is calculated assuming normal overlap and adverse axial power distributions, while adhering to the power dependent rod insertion limits.

### Maximum Differential Rod Withdrawal from Subcritical

The maximum differential rod worth from subcritical is calculated for each reload core at BOC and EOC. This calculation is performed to ensure that inputs to the uncontrolled bank withdrawal from subcritical or low power accident are bounded. The calculation of this parameter assumes the combination of two sequential control banks moving in 100% overlap with the reactor at HZP. The impact of adverse axial power distributions is also considered in the calculation of the maximum differential rod worth.

### Dropped Rod Worth

The maximum allowed dropped rod worth is calculated, which occurs at EOC. Limiting combinations of dropped rods are evaluated to determine the maximum dropped rod worth. This value is compared against the reference analysis value to ensure that the safety analysis remains bounding. Dropped rod worths are calculated by evaluating the reactivity difference produced from a control rod or rods dropped from the HFP ARO RIL condition.

### Ejected Rod Worth

Ejected rod worths are calculated at BOC and EOC for both HFP and HZP conditions. Initial conditions for the ejected rod worth calculation are established by assuming that the control rods are at their rod insertion limit and by imposing a positively skewed power distribution. The rod worth calculation is performed by ejecting the control rod from the rod insertion limit to the ARO condition and calculating the reactivity difference. All possible rods are analyzed to determine the highest worth ejected rod. Conservatisms in the calculation of this rod worth and the resulting peaking factors produced from the rod ejection are retained by holding both the moderator and fuel temperature distributions constant.

## 3.2 Reactivity Coefficients and Kinetics Parameters

The dynamic behavior of a reactor core during load follow maneuvers, transients, and accident conditions can be described in terms of reactivity coefficients. The magnitude and sign of these coefficients affect the reactor stability during transient and accident conditions. Reactivity coefficients are defined as the change in reactivity produced from a change in reactor power, moderator density, fuel temperature or boron concentration. The moderator density effects are often expressed in terms of moderator temperature. Since these coefficients are a strong function of exposure, they are calculated at several exposure statepoints during core life. Reactivity coefficients are also influenced by changes in moderator temperature, reactor power, and soluble boron concentration.

The statepoints at which reactivity coefficients are evaluated are chosen to ensure that the assumptions made in the specific accident analyses remain bounded. For example, the moderator



dilution accident at power is sensitive to the most positive moderator temperature coefficient and the steam line break accident is sensitive to the most negative (or least positive) isothermal temperature coefficient. The calculation of the moderator temperature coefficient, and fuel temperature coefficients and the statepoints at which these coefficients are evaluated are discussed below. The calculation of critical boron concentrations, boron worths and kinetics parameters follow.

### Moderator Temperature Coefficient

The moderator temperature coefficient (MTC) is defined as the change in core reactivity resulting from a change in moderator temperature. Bounding coefficients (least and most negative) are calculated for each reload core. The following parameters are considered in the evaluation of the moderator temperature coefficient to ensure that conservative results are obtained.

- Soluble boron
- Cycle exposure
- Control rods
- Moderator temperature

The calculation of the MTC is typically performed using a three-dimensional core model. The moderator temperature coefficient is calculated by inducing a change in moderator temperature (and, therefore, density) about the average temperature of interest and dividing the resulting reactivity change by the change in moderator temperature.

### Doppler Temperature Coefficient

The Doppler (or fuel) temperature coefficient (DTC) is defined as the change in core reactivity resulting from a change in fuel temperature. The most and least negative DTCs are calculated for each reload core considering the core burnup and power level. The DTC is calculated by performing a set of two cases which vary the fuel temperature about a mean fuel temperature. The reactivity difference between the two fuel temperatures divided by the change in fuel

temperature is the definition of the DTC. DTCs are often quoted at various power levels by equating changes in reactor power to changes in mean fuel temperature.

### Kinetics Parameters

The dynamic behavior of the reactor core is determined to a large degree by the presence of delayed neutrons. Delayed neutron fractions and decay constants are calculated for six effective delayed neutron groups. The total beta-effective is the sum of the six group effective fractions and is, along with prompt neutron lifetime, calculated at BOC and EOC conditions.

### Critical Boron Concentrations and Boron Worths

Critical and shutdown boron concentrations are calculated as a function of reactor power, exposure, temperature, and control rod positions as allowed by the power dependent rod insertion limits. Differential boron worths are also calculated as a function of various combinations of the above variables. The results of these calculations are compared to inputs for several accident analyses.

### References

- 3-1 Nuclear Physics Methodology for Reload Design, DPC-NF-2010A, Duke Power Company, June 1985.
- 3-2 Nuclear Design Methodology Using CASMO-3/SIMULATE-3P, DPC-NE-1004-A, Revision 1, Duke Power Company, December 1997.
- 3-3 Nuclear Design Methodology for Core Operating Limits of Westinghouse Reactors, DPC-NE-2011P-A, Duke Power Company, March 1990.

## 4.0 ROD EJECTION ANALYSIS

### 4.1 Overview

#### 4.1.1 Description of Rod Ejection Accident

The rod ejection accident is described in FSAR Section 15.4.8 (Reference 4-1). The accident is initiated by a failure of the control rod drive mechanism housing, which allows a control rod to be rapidly ejected from the reactor by the Reactor Coolant System pressure. If the reactivity worth of the ejected control rod is large enough, the reactor will become prompt critical. The resulting power excursion will be limited by the fuel temperature feedback and the accident will be terminated when the Reactor Protection System trips the reactor on high neutron flux and the remaining control rods fall into the core. The mechanical design and testing of the control rod drive mechanisms and housings make this event unlikely. If a control rod ejection should occur, the nuclear design of the reactor core and limits on control rod insertion will limit any potential fuel damage to acceptable levels.

#### 4.1.2 Acceptance Criteria

The rod ejection accident is classified as an ANS Condition IV event. Three acceptance criteria are applicable as required per NUREG-0800, Section 15.4.8 (Reference 4-2). The radially averaged fuel pellet enthalpy shall not exceed 280 cal/gm at any axial location. This criterion ensures that a coolable core geometry is maintained. Acceptable offsite dose consequences must be shown by being "well within" the 10CFR100 dose limits of 25 rem whole-body and 300 rem to the thyroid. "Well within" is to be interpreted as less than 25% of the above values. The radionuclide source term is determined by conservatively predicting the number of fuel pins exceeding the DNB limit and the percentage of melted fuel. The peak Reactor Coolant System pressure must be within Service Limit C as defined by the ASME Code (Reference 4-3), which is 3000 psia (120% of the 2500 psia design pressure).

#### 4.1.3 Analytical Approach

The complexity of the core and system response to a rod ejection event requires the application of a sequence of computer codes. The rapid core power excursion is simulated with a three-dimensional transient neutronic and thermal-hydraulic model using the ARROTTA code (Reference 4-4). The resulting transient core power distribution results are then input to VIPRE-01 (Reference 4-5) core thermal-hydraulic models. The VIPRE models calculate the peak fuel pellet enthalpy, the allowable power peaking to avoid exceeding the DNBR limit, and the core coolant expansion rate. The allowable power peaking is then used along with a post-ejected condition fuel pin census to determine the percent of pins in DNB. The coolant expansion rate is input to a RETRAN-02 (Reference 4-6) model of the Reactor Coolant System to determine the peak pressure resulting from the core power excursion.

### 4.2 Simulation Codes and Models

#### 4.2.1 Nuclear Analysis

The response of the reactor core to the rapid reactivity insertion from the control rod ejection is simulated with the ARROTTA code. ARROTTA computes a three-dimensional power distribution (in rectangular coordinates) and reactivity or power level for both static and transient applications. The neutronics solution in ARROTTA is based on the Analytic Nodalization Method as developed for QUANDRY (Reference 4-7).

The neutronics method generates an exact solution to the neutron diffusion equations if the shape of the transverse leakage function is assumed to be of a known quadratic form. In the limit of small node sizes, the equations revert to the same limit as the standard flux-centered finite difference equations. ARROTTA uses a full two group representation of the diffusion equations and up to six delayed neutron groups. A complete description of the theory and equations solved in ARROTTA can be found in Reference 4-4.

The ARROTTA model for the rod ejection analysis is based on a best estimate model of Catawba 1 Cycle 2 that is adjusted as described in Section 4.3.1 to produce conservative results. The assembly enrichments, burnable poison loading and assembly exposures for Catawba 1 Cycle 2

are shown in Figure 4-1. The neutronics model is based on the Westinghouse optimized fuel loaded in the reactor for that cycle. The ARROTTA model has one node per fuel assembly in the radial direction and a minimum of twelve equal length fuel nodes in the axial direction. In addition to the fuel, there are two rows of reflector in the radial direction on the outside of the core and one plane of reflector nodes on both the top and bottom of the core. The reflector row next to the fuel consists of homogenized steel baffle and reactor coolant while the outer row contains just coolant. The axial reflector planes consist of homogenized reactor coolant, assembly structure, and some vessel structure.

All fuel and reflector cross sections and assembly discontinuity factors (ADFs) were taken from CASMO-3 (Reference 4-8) assembly lattice calculations. The two group conventional cross sections are processed by a series of auxiliary programs and input to ARROTTA in the following form:

$$\Sigma = R(A + BX + CX^2) + (1 - R)(D + EX + FX^2) + \frac{d\Sigma}{dT_m}(T_m - T_m') + \frac{d\Sigma}{dT_f}(\sqrt{T_f} - \sqrt{T_f'})$$

where  $R=0$  for no control rod,  $R=1$  for a control rod fully inserted in the node.  $A, B, C, D, E, F, d\Sigma/dT_m$  and  $d\Sigma/dT_f$  are determined from the CASMO-3 cross sections for both energy groups for all cross sections including  $\Sigma_{tr}, \Sigma_a, v\Sigma_f$  and  $\kappa\Sigma_f$ . The  $d\Sigma/dT_f$  term is only used for the fast group cross sections. For a PWR, the  $X$  term is defined as the change in relative water density from a reference value (density/reference density - 1). Also, there are microscopic contributions to absorption and removal for soluble boron and to just absorption for xenon, iodine, samarium, and promethium. Because of limitations in the auxiliary programs, the variations of all cross sections against  $X$  are the same either with or without a control rod present ( $A \neq D$ , but  $E=B$  and  $F=C$ ).

The cross sections are not functionalized against fuel exposure because each set of cross sections, called a composition, is only valid for a unique fuel exposure and enrichment combination. The auxiliary program that functionalizes the cross sections finds fuel nodes of similar exposure and identical enrichment and assigns a single composition to those nodes at their average exposure.

ADFs are used to account for heterogeneities within assemblies for which the homogeneous flux solution cannot account. ARROTTA allows a different ADF for each face of a node, but CASMO-3, because it is an infinite lattice program, provides only a single radial ADF. These ADFs are input to ARROTTA as a single radial value for each fuel node and reflector-fuel interface. Since ADFs are not strong functions of fuel exposure, they are input as single values for each assembly instead of a value for each composition. ADFs are not used in the axial direction.

The ARROTTA thermal-hydraulic model is comprised of a fluid dynamics model and a fuel pin heat transfer model. The fluid dynamics model is an inhomogeneous, non-equilibrium, two-phase, closed channel model that uses separate energy equations for each phase and accounts for six possible flow regimes. The heat conduction model is based on spatially averaged, time dependent equations for the average pellet temperature. The thermal-hydraulic parameters calculated by ARROTTA are used to update the cross section model for the nuclear calculations; they are not used to determine fuel performance during the transient.

The ARROTTA code has been benchmarked against numerical steady-state and transient standard benchmark problems. The results of these benchmarks are documented in Reference 4-9 and show that ARROTTA agrees very well with the reference solutions. ARROTTA has also been benchmarked to a separate rod ejection transient simulation for a four-loop Westinghouse reactor (Reference 4-10). The benchmark case compares ARROTTA to HERMITE, a code which has received NRC review and approval for use in control rod ejection analyses.

The ARROTTA model for this benchmark problem is very similar to the model used in this control rod ejection analysis. The results from this benchmark problem also show excellent agreement. These benchmark problems clearly demonstrate that ARROTTA is an acceptable code to use in analyzing the rod ejection accident.

ARROTTA is used to calculate the core power level versus time during the rod ejection transient. Also, the radial, axial, and total peaking by assembly is calculated at each time step during the transient. This information is used by VIPRE to determine the fuel temperature, enthalpy and the amount of fuel failure due to DNB.

## 4.2.2 Core Thermal-Hydraulic Analysis

### 4.2.2.1 VIPRE-01 Code Description

The VIPRE-01 code is used for the rod ejection analysis thermal evaluations. VIPRE-01 is a subchannel thermal-hydraulic computer code developed for EPRI by Battelle Pacific Northwest Laboratories (BPNL). The VIPRE-01 code has been reviewed by the NRC and was found to be acceptable for referencing in licensing applications (Reference 4-11).

With the subchannel analysis approach, the nuclear fuel element is divided into a number of quasi one-dimensional channels that communicate laterally by diversion crossflow and turbulent mixing. However, VIPRE-01 is also capable of simulating single subchannel geometry. Given the geometry of the reactor core and coolant channel, and the boundary conditions or forcing functions, VIPRE-01 calculates core flow distributions, coolant conditions, fuel rod temperatures and the departure from nucleate boiling ratio (DNBR) for steady-state and transient conditions. VIPRE-01 accepts all necessary boundary conditions that originate either from a system transient simulation code such as RETRAN, or a transient core neutronics simulation code such as ARROTTA. Included is the capability to impose different boundary conditions on different segments of the core model. For example, different transient inlet temperatures, flow rates, heat flux transients, and even different transient assembly and pin radial powers or axial flux shapes can be modeled.

### 4.2.2.2 Fuel Temperature and Enthalpy Calculation

In order to show that the peak fuel enthalpy acceptance criteria described in Section 4.1.2 is met, the standard [ ] VIPRE model (Reference 4-15) with fuel conduction is utilized to calculate the maximum hot spot fuel temperature and enthalpy during the transient. Given the

[ ]

VIPRE calculates the transient maximum hot spot average fuel temperature and the maximum radial average fuel enthalpy. Details regarding the [ ] VIPRE model and initial and boundary conditions follow.

### Model Description



### Axial Power Distributions

During the transient the hot assembly axial power distributions change mainly due to the motions of the ejected control rod and due to the insertion of control rods as the reactor trips. VIPRE is able to accept different axial power distributions during the transient. For each transient case,

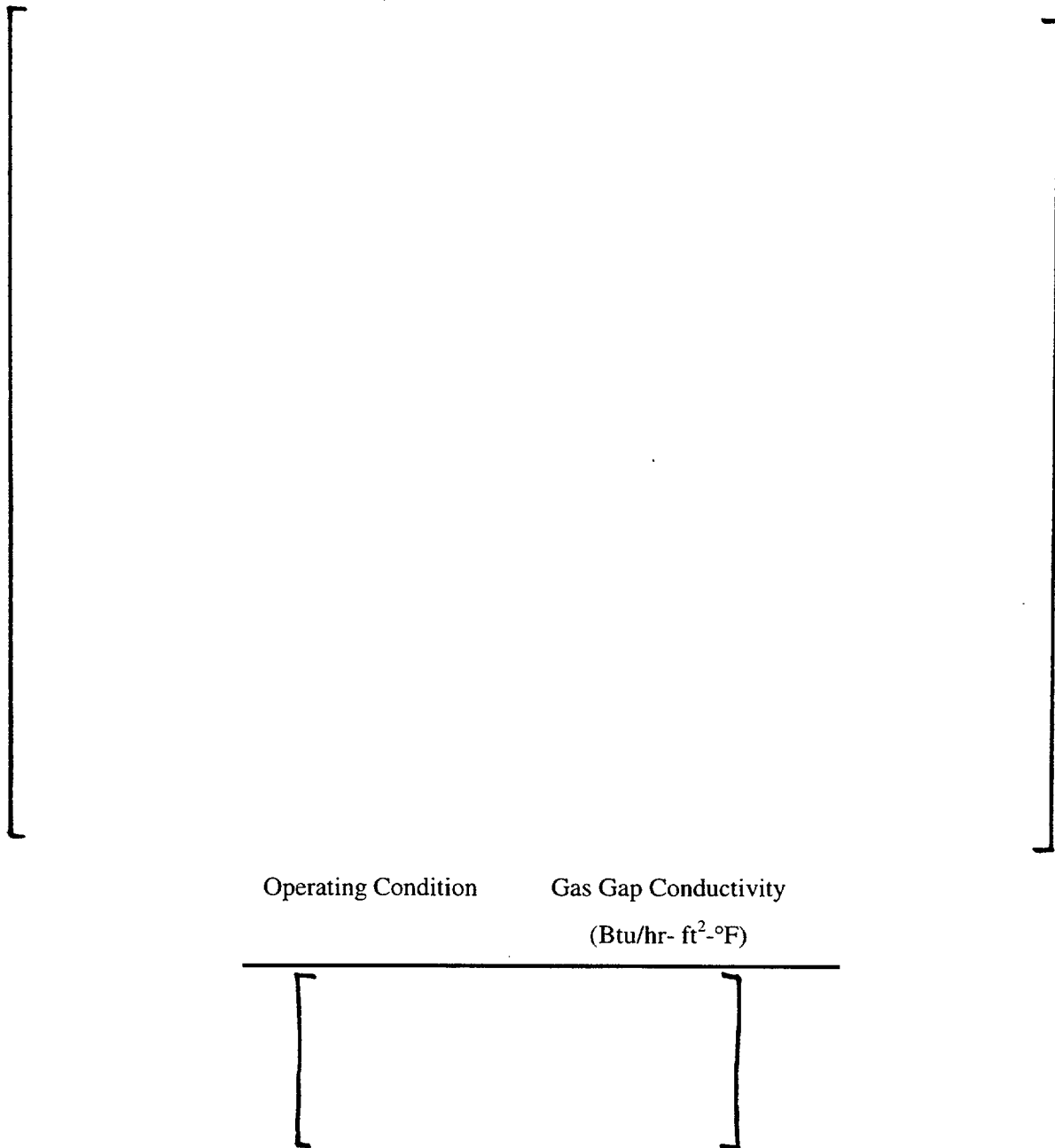


### Radial Power Distributions





### Fuel Conduction Model



### Heat Transfer Correlations

Sensitivity studies have been performed to justify the use of the heat transfer correlations for the four major segments of the boiling curve as shown below.

For single-phase forced convection - [ ]  
 For saturated nucleate boiling regime - [ ]  
 For transition boiling regime - [ ]  
 For film boiling regime - [ ]

The critical heat flux correlation used to define the peak of the boiling curve is the same as the correlation used for the DNBR evaluation. The minimum DNBR value for which transition boiling occurs is set to be the DNBR limit for that correlation.

### Flow Correlations

For the rod ejection analysis, the subcooled void, the bulk void, and the two-phase friction multiplier are modeled by using the [ ] correlations, respectively.

The justification of using these models is based on the results of the sensitivity analysis of different void models to the transient fuel temperature calculation.

### Other Thermal-Hydraulic Correlations

Pressure losses due to frictional drag are calculated in VIPRE for axial flow. The friction factor for the pressure loss in the axial direction is determined from an empirical correlation as:

$$f = A \times Re^B$$

where Re is the Reynolds number. The code evaluates both a turbulent and laminar set of coefficients and selects the maximum. The values selected for parameters A and B are based on smooth tubes and are taken from Reference 4-5.

|                 |         |           |
|-----------------|---------|-----------|
| Turbulent flow: | A = [ ] | B = - [ ] |
| Laminar flow:   | A = [ ] | B = - [ ] |

The local hydraulic form loss coefficient is set as a constant to model the irrecoverable axial pressure loss as shown below.

$$\Delta P = KG^2/2\rho g_c$$

where:        K        = spacer grid form loss coefficient  
               G        = mass flux, lbm/sec-ft<sup>2</sup>  
               ρ        = density, lbm/ft<sup>3</sup>  
               g<sub>c</sub>       = 32.174 lb-ft/sec<sup>2</sup>-lb<sub>f</sub>

#### Conservative Factors

Flow area reduction - the hot subchannel flow area is reduced by 2% to account for variations in as-built subchannel flow area.

Hot channel flow rate reduction - the hot assembly inlet flow is conservatively reduced by 5% from the nominal assembly flow.

An appropriate engineering hot channel factor is applied to account for variations in the fabrication variables which affect the heat generation rate along the flow channel.

#### Direct Coolant Heating

The amount of heat generated in the coolant is 2.6% of the total power.

#### Fuel Enthalpy Calculation

VIPRE-01 does not perform a fuel enthalpy calculation. Thus, the fuel enthalpy for a given fuel temperature during the transient is calculated separately from VIPRE based on the equation obtained from MATPRO (Reference 4-13).

$$\text{FENTHL} = \text{FENTHL}(T) - \text{FENTHL}(T_{\text{ref}})$$

With:

$$\text{FENTHL} = \frac{K_1 \Theta}{\exp(\Theta/T) - 1} + \frac{K_2 T^2}{2} + \frac{Y K_3}{2} \exp(-E_D/RT)$$

Where:

FENTHL = fuel enthalpy (J/kg)

T = temperature (K)

Y = oxygen to metal ratio = 2.0

R = 8.3143 (J/mol-K)

Θ = the Einstein temperature (K)

= 535.285 for UO<sub>2</sub>

K<sub>1</sub> = 296.7 (J/kg-K)

K<sub>2</sub> = 2.42 x 10<sup>-2</sup> (J/kg-K<sup>2</sup>)

K<sub>3</sub> = 8.745 x 10<sup>7</sup> (J/kg)

E<sub>D</sub> = 1.577 x 10<sup>5</sup> (J/mol)

FENTHL(T<sub>ref</sub>) = fuel enthalpy at any desired reference temperature

The above fuel enthalpy correlation is only valid for a fuel temperature greater than about 300K (80.3°F) (Reference 4-13). The reference temperature is 300°K.

#### 4.2.2.3 Coolant Expansion Rate Calculation

If the peak fuel enthalpy criterion is met, there is little chance of fuel dispersal into the coolant. Therefore, the Reactor Coolant System expansion rate may be calculated using conventional heat transfer from the fuel and prompt heat generation in the coolant. This rate must be calculated with the consideration of the spatial power distribution before and during the transient since this rate, at any location in the reactor core, depends on the initial amount of subcooling and the rate of change of the heat added into the coolant channels. A [ ]VIPRE model is constructed

for this purpose. Using the [ , VIPRE calculates the flow rate in each channel during the transient. Using the VIPRE channel flow rates, the total coolant expansion rate can be calculated. This total coolant expansion rate is input to a RETRAN plant transient model for simulating the resulting pressure response.

#### Model Description



#### Axial Power Distributions



### Radial Power Distributions

[

]

### Fuel Conduction Model

[

]

### Heat Transfer Correlations

Heat transfer correlations used for the four major segments of the boiling curve are as shown below.

For single-phase forced convection - [ ]  
For saturated nucleate boiling regime - [ ]  
For transition boiling regime - [ ]  
For film boiling regime - [ ]

The critical heat flux correlation used to define the peak of the boiling curve is the same as the correlation used for the DNBR evaluation. The minimum DNBR value for which transition boiling occurs is set to be the DNBR limit for that correlation.

### Flow Correlations

For the coolant volume expansion calculations, the subcooled void, the bulk void, and the two-phase friction multiplier are modeled by using the [ ]

### Other Thermal-Hydraulic Correlations

Refer to Section 4.2.2.2.

### Calculation of the Reactor Coolant Expansion Rate From VIPRE Flow Rates

From the [ ] model results, the inlet and exit mass flow rates and densities for each channel can be obtained. The instantaneous volume expansion rate at time t for each channel,  $Q_i$  (ft<sup>3</sup>/sec), is first calculated as shown below.

$$Q_i \text{ (ft}^3\text{/sec)} = \frac{M_{i, \text{ exit}}}{\rho_{i, \text{ exit}}} - \frac{M_{i, \text{ inlet}}}{\rho_{i, \text{ inlet}}}$$

Where: i = channel index

M = mass flow rate, lbm/sec

r = density, lbm/ft<sup>3</sup>

Then the instantaneous core volume expansion rate at time t is:

$$Q \text{ (ft}^3\text{/sec)} = \sum_{i=1}^I Q_i$$

The above calculations are repeated for different times to obtain Q(t) during the transient.

#### 4.2.2.4 DNBR Evaluation

To determine the offsite dose consequences, an analysis is performed using the VIPRE code to determine the percentage of the core experiencing DNB. Those fuel pins which exceed the DNBR limit are assumed to fail. The standard [ ] model (Reference 4-15) described in Section 4.2.2.2 is used for the DNBR evaluation. Utilizing the [

] One CHF correlation used is the BWCMV correlation (Reference 4-14) and the DNBR limit is 1.331 ( $1.331 = 1.10 \times 1.21$  where 1.210 is the correlation design limit and the 1.10 factor adds 10% margin). The second CHF correlation used to perform DNB analysis is the BWU-Z CHF correlation (Reference 4-18). The BWU-Z correlation was reviewed and approved by the NRC for use in McGuire/Catawba analyses in References 4-19 and 4-20. The BWU-Z correlation limit is 1.193 for this analysis. [

] A fuel pin census is then performed to determine the number of fuel pins in the core experiencing DNB.

[

] Last, the pin power for every pin is compared to the appropriate MARP value. If the pin power is higher than the MARP, then that pin is in DNB.

[

]



### Model Description

The [ ] model used for the rod ejection DNBR calculations is identical to the one used in Section 4.2.2.2 (Figure 4-2).

### Cases Analyzed

The methodology and results presented show the analysis for HFP and HZP initial conditions for both BOC and EOC. Based on analysis experience, the HZP cases are no longer analyzed for the following reason. The DNBR evaluation is performed to determine the number of failed fuel pins for input to the dose analysis. A key element of the dose analysis is the duration of steam generator tube bundle uncover following the post-reactor trip boiloff. For the HZP cases there is no steam generator tube bundle uncover, and the doses will be less than the HFP case doses even with 100% fuel pin failure. The methodology and results are retained for completeness.

### Axial Power Distributions



### Radial Power Distributions



### Fuel Conduction Model



### Heat Transfer Correlations

For the DNBR calculations, only the single-phase forced convection and nucleate boiling heat transfer modes are applicable. The [ ] correlation is used for the single-phase forced convection mode. The [ ] correlation is used for the nucleate boiling regime. Justification for using these correlations is based on [ ]

[ ] The critical heat flux correlation used to define the peak of the boiling curve is the same as the correlation used for the DNBR evaluation. The minimum DNBR value for which transition boiling occurs is set to be the DNBR limit for that correlation.

### Flow Correlations

The [ ] correlation for the two-phase friction multiplier. Justification for using these correlations is based on [ ]

### Other Thermal-Hydraulic Correlations

Refer to Section 4.2.2.2.

#### 4.2.3 System Thermal-Hydraulic Analysis

The Reactor Coolant System response to a rod ejection accident is primarily a rapid pressurization due to the increase in heat transfer associated with the power excursion. The VIPRE analysis of the coolant expansion rate described in Section 4.2.2.3 produces an expansion rate which conservatively models [ ] The VIPRE result is input to a RETRAN-02 model of McGuire/Catawba as [ ] The RETRAN-02 model is the base model described in detail in Reference 4-15.

### 4.3 ARROTTA Analysis

#### 4.3.1 Initial Conditions

The control rod ejection transient is analyzed at four statepoints for Catawba Unit 1, Cycle 2: beginning-of-cycle (BOC) at hot zero power (HZP) and hot full power (HFP) and end-of-cycle (EOC) at HZP and HFP. Because of the modifications to the ARROTTA model that are described below, analysis of this core is expected to bound any expected future reload cycle. The ejected control rod is located at core location D-12. Figure 4-4 shows this location in the reactor. The control rod in location D-12 is part of Control Bank D (hereafter referred to as Bank D). At the HZP rod insertion limit, D is the only bank fully inserted. At the HFP insertion limit, it is the only bank in the core. The central control rod (location H-8, also a member of Bank D) is not chosen as the ejected rod because sensitivity studies showed that a higher  $F_Q$  would be achieved by ejecting a given worth from D-12 than from H-8 due to the asymmetric power distributions produced when D-12 is ejected. Since the higher  $F_Q$  is more conservative, D-12 is chosen as the ejected rod.

For the HZP statepoints, the reactor is initially critical at a very low power level with control rods at the insertion limit: Bank D at 0 steps withdrawn (swd), Bank C at 47 swd, and Bank B at 162 swd. The rod is fully withdrawn at approximately 226 swd and at 0 swd the control rod tip is approximately 2.65 inches above the bottom of the core. No allowance is made for a bank of rods being mispositioned lower than indicated (higher worth) because the ejected rod is initially fully inserted. If either Bank C or B were mispositioned, the worst effect would be to increase

the ejected rod worth. However, the ejected rod worth is already assumed to be conservatively high, so this effect is accounted for.

The control rod is ejected in 0.1 seconds at constant velocity for the HZP cases. This is significantly faster than physically possible, even when friction is ignored in the ejection time calculation. Sensitivity studies show that the peak power level attained during the transient is slightly higher (more conservative) for a faster ejection time. Thus, the control rod ejection results are conservative with respect to control rod ejection time.

For the HFP statepoints, the reactor is initially at 102% of rated power with Bank D at 149 swd. This is 12 steps beyond the insertion limit to make allowance for the bank being mispositioned. The control rod at D-12 is ejected in 0.058 seconds at constant acceleration. This acceleration is consistent with the ejection time of 0.1 seconds used in the HZP cases.

[ ]

The moderator temperature coefficient (MTC) is adjusted to the values shown in Table 4-1. Although the MTC has very little effect on the transient results, it was adjusted to be greater than the technical specification limits for the BOC statepoints. For the EOC statepoints, the MTC was adjusted to be greater (less negative) than any expected for future reload cycles. The MTC was adjusted in the ARROTTA model by [ ]

The Doppler (or fuel) temperature coefficient (DTC) is important to this transient because the negative reactivity from the increased fuel temperature is the only effect that limits the power excursion and starts to shut down the reactor. The DTC is adjusted to the values shown in Table 4-1. These values are greater (less negative) than any expected for future reload cycles. The DTC is adjusted by [ ]

The effective delayed neutron fraction ( $\beta$ ) and the ejected rod worth both determine the transient response of the reactor. The peak power level attained during the transient will increase for smaller values of  $\beta$  and larger values of the ejected rod worth. The ejected rod worth is adjusted by [ ]

$\beta$  is input to the model by six delayed groups for each composition. Since  $\beta$  is dependent on enrichment and burnup, all the compositions are different from each other.  $\beta$  is adjusted by [ ]

The total effect of all of the changes to the Catawba Unit 1 Cycle 2 model is to create an ARROTTA model that will bound all expected reload cycles for both McGuire and Catawba Nuclear Stations. The various limiting parameters are listed in Table 4-1.

#### 4.3.2 Boundary Conditions

The fuel and core thermal-hydraulic boundary conditions are listed on Table 4-2. The thermal-hydraulic description of the fuel used in ARROTTA represents B&W Mark-BW fuel. The rod ejection transient is very nearly adiabatic through the time that the peak power level is limited by the fuel temperature feedback. Since the Mark-BW fuel contains a higher mass of fuel than the Westinghouse OFA fuel, it will heat up more slowly during adiabatic events. The slow heatup decreases the fuel temperature feedback, resulting in a higher, more conservative, transient core power response.

The reactor trip signal is generated when the third highest excore detector reaches either 37% for the HZP cases or 118% for the HFP cases. This modeling is based on a single failure of the highest detector and a two-out-of-the-remaining-three trip coincidence logic. The excore signals are synthesized from the power densities of several assemblies that are near the excore locations. The remaining control rods fall into the reactor starting at 0.5 seconds after the trip signal is generated.

During the reactor trip, the ejected rod and the remaining rod with the highest worth are assumed not to fall into the reactor. To conservatively model the reactor trip, not all of the control rod banks are allowed to drop, and some of the banks that are dropped have their worth reduced by cross section adjustments. The net shutdown margin in all cases is less than 250 pcm. Also, the negative reactivity inserted due to the reactor trip is not allowed to exceed the conservative trip reactivity curve that is shown on Figure 4-7. The integral worth of the falling control rods is computed for several different axial positions of the rods at the initial conditions. [

]

Core power versus time, as calculated by ARROTTA, is shown in Figures 4-8, 4-11, 4-15, and 4-18 for the four cases. Table 4-3 summarizes the results of the four cases. The ARROTTA analysis used time steps of 0.001 seconds through the time of peak power. After the peak power occurred, the time step size was relaxed to no greater than 0.01 seconds. Sensitivity studies showed that for the initial power excursion the peak core power level is reduced for time steps shorter than 0.001 seconds. Thus, the time step selection of 0.001 seconds through the time of the peak power level is conservative. After the peak, sensitivity studies showed very little change in the results for time steps up to 0.01 seconds.

For the HFP statepoints, the core power increases rapidly as the control rod is ejected (Figures 4-8 and 4-15). The power continues to increase until the Doppler feedback, caused by the increasing fuel temperature, becomes large enough to turn the excursion around. The power level then continues to decrease as the fuel temperature approaches an equilibrium value. Due to the rapid initial power increase, the reactor trip on high flux occurs very early. Rod insertion completes shutdown of the reactor. Insertion begins after the peak power due to the trip delay. Since the trip reactivity for each transient is normalized to the conservative trip reactivity curve of Figure 4-7, rod motion has a minimal effect until the rods approach the bottom of the core.

The HZP statepoints differ from the HFP statepoints in that there is no initial thermal-hydraulic feedback and the reactor becomes prompt critical. The initial power increase continues long after the control rod is ejected (Figures 4-11 and 4-18). Since the reactor is prompt critical, it quickly reaches a high power level before the fuel heats up enough for the Doppler feedback to turn the power excursion around. The power level then decreases almost as fast as it increased, until near-equilibrium is reached. The reactor is then shut down by control rod insertion resulting from the high flux trip.

The ARROTTA initial radial power distribution for the BOC HFP case is shown on Figure 4-9. The power distribution at the time of the peak power, which is concurrent with the highest radial and nodal peaks, is shown in Figure 4-10. For the EOC HFP statepoint, these power distributions are shown in Figures 4-16 and 4-17. The initial power distribution for BOC HZP statepoint is shown in Figure 4-12. The power distribution at the time of the highest radial and nodal peaks is

shown on Figure 4-13 and the power distribution at the time of the highest power is shown on Figure 4-14. For the EOC HZP statepoint, these power distributions are shown on Figures 4-19, 4-20, and 4-21.

The core power level versus time is a key input from the neutronics calculation to the thermal-hydraulic evaluation discussed in the next section. In addition to total core power versus time,

[ ] as discussed in Section 4.2.2.4.  
The [ ]  
[ ] to evaluate the number of pin  
failures due to DNB as described in Section 4.4.4.

#### 4.4 VIPRE Analysis

##### 4.4.1 Initial Conditions

During the rod ejection transient, the reactor core coolant pressure increases due to the coolant expansion as a result of the reactor power excursion. [ ]

[ ] The core inlet flowrate for the HFP case is derived by reducing the technical specification minimum measured flow by 9% for assumed bypass flow and by 2.2% for measurement uncertainty. The three-pump core inlet flowrate for HZP is 75% of the 4 pump HFP flow based on the technical specification flow required in this mode. Note that the two-pump flowrate of 46% was used in the analysis results presented due to only two pumps being required by technical specifications at the time that this report was originally submitted. The initial core inlet flowrates for the analysis results presented are 339,972 gpm and 156,387 gpm for HFP and HZP respectively, based on a technical specification flow of 382,000 gpm. [ ]

]

The initial core coolant inlet temperatures include an allowance of +4°F for control deadband and measurement error. Core inlet temperatures of 561.4°F and 561.0°F are used throughout the transient analyses for HFP and HZP, respectively.



The initial core power for the HZP and HFP cases are 0.0% and 102.0% of 3411 MWt. However, for the HZP case an assumed 2% of 3411 MWt of decay heat is added into the average power generated by ARROTTA. The transient core average power for the four operating conditions are shown in Figures 4-8, 11, 15, and 18.

#### 4.4.2 Fuel Temperature and Enthalpy

The fuel temperatures and enthalpies are calculated for the four transient cases. The maximum fuel temperature and enthalpy during the transient are shown below.

| Case     | Maximum<br>Centerline Fuel<br>Temp. (°F) | Maximum<br>Fuel Average<br>Temp.<br>(°F) | Maximum<br>Clad Surface<br>Temp.<br>(°F) | Maximum<br>Fuel Average<br>Enthalpy<br>(cal/gm) |
|----------|--|--|--|---|
| HZP, BOL | 4090                                     | 3220                                     | 1410                                     | 133   |
| HFP, BOL | 3890                                     | 2812                                     | 1101                                     | 113   |
| HZP, EOL | 3190                                     | 2872                                     | 1172                                     | 116   |
| HFP, EOL | 3066                                     | 1956                                     | 940                                      | 75  |

The above results show that during the transient the maximum centerline fuel temperature is well below the fuel melting temperature of 4700°F (Reference 4-1), and that the maximum fuel average enthalpy is well below the acceptance criterion radially averaged fuel enthalpy of 280 cal/gm. Since the fuel pellet does not melt during the accident, the activity due to the fuel pellet will not contribute to the dose calculation results.

#### 4.4.3 Coolant Expansion Rate

The BOC HFP rod ejection transient results in the highest coolant expansion rate. Figure 4-31 shows the instantaneous core coolant expansion rate (ft<sup>3</sup>/sec) as a function of transient time. The initial expansion rate corresponds to the full power initial condition and the resulting decrease in coolant density due to sensible heating in the core. The result shows that a peak expansion rate

of [ ]

#### 4.4.4 DNBR and Fuel Pin Census

The DNBR calculations are performed for the four operating conditions. The DNBR results are expressed as a family of curves of maximum allowed radial power (MARF) versus assembly axial peak and location (Figures 4-22 through 4-25). When the radial power peak of the fuel pin exceeds the MARF during the transient, DNBR is assumed to occur and the cladding fails. The fuel pin census is performed to determine the number of failed fuel pins during the accident. Results are shown in Figures 4-26 through 4-29 and are summarized below.

| Operating Conditions | % of Fuel Pins Experiencing<br>DNB |
|----------------------|------------------------------------|
| HZP, BOL             | 10.7                               |
| HFP, BOL             | 36.9                               |
| HZP, EOL             | 19.6                               |
| HFP, EOL             | 14.4                               |

The above results show that the HFP, BOC case has the largest number of pins experiencing DNBR. The offsite dose consequences are analyzed based on 50% of the fuel pins experiencing DNBR to conservatively bound the above results.

#### 4.5 RETRAN Analysis

##### 4.5.1 Initial Conditions

The RETRAN model pressure response to the rod ejection transient is primarily a function of the coolant expansion rate and the pressurizer code safety valve relief capacity, which are input as boundary conditions as discussed in the following section. Most parameters such as initial primary temperature have little impact on the pressure response due to the very short duration of the simulation (3.5 seconds) which results in minimizing temperature transport effects.

Sensitivity studies were performed which demonstrated that thermal effects were not significant.

Therefore, the transient was evaluated with nominal hot full power initial conditions with the exception of pressurizer pressure and level. These two parameters clearly impact the system pressure response to the coolant expansion.

#### Pressurizer Pressure

The peak pressure response is conservatively bounded by using a maximum error-adjusted value of 2295 psig. This is the nominal hot full power pressure of 2235 psig with a 60 psi uncertainty allowance for elevated pressurizer pressure.

#### Pressurizer Level

A high initial pressurizer level decreases the volume of the steam bubble thereby increasing the compressibility effect. The limiting hot full power programmed pressurizer level is 61.5%. The initial condition uncertainty allowance for reduced level is 9%. The initial level is therefore 70.5%.

#### 4.5.2 Boundary Conditions

Primary system boundary conditions which significantly effect the pressure response include the coolant volume expansion rate, reactor power, and pressurizer safety valve modeling. These boundary conditions are discussed separately below. In order to conservatively bound the pressure response, the pressurizer PORVs and spray are defeated. Full primary system flow is maintained to maximize the reactor vessel pressure drop and hence maximize the lower plenum pressure. The maximum system pressure occurs at the bottom of the lower plenum.

Secondary side boundary conditions were determined to have minimal impact on the transient due to the short duration of the simulation. Nevertheless, conservative assumptions were made to conservatively bound the pressure response. The turbine is assumed to trip immediately on reactor trip. Main feedwater isolation is assumed to be initiated at time 0.0, and the isolation valves are ramped closed over a bounding 2.5 second interval. The condenser is assumed not to be available, and the steam generator PORVs are assumed to be inoperable. The steam generator

safety valves are available for secondary steam relief, however, the simulation is terminated before these valves are challenged.

#### Reactor Coolant Volume Expansion Rate



#### Reactor Power



#### Pressurizer Safety Valve Modeling

The pressurizer code safety valves function as overpressure mitigation equipment. The nominal lift setpoint is increased by 3% to account for calibration allowance. The valves are assumed to open linearly until they are fully open at a pressure 3% above the adjusted lift setpoint. The valve modeling then includes a hysteresis effect that keeps the valves fully open until the pressure decreases to 5% below the adjusted lift setpoint.

#### 4.5.3 Results

The Reactor Coolant System pressure response to the rod ejection is shown in Figure 4-31. The pressure plotted represents the pressure at the bottom of the reactor vessel lower plenum where

the highest system pressure occurs. Figure 4-31 shows that a peak system pressure of 2728 psig is reached in 1.9 seconds. The peak pressure is within the acceptance criterion of 3000 psia discussed in Section 4.1.2.

#### 4.6 Dose Consequences

A conservative evaluation of the rod ejection accident is performed to determine the resulting radiological consequences. Methods used to perform this evaluation are identical to those used in the present licensing evaluation for Catawba Nuclear Station. No fuel melting occurs for either Catawba or McGuire Nuclear Stations. The value for the number of pins assumed to enter DNB is conservatively selected to be 50% to bound the results given in Section 4.4.4. Dose results for McGuire and Catawba Nuclear Stations are as follows:

##### Exclusion Area Boundary

|            | McGuire | Catawba | Acceptance<br>Criterion |
|------------|---------|---------|-------------------------|
| Whole Body | 0.598   | 0.480   | 6.25                    |
| Thyroid    | 50.29   | 30.55   | 75                      |

##### Low Population Zone

|            | McGuire | Catawba | Acceptance<br>Criterion |
|------------|---------|---------|-------------------------|
| Whole Body | 0.080   | 0.057   | 6.25                    |
| Thyroid    | 9.283   | 3.165   | 75                      |

These results show that the offsite dose consequences from a conservative rod ejection analysis are well within the dose limits stated in 10CFR100.

#### 4.7 Cycle Specific Evaluation

Due to the conservative assumptions and modeling used in the ARROTTA model, it is anticipated that for reload cores, no new ARROTTA cases will be necessary. The determination as to whether the existing ARROTTA cases remain bounding will be made by performing a cycle-specific reload check of the key physics input parameters listed in Table 4-4. These parameters will be calculated using standard steady-state neutronics codes approved by the NRC for reload design. If the key parameters remain bounded then no new ARROTTA analyses are necessary; otherwise, an evaluation, reanalysis, or redesign of the reload core will be performed.

A DNB pin census will be performed for the reload cycle, as described in Section 4.4.4, with the radial pin information being calculated with SIMULATE-3P. The ejected rod worth shall be calculated with the fuel and moderator temperatures frozen in the pre-ejected condition or uniform throughout the core (either method will generate conservative results). Also, the xenon distribution will be skewed to force a top peaked power distribution to make the ejected rod worth higher (for the HFP cases) and to make the DNB pin census more conservative. The power distribution with the ejected rod out will be used for the DNB pin census. The calculated percent fuel failure due to DNB will be compared for each cycle to the fuel failure limit assumed in the dose calculation. If the cycle specific value is less than the limit, then the existing safety analysis is still valid. Otherwise, an evaluation, a new dose calculation, reanalysis, or new reload design will be performed as appropriate.

## References

- 4-1     McGuire Nuclear Station, Final Safety Analysis Report, 1988 Update.
  
- 4-2     USNRC Standard Review Plan, Section 15.4.8, NUREG-0800, Rev. 2, July 1981.
  
- 4-3     ASME Boiler and Pressure Vessel Code, Section III, "Nuclear Power Plant Components," ASME.
  
- 4-4     ARROTTA: Advanced Rapid Reactor Operational Transient Analysis Computer Code, Computer Code Documentation Package, EPRI.
  
- 4-5     VIPRE-01: A Thermal-Hydraulic Code for Reactor Cores; EPRI NP-2511-CCMA Revision 3, EPRI, August 1989
  
- 4-6     RETRAN-02: A Program for Transient Thermal-Hydraulic Analysis of Complex Fluid Flow Systems, EPRI NP-1850-CCMA Revision 4, EPRI, November 1988.
  
- 4-7     K. S. Smith, An Analytic Nodal Method for Solving the 2-Group, Multidimensional, Static and Transient Neutron Diffusion Equations, Nuc. Eng. Thesis, Dept. of Nuc. Eng., MIT, Cambridge, MA., (February, 1979).
  
- 4-8     Nuclear Design Methodology Using CASMO-3/SIMULATE-3P, DPC-NE-1004-A, Revision 1, Duke Power Company, December 1997
  
- 4-9     "ARROTTA Validation and Verification - Standard Benchmarks Set," EPRI Research Project 1936-6, July 1989, Prepared by S. Levy, Inc.
  
- 4-10    ARROTTA-HERMITE Code Comparison, EPRI NP-6614, December 1989.

- 4-11 Letter from C. E. Rossi (NRC) to J. A. Blaisdell (UGRA), Acceptance for Referencing of Licensing Topical Report, VIPRE-01: A Thermal-Hydraulic Analysis Code for Reactor Cores, EPRI-NP-2511-CCM, Vol. 1-5, May 1986.
- 4-12 Y. H. Hsui, et al., TACO2: Fuel Pin Performance Analysis, Revision 1, BAW-10141PA, June 1983.
- 4-13 Donald L. Hagermann, et al., MATPRO-Version 11 (Revision 2): A Handbook of Materials Properties for Use in the Analysis of Light Water Reactor Fuel Rod Behavior, NUREG/CR-0479, August 1981.
- 4-14 D. A. Farnsworth and G. A. Meyer, BWCMV Correlation of Critical Heat Flux in Mixing Vane Grid Fuel Assemblies, BAW-10159P, Babcock and Wilcox, May 1986.
- 4-15 Thermal-Hydraulic Transient Analysis Methodology, DPC-NE-3000-PA, Revision 2, Duke Power Company, December 2000
- 4-16 Nuclear Physics Methodology for Reload Design, DPC-NF-2010-A, Duke Power Company, March 1990
- 4-17 D. A. Wesley and K. J. Firth, TACO3 - Fuel Pin Thermal Analysis Code, BAW-10162P-A, Babcock & Wilcox, November 1989
- 4-18 D. A. Farnsworth and G. A. Meyer, The BWU Critical Heat Flux Correlations, BAW-10199P, BWFC, November 1994
- 4-19 Letter , H. N. Berkow (NRC) to M. S. Tuckman (Duke), November 7, 1996
- 4-20 Letter, P. S. Tam (NRC) to M. S. Tuckman (Duke), February 20, 1997



Table 4-1

Rod Ejection Transient  
Kinetics Parameters

| Parameter                | BOC HZP | BOC HFP | EOC HZP | EOC HFP |
|--------------------------|---------|---------|---------|---------|
| Ejected rod worth (pcm)  | 763     | 201     | 907     | 200     |
| MTC (pcm/°F)             | 7.1     | 0.5     | -9.3    | -9.9    |
| DTC (pcm/°F)             | -0.9    | -0.9    | -1.2    | -1.2    |
| Delayed neutron fraction | 0.00551 | 0.0055  | 0.004   | 0.004   |

Table 4-2

Rod Ejection Transient  
Initial Conditions

| Parameter                         | BOC HZP  | BOC HFP  | EOC HZP  | EOC HFP  |
|-----------------------------------|----------|----------|----------|----------|
| Initial power (MWt)               | 3411E-9  | 3479.22  | 3411E-9  | 3479.22  |
| Initial power (%)                 | 1.00E-7  | 102.0    | 1.00E-7  | 102.0    |
| Core flow (gpm)                   | 156387.3 | 339972.4 | 156387.3 | 339972.4 |
| Inlet temperature (°F)            | 561.0    | 561.4    | 561.0    | 561.4    |
| Reactor pressure (psia)           | 2305.0   | 2305.0   | 2305.0   | 2305.0   |
| Fission power fraction in coolant | 0.026    | 0.026    | 0.026    | 0.026    |

Table 4-3  
Rod Ejection ARROTTA Results

| Parameter                                       | BOC HZP | BOC HFP | EOC HZP | EOC HFP |
|---|---------|---------|---------|---------|
| Time of peak power, sec.                        | 0.339   | 0.097   | 0.172   | 0.097   |
| Peak power level, % of full power               | 1476    | 142     | 5555    | 167     |
| Peak nodal power relative to core average       | 12.79   | 3.17    | 18.11   | 3.76    |
| Peak assembly power relative to core average    | 6.16    | 1.92    | 7.90    | 2.18    |
| Time that trip setpoint reached, sec.           | 0.296   | 0.064   | 0.156   | 0.061   |
| Time of the beginning of the tripped rod motion | 0.796   | 0.564   | 0.656   | 0.561   |

Table 4-4  
Rod Ejection Reload Checklist

| Parameter               |              | BOC HFP | BOC HZP | EOC HFP | EOC HZP |
|-------------------------|--------------|---------|---------|---------|---------|
| Ejected Rod Worth (pcm) | less than    | 200     | 720     | 200     | 900     |
| $\beta$                 | greater than | 0.0055  | .00551  | .004    | .004    |
| DTC (pcm/°F)            | less than    | -0.9    | -0.9    | -1.2    | -1.2    |
| MTC (pcm/°F)            | less than    | 0.0     | +7.0    | -10.0   | -10.0   |
| DNB Census              | less than    | 50%     | 50%     | 50%     | 50%     |
| $F_Q$                   | less than    | 4.12    | 16.62   | 4.88    | 23.55   |

Figure 4-1  
Catawba Unit 1, Cycle 2  
Assembly Enrichments and Fuel Exposures

|   | H                        | G                        | F                        | E                        | D                        | C                        | B                        | A  |    |
|---|--------------------------|--------------------------|--------------------------|--------------------------|--------------------------|--------------------------|--------------------------|--|----|
| 8 | 1.6*00<br>12.43<br>21.79 | 3.1*06<br>11.72<br>24.19 | 3.1*20<br>15.39<br>27.73 | 3.1*06<br>10.84<br>23.68 | 2.4*15<br>14.91<br>25.82 | 3.1*06<br>10.84<br>23.35 | 3.1*15<br>14.01<br>26.04 | 3.4/00<br>0.00<br>10.74  |    |
|   |                          | 3.1*20<br>15.39<br>27.65 | 3.1*00<br>11.98<br>24.67 | 2.4*16<br>14.50<br>25.88 | 3.1*00<br>8.86<br>21.99  | 2.4*16<br>15.26<br>26.23 | 3.1*00<br>13.08<br>25.04 | 3.2/00<br>0.00<br>10.27  | 9  |
|   |                          |                          | 2.4*16<br>14.59<br>26.26 | 3.2/08<br>0.00<br>14.31  | 2.4*12<br>15.53<br>27.12 | 3.2/08<br>0.00<br>14.17  | 3.1*16<br>14.10<br>26.18 | 3.4/00<br>0.00<br>9.53   | 10 |
|   |                          |                          |                          | 2.4*00<br>16.24<br>27.72 | 3.2/12<br>0.00<br>13.63  | 2.4*16<br>14.44<br>25.91 | 3.2/04<br>0.00<br>12.55  | 2.4*12<br>15.74<br>20.48                                       | 11 |
|   |                          |                          |                          |                          | 2.4*12<br>15.76<br>26.63 | 3.1*00<br>9.47<br>22.14  | 3.2/00<br>0.00<br>10.00  |  | 12 |
|   |                          |                          |                          |                          |                          | 3.1/00<br>0.00<br>12.18  | 2.4*12<br>15.76<br>20.29 |  | 13 |
|   |                          |                          |                          |                          |                          |                          |                          | Enrichment/ # of BPs<br>BOC Exposure (GWD/MTU)<br>EOC Exposure |    |

Note: 2.4\*12 means a 12 BP cluster was pulled from the 2.4% enriched assembly at the end of the last cycle.  
3.2/12 means the 3.2% enriched assembly currently has a 12 BP cluster.

Figure 4-2  
VIPRE 14 Channel Model

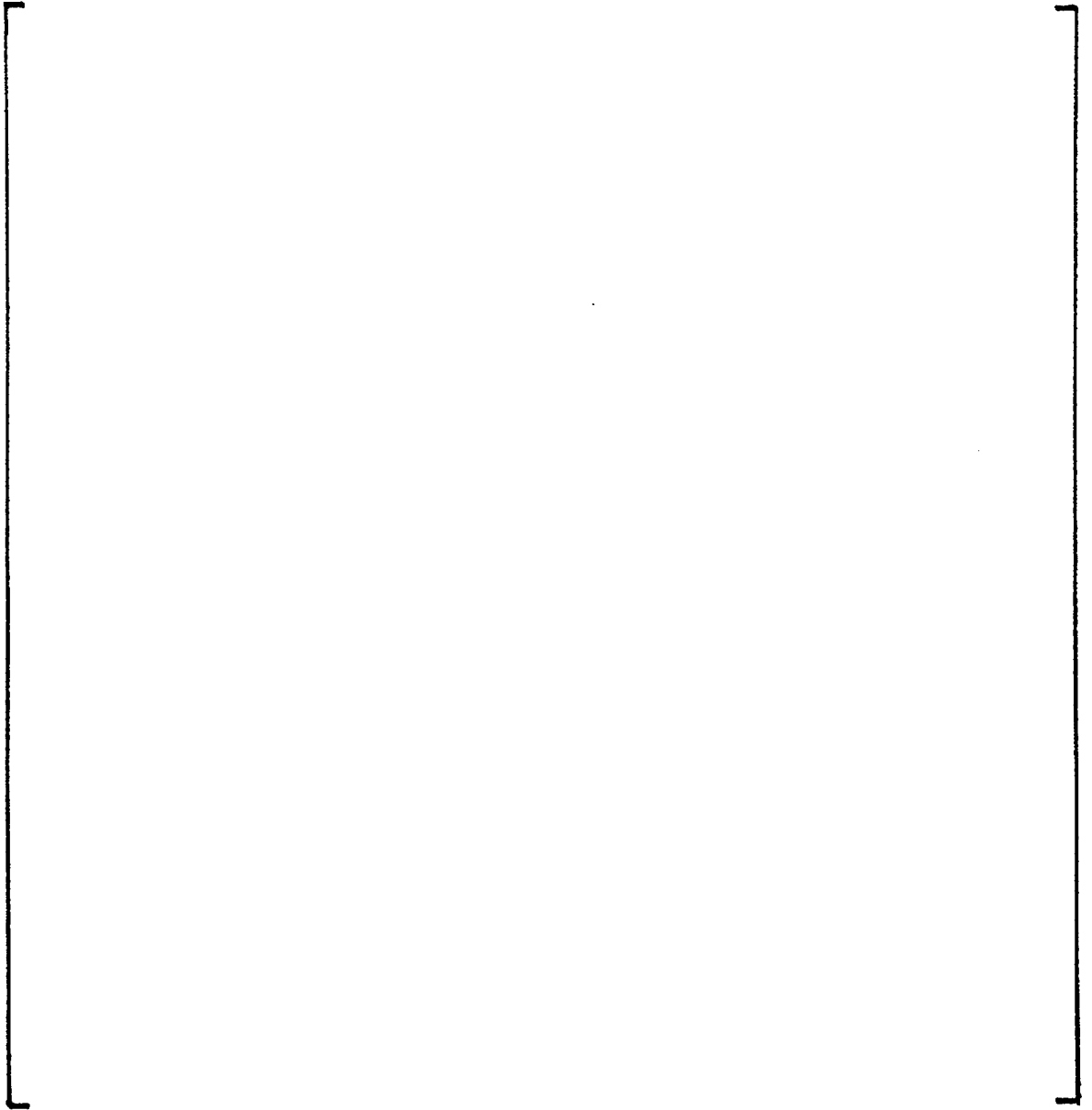


Figure 4-3

[ ] VIPRE Model for  
Reactor Coolant Expansion Rate  
Calculation

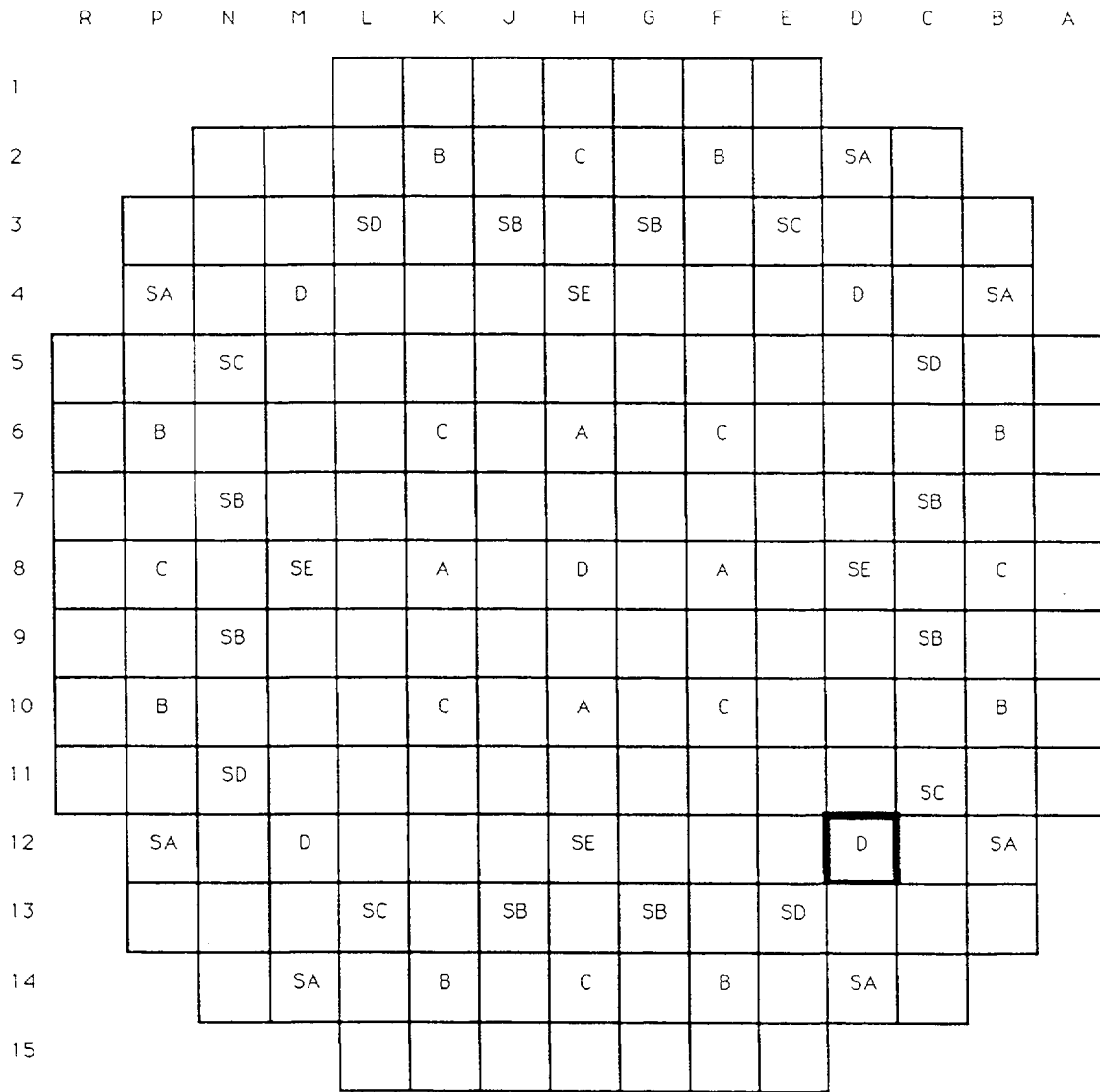


rod number



channel number

Figure 4-4  
FSAR Section 15.4.8 - Rod Ejection Accident  
Control Rod Locations



| Control Bank | Number Of Rods |
|--------------|----------------|
| A            | 4              |
| B            | 8              |
| C            | 8              |
| D            | 5              |
| Total        | 25             |

| Shutdown Bank | Number Of Rods |
|---------------|----------------|
| SA            | 8              |
| SB            | 8              |
| SC            | 4              |
| SD            | 4              |
| SE            | 4              |
| Total         | 28             |

Ejected Rod Location

Figure 4-5

FSAR Section 15.4.8 - Control Rod Ejection  
BOC, HFP, ARO Power Distributions  
Before and After

|    | H    | G    | F    | E    | D                             | C    | B    | A    |
|----|------|------|------|------|-------------------------------|------|------|------|
| 8  | 0.80 | 1.14 | 1.12 | 1.15 | 0.95                          | 1.13 | 1.12 | 1.04 |
|    | 0.65 | 0.95 | 0.96 | 1.01 | 0.84                          | 1.01 | 0.98 | 0.91 |
|    | 0.67 | 1.03 | 1.06 | 1.09 | 0.93                          | 1.07 | 1.04 | 1.19 |
| 9  | 1.14 | 1.11 | 1.15 | 0.98 | 1.17                          | 0.96 | 1.11 | 0.99 |
|    | 0.95 | 0.94 | 1.01 | 0.88 | 1.08                          | 0.88 | 1.00 | 0.88 |
|    | 1.03 | 1.03 | 1.09 | 0.97 | 1.18                          | 0.96 | 1.10 | 1.16 |
| 10 | 1.12 | 1.15 | 0.98 | 1.13 | 0.95                          | 1.23 | 1.07 | 0.88 |
|    | 0.96 | 1.01 | 0.93 | 1.26 | 0.97                          | 1.26 | 1.04 | 0.82 |
|    | 1.06 | 1.09 | 1.03 | 1.36 | 1.09                          | 1.34 | 1.17 | 1.16 |
| 11 | 1.14 | 0.98 | 1.23 | 0.94 | 1.13                          | 0.95 | 1.10 | 0.40 |
|    | 1.00 | 0.89 | 1.26 | 1.32 | 1.25                          | 1.25 | 1.18 | 0.40 |
|    | 1.08 | 0.97 | 1.36 | 1.39 | 1.40                          | 1.40 | 1.37 | 0.71 |
| 12 | 0.95 | 1.17 | 0.95 | 1.13 | 0.91                          | 1.10 | 0.90 |      |
|    | 0.84 | 1.08 | 0.97 | 1.25 | 1.35                          | 1.32 | 0.98 |      |
|    | 0.93 | 1.18 | 1.09 | 1.40 | 1.50                          | 1.40 | 1.35 |      |
| 13 | 1.14 | 0.96 | 1.23 | 0.95 | 1.10                          | 1.09 | 0.38 |      |
|    | 1.01 | 0.88 | 1.26 | 1.25 | 1.32                          | 1.13 | 1.40 |      |
|    | 1.07 | 0.96 | 1.34 | 1.40 | 1.40                          | 1.41 | 0.76 |      |
| 14 | 1.11 | 1.11 | 1.06 | 1.10 | 0.89                          | 0.38 |      |      |
|    | 0.98 | 1.01 | 1.04 | 1.18 | 0.98                          | 0.40 |      |      |
|    | 1.05 | 1.10 | 1.17 | 1.37 | 1.35                          | 0.76 |      |      |
| 15 | 1.05 | 0.99 | 0.88 | 0.40 | Assembly Power Before Changes |      |      |      |
|    | 0.91 | 0.88 | 0.82 | 0.40 | Assembly Power After Changes  |      |      |      |
|    | 1.19 | 1.16 | 1.15 | 0.71 | Peak Pin After Changes        |      |      |      |

Figure 4-6

FSAR Section 15.4.8 - Control Rod Ejection  
EOC, HFP, ARO Power Distributions  
Before and After [ ]

|    | H    | G    | F    | E    | D   | C    | B    | A    |
|----|------|------|------|------|---|------|------|------|
| 8  | 0.76 | 1.00 | 0.98 | 1.03 | 0.90  | 1.05 | 1.04 | 1.01 |
|    | 0.62 | 0.83 | 0.84 | 0.90 | 0.79  | 0.93 | 0.91 | 0.87 |
|    | 0.63 | 0.88 | 0.88 | 0.93 | 0.84  | 0.97 | 0.95 | 1.09 |
| 9  | 1.00 | 0.97 | 1.03 | 0.92 | 1.10  | 0.94 | 1.06 | 0.98 |
|    | 0.83 | 0.82 | 0.90 | 0.84 | 1.01  | 0.86 | 0.95 | 0.86 |
|    | 0.87 | 0.87 | 0.99 | 0.90 | 1.07  | 0.92 | 1.06 | 1.08 |
| 10 | 0.98 | 1.03 | 0.95 | 1.27 | 0.99  | 1.28 | 1.05 | 0.93 |
|    | 0.84 | 0.91 | 0.90 | 1.29 | 1.00  | 1.29 | 1.02 | 0.86 |
|    | 0.88 | 0.99 | 0.98 | 1.33 | 1.08  | 1.33 | 1.12 | 1.13 |
| 11 | 1.03 | 0.92 | 1.27 | 1.01 | 1.30  | 1.00 | 1.14 | 0.50 |
|    | 0.90 | 0.84 | 1.29 | 1.38 | 1.36  | 1.30 | 1.22 | 0.50 |
|    | 0.93 | 0.91 | 1.33 | 1.40 | 1.40  | 1.40 | 1.37 | 0.82 |
| 12 | 0.90 | 1.10 | 0.99 | 1.30 | 0.99  | 1.12 | 0.96 |      |
|    | 0.79 | 1.01 | 1.00 | 1.36 | 1.38  | 1.36 | 1.06 |      |
|    | 0.84 | 1.07 | 1.08 | 1.40 | 1.50  | 1.40 | 1.37 |      |
| 13 | 1.05 | 0.94 | 1.28 | 1.00 | 1.12  | 1.10 | 0.47 |      |
|    | 0.93 | 0.86 | 1.28 | 1.30 | 1.36  | 1.19 | 0.52 |      |
|    | 0.97 | 0.92 | 1.33 | 1.40 | 1.40  | 1.40 | 0.89 |      |
| 14 | 1.04 | 1.06 | 1.05 | 1.14 | 0.96  | 0.47 |      |      |
|    | 0.91 | 0.95 | 1.02 | 1.21 | 1.06  | 0.52 |      |      |
|    | 0.95 | 1.06 | 1.12 | 1.37 | 1.37  | 0.89 |      |      |
| 15 | 1.01 | 0.98 | 0.92 | 0.49 | Assembly Power Before Changes<br>Assembly Power After Changes<br>Peak Pin After Changes |      |      |      |
|    | 0.88 | 0.86 | 0.85 | 0.50 |   |      |      |      |
|    | 1.09 | 1.08 | 1.13 | 0.82 |   |      |      |      |



Figure 4-7  
FSAR Section 15.4.8 - Control Rod Ejection  
Trip Reactivity Curve

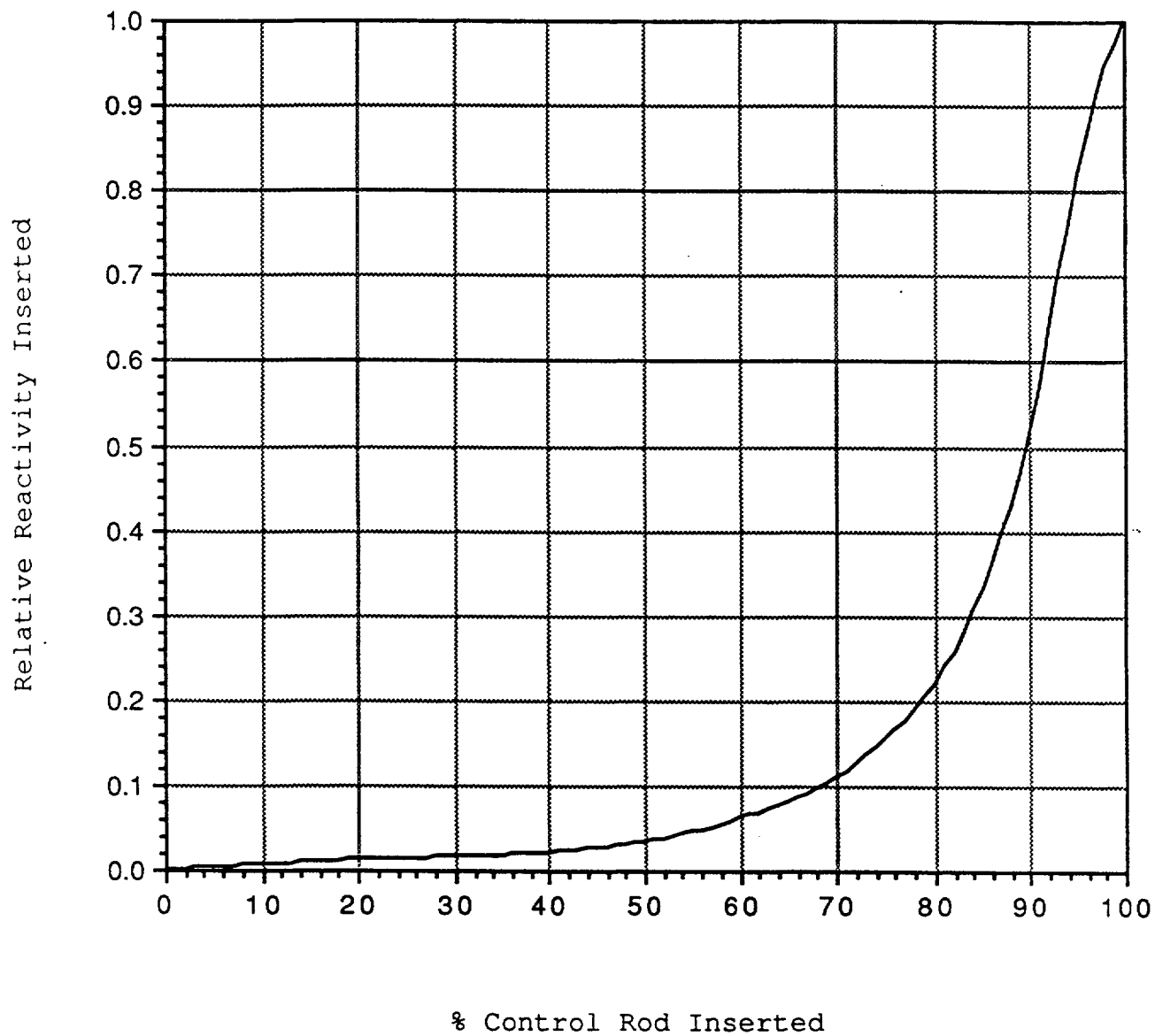


Figure 4-8  
FSAR Section 15.4.8 - Control Rod Ejection  
BOC HFP Core Power vs. Time

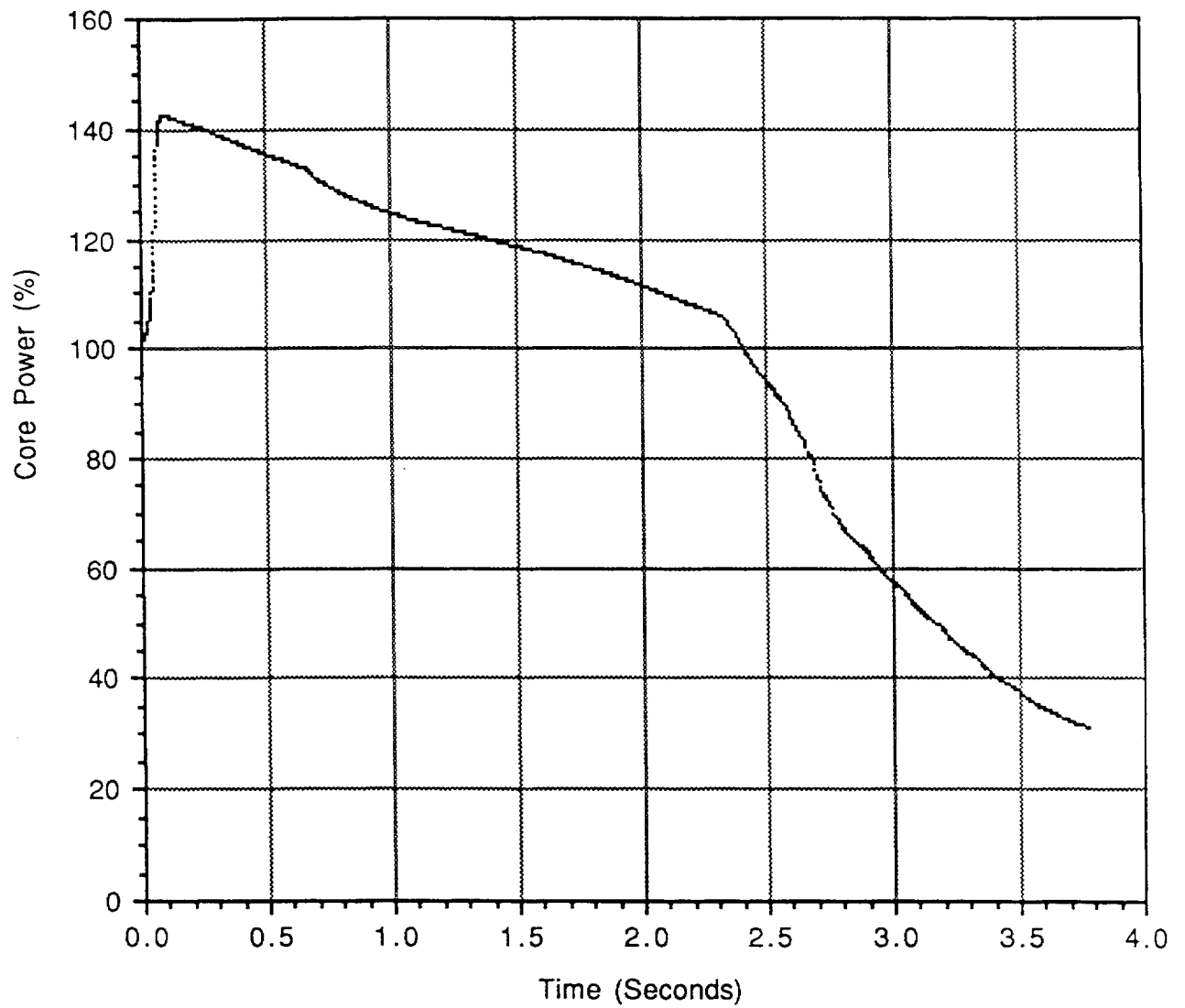


Figure 4-9  
FSAR Section 15.4.8 – Control Rod Ejection  
BOC HFP Assembly Power Distribution at 0.0 Seconds

|    | R    | P    | N    | M    | L    | K    | J    | H    | G    | F    | E    | D    | C    | B    | A    |
|----|------|------|------|------|------|------|------|------|------|------|------|------|------|------|------|
| 1  |      |      |      |      | 0.40 | 0.85 | 0.92 | 0.96 | 0.92 | 0.85 | 0.40 |      |      |      |      |
| 2  |      |      | 0.38 | 0.95 | 1.18 | 1.07 | 1.05 | 1.03 | 1.05 | 1.07 | 1.18 | 0.95 | 0.38 |      |      |
| 3  |      | 0.38 | 1.05 | 1.22 | 1.22 | 1.28 | 0.91 | 1.05 | 0.91 | 1.28 | 1.22 | 1.22 | 1.05 | 0.38 |      |
| 4  |      | 0.95 | 1.22 | 1.08 | 1.19 | 0.99 | 1.12 | 0.88 | 1.12 | 0.99 | 1.19 | 1.19 | 1.22 | 0.95 |      |
| 5  | 0.40 | 1.18 | 1.22 | 1.19 | 1.30 | 1.29 | 0.92 | 1.04 | 0.92 | 1.29 | 1.30 | 1.19 | 1.22 | 1.19 | 0.40 |
| 6  | 0.85 | 1.07 | 1.28 | 0.99 | 1.29 | 0.96 | 1.04 | 0.97 | 1.03 | 0.96 | 1.29 | 0.99 | 1.28 | 1.07 | 0.85 |
| 7  | 0.92 | 1.05 | 0.92 | 1.12 | 0.92 | 1.03 | 0.93 | 0.91 | 0.93 | 1.04 | 0.92 | 1.12 | 0.91 | 1.05 | 0.92 |
| 8  | 0.96 | 1.03 | 1.06 | 0.88 | 1.04 | 0.97 | 0.92 | 0.51 | 0.92 | 0.97 | 1.04 | 0.88 | 1.06 | 1.03 | 0.96 |
| 9  | 0.92 | 1.05 | 0.91 | 1.12 | 0.92 | 1.04 | 0.93 | 0.92 | 0.93 | 1.03 | 0.92 | 1.12 | 0.92 | 1.05 | 0.92 |
| 10 | 0.85 | 1.07 | 1.28 | 0.99 | 1.29 | 0.96 | 1.03 | 0.97 | 1.04 | 0.96 | 1.29 | 0.99 | 1.28 | 1.07 | 0.85 |
| 11 | 0.40 | 1.19 | 1.22 | 1.19 | 1.30 | 1.29 | 0.92 | 1.04 | 0.92 | 1.29 | 1.30 | 1.19 | 1.22 | 1.18 | 0.40 |
| 12 |      | 0.95 | 1.22 | 1.08 | 1.19 | 0.99 | 1.12 | 0.88 | 1.12 | 0.99 | 1.19 | 1.08 | 1.22 | 0.95 |      |
| 13 |      | 0.38 | 1.05 | 1.22 | 1.22 | 1.28 | 0.91 | 1.06 | 0.91 | 1.28 | 1.22 | 1.22 | 1.05 | 0.38 |      |
| 14 |      |      | 0.38 | 0.95 | 1.18 | 1.07 | 1.05 | 1.03 | 1.05 | 1.07 | 1.18 | 0.95 | 0.38 |      |      |
| 15 |      |      |      |      | 0.40 | 0.85 | 0.92 | 0.96 | 0.92 | 0.85 | 0.40 |      |      |      |      |



- Peak Assembly Power

Figure 4-10  
FSAR Section 15.4.8 - Control Rod Ejection  
BOC HFP Assembly Power Distribution at 0.09 Seconds

|    | R    | P    | N    | M    | L    | K    | J    | H    | G    | F    | E    | D    | C    | B    | A    |
|----|------|------|------|------|------|------|------|------|------|------|------|------|------|------|------|
| 1  |      |      |      |      | 0.33 | 0.70 | 0.76 | 0.80 | 0.77 | 0.72 | 0.34 |      |      |      |      |
| 2  |      |      | 0.31 | 0.77 | 0.97 | 0.88 | 0.87 | 0.86 | 0.89 | 0.91 | 1.02 | 0.82 | 0.33 |      |      |
| 3  |      | 0.31 | 0.85 | 0.99 | 1.00 | 1.06 | 0.76 | 0.90 | 0.79 | 1.11 | 1.06 | 1.07 | 0.93 | 0.34 |      |
| 4  |      | 0.77 | 0.99 | 0.87 | 0.97 | 0.82 | 0.94 | 0.75 | 0.97 | 0.87 | 1.05 | 0.94 | 1.10 | 0.87 |      |
| 5  | 0.33 | 0.97 | 1.00 | 0.97 | 1.08 | 1.08 | 0.79 | 0.92 | 0.82 | 1.16 | 1.19 | 1.09 | 1.14 | 1.12 | 0.39 |
| 6  | 0.70 | 0.88 | 1.06 | 0.82 | 1.08 | 0.82 | 0.91 | 0.88 | 0.95 | 0.90 | 1.22 | 0.96 | 1.25 | 1.06 | 0.85 |
| 7  | 0.76 | 0.87 | 0.77 | 0.94 | 0.79 | 0.91 | 0.83 | 0.85 | 0.90 | 1.03 | 0.93 | 1.15 | 0.95 | 1.11 | 0.97 |
| 8  | 0.80 | 0.87 | 0.90 | 0.75 | 0.92 | 0.88 | 0.85 | 0.48 | 0.94 | 1.04 | 1.14 | 0.98 | 1.19 | 1.16 | 1.07 |
| 9  | 0.78 | 0.89 | 0.78 | 0.98 | 0.82 | 0.96 | 0.90 | 0.94 | 1.01 | 1.18 | 1.09 | 1.36 | 1.12 | 1.27 | 1.09 |
| 10 | 0.72 | 0.91 | 1.11 | 0.87 | 1.16 | 0.90 | 1.03 | 1.04 | 1.18 | 1.17 | 1.65 | 1.31 | 1.69 | 1.39 | 1.07 |
| 11 | 0.35 | 1.02 | 1.06 | 1.05 | 1.19 | 1.22 | 0.93 | 1.14 | 1.09 | 1.65 | 1.82 | 1.76 | 1.78 | 1.64 | 0.55 |
| 12 |      | 0.83 | 1.07 | 0.94 | 1.09 | 0.95 | 1.15 | 0.98 | 1.36 | 1.31 | 1.76 | 1.88 | 1.92 | 1.40 |      |
| 13 |      | 0.33 | 0.93 | 1.10 | 1.14 | 1.25 | 0.95 | 1.19 | 1.12 | 1.69 | 1.77 | 1.92 | 1.64 | 0.59 |      |
| 14 |      |      | 0.34 | 0.87 | 1.12 | 1.06 | 1.10 | 1.16 | 1.27 | 1.39 | 1.64 | 1.40 | 0.59 |      |      |
| 15 |      |      |      |      | 0.39 | 0.85 | 0.96 | 1.07 | 1.09 | 1.07 | 0.55 |      |      |      |      |



- Peak Assembly Power

Figure 4-11  
FSAR Section 15.4.8 - Control Rod Ejection  
BOC HZP Core Power vs. Time

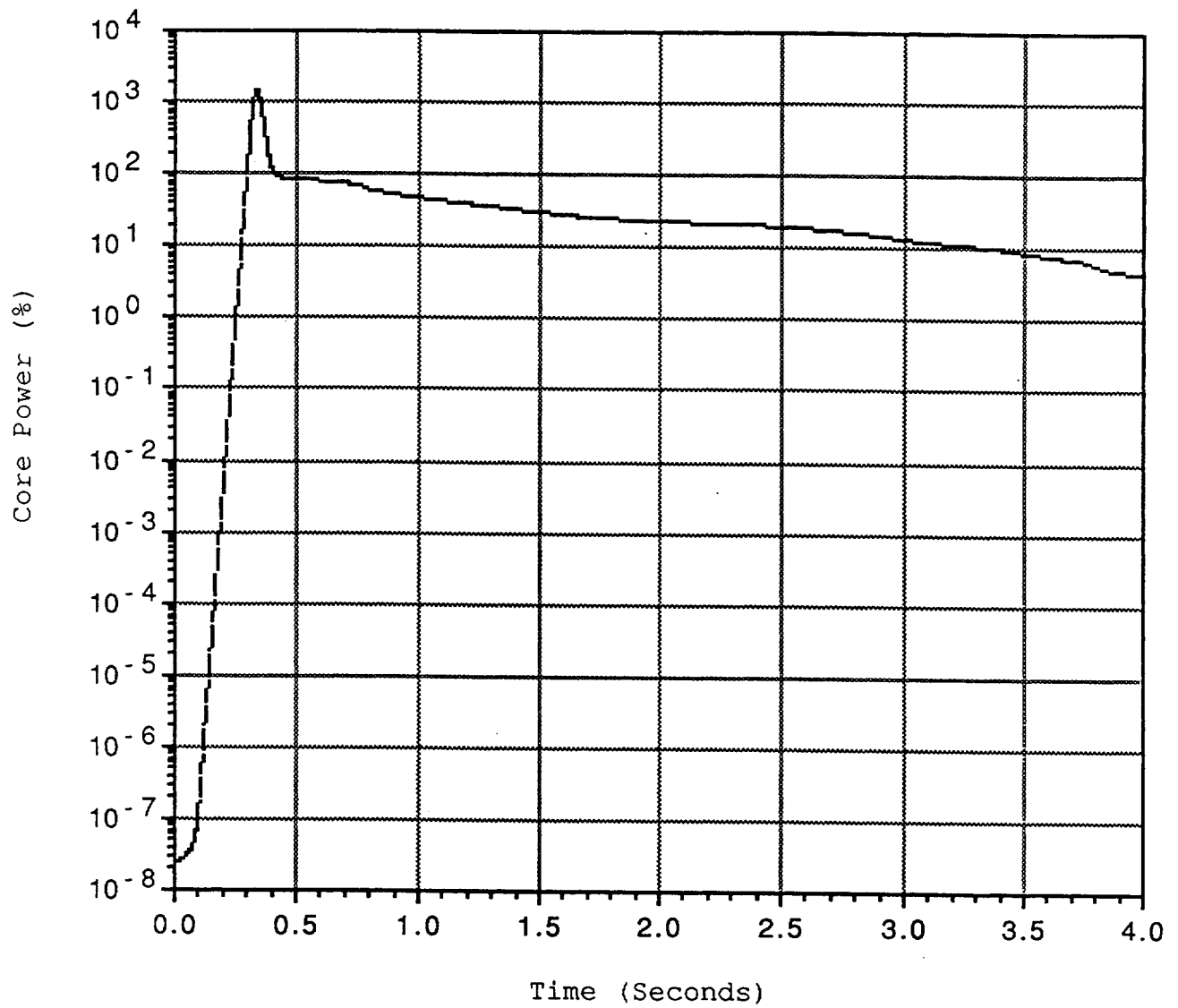


Figure 4-12  
FSAR Section 15.4.8 - Control Rod Ejection  
BOC HZP Assembly Power Distribution at 0.0 Seconds

|    | R    | P    | N    | M    | L    | K    | J    | H    | G    | F    | E    | D    | C    | B    | A    |
|----|------|------|------|------|------|------|------|------|------|------|------|------|------|------|------|
| 1  |      |      |      |      | 0.38 | 0.68 | 0.63 | 0.58 | 0.63 | 0.68 | 0.38 |      |      |      |      |
| 2  |      |      | 0.50 | 1.19 | 1.33 | 0.84 | 0.76 | 0.45 | 0.76 | 0.84 | 1.33 | 1.19 | 0.50 |      |      |
| 3  |      | 0.50 | 1.41 | 1.59 | 1.57 | 1.39 | 0.82 | 0.86 | 0.82 | 1.39 | 1.57 | 1.59 | 1.41 | 0.50 |      |
| 4  |      | 1.20 | 1.59 | 0.89 | 1.51 | 1.19 | 1.16 | 0.84 | 1.16 | 1.19 | 1.51 | 0.89 | 1.59 | 1.20 |      |
| 5  | 0.40 | 1.35 | 1.58 | 1.51 | 1.67 | 1.35 | 0.89 | 1.02 | 0.89 | 1.35 | 1.67 | 1.51 | 1.58 | 1.35 | 0.40 |
| 6  | 0.70 | 0.85 | 1.40 | 1.20 | 1.35 | 0.54 | 0.88 | 0.89 | 0.88 | 0.54 | 1.35 | 1.20 | 1.40 | 0.85 | 0.70 |
| 7  | 0.64 | 0.77 | 0.83 | 1.16 | 0.89 | 0.88 | 0.78 | 0.76 | 0.78 | 0.88 | 0.89 | 1.16 | 0.82 | 0.77 | 0.64 |
| 8  | 0.58 | 0.45 | 0.87 | 0.85 | 1.03 | 0.89 | 0.76 | 0.27 | 0.76 | 0.89 | 1.03 | 0.85 | 0.87 | 0.45 | 0.58 |
| 9  | 0.64 | 0.77 | 0.82 | 1.16 | 0.89 | 0.88 | 0.78 | 0.76 | 0.78 | 0.88 | 0.89 | 1.16 | 0.83 | 0.77 | 0.64 |
| 10 | 0.70 | 0.85 | 1.40 | 1.20 | 1.35 | 0.54 | 0.88 | 0.89 | 0.88 | 0.54 | 1.35 | 1.20 | 1.40 | 0.85 | 0.70 |
| 11 | 0.40 | 1.35 | 1.58 | 1.51 | 1.67 | 1.35 | 0.89 | 1.02 | 0.89 | 1.35 | 1.67 | 1.51 | 1.58 | 1.35 | 0.40 |
| 12 |      | 1.20 | 1.59 | 0.89 | 1.51 | 1.19 | 1.16 | 0.84 | 1.16 | 1.20 | 1.51 | 0.89 | 1.59 | 1.20 |      |
| 13 |      | 0.50 | 1.41 | 1.59 | 1.57 | 1.39 | 0.82 | 0.86 | 0.82 | 1.39 | 1.57 | 1.59 | 1.41 | 0.50 |      |
| 14 |      |      | 0.50 | 1.19 | 1.33 | 0.84 | 0.76 | 0.45 | 0.76 | 0.84 | 1.33 | 1.19 | 0.50 |      |      |
| 15 |      |      |      |      | 0.38 | 0.68 | 0.63 | 0.58 | 0.63 | 0.68 | 0.38 |      |      |      |      |



- Peak Assembly Power

Figure 4-13  
FSAR Section 15.4.8 - Control Rod Ejection  
BOC HZP Assembly Power Distribution at 0.2 Seconds

|    | R    | P    | N    | M    | L    | K    | J    | H    | G    | F    | E    | D    | C    | B    | A    |
|----|------|------|------|------|------|------|------|------|------|------|------|------|------|------|------|
| 1  |      |      |      |      | 0.06 | 0.12 | 0.12 | 0.13 | 0.17 | 0.21 | 0.12 |      |      |      |      |
| 2  |      |      | 0.08 | 0.19 | 0.21 | 0.14 | 0.15 | 0.11 | 0.22 | 0.27 | 0.46 | 0.43 | 0.19 |      |      |
| 3  |      | 0.08 | 0.22 | 0.25 | 0.27 | 0.26 | 0.18 | 0.23 | 0.26 | 0.49 | 0.58 | 0.62 | 0.58 | 0.22 |      |
| 4  |      | 0.19 | 0.25 | 0.15 | 0.27 | 0.25 | 0.28 | 0.25 | 0.41 | 0.47 | 0.63 | 0.39 | 0.73 | 0.57 |      |
| 5  | 0.06 | 0.22 | 0.27 | 0.27 | 0.33 | 0.30 | 0.25 | 0.36 | 0.36 | 0.62 | 0.83 | 0.79 | 0.84 | 0.73 | 0.23 |
| 6  | 0.12 | 0.14 | 0.26 | 0.25 | 0.30 | 0.14 | 0.31 | 0.39 | 0.46 | 0.32 | 0.86 | 0.79 | 0.92 | 0.57 | 0.49 |
| 7  | 0.12 | 0.15 | 0.18 | 0.28 | 0.25 | 0.31 | 0.34 | 0.43 | 0.57 | 0.77 | 0.82 | 1.09 | 0.77 | 0.72 | 0.61 |
| 8  | 0.13 | 0.11 | 0.23 | 0.25 | 0.36 | 0.39 | 0.42 | 0.21 | 0.78 | 1.07 | 1.38 | 1.21 | 1.27 | 0.65 | 0.83 |
| 9  | 0.17 | 0.22 | 0.26 | 0.41 | 0.36 | 0.46 | 0.57 | 0.78 | 1.02 | 1.40 | 1.68 | 2.40 | 1.75 | 1.60 | 1.27 |
| 10 | 0.21 | 0.27 | 0.48 | 0.47 | 0.61 | 0.31 | 0.77 | 1.07 | 1.40 | 1.12 | 3.41 | 3.23 | 3.79 | 2.17 | 1.70 |
| 11 | 0.13 | 0.46 | 0.58 | 0.63 | 0.83 | 0.85 | 0.82 | 1.37 | 1.68 | 3.40 | 5.08 | 5.24 | 5.22 | 4.12 | 1.14 |
| 12 |      | 0.43 | 0.61 | 0.39 | 0.79 | 0.79 | 1.09 | 1.20 | 2.39 | 3.22 | 5.23 | 5.23 | 6.16 | 4.09 |      |
| 13 |      | 0.19 | 0.57 | 0.72 | 0.83 | 0.91 | 0.77 | 1.26 | 1.74 | 3.78 | 5.20 | 6.15 | 5.35 | 1.82 |      |
| 14 |      |      | 0.21 | 0.56 | 0.71 | 0.56 | 0.71 | 0.64 | 1.58 | 2.15 | 4.07 | 4.07 | 1.81 |      |      |
| 15 |      |      |      |      | 0.22 | 0.48 | 0.60 | 0.82 | 1.25 | 1.66 | 1.08 |      |      |      |      |

 - Peak Assembly Power

Figure 4-14  
FSAR Section 15.4.8 – Control Rod Ejection  
BOC HZP Assembly Power Distribution at 0.34 Seconds

|    | R    | P    | N    | M    | L    | K    | J    | H    | G    | F    | E    | D    | C    | B    | A    |
|----|------|------|------|------|------|------|------|------|------|------|------|------|------|------|------|
| 1  |      |      |      |      | 0.09 | 0.16 | 0.16 | 0.18 | 0.22 | 0.26 | 0.15 |      |      |      |      |
| 2  |      |      | 0.11 | 0.26 | 0.30 | 0.20 | 0.20 | 0.14 | 0.28 | 0.33 | 0.56 | 0.53 | 0.23 |      |      |
| 3  |      | 0.11 | 0.30 | 0.35 | 0.36 | 0.35 | 0.23 | 0.29 | 0.32 | 0.59 | 0.70 | 0.73 | 0.69 | 0.25 |      |
| 4  |      | 0.26 | 0.35 | 0.20 | 0.37 | 0.32 | 0.36 | 0.31 | 0.49 | 0.55 | 0.74 | 0.46 | 0.85 | 0.66 |      |
| 5  | 0.09 | 0.30 | 0.36 | 0.37 | 0.43 | 0.39 | 0.31 | 0.42 | 0.42 | 0.71 | 0.94 | 0.89 | 0.95 | 0.83 | 0.26 |
| 6  | 0.16 | 0.20 | 0.35 | 0.32 | 0.39 | 0.18 | 0.36 | 0.44 | 0.51 | 0.35 | 0.93 | 0.85 | 1.01 | 0.64 | 0.55 |
| 7  | 0.16 | 0.20 | 0.23 | 0.36 | 0.31 | 0.36 | 0.38 | 0.46 | 0.60 | 0.79 | 0.84 | 1.13 | 0.81 | 0.76 | 0.65 |
| 8  | 0.18 | 0.14 | 0.29 | 0.31 | 0.42 | 0.44 | 0.46 | 0.22 | 0.79 | 1.06 | 1.35 | 1.18 | 1.26 | 0.66 | 0.85 |
| 9  | 0.22 | 0.28 | 0.32 | 0.49 | 0.42 | 0.51 | 0.60 | 0.78 | 1.00 | 1.35 | 1.60 | 2.26 | 1.67 | 1.56 | 1.26 |
| 10 | 0.26 | 0.33 | 0.59 | 0.55 | 0.70 | 0.35 | 0.79 | 1.05 | 1.35 | 1.07 | 3.16 | 2.96 | 3.54 | 2.11 | 1.65 |
| 11 | 0.16 | 0.56 | 0.69 | 0.73 | 0.93 | 0.92 | 0.83 | 1.34 | 1.59 | 3.15 | 4.61 | 4.77 | 4.76 | 3.82 | 1.07 |
| 12 |      | 0.52 | 0.73 | 0.45 | 0.88 | 0.85 | 1.12 | 1.18 | 2.25 | 2.95 | 4.76 | 4.72 | 5.55 | 3.74 |      |
| 13 |      | 0.23 | 0.68 | 0.84 | 0.94 | 1.00 | 0.80 | 1.25 | 1.66 | 3.53 | 4.74 | 5.54 | 4.83 | 1.64 |      |
| 14 |      |      | 0.25 | 0.65 | 0.82 | 0.63 | 0.75 | 0.66 | 1.55 | 2.09 | 3.79 | 3.72 | 1.64 |      |      |
| 15 |      |      |      |      | 0.25 | 0.54 | 0.64 | 0.84 | 1.24 | 1.61 | 1.02 |      |      |      |      |



– Peak Assembly Power



Figure 4-15  
FSAR Section 15.4.8 - Control Rod Ejection  
EOC HFP Core Power vs. Time

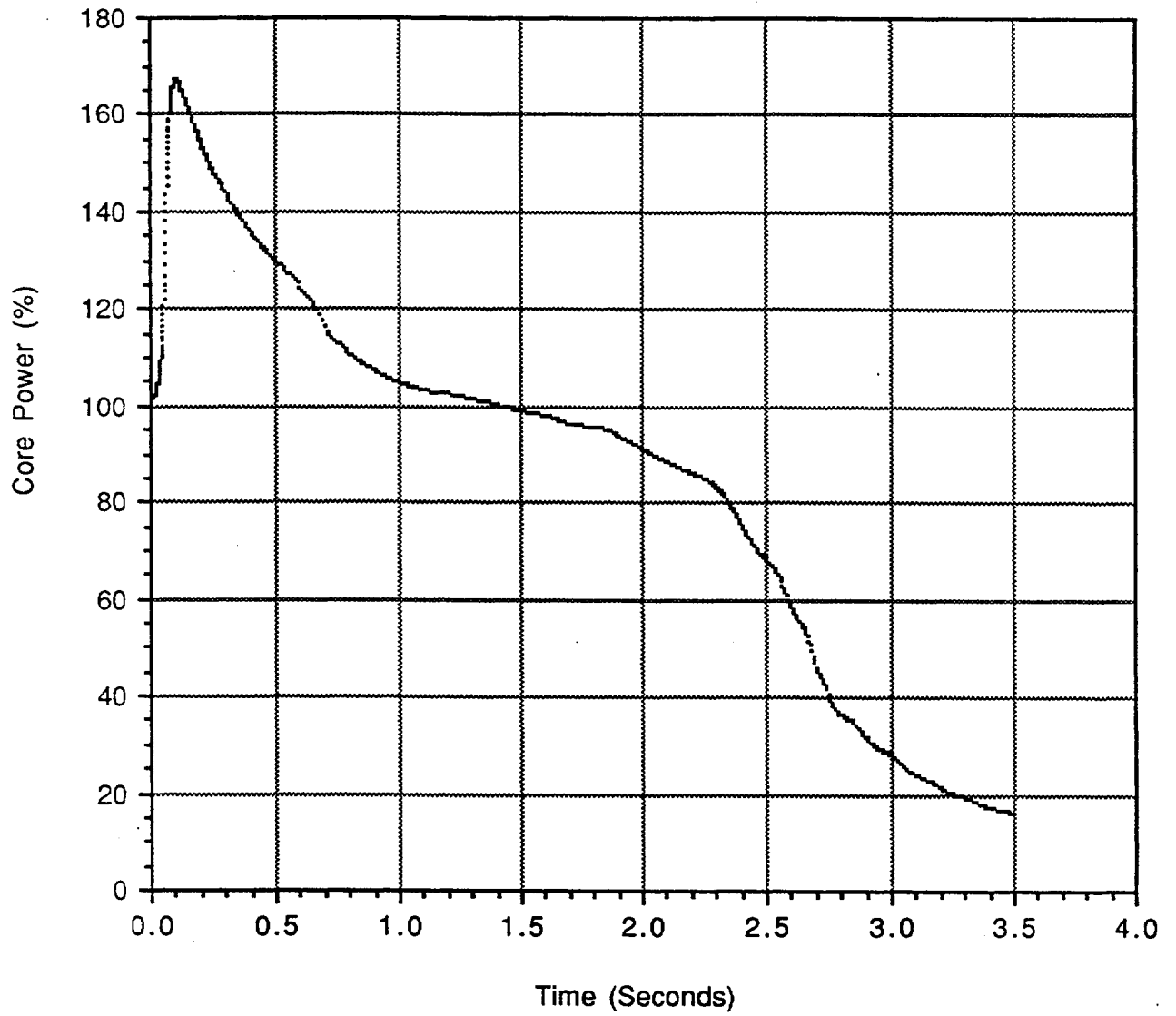


Figure 4-16  
 FSAR Section 15.4.8 - Control Rod Ejection  
 EOC HFP Assembly Power Distribution at 0.0 Seconds

|    | R    | P    | N    | M    | L    | K    | J    | H    | G    | F    | E    | D    | C    | B    | A    |
|----|------|------|------|------|------|------|------|------|------|------|------|------|------|------|------|
| 1  |      |      |      |      | 0.50 | 0.88 | 0.89 | 0.90 | 0.89 | 0.88 | 0.50 |      |      |      |      |
| 2  |      |      | 0.50 | 1.05 | 1.23 | 1.04 | 0.98 | 0.94 | 0.98 | 1.04 | 1.23 | 1.05 | 0.50 |      |      |
| 3  |      | 0.50 | 1.15 | 1.31 | 1.29 | 1.31 | 0.88 | 0.96 | 0.88 | 1.31 | 1.29 | 1.31 | 1.15 | 0.50 |      |
| 4  |      | 1.05 | 1.31 | 1.20 | 1.33 | 1.01 | 1.03 | 0.81 | 1.03 | 1.01 | 1.33 | 1.20 | 1.31 | 1.05 |      |
| 5  | 0.50 | 1.23 | 1.29 | 1.33 | 1.38 | 1.31 | 0.85 | 0.91 | 0.85 | 1.31 | 1.38 | 1.33 | 1.29 | 1.23 | 0.50 |
| 6  | 0.88 | 1.05 | 1.31 | 1.01 | 1.31 | 0.91 | 0.90 | 0.82 | 0.90 | 0.91 | 1.31 | 1.01 | 1.31 | 1.05 | 0.88 |
| 7  | 0.89 | 0.98 | 0.88 | 1.03 | 0.85 | 0.90 | 0.78 | 0.77 | 0.78 | 0.90 | 0.85 | 1.03 | 0.88 | 0.98 | 0.89 |
| 8  | 0.90 | 0.94 | 0.96 | 0.81 | 0.91 | 0.82 | 0.77 | 0.49 | 0.77 | 0.82 | 0.91 | 0.81 | 0.96 | 0.94 | 0.90 |
| 9  | 0.89 | 0.98 | 0.88 | 1.03 | 0.85 | 0.90 | 0.78 | 0.77 | 0.78 | 0.90 | 0.85 | 1.03 | 0.88 | 0.98 | 0.89 |
| 10 | 0.88 | 1.05 | 1.31 | 1.01 | 1.31 | 0.91 | 0.90 | 0.82 | 0.90 | 0.91 | 1.31 | 1.01 | 1.31 | 1.05 | 0.88 |
| 11 | 0.50 | 1.23 | 1.29 | 1.33 | 1.38 | 1.31 | 0.85 | 0.91 | 0.85 | 1.31 | 1.38 | 1.33 | 1.29 | 1.23 | 0.50 |
| 12 |      | 1.05 | 1.31 | 1.20 | 1.33 | 1.01 | 1.03 | 0.81 | 1.03 | 1.01 | 1.33 | 1.20 | 1.31 | 1.05 |      |
| 13 |      | 0.50 | 1.15 | 1.31 | 1.29 | 1.31 | 0.88 | 0.96 | 0.88 | 1.31 | 1.29 | 1.31 | 1.15 | 0.50 |      |
| 14 |      |      | 0.50 | 1.05 | 1.23 | 1.04 | 0.98 | 0.94 | 0.98 | 1.04 | 1.23 | 1.05 | 0.50 |      |      |
| 15 |      |      |      |      | 0.50 | 0.88 | 0.89 | 0.90 | 0.89 | 0.88 | 0.50 |      |      |      |      |



- Peak Assembly Power

Figure 4-17  
 FSAR Section 15.4.8 - Control Rod Ejection  
 EOC HFP Assembly Power Distribution at 0.09 Seconds

|    | R    | P    | N    | M    | L    | K    | J    | H    | G    | F    | E    | D    | C    | B    | A    |
|----|------|------|------|------|------|------|------|------|------|------|------|------|------|------|------|
| 1  |      |      |      |      | 0.39 | 0.68 | 0.70 | 0.72 | 0.72 | 0.72 | 0.42 |      |      |      |      |
| 2  |      |      | 0.38 | 0.80 | 0.94 | 0.81 | 0.77 | 0.75 | 0.80 | 0.86 | 1.03 | 0.88 | 0.43 |      |      |
| 3  |      | 0.38 | 0.87 | 0.99 | 0.99 | 1.02 | 0.70 | 0.77 | 0.73 | 1.10 | 1.09 | 1.11 | 0.99 | 0.44 |      |
| 4  |      | 0.80 | 0.99 | 0.91 | 1.03 | 0.79 | 0.82 | 0.66 | 0.87 | 0.87 | 1.15 | 1.02 | 1.15 | 0.95 |      |
| 5  | 0.39 | 0.94 | 0.99 | 1.03 | 1.07 | 1.04 | 0.69 | 0.76 | 0.74 | 1.15 | 1.23 | 1.20 | 1.19 | 1.15 | 0.48 |
| 6  | 0.68 | 0.81 | 1.02 | 0.79 | 1.04 | 0.74 | 0.75 | 0.71 | 0.81 | 0.84 | 1.22 | 0.97 | 1.27 | 1.03 | 0.88 |
| 7  | 0.70 | 0.77 | 0.70 | 0.82 | 0.69 | 0.75 | 0.68 | 0.69 | 0.75 | 0.89 | 0.87 | 1.07 | 0.93 | 1.05 | 0.95 |
| 8  | 0.72 | 0.75 | 0.77 | 0.66 | 0.77 | 0.71 | 0.69 | 0.46 | 0.79 | 0.90 | 1.03 | 0.94 | 1.12 | 1.10 | 1.05 |
| 9  | 0.72 | 0.80 | 0.73 | 0.87 | 0.74 | 0.81 | 0.75 | 0.79 | 0.88 | 1.08 | 1.07 | 1.33 | 1.15 | 1.26 | 1.12 |
| 10 | 0.72 | 0.86 | 1.10 | 0.87 | 1.15 | 0.84 | 0.89 | 0.90 | 1.08 | 1.19 | 1.78 | 1.43 | 1.84 | 1.45 | 1.19 |
| 11 | 0.42 | 1.03 | 1.09 | 1.15 | 1.23 | 1.22 | 0.87 | 1.03 | 1.07 | 1.78 | 2.03 | 2.05 | 1.97 | 1.80 | 0.72 |
| 12 |      | 0.89 | 1.11 | 1.02 | 1.20 | 0.97 | 1.07 | 0.94 | 1.33 | 1.43 | 2.05 | 2.18 | 2.13 | 1.62 |      |
| 13 |      | 0.43 | 0.99 | 1.15 | 1.19 | 1.27 | 0.93 | 1.12 | 1.15 | 1.84 | 1.96 | 2.13 | 1.86 | 0.80 |      |
| 14 |      |      | 0.44 | 0.94 | 1.15 | 1.03 | 1.05 | 1.10 | 1.26 | 1.45 | 1.80 | 1.62 | 0.80 |      |      |
| 15 |      |      |      |      | 0.48 | 0.88 | 0.95 | 1.05 | 1.12 | 1.19 | 0.72 |      |      |      |      |



- Peak Assembly Power

Figure 4-18  
FSAR Section 15.4.8 - Control Rod Ejection  
EOC HZP Core Power vs. Time

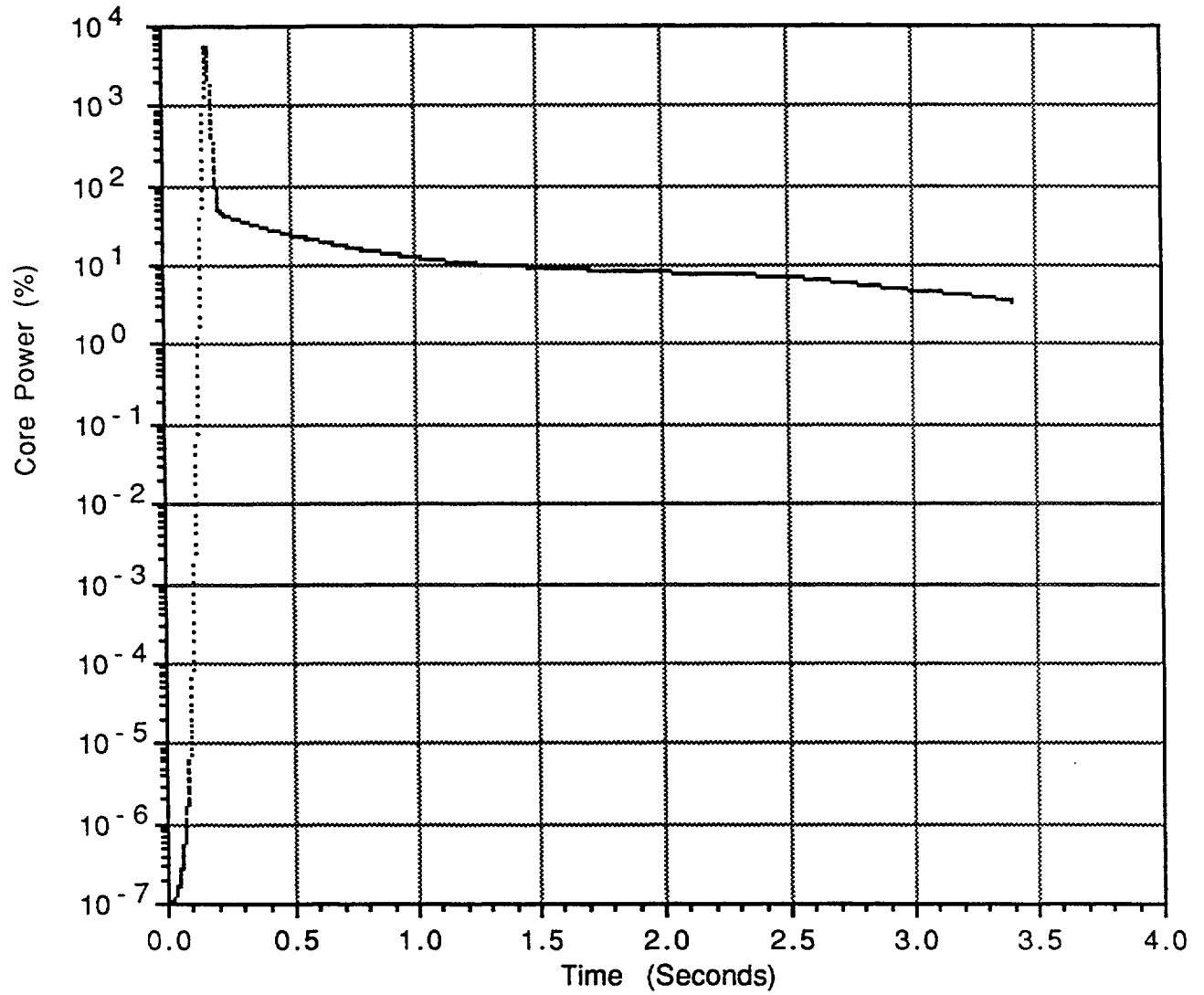


Figure 4-19  
FSAR Section 15.4.8 - Control Rod Ejection  
EOC HZP Assembly Power Distribution at 0.0 Seconds

|    | R    | P    | N    | M    | L    | K    | J    | H    | G    | F    | E    | D    | C    | B    | A    |
|----|------|------|------|------|------|------|------|------|------|------|------|------|------|------|------|
| 1  |      |      |      |      | 0.52 | 0.77 | 0.64 | 0.56 | 0.64 | 0.77 | 0.52 |      |      |      |      |
| 2  |      |      | 0.68 | 1.44 | 1.50 | 0.92 | 0.72 | 0.44 | 0.72 | 0.92 | 1.50 | 1.44 | 0.68 |      |      |
| 3  |      | 0.68 | 1.71 | 1.82 | 1.74 | 1.44 | 0.76 | 0.72 | 0.76 | 1.44 | 1.74 | 1.82 | 1.71 | 0.68 |      |
| 4  |      | 1.44 | 1.82 | 1.11 | 1.68 | 1.11 | 0.96 | 0.69 | 0.96 | 1.11 | 1.68 | 1.11 | 1.82 | 1.44 |      |
| 5  | 0.52 | 1.50 | 1.74 | 1.68 | 1.69 | 1.26 | 0.71 | 0.74 | 0.71 | 1.26 | 1.69 | 1.68 | 1.74 | 1.50 | 0.52 |
| 6  | 0.78 | 0.93 | 1.45 | 1.11 | 1.26 | 0.49 | 0.60 | 0.57 | 0.60 | 0.49 | 1.26 | 1.11 | 1.45 | 0.93 | 0.78 |
| 7  | 0.65 | 0.72 | 0.76 | 0.96 | 0.71 | 0.60 | 0.48 | 0.44 | 0.48 | 0.60 | 0.71 | 0.96 | 0.76 | 0.72 | 0.65 |
| 8  | 0.56 | 0.44 | 0.72 | 0.69 | 0.74 | 0.58 | 0.44 | 0.18 | 0.44 | 0.58 | 0.74 | 0.69 | 0.72 | 0.44 | 0.56 |
| 9  | 0.65 | 0.72 | 0.76 | 0.96 | 0.71 | 0.60 | 0.48 | 0.44 | 0.48 | 0.60 | 0.71 | 0.96 | 0.76 | 0.72 | 0.65 |
| 10 | 0.78 | 0.93 | 1.45 | 1.11 | 1.26 | 0.49 | 0.60 | 0.57 | 0.60 | 0.49 | 1.26 | 1.11 | 1.45 | 0.93 | 0.78 |
| 11 | 0.52 | 1.50 | 1.74 | 1.68 | 1.69 | 1.26 | 0.71 | 0.74 | 0.71 | 1.26 | 1.69 | 1.68 | 1.74 | 1.50 | 0.52 |
| 12 |      | 1.44 | 1.82 | 1.11 | 1.68 | 1.11 | 0.96 | 0.69 | 0.96 | 1.11 | 1.68 | 1.11 | 1.82 | 1.44 |      |
| 13 |      | 0.68 | 1.71 | 1.82 | 1.74 | 1.44 | 0.76 | 0.72 | 0.76 | 1.44 | 1.74 | 1.82 | 1.71 | 0.68 |      |
| 14 |      |      | 0.68 | 1.44 | 1.50 | 0.92 | 0.72 | 0.44 | 0.72 | 0.92 | 1.50 | 1.44 | 0.68 |      |      |
| 15 |      |      |      |      | 0.52 | 0.77 | 0.64 | 0.56 | 0.64 | 0.77 | 0.52 |      |      |      |      |



- Peak Assembly Power

Figure 4-20  
FSAR Section 15.4.8 - Control Rod Ejection  
EOC HZP Assembly Power Distribution at 0.13 Seconds

|    | R    | P    | N    | M    | L    | K    | J    | H    | G    | F    | E    | D    | C    | B    | A    |
|----|------|------|------|------|------|------|------|------|------|------|------|------|------|------|------|
| 1  |      |      |      |      | 0.03 | 0.05 | 0.05 | 0.06 | 0.09 | 0.13 | 0.10 |      |      |      |      |
| 2  |      |      | 0.04 | 0.08 | 0.09 | 0.06 | 0.06 | 0.05 | 0.12 | 0.16 | 0.31 | 0.32 | 0.16 |      |      |
| 3  |      | 0.04 | 0.09 | 0.10 | 0.11 | 0.10 | 0.07 | 0.10 | 0.14 | 0.30 | 0.39 | 0.44 | 0.44 | 0.18 |      |
| 4  |      | 0.08 | 0.10 | 0.07 | 0.11 | 0.09 | 0.11 | 0.11 | 0.20 | 0.27 | 0.44 | 0.31 | 0.53 | 0.43 |      |
| 5  | 0.03 | 0.09 | 0.11 | 0.11 | 0.13 | 0.11 | 0.10 | 0.15 | 0.18 | 0.38 | 0.56 | 0.58 | 0.61 | 0.53 | 0.20 |
| 6  | 0.05 | 0.06 | 0.10 | 0.09 | 0.11 | 0.06 | 0.12 | 0.17 | 0.23 | 0.20 | 0.58 | 0.53 | 0.67 | 0.42 | 0.38 |
| 7  | 0.05 | 0.06 | 0.07 | 0.11 | 0.10 | 0.12 | 0.14 | 0.20 | 0.32 | 0.48 | 0.58 | 0.79 | 0.60 | 0.54 | 0.49 |
| 8  | 0.06 | 0.05 | 0.10 | 0.11 | 0.15 | 0.17 | 0.20 | 0.14 | 0.50 | 0.77 | 1.09 | 1.05 | 1.08 | 0.58 | 0.75 |
| 9  | 0.09 | 0.12 | 0.14 | 0.20 | 0.18 | 0.23 | 0.32 | 0.50 | 0.74 | 1.16 | 1.62 | 2.31 | 1.80 | 1.57 | 1.31 |
| 10 | 0.13 | 0.16 | 0.30 | 0.27 | 0.38 | 0.20 | 0.48 | 0.76 | 1.16 | 1.20 | 3.83 | 3.52 | 4.38 | 2.40 | 1.96 |
| 11 | 0.10 | 0.31 | 0.39 | 0.44 | 0.56 | 0.58 | 0.58 | 1.09 | 1.61 | 3.83 | 6.20 | 6.75 | 6.47 | 4.98 | 1.56 |
| 12 |      | 0.32 | 0.44 | 0.31 | 0.58 | 0.53 | 0.78 | 1.05 | 2.31 | 3.52 | 6.75 | 7.19 | 7.90 | 5.39 |      |
| 13 |      | 0.16 | 0.44 | 0.53 | 0.61 | 0.67 | 0.59 | 1.07 | 1.80 | 4.37 | 6.46 | 7.90 | 7.17 | 2.68 |      |
| 14 |      |      | 0.18 | 0.43 | 0.53 | 0.41 | 0.53 | 0.57 | 1.56 | 2.39 | 4.97 | 5.38 | 2.68 |      |      |
| 15 |      |      |      |      | 0.19 | 0.38 | 0.49 | 0.75 | 1.30 | 1.95 | 1.56 |      |      |      |      |



- Peak Assembly Power

Figure 4-21  
FSAR Section 15.4.8 - Control Rod Ejection  
EOC HZP Assembly Power Distribution at 0.17 Seconds

|    | R    | P    | N    | M    | L    | K    | J    | H    | G    | F    | E    | D    | C    | B    | A    |
|----|------|------|------|------|------|------|------|------|------|------|------|------|------|------|------|
| 1  |      |      |      |      | 0.06 | 0.09 | 0.09 | 0.11 | 0.16 | 0.21 | 0.16 |      |      |      |      |
| 2  |      |      | 0.07 | 0.15 | 0.16 | 0.11 | 0.11 | 0.09 | 0.19 | 0.26 | 0.48 | 0.48 | 0.24 |      |      |
| 3  |      | 0.07 | 0.18 | 0.19 | 0.20 | 0.18 | 0.12 | 0.16 | 0.22 | 0.46 | 0.59 | 0.65 | 0.64 | 0.27 |      |
| 4  |      | 0.15 | 0.19 | 0.12 | 0.20 | 0.15 | 0.17 | 0.17 | 0.30 | 0.40 | 0.64 | 0.45 | 0.76 | 0.62 |      |
| 5  | 0.06 | 0.16 | 0.20 | 0.20 | 0.22 | 0.19 | 0.15 | 0.21 | 0.26 | 0.52 | 0.76 | 0.79 | 0.83 | 0.73 | 0.27 |
| 6  | 0.09 | 0.11 | 0.18 | 0.15 | 0.19 | 0.09 | 0.16 | 0.22 | 0.29 | 0.26 | 0.73 | 0.66 | 0.86 | 0.55 | 0.51 |
| 7  | 0.09 | 0.11 | 0.12 | 0.17 | 0.15 | 0.16 | 0.18 | 0.24 | 0.36 | 0.54 | 0.65 | 0.88 | 0.68 | 0.64 | 0.60 |
| 8  | 0.11 | 0.09 | 0.16 | 0.17 | 0.21 | 0.22 | 0.24 | 0.15 | 0.52 | 0.79 | 1.11 | 1.06 | 1.11 | 0.63 | 0.83 |
| 9  | 0.16 | 0.19 | 0.21 | 0.30 | 0.26 | 0.29 | 0.36 | 0.52 | 0.75 | 1.14 | 1.54 | 2.20 | 1.74 | 1.58 | 1.35 |
| 10 | 0.21 | 0.26 | 0.45 | 0.39 | 0.52 | 0.26 | 0.53 | 0.78 | 1.14 | 1.15 | 3.51 | 3.19 | 4.06 | 2.37 | 1.94 |
| 11 | 0.15 | 0.47 | 0.58 | 0.63 | 0.75 | 0.72 | 0.64 | 1.10 | 1.54 | 3.49 | 5.46 | 5.92 | 5.71 | 4.52 | 1.47 |
| 12 |      | 0.48 | 0.64 | 0.44 | 0.78 | 0.65 | 0.87 | 1.06 | 2.19 | 3.19 | 5.92 | 6.17 | 6.76 | 4.74 |      |
| 13 |      | 0.24 | 0.63 | 0.75 | 0.82 | 0.85 | 0.68 | 1.10 | 1.73 | 4.04 | 5.70 | 6.75 | 6.15 | 2.34 |      |
| 14 |      |      | 0.26 | 0.61 | 0.72 | 0.55 | 0.63 | 0.63 | 1.57 | 2.36 | 4.51 | 4.73 | 2.34 |      |      |
| 15 |      |      |      |      | 0.27 | 0.49 | 0.58 | 0.81 | 1.34 | 1.93 | 1.47 |      |      |      |      |



- Peak Assembly Power

Figure 4-22  
FSAR Section 15.4.8 - Control Rod Ejection  
BOC HFP MARP Curves

Allowed Radial Peak



Figure 4-23  
FSAR Section 15.4.8 - Control Rod Ejection  
BOC HZP MARP Curves

Allowed Radial Peak




Figure 4-24  
FSAR Section 15.4.8 - Control Rod Ejection  
EOC HFP MARP Curves

Allowed Radial Peak

Figure 4-25  
FSAR Section 15.4.8 - Control Rod Ejection  
EOC HZP MARP Curves

Allowed Radial Peak



Figure 4-26  
FSAR Section 15.4.8 - Control Rod Ejection  
BOC HFP Pins in DNB by Assembly

|    | R | P  | N   | M  | L   | K   | J   | H   | G   | F   | E   | D   | C   | B   | A   |
|----|---|----|-----|----|-----|-----|-----|-----|-----|-----|-----|-----|-----|-----|-----|
| 1  |   |    |     |    | 0   | 0   | 0   | 0   | 0   | 0   | 0   |     |     |     |     |
| 2  |   |    | 0   | 0  | 12  | 0   | 0   | 0   | 0   | 0   | 48  | 4   | 0   |     |     |
| 3  |   | 0  | 0   | 0  | 0   | 55  | 0   | 0   | 0   | 149 | 0   | 0   | 6   | 0   |     |
| 4  |   | 0  | 0   | 0  | 0   | 0   | 0   | 0   | 4   | 0   | 7   | 0   | 38  | 34  |     |
| 5  | 0 | 12 | 0   | 0  | 109 | 150 | 0   | 0   | 0   | 244 | 264 | 32  | 167 | 163 | 0   |
| 6  | 0 | 0  | 56  | 0  | 149 | 0   | 0   | 0   | 70  | 4   | 264 | 0   | 264 | 109 | 63  |
| 7  | 0 | 0  | 0   | 0  | 0   | 0   | 0   | 0   | 10  | 256 | 73  | 264 | 46  | 264 | 131 |
| 8  | 0 | 0  | 0   | 0  | 0   | 0   | 0   | 0   | 43  | 264 | 264 | 225 | 264 | 264 | 169 |
| 9  | 0 | 0  | 0   | 3  | 0   | 70  | 10  | 41  | 240 | 264 | 264 | 264 | 264 | 264 | 180 |
| 10 | 0 | 0  | 148 | 0  | 244 | 4   | 254 | 264 | 264 | 264 | 264 | 264 | 264 | 264 | 165 |
| 11 | 0 | 49 | 1   | 6  | 264 | 264 | 65  | 264 | 264 | 264 | 264 | 264 | 264 | 264 | 0   |
| 12 |   | 4  | 0   | 0  | 31  | 0   | 264 | 233 | 264 | 264 | 264 | 264 | 264 | 219 |     |
| 13 |   | 0  | 6   | 36 | 163 | 264 | 52  | 264 | 264 | 264 | 264 | 264 | 256 | 28  |     |
| 14 |   |    | 0   | 34 | 162 | 106 | 264 | 264 | 264 | 264 | 264 | 219 | 28  |     |     |
| 15 |   |    |     |    | 0   | 61  | 130 | 168 | 180 | 164 | 0   |     |     |     |     |

Total Pins in DNB = 18806 (36.91%)

Figure 4-27  
FSAR Section 15.4.8 - Control Rod Ejection  
BOC HZP Pins in DNB by Assembly

|    | R | P | N | M | L | K | J | H | G   | F   | E   | D   | C   | B   | A |
|----|---|---|---|---|---|---|---|---|-----|-----|-----|-----|-----|-----|---|
| 1  |   |   |   |   | 0 | 0 | 0 | 0 | 0   | 0   | 0   |     |     |     |   |
| 2  |   |   | 0 | 0 | 0 | 0 | 0 | 0 | 0   | 0   | 0   | 0   | 0   |     |   |
| 3  |   | 0 | 0 | 0 | 0 | 0 | 0 | 0 | 0   | 0   | 0   | 0   | 0   | 0   |   |
| 4  |   | 0 | 0 | 0 | 0 | 0 | 0 | 0 | 0   | 0   | 0   | 0   | 0   | 0   |   |
| 5  | 0 | 0 | 0 | 0 | 0 | 0 | 0 | 0 | 0   | 0   | 0   | 0   | 0   | 0   | 0 |
| 6  | 0 | 0 | 0 | 0 | 0 | 0 | 0 | 0 | 0   | 0   | 0   | 0   | 0   | 0   | 0 |
| 7  | 0 | 0 | 0 | 0 | 0 | 0 | 0 | 0 | 0   | 0   | 0   | 0   | 0   | 0   | 0 |
| 8  | 0 | 0 | 0 | 0 | 0 | 0 | 0 | 0 | 0   | 0   | 0   | 0   | 0   | 0   | 0 |
| 9  | 0 | 0 | 0 | 0 | 0 | 0 | 0 | 0 | 0   | 0   | 17  | 162 | 0   | 0   | 0 |
| 10 | 0 | 0 | 0 | 0 | 0 | 0 | 0 | 0 | 0   | 1   | 251 | 264 | 264 | 46  | 0 |
| 11 | 0 | 0 | 0 | 0 | 0 | 0 | 0 | 0 | 21  | 250 | 264 | 264 | 264 | 257 | 0 |
| 12 |   | 0 | 0 | 0 | 0 | 0 | 0 | 0 | 157 | 264 | 264 | 264 | 264 | 220 |   |
| 13 |   | 0 | 0 | 0 | 0 | 0 | 0 | 0 | 0   | 264 | 264 | 264 | 263 | 70  |   |
| 14 |   |   | 0 | 0 | 0 | 0 | 0 | 0 | 0   | 42  | 251 | 220 | 68  |     |   |
| 15 |   |   |   |   | 0 | 0 | 0 | 0 | 0   | 0   | 0   |     |     |     |   |

Total Pins in DNB = 5464 (10.72%)

Figure 4-28  
FSAR Section 15.4.8 - Control Rod Ejection  
EOC HFP Pins in DNB by Assembly

|    | R | P | N | M | L | K  | J | H  | G   | F   | E   | D   | C   | B   | A   |
|----|---|---|---|---|---|----|---|----|-----|-----|-----|-----|-----|-----|-----|
| 1  |   |   |   |   | 0 | 0  | 0 | 0  | 0   | 0   | 0   |     |     |     |     |
| 2  |   |   | 0 | 0 | 0 | 0  | 0 | 0  | 0   | 0   | 0   | 0   | 0   |     |     |
| 3  |   | 0 | 0 | 0 | 0 | 0  | 0 | 0  | 0   | 0   | 0   | 0   | 0   | 0   |     |
| 4  |   | 0 | 0 | 0 | 0 | 0  | 0 | 0  | 0   | 0   | 0   | 0   | 0   | 0   |     |
| 5  | 0 | 0 | 0 | 0 | 0 | 0  | 0 | 0  | 0   | 0   | 0   | 0   | 0   | 5   | 0   |
| 6  | 0 | 0 | 0 | 0 | 0 | 0  | 0 | 0  | 0   | 0   | 12  | 0   | 29  | 0   | 0   |
| 7  | 0 | 0 | 0 | 0 | 0 | 0  | 0 | 0  | 0   | 0   | 0   | 0   | 0   | 0   | 0   |
| 8  | 0 | 0 | 0 | 0 | 0 | 0  | 0 | 0  | 0   | 0   | 0   | 0   | 0   | 0   | 56  |
| 9  | 0 | 0 | 0 | 0 | 0 | 0  | 0 | 0  | 0   | 18  | 12  | 253 | 70  | 170 | 111 |
| 10 | 0 | 0 | 0 | 0 | 0 | 0  | 0 | 0  | 18  | 113 | 264 | 264 | 264 | 261 | 135 |
| 11 | 0 | 0 | 0 | 0 | 0 | 9  | 0 | 0  | 15  | 264 | 264 | 264 | 264 | 262 | 0   |
| 12 |   | 0 | 0 | 0 | 0 | 0  | 0 | 0  | 254 | 264 | 264 | 264 | 264 | 217 |     |
| 13 |   | 0 | 0 | 0 | 0 | 29 | 0 | 0  | 64  | 264 | 264 | 264 | 256 | 38  |     |
| 14 |   |   | 0 | 0 | 3 | 0  | 0 | 0  | 169 | 260 | 262 | 217 | 38  |     |     |
| 15 |   |   |   |   | 0 | 0  | 0 | 54 | 111 | 134 | 0   |     |     |     |     |

Total Pins in DNB = 7351 (14.43%)

Figure 4-29  
FSAR Section 15.4.8 - Control Rod Ejection  
EOC HZP Pins in DNB by Assembly

|    | R | P  | N   | M   | L   | K  | J | H  | G   | F   | E   | D   | C   | B   | A   |
|----|---|----|-----|-----|-----|----|---|----|-----|-----|-----|-----|-----|-----|-----|
| 1  |   |    |     |     | 0   | 0  | 0 | 0  | 0   | 0   | 0   |     |     |     |     |
| 2  |   |    | 0   | 0   | 0   | 0  | 0 | 0  | 0   | 0   | 10  | 36  | 0   |     |     |
| 3  |   | 0  | 0   | 0   | 0   | 0  | 0 | 0  | 0   | 0   | 39  | 176 | 123 | 0   |     |
| 4  |   | 0  | 0   | 0   | 0   | 0  | 0 | 0  | 0   | 0   | 68  | 5   | 170 | 62  |     |
| 5  | 0 | 0  | 0   | 0   | 0   | 0  | 0 | 0  | 0   | 0   | 149 | 147 | 186 | 69  | 0   |
| 6  | 0 | 0  | 0   | 0   | 0   | 0  | 0 | 0  | 0   | 0   | 0   | 0   | 13  | 0   | 0   |
| 7  | 0 | 0  | 0   | 0   | 0   | 0  | 0 | 0  | 0   | 0   | 0   | 0   | 0   | 0   | 0   |
| 8  | 0 | 0  | 0   | 0   | 0   | 0  | 0 | 0  | 0   | 0   | 5   | 0   | 1   | 2   | 0   |
| 9  | 0 | 0  | 0   | 0   | 0   | 0  | 0 | 0  | 0   | 4   | 58  | 207 | 111 | 107 | 67  |
| 10 | 0 | 0  | 0   | 0   | 0   | 0  | 0 | 0  | 4   | 39  | 264 | 264 | 264 | 251 | 164 |
| 11 | 0 | 13 | 45  | 69  | 150 | 0  | 0 | 0  | 60  | 264 | 264 | 264 | 264 | 264 | 70  |
| 12 |   | 37 | 182 | 6   | 148 | 0  | 0 | 0  | 207 | 264 | 264 | 264 | 264 | 260 |     |
| 13 |   | 0  | 127 | 171 | 187 | 13 | 0 | 16 | 110 | 264 | 264 | 264 | 264 | 145 |     |
| 14 |   |    | 0   | 63  | 69  | 0  | 0 | 3  | 107 | 250 | 264 | 260 | 145 |     |     |
| 15 |   |    |     |     | 0   | 0  | 0 | 0  | 67  | 160 | 69  |     |     |     |     |

Total Pins in DNB = 9970 (19.57%)

Figure 4-30  
Core Coolant Volume Expansion Rate for  
HFP, BOC Case

Expansion Rate (Ft<sup>3</sup>/sec)

Time (seconds)



# ROD EJECTION

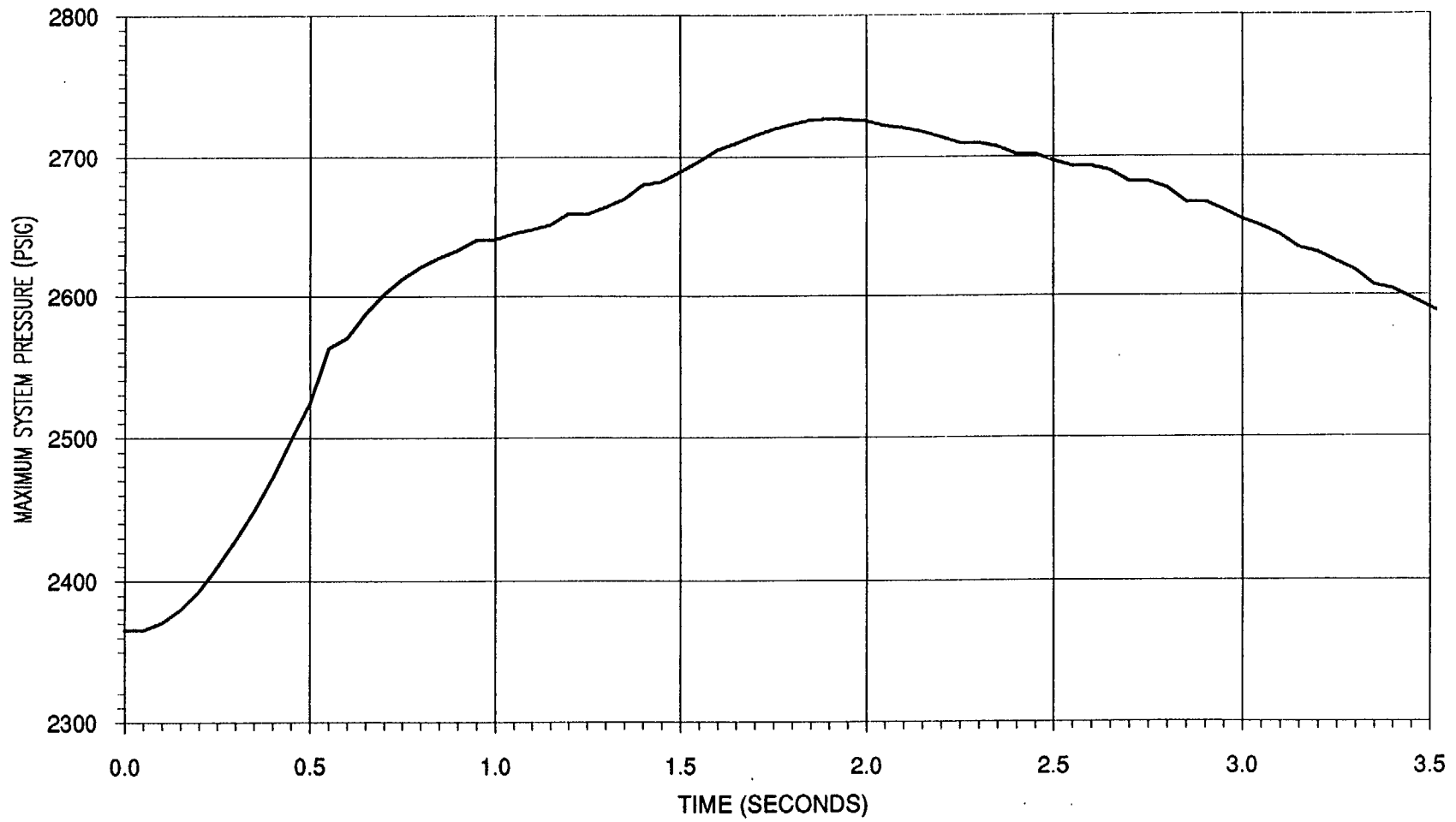


Figure 4-31

## 5.0 STEAM LINE BREAK ANALYSIS

### 5.1 Overview

#### 5.1.1 Description of Steam Line Break Accident

The steam line break transient is described in FSAR Section 15.1.5 (Reference 5-1). The steam release arising from a break in a main steam line would result in an initial increase in steam flow, with a subsequent decrease during the accident as the steam pressure falls. The energy removal from the Reactor Coolant System (RCS) causes a reduction of coolant temperature and pressure. In the presence of a negative moderator temperature coefficient, the cooldown results in an insertion of positive reactivity. If the most reactive control rod is assumed stuck in its fully withdrawn position after reactor trip, the core might become critical and return to power. A return to power following a steam line rupture is a potential problem mainly because of the high power peaking factors which exist assuming the most reactive control rod to be stuck in its fully withdrawn position. The core is ultimately shut down by the boric acid injection delivered by the Safety Injection System.

#### 5.1.2 Acceptance Criteria

A major steam line break is classified as an ANS Condition IV event, a limiting fault. Minor secondary system pipe breaks are classified as ANS Condition III or infrequent events. The analysis is performed assuming a stuck control rod, a single failure in the engineered safety features, and with consideration of both offsite power maintained and offsite power lost. The following two criteria must be satisfied. First, the core must remain in place and intact. The analysis submitted herein meets this criterion by showing that the 95/95 DNB limit of Reference 5-2, Section 4.4 is satisfied. Future analyses using these same methods might meet the criterion by demonstrating continued core cooling capability based on an acceptable fuel damage model and result. Second, radiation doses must not exceed the guidelines of 10CFR100. These dose limits are 25 rem whole body and 300 rem thyroid. The Condition III and IV criteria regarding overpressurization are not challenged by a steam line break transient.

### 5.1.3 Analytical Approach

The steam line break transient requires a limiting set of physics parameters to be determined for use as initial and boundary conditions. These parameters are input to a McGuire/Catawba RETRAN-02 (Reference 5-3) model for the system thermal-hydraulic analysis. The RETRAN-02 analysis generates the core statepoint conditions which correspond to the transient time of minimum DNBR. Neutronics codes such as EPRI-NODE-P (Reference 5-4) or SIMULATE-3P (Reference 5-5) are used to generate core power distributions corresponding to the statepoint conditions. The core power distribution along with the core thermal-hydraulic boundary conditions from the RETRAN-02 analysis are then input to a McGuire/Catawba VIPRE-01 (Reference 5-6) model to calculate the minimum DNBR. If this value were below the DNBR limit, then a fuel rod census would be performed to determine the number of fuel rods in DNB and therefore the fraction of gap activity released. The dose consequences of this release would then be evaluated.

## 5.2 Simulation Codes and Models

### 5.2.1 System Thermal-Hydraulic Analysis

#### 5.2.1.1 Selection of a Bounding Unit

Differences between the McGuire and Catawba units are discussed in Section 3.1.6 of Reference 5-7 for the steam line break transient. The most important differences with respect to steam line break are the steam generator type and the differences in the Auxiliary Feedwater System flowrates. McGuire and Catawba Unit 1 steam generators have been replaced with BWI feeding steam generators. Catawba Unit 2 has Westinghouse Model D5 preheater steam generators. The steam generators influence the transient response due to design differences such as heat transfer areas, tube alloys, tube bundle height, and initial liquid inventory. The Auxiliary Feedwater System flowrates are different due to pump discharge piping resistance and throttle valve positions, and pump capacity. Both steam generator designs are analyzed separately. The Auxiliary Feedwater System flowrates used are conservative for the unit for which the analysis is applicable. The Catawba Unit 2 analysis results are presented.

5.2.1.2 Modifications to Base Plant Model

Renodalization of Reactor Vessel



Renodalization of Steam Generator Secondary



Since the main feedwater piping contains only subcooled water connected to the steam generator, this inventory would remain inactive during a steam line break and would not affect the transient analysis. In order to save computational costs, the main feedwater piping nodes are eliminated and the feedwater is added directly to the steam generator via a positive fill junction, similar to the junction already used for auxiliary feedwater.

#### 5.2.1.3 Break Modeling

The full cross-sectional area of the 34" main steam line is 5.4 ft<sup>2</sup>. The area of the flow restrictor at the steam generator outlet is 1.4 ft<sup>2</sup>. [

] This analysis uses the Moody critical flow model. For the timeframe of interest, the break flow is always limited by critical flow.

#### 5.2.2 Nuclear Analysis

The transient system response during a steam line break accident is sensitive to core reactivity versus temperature and the Doppler Temperature Coefficient. The core thermal-hydraulic response is sensitive to the three dimensional core power distribution. Therefore, the nuclear analysis for this event must specify pre-break core physics characteristics and post-break power distributions based on the calculated system response.

##### 5.2.2.1 Core Physics Parameters

The k-effective versus temperature curve (Figure 5-2) and Doppler temperature coefficient are selected such that a limiting return to power occurs in the RETRAN analysis. This curve represents the effect on reactivity of an asymmetric cooldown from the technical specification shutdown margin limit. The

Doppler coefficient was chosen to be  $-3.5 \text{ pcm}/^{\circ}\text{F}$  for this analysis. The conservatism of the k-effective versus temperature curve and Doppler coefficient will be confirmed each cycle as described in Section 5.5.

#### 5.2.2.2 Power Distributions

[

]SIMULATE-3P, or PDQ

(Reference 5-4) in conjunction with EPRI NODE-P, are used to calculate the peak pin to assembly average ratio for the hot assembly. This pin to assembly factor is applied to the assembly average power calculated for the limiting RETRAN statepoints. Alternatively, SIMULATE-3P can be used to explicitly calculate the peak pin value at limiting RETRAN statepoints. The three-dimensional power distribution and the system analysis results are then combined for the thermal-hydraulic evaluation.

#### 5.2.3 Core Thermal-Hydraulic Analysis

##### 5.2.3.1 VIPRE Code Description

The VIPRE-01 code (Reference 5-6) is used for the steam line break core thermal-hydraulic analyses. VIPRE-01 is a subchannel thermal-hydraulic computer code. With this subchannel analysis approach, the nuclear fuel element is divided into a number of quasi one-dimensional channels that communicate laterally by diversion crossflow and turbulent mixing. Given the geometry of the reactor core and coolant channels and the boundary conditions or forcing functions, VIPRE-01 calculates core flow distributions, coolant conditions, fuel rod temperatures and the minimum departure from nucleate boiling ratio (MDNBR) for steady-state conditions and for transients. VIPRE-01 accepts all necessary boundary conditions that originate either from the RETRAN system transient simulation or the core neutronics simulation. Included is the capability to impose different boundary conditions on different regions of the core model. For example, different core region inlet temperatures, flow rates, heat flux, and even different assembly and pin radial powers or axial flux shapes can be modeled in steady-state or transient modes.

#### 5.2.3.2 Analysis Methodology

[

]

VIPRE model is used. Given the RETRAN statepoint core quadrant inlet temperatures, core quadrant inlet flow rates, core exit pressure, core average surface heat flux, and the assembly axial and radial power distributions from the neutronics code, this 45 channel model calculates the statepoint local coolant properties and the DNBR. One critical heat flux (CHF) correlation used to evaluate the DNBR is the Westinghouse W-3S correlation (Reference 5-6, Appendix D). The W-3S CHF correlation has been recently approved by the NRC for analysis with system pressures as low as 500 psia (Reference 5-8). The second CHF correlation used to perform DNB analysis is the BWU-Z CHF correlation (Reference 5-9). The BWU-Z correlation was reviewed and approved by the NRC for use in McGuire/Catawba analyses in References 5-10 and 5-11. The BWU-Z correlation limit is pressure dependent and has the following limits:

| <u>Pressure Range (psia)</u> | <u>DNBR Limit</u> |
|------------------------------|-------------------|
| 400-700                      | 1.590             |
| 700-1000                     | 1.199             |
| 1000-1500                    | 1.125             |
| 1500-2400                    | 1.193             |

Two steady-state cases are analyzed: the first case with offsite power available, and the second case with offsite power unavailable. A statepoint DNBR calculation is performed instead of a transient DNBR calculation since the steam line break accident is a slow transient and a statepoint consisting of the limiting surface heat flux and inlet boundary conditions provides conservative DNBR results.

#### Model Description

[

]

### Axial Power Distributions

### Radial Power Distributions

## 5.3 Transient Analysis

### 5.3.1 Initial Conditions

#### Pressurizer Pressure

Since this transient is being evaluated for minimum DNBR, a low initial pressurizer pressure is used. The low initial pressure causes an earlier safety injection actuation since the transient starts closer to the



setpoint. This is compensated for in the safety injection setpoint as described below. Nominal pressurizer pressure with any control rods withdrawn is 2235 psig. The initial condition uncertainty allowance for reduced pressurizer pressure is 30 psi. The initial condition for this transient is, therefore, 2205 psig.

#### Pressurizer Level

A low initial pressurizer level minimizes RCS inventory during the transient. This minimizes core outlet pressure and is, therefore, conservative for evaluation of minimum DNBR. This effect more than compensates for the slightly quicker boration when the safety injection fluid mixes with the smaller RCS mass. The hot zero power programmed pressurizer level is 25%. The initial condition uncertainty allowance for reduced pressurizer level is 9%. The initial condition for this transient is, therefore, 16%.

#### RCS Temperature

Since this transient is being evaluated for minimum DNBR, a high initial RCS temperature is used. A slightly greater reactivity insertion results from starting from a high initial temperature since the slope of the k-effective vs. temperature curve is greater at higher temperatures. The hot zero power programmed RCS temperature is 557°F. The initial condition uncertainty allowance for increased RCS temperature is 4°F. The initial condition for this transient is, therefore, 561°F.

#### RCS Flow

Since this transient is being evaluated for minimum DNBR, a low initial RCS flow is used. The effect of lower flow on DNBR more than offsets the decrease in primary-to-secondary heat transfer. The Technical Specification minimum measured flow assumed for this analysis is 382,000 gpm. The Catawba flow measurement uncertainty is 2.2%, which is larger than the corresponding McGuire value. The initial condition for this transient is, therefore, 373,596 gpm.

#### Steam Generator Water Inventory

Since the primary-to-secondary heat transfer is the driving force behind the excessive RCS cooldown and depressurization, steam generator inventory is maximized to provide the largest cooldown capacity and to

prolong the time prior to U-tube uncover and heat transfer degradation. The normal hot zero power mass is approximately [ ] lbm per steam generator. The initial condition uncertainty allowance for increased steam generator level is 8%. In this region of the steam generator, this is equivalent to an additional [ ] lbm. The initial condition for this transient is, therefore, approximately [ ] lbm.

### Core Power

Initial core heat output would result in a lower temperature decrease since this energy would have to be removed in addition to that stored in the RCS fluid and metal. This would result in a milder transient and would be nonconservative. The core is, therefore, initially at hot zero power, here defined as  $10^{-9}$  times full power.

### Steam Generator Tube Plugging

Assuming no steam generator tube plugging maximizes the steam generator heat transfer area and minimizes the RCS loop flow resistance. Both of these effects enhance primary-to-secondary heat transfer and are, therefore, conservative. These effects more than offset the slight decrease in RCS inventory which would result from plugged tubes. Therefore, no tube plugging is assumed for this analysis.

### Core Bypass Flow

Core bypass flow is assumed to be 6% of total core flow.

## 5.3.2 Boundary Conditions

### 5.3.2.1 Availability of Systems and Components

### Reactor Coolant Pumps

The reactor coolant pumps are assumed to trip when offsite power is lost. For portions of the analysis during which offsite power is maintained, all reactor coolant pumps are assumed to be operating.

### Pressurizer Pressure Control

No credit is taken for pressurizer heater operation. This assumption enhances the RCS depressurization and is therefore conservative for the evaluation of minimum DNBR.

### Pressurizer Level Control

No credit is taken for the automatic operation of the Chemical and Volume Control System (CVCS) to attempt to increase RCS mass and thereby maintain pressurizer level and pressure. The charging and letdown flows are assumed to isolate simultaneously and to be balanced prior to isolation. Not taking credit for CVCS action to maintain pressure is conservative for the evaluation of minimum DNBR.

### Condenser Steam Dump

The condenser steam dump valves are initially assumed to be open slightly to release the steam generated by the relatively small heat input to the RCS from the reactor coolant pumps. These valves are assumed to be closed after reactor trip. However, since the flow through these valves is very small compared to break flow, the opening or closing these valves has an insignificant effect on the analysis.

### Main Feedwater

The main feedwater pumps take suction from the hotwell pumps via the condensate booster pumps. Both of the latter sets of pumps are run from offsite power. When offsite power is lost, both of these types of pumps trip, causing the main feedwater pumps to trip on low suction pressure, condensate booster pump trip, or safety injection. It is assumed that this process takes no more than 5 seconds. For events in which offsite power is maintained, no main feedwater pump trip is assumed. For all cases, no credit is taken for feedwater isolation on low-low RCS average temperature coincident with reactor trip.

### Auxiliary Feedwater

All three auxiliary feedwater pumps are assumed to start on loss of offsite power and deliver flow to all four steam generators. This is conservative since it maximizes the secondary heat sink.

### Offsite Power

As instructed by Section 15.1.5 of Reference 5-2, the assumptions regarding the loss of offsite power and the timing of such a loss were studied to determine their effects on the consequences of the accident.

Analyses were performed with offsite power both maintained throughout the transient and lost during the transient. The core is ultimately shut down by borated water from the high and intermediate-head safety injection pumps. In the absence of offsite power, the pumps are powered from emergency buses energized by diesel generators. The diesels start on either a safety injection signal or an undervoltage condition on the emergency buses (indicative of the loss of offsite power). Since delaying diesel generator start delays borated water delivery, and is therefore conservative, the loss of offsite power is timed to coincide with the safety injection actuation.

### Safety Injection Pumps

The injection of borated water introduces negative reactivity and is therefore a benefit. The injection of cold, unborated water is a penalty, however, since it makes the cooldown more severe. Because of this, the single failure, the loss of one train of safety injection, is timed to coincide with the point at which the high-head safety injection piping is purged of unborated water.

#### 5.3.2.2 Response Times

### Pumped Safety Injection Flow

A delay is assumed from the SI setpoint being reached until the SI signal is generated. An additional delay is assumed from the diesel generator start signal until the first load group, which includes the high-head safety injection pump discharge valves, is sequenced onto the emergency bus. A third delay is assumed from the sequencing of the first load group onto the emergency bus until delivery of unborated water to the RCS. The total of these three delays is 33 seconds. For the case in which offsite power is maintained, the corresponding delay is 19 seconds.

### Feedwater Isolation Valves

Following the receipt of a safety injection signal, an additional delay is assumed to generate a feedwater isolation signal and complete closure of the isolation valves. The total response time for the feedwater isolation function is 12 seconds.

### Main Steam Isolation Valves

Following the receipt of a steam line isolation signal, an additional delay is assumed to close the main steam isolation and main steam isolation bypass valves. The total response time for the steam line isolation function is 10 seconds.

### Auxiliary Feedwater Pumps

Since cold auxiliary feedwater flow into the steam generator makes the cooldown more severe, no time delay is assumed between the loss of offsite power and the delivery of flow to the steam generators.

#### 5.3.2.3 Flow From Interfacing Systems

### Safety Injection

Safety injection flow is varied as a function of RCS pressure. The limiting head-flow curves among the high and intermediate head pumps are adjusted to conservatively account for pump head degradation.

### Main Feedwater

At hot zero power, the main feedwater control valve is closed, and the feedwater is delivered to the steam generator upper nozzle through the main feedwater control bypass valve. In assessing the amount of main feedwater flow during a steam line break, the following aspects must be considered: automatic control of pump speed, automatic control of bypass valve position, and line resistance of the piping to the upper nozzle. The speed controller will initially attempt to reduce pump speed. No credit is taken in the analysis for a flow reduction due to this effect. Rather than model the bypass valve controller in detail, the analysis conservatively assumes that the valve instantaneously travels to its full open position. A

lower limit is placed on the upper nozzle piping resistance in this configuration. The flow boundary condition is then conservatively increased as steam generator pressure decreases, by assuming that feedwater pump discharge pressure remains constant at the initial value corresponding to the low resistance limit.

#### Auxiliary Feedwater

Auxiliary feedwater flow is varied as a function of steam generator pressure. The limiting head-flow curves among the motor and turbine-driven pumps are adjusted to conservatively account for installed pump performance being better than the curves and for pump motor speed being higher than predicted.

#### 5.3.2.4 Engineered Safety Features Actuation Setpoints

##### Safety Injection

Safety injection is assumed to be actuated at 1700 psig pressurizer pressure.

##### Steam Line Isolation

Steam line isolation is assumed to occur at 700 psig steam line pressure. No credit is taken for steam line isolation on high containment pressure for breaks inside containment.

##### Dynamic Compensation of Steam Line Pressure Signal

No credit is taken for the lead/lag compensation on the steam line pressure signal for actuation of steam line isolation. This results in later actuation and prolonged blowdown of the intact steam generators. This effect makes the transient more severe, and this modeling therefore bounds both the presence and the absence of the lead/lag compensation.

#### 5.3.2.5 Boron Injection Modeling

##### Transport

The boron transport model used is described in Section VII.2.5 of Reference 5-3. The boron is assumed to be soluble in the transport medium and to have no direct effect on the fluid equations. The basic equation computes the time rate of change of boron mass in a control volume from the net inflow from connected volumes plus the net generation within that volume.

##### Purge Volumes

Purge volumes from the outlet of the refueling water storage tank to the inlet of the RCS are separately calculated for both the high and intermediate-head safety injection pumps. These piping volumes are assumed to be initially at a concentration of 0 ppm. Borated water is assumed to reach the RCS only after an amount of unborated water equal to the purge volume has been injected. This purging is done separately for the high and intermediate head pumps.

##### Concentration

The boron concentration in the injection water is an assumed 1900 ppm Refueling Water Storage Tank Technical Specification lower limit value minus a 1% concentration measurement error, or 1881 ppm.

#### 5.3.2.6 Core Kinetics Modeling

##### Point Kinetics

The RETRAN point kinetics model is used for the system thermal-hydraulic analysis. The particular option employed uses one prompt neutron group, six delayed neutron groups, eleven delayed gamma emitters, plus U-239 and Np-239. The point kinetics model is adequate for this application since the system analysis does not require detailed modeling of power distribution effects. The power distributions used in the system analysis are determined to be conservative as discussed below. The effective delayed neutron fraction and the prompt neutron lifetime values are chosen to minimize the

ratio of the former to the latter. This ratio is a RETRAN input. Minimizing it increases the neutron power spike when prompt criticality is achieved.

### Temperature Feedback

The basis for the temperature feedback is a relationship between the reactivity vs. temperature curve and

[

] which

is input to the point kinetics model.

### Axial Power Distribution

The axial power distribution for the RETRAN analysis is simply the energy deposition fraction for each of the three axial core conductors. These fractions approximate the axial power distribution calculated by the three dimensional core model described in Section 5.2.2.2. The RETRAN axial power distribution at the peak heat flux statepoint is more top-peaked than the distribution calculated by the three dimensional model. This approach is conservative since it results in a more severe return to power.

### Radial Power Distribution

[

] This approach is conservative since it results in a more severe

return to power.



### Control Rod Reactivity

Since the steam line break transient is a concern chiefly because of power peaking in the vicinity of a stuck rod, the control rods are assumed to begin the transient outside of the core; i.e., the reactor is initially not tripped. Manual action by the operator is assumed to immediately trip the reactor. This assumption is conservative since any cooldown prior to rod insertion would introduce positive reactivity which would increase core power. This would increase RCS stored energy and cause decay heat generation, both of which cause a less severe cooldown. The amount of negative reactivity introduced by rod insertion is sufficient to make the core subcritical by the technical specification shutdown margin.

### Boron Reactivity

The negative reactivity inserted by boration is modeled by 
$$\left[ \frac{\text{boron concentration}}{\text{boron concentration at shutdown}} \right] \text{core boron concentration}$$
 This concentration is multiplied by a boron worth to give a reactivity.

## 5.4 Results and Conclusions

### 5.4.1 Primary and Secondary System Response

Sensitivity studies were performed to demonstrate that the 1.4 ft<sup>2</sup> break size is limiting. The steam line break transient is analyzed both with offsite power maintained and with offsite power lost coincident with safety injection actuation. The event sequences for the two cases are presented in Tables 5-1 and 5-2. Figures 5-4 through 5-14 correspond to the case with offsite power maintained and 5-15 through 5-25 to the case with offsite power lost.

#### Offsite Power Maintained

Steam line pressure in the faulted steam line (Figure 5-4) decreases after the break occurs. The depressurization rate initially increases after steam line isolation occurs, since beyond this point only the faulted steam generator is supplying steam to the break. The depressurization rate then decreases as the steam line continues to blow down towards atmospheric pressure. Steam line pressure in the intact steam

line (shown on the same figure) also decreases until steam line isolation occurs. Beyond this point the intact steam generators, and therefore their associated steam lines, experience a slight pressurization.

The cold leg temperatures (Figure 5-5) closely follow the pressures in the respective steam lines. The hot leg temperatures (Figure 5-6) follow the cold leg temperatures until the return to power occurs. A larger difference between the hot and cold leg temperatures develops beyond this point due to the core heat output.

Core boron concentration (Figure 5-7) is zero until after the unborated water is purged from the safety injection piping. Thereafter, it slowly increases as the borated safety injection water mixes with the unborated RCS inventory.

The temperatures drive the core reactivity transient shown in Figure 5-8. Reactivity initially drops to the technical specification shutdown margin on reactor trip as the rods fall into the core. The positive reactivity inserted due to the decreasing temperatures causes total reactivity to increase until prompt criticality is momentarily achieved. The fuel temperature feedback caused by the sudden power increase causes reactivity to decrease rapidly to near zero. Reactivity decreases slowly as power increases due to increasing fuel temperature feedback. Reactivity decreases further with the addition of borated water from the Safety Injection System.

The neutron power transient (Figure 5-9) caused by this reactivity transient, is zero until prompt criticality occurs. At this point power spikes up and then immediately decreases sharply due to the negative Doppler feedback. Power then increases in equilibrium with reactivity until just after boron reaches the core. This is followed by a slow decrease toward shutdown. The core heat flux (Figure 5-10) is similar to the core power with two exceptions. First, there is some heat flux generated prior to prompt criticality by removal of stored energy from the fuel. Second, the power spike at prompt criticality is too brief to be reflected in the heat flux.

Pressurizer level (Figure 5-11) decreases rapidly until the pressurizer empties. It stays at zero until enough water inventory is added by the Safety Injection System to offset the contraction of the original inventory due to the cooldown. Pressurizer pressure (Figure 5-12) decreases relatively slowly until the pressurizer empties. The decrease is more rapid until the saturation pressure is reached in the hottest

parts of the RCS. Thereafter, pressure increases slowly as inventory addition from the Safety Injection System offsets inventory contraction from the cooldown.

Break flow (Figure 5-13) initially decreases as the steam line pressure decreases. After steam line isolation, flow from the intact loops stops. Beyond this point flow decreases with decreasing pressure.

The core mass fluxes (Figure 5-14) increase with time since the reactor coolant pumps provide essentially constant volumetric flow which, with the decreasing RCS temperatures, is equivalent to an increasing mass flow rate.

### Offsite Power Lost

Although Figures 5-4 through 5-14 depict the case in which offsite power is maintained, the discussion is generally applicable to Figures 5-15 through 5-25, the case in which offsite power is lost at safety injection. Important exceptions are noted below.

Neutron power (Figure 5-22) does not begin a sustained decrease until after boron from both the high-head and intermediate-head safety injection pumps has reached the core.

The core mass fluxes (Figure 5-25) decrease beyond the point at which offsite power is lost due to the coastdown of the reactor coolant pumps.

The system transient response for each case is reviewed to select the statepoint(s) for the power peaking and DNBR analysis. Values provided for each statepoint include neutron power, core heat flux, core outlet pressure, [

## 5.4.2 Core Response

### 5.4.2.1 Axial and Radial Power Distributions

Using the limiting statepoints from the RETRAN analyses discussed in Section 5.4.1, axial and radial power distributions are calculated as described in Section 5.2.2.2. The axial power distribution for the

offsite power maintained case has a top peaked shape, whereas the offsite power lost case has a bottom peaked shape. This effect is caused by the difference in moderator temperature feedback resulting from the large difference in RCS flow. Typical values of the maximum axial peaking factors for the peak radial location are [ ] for the offsite power maintained and offsite power lost cases, respectively. Figures 5-26 and 5-27 show the asymmetric core assembly radial power distributions. The cold quadrant, which contains the stuck rod, has a more highly peaked assembly radial power distribution than the rest of the core. Typical maximum hot assembly pin radial power peaking factors are [ ] for the offsite power maintained and offsite power lost cases, respectively.

#### 5.4.2.2 Minimum DNBR Results

Using the limiting statepoints from the RETRAN analyses discussed in Section 5.4.1, together with the power distributions discussed in Section 5.4.2.1, the VIPRE [ ] model is used to calculate the core local fluid properties and MDNBR. The MDNBRs predicted by the W-3S CHF correlation are greater than 1.45 for both the offsite power maintained and offsite power lost cases. Therefore, the criterion that the core remain in place and intact, as discussed in Section 5.1.2, is met. Because this criterion is met, the current FSAR dose analysis, which assumes no DNBR-related fuel failures, remains valid.

### 5.5 Cycle Specific Evaluation

The cycle-specific reload evaluation for the steam line break accident focuses on the conservative core physics parameters input to the system transient modeling. Each reload cycle is evaluated to determine whether the reactor is subcritical at the core and system conditions corresponding to the limiting peak heat flux statepoint of the system transient. There is a high degree of confidence that each reload core will be bounded since the system model was developed with:

- The minimum shutdown margin allowed by the technical specifications
- A conservative reactivity versus temperature response
- A conservative Doppler coefficient.

If the cycle-specific reactivity check shows the reactor to be subcritical with respect to the core assumed in the existing licensing basis analysis, including a stuck rod, then the response predicted by the system

analysis bounds the reload core. If the reload core is not subcritical at these conditions, two approaches are available to obtain acceptable steam line break analysis results: redesign the reload core, or reanalyze the transient.

## References

- 5-1 Catawba Nuclear Station Final Safety Analysis Report, 1988 Update.
- 5-2 Standard Review Plan, Volume III, NUREG-0800, NRC, Revision 2, July 1981.
- 5-3 RETRAN-02: A Program for Transient Thermal-Hydraulic Analysis of Complex Fluid Flow Systems, EPRI NP-1850-CCM, Revision 4, EPRI, November 1988.
- 5-4 Nuclear Physics Methodology for Reload Design, DPC-NF-2010A, Duke Power Company, June 1985.
- 5-5 Nuclear Design Methodology Using CASMO-3/SIMULATE-3P, DPC-NE-1004-A, Revision 1, Duke Power Company, December 1997.
- 5-6 VIPRE-01: A Thermal-Hydraulic Code for Reactor Cores, EPRI NP-2511-CCM-A, Revision 3, EPRI, August 1989.
- 5-7 Thermal-Hydraulic Transient Analysis Methodology, DPC-NE-3000-PA, Revision 2, Duke Power Company, December 2000
- 5-8 January 31, 1989 letter from A. S. Thadani (NRC) to W. J. Johnson (Westinghouse), "Acceptance for Referencing of licensing Topical Report, WCAP-9226-P/9227-NP, 'Reactor Core Response to Excessive Secondary Steam Releases.'"
- 5-9 D. A. Farnsworth and G. A. Meyer, The BWU Critical Heat Flux Correlations, BAW-10199P, BWFC, November 1994
- 5-10 Letter , H. N. Berkow (NRC) to M. S. Tuckman (Duke), November 7, 1996
- 5-11 Letter, P. S. Tam (NRC) to M. S. Tuckman (Duke), February 20, 1997

Table 5-1

Sequence of Events for 1.4 ft<sup>2</sup> Split Break  
With Offsite Power Maintained

| Event   | Time<br>(seconds) |
|---|-------------------|
| Break occurs / Operator manually trips reactor                          | 0.01              |
| Pressurizer level goes offscale low                                     | 22                |
| SI actuation on low pressurizer pressure                                | 35                |
| Steam line isolation on low steam line pressure                         | 36                |
| Criticality occurs  | 46                |
| SI pumps begin to deliver unborated water to RCS                        | 52                |
| High-head SI lines purged of unborated water /<br>One train of SI fails | 119               |
| Peak heat flux occurs   | 120               |
| Intermediate-head SI lines purged of unborated water                    | 191               |

Table 5-2

Sequence of Events for 1.4 ft<sup>2</sup> Split Break  
With Offsite Power Lost at SI Actuation

| Event   | Time<br>(seconds) |
|---|-------------------|
| Break occurs / Operator manually trips reactor  | 0.01              |
| Pressurizer level goes offscale low   | 22                |
| SI actuation on low pressurizer pressure /<br>Offsite power lost<br>Reactor coolant pumps begin to coast down | 35                |
| Steam line isolation on low steam line pressure   | 36                |
| Criticality occurs  | 52                |
| SI pumps begin to deliver unborated water to RCS  | 66                |
| High-head SI lines purged of unborated water /<br>One train of SI fails                                       | 134               |
| Intermediate-head SI lines purged of unborated water  | 223               |
| Peak heat flux occurs   | 228               |

Pages 5-23 and 5-24 intentionally blank



Figure 5-1

RETRAN Reactor Vessel Model

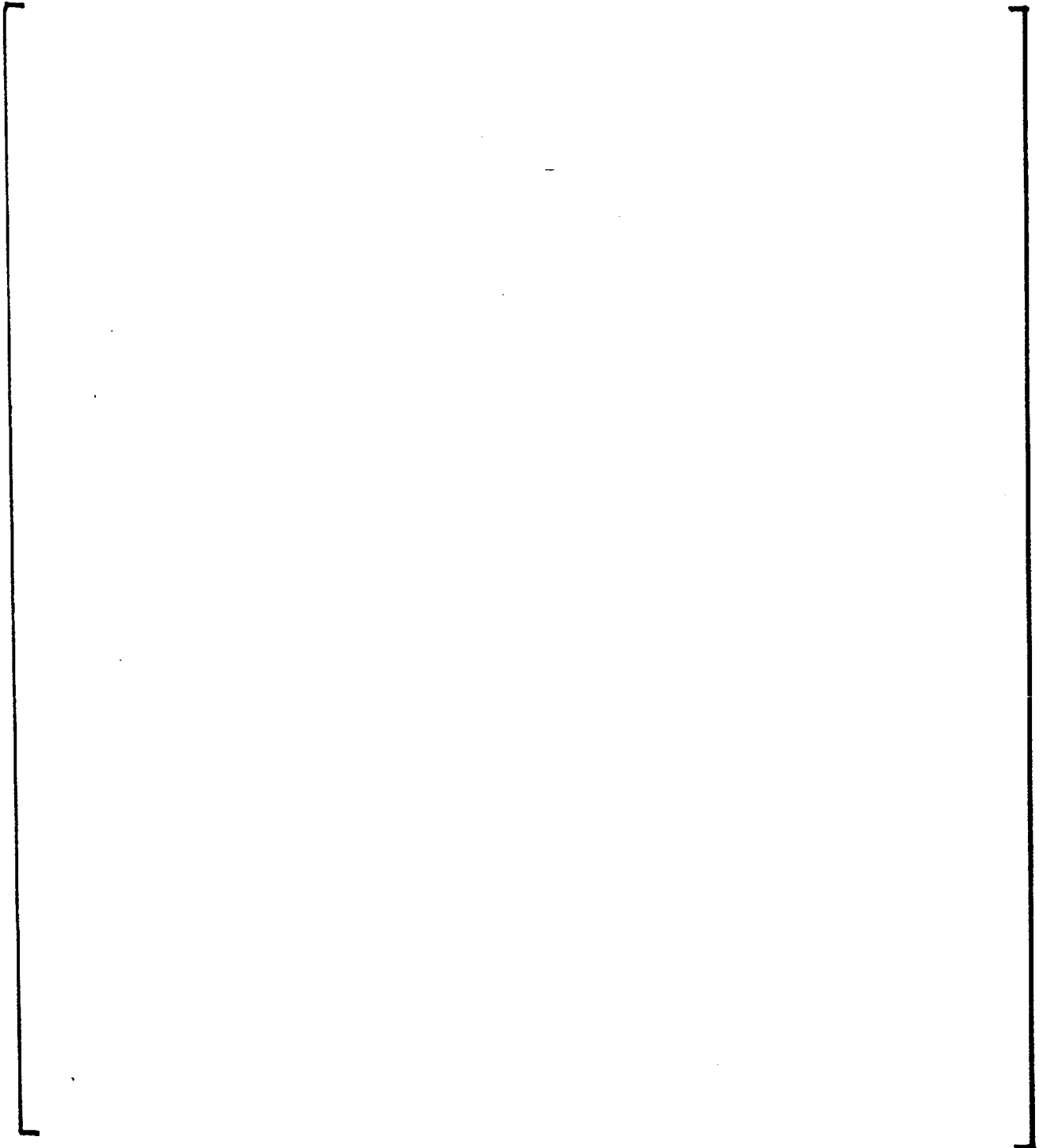


Figure 5-2

K-effective versus Moderator Temperature

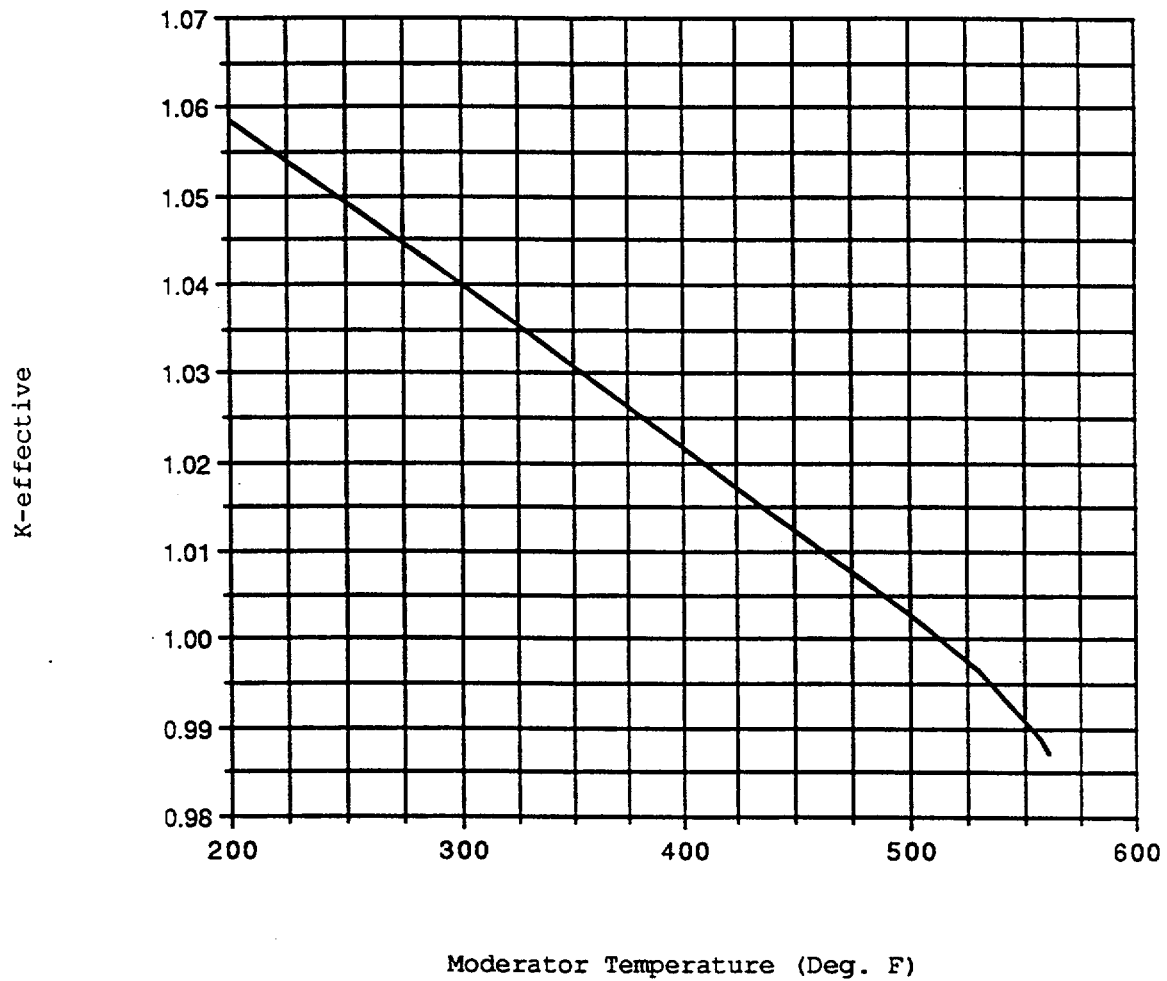


Figure 5-3  
[ ] VIPRE Model for Steam Line  
Break Core Thermal-Hydraulic Analyses

# FSAR SECTION 15.1.5 – STEAM LINE BREAK

OFFSITE POWER MAINTAINED

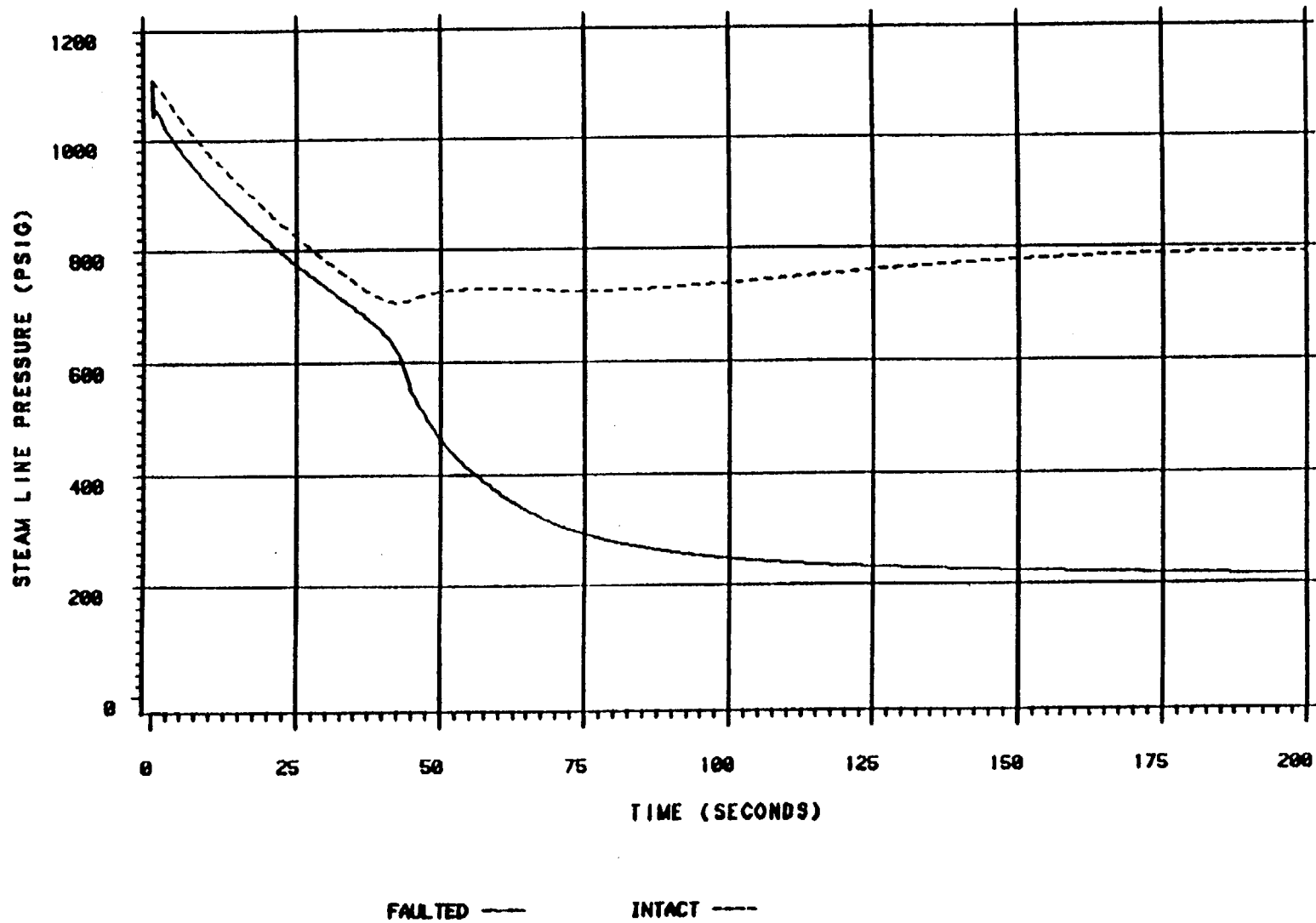


Figure 5-4

# FSAR SECTION 15.1.5 – STEAM LINE BREAK

OFFSITE POWER MAINTAINED

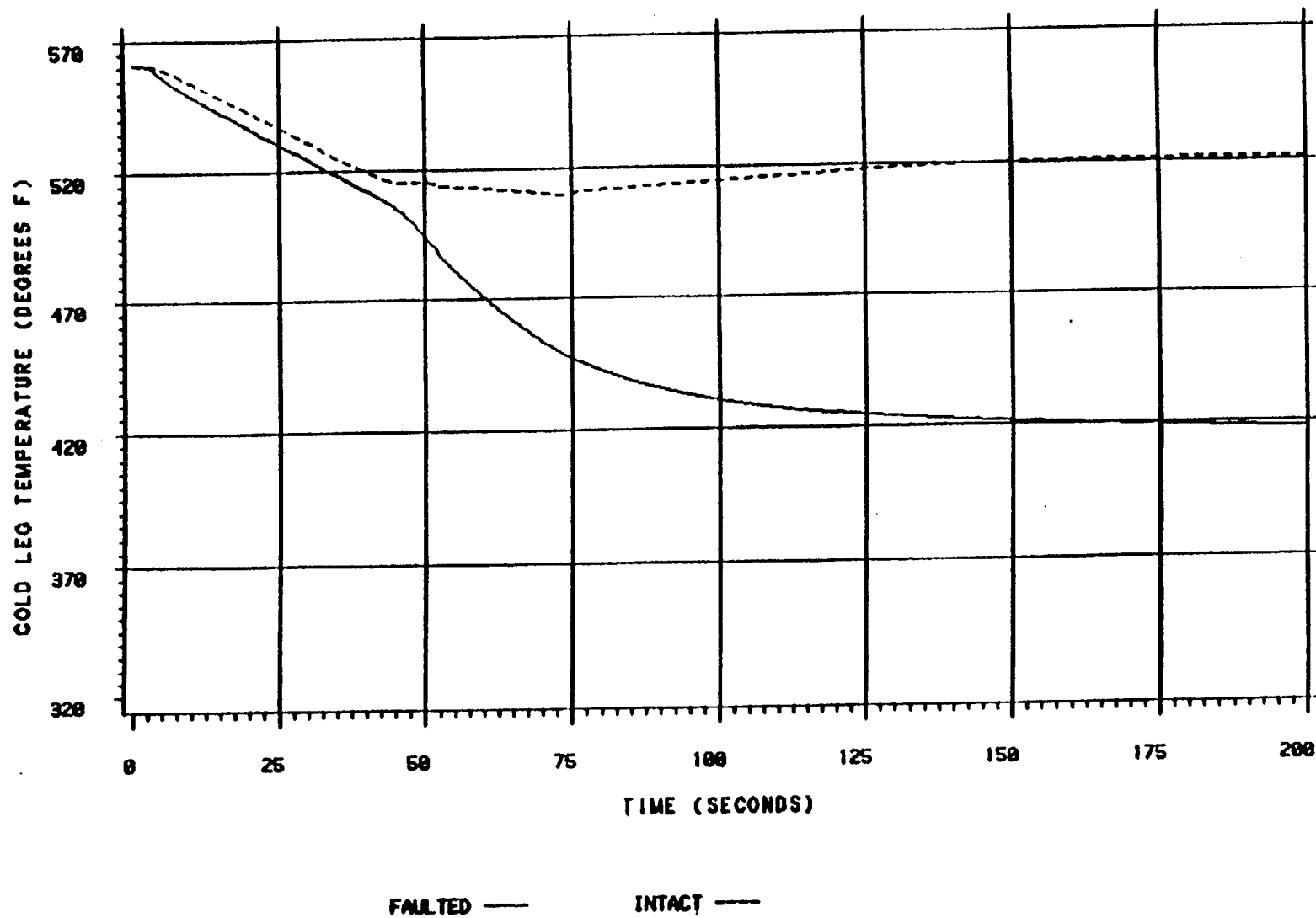


Figure 5-5

# FSAR SECTION 15.1.5 – STEAM LINE BREAK

OFFSITE POWER MAINTAINED

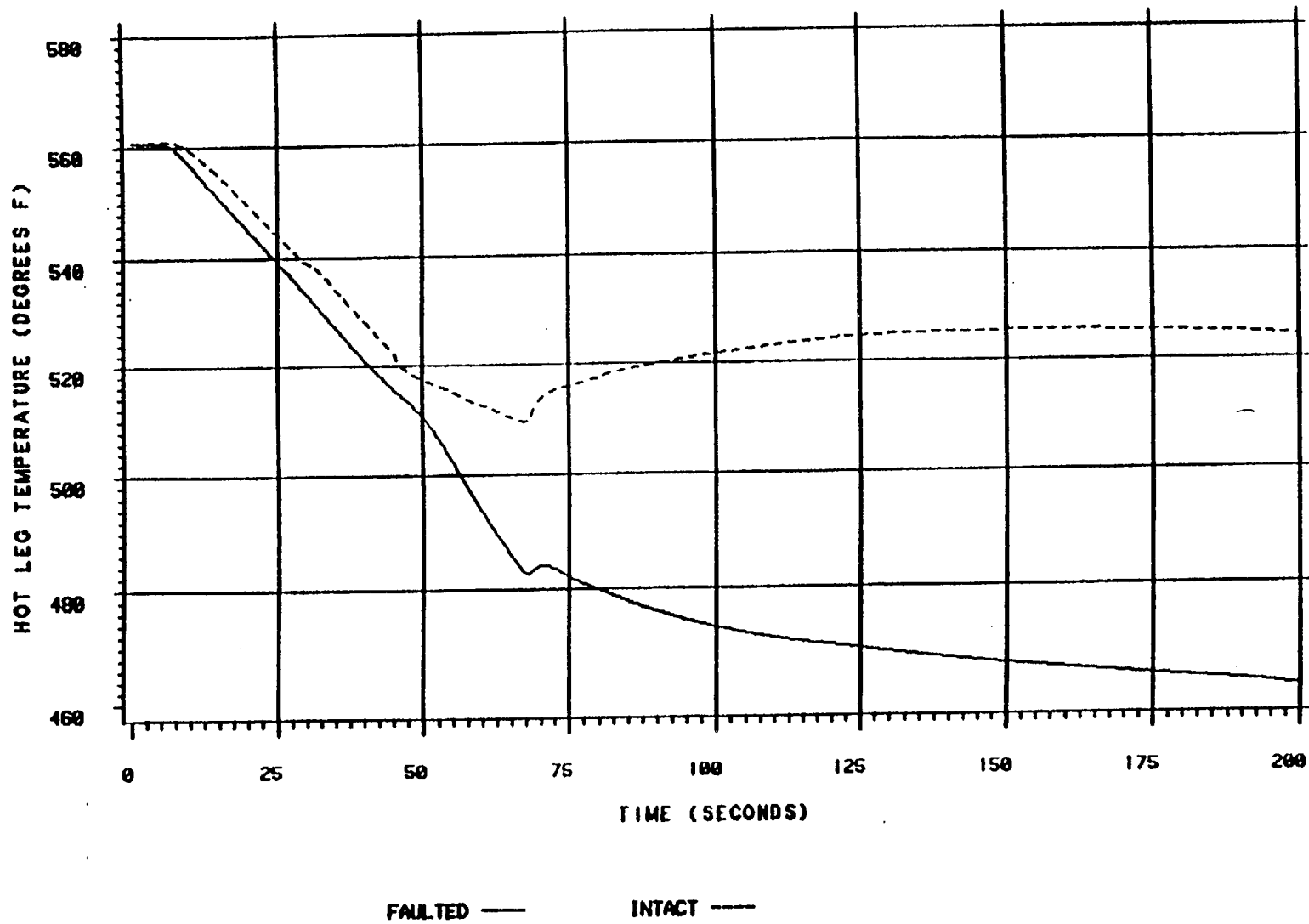


Figure 5-6

# FSAR SECTION 15.1.5 – STEAM LINE BREAK

OFFSITE POWER MAINTAINED

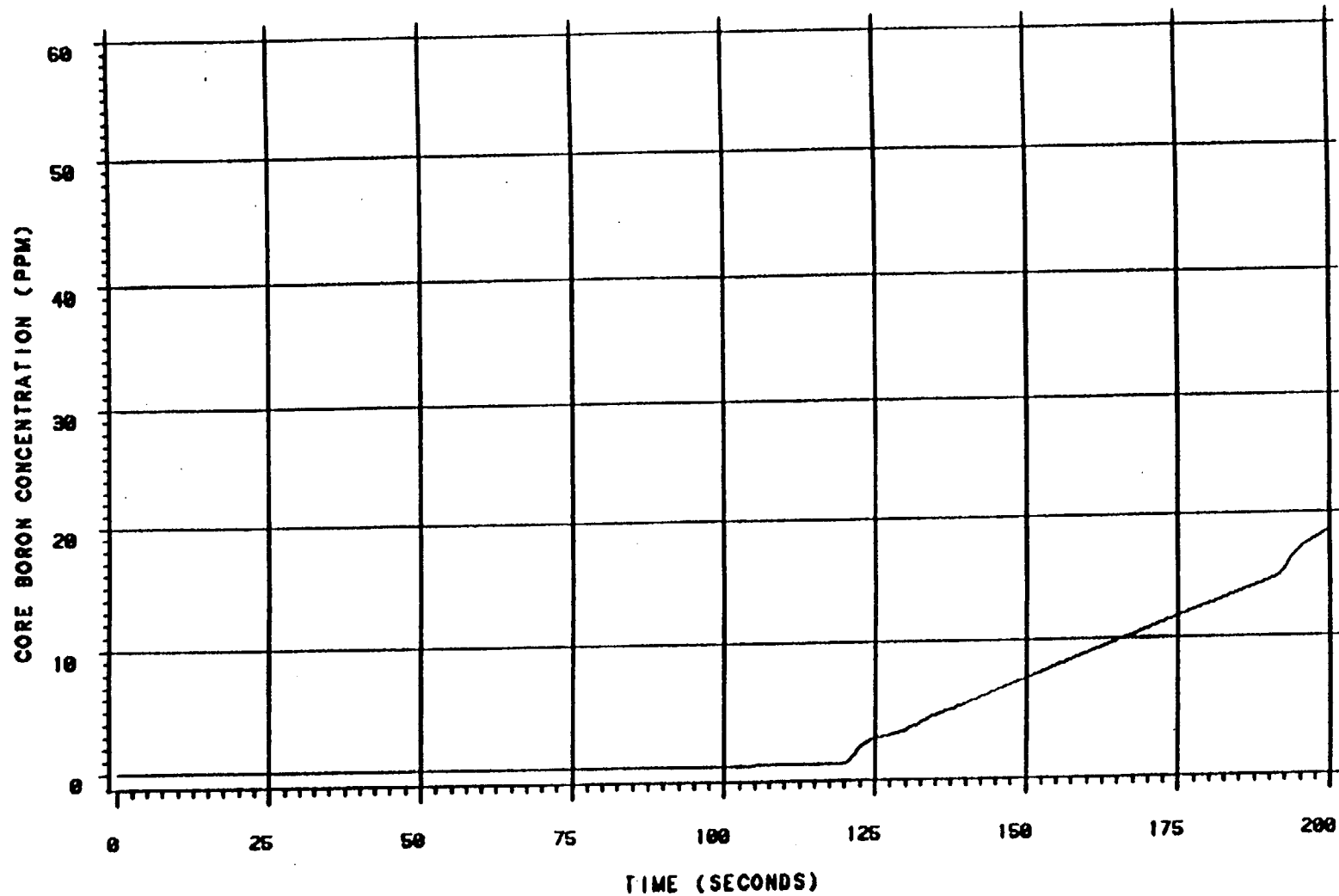


Figure 5-7

# FSAR SECTION 15.1.5 – STEAM LINE BREAK

OFFSITE POWER MAINTAINED

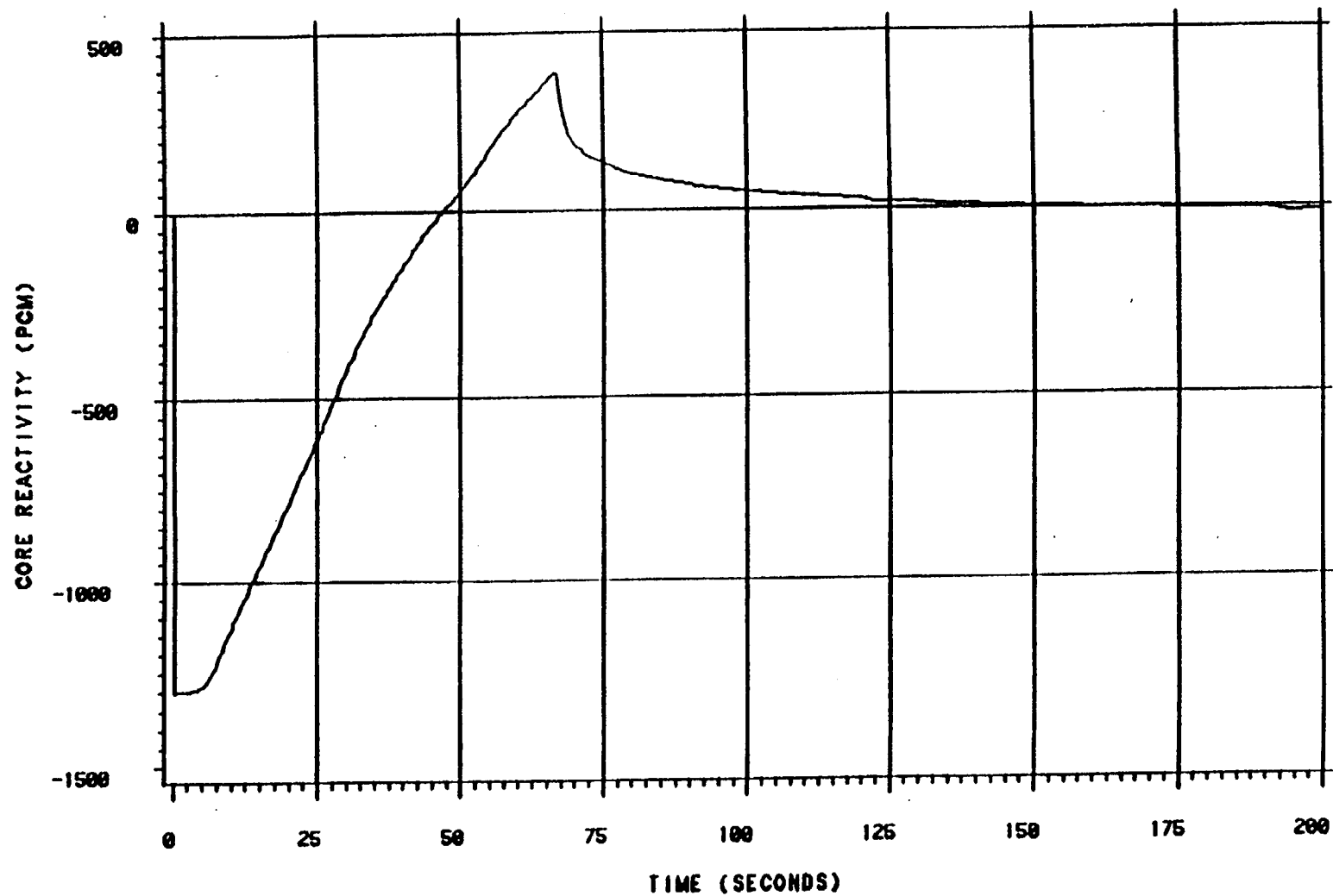


Figure 5-8



# FSAR SECTION 15.1.5 – STEAM LINE BREAK

OFFSITE POWER MAINTAINED

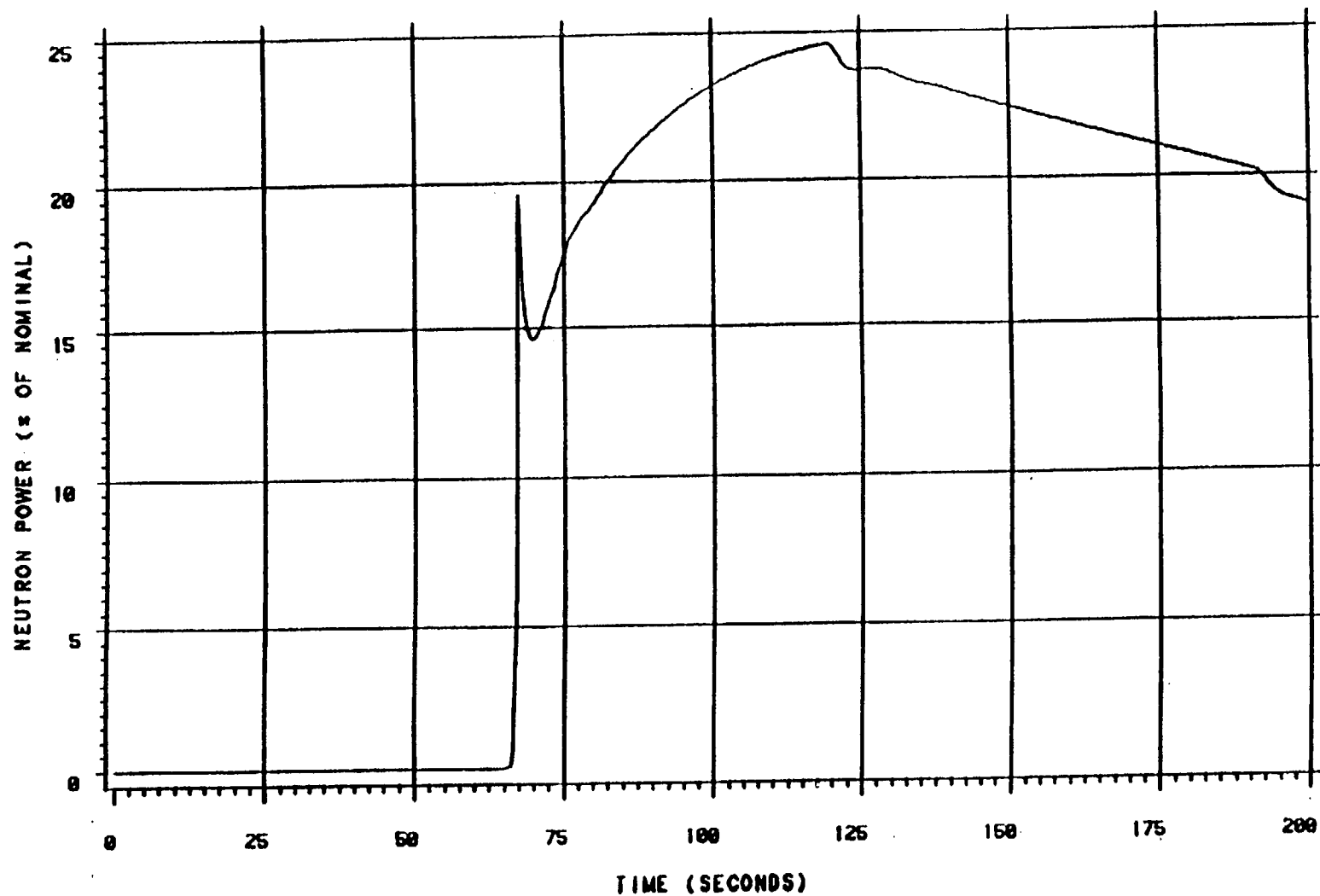


Figure 5-9

# FSAR SECTION 15.1.5 – STEAM LINE BREAK

OFFSITE POWER MAINTAINED

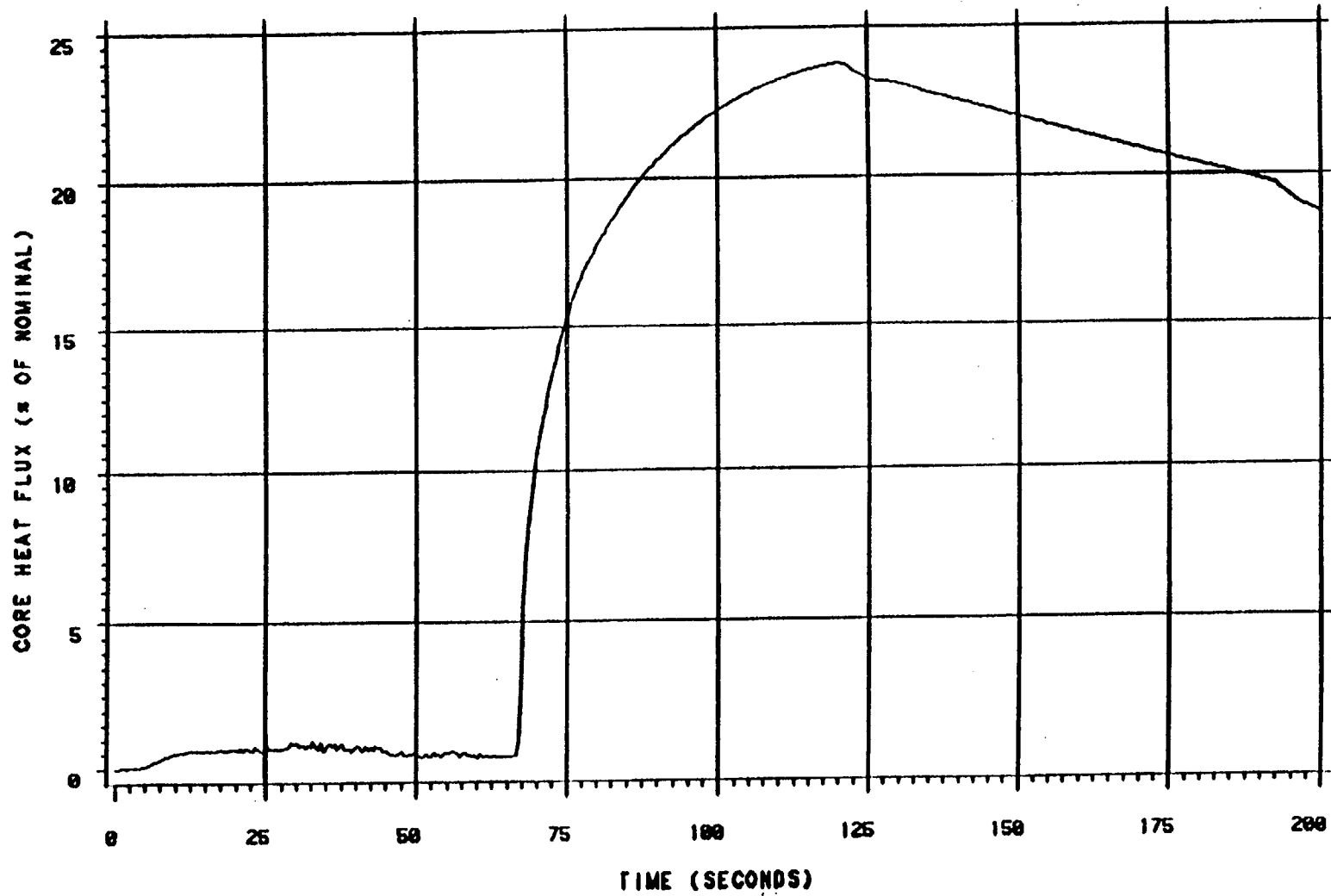


Figure 5-10

# FSAR SECTION 15.1.5 - STEAM LINE BREAK

OFFSITE POWER MAINTAINED

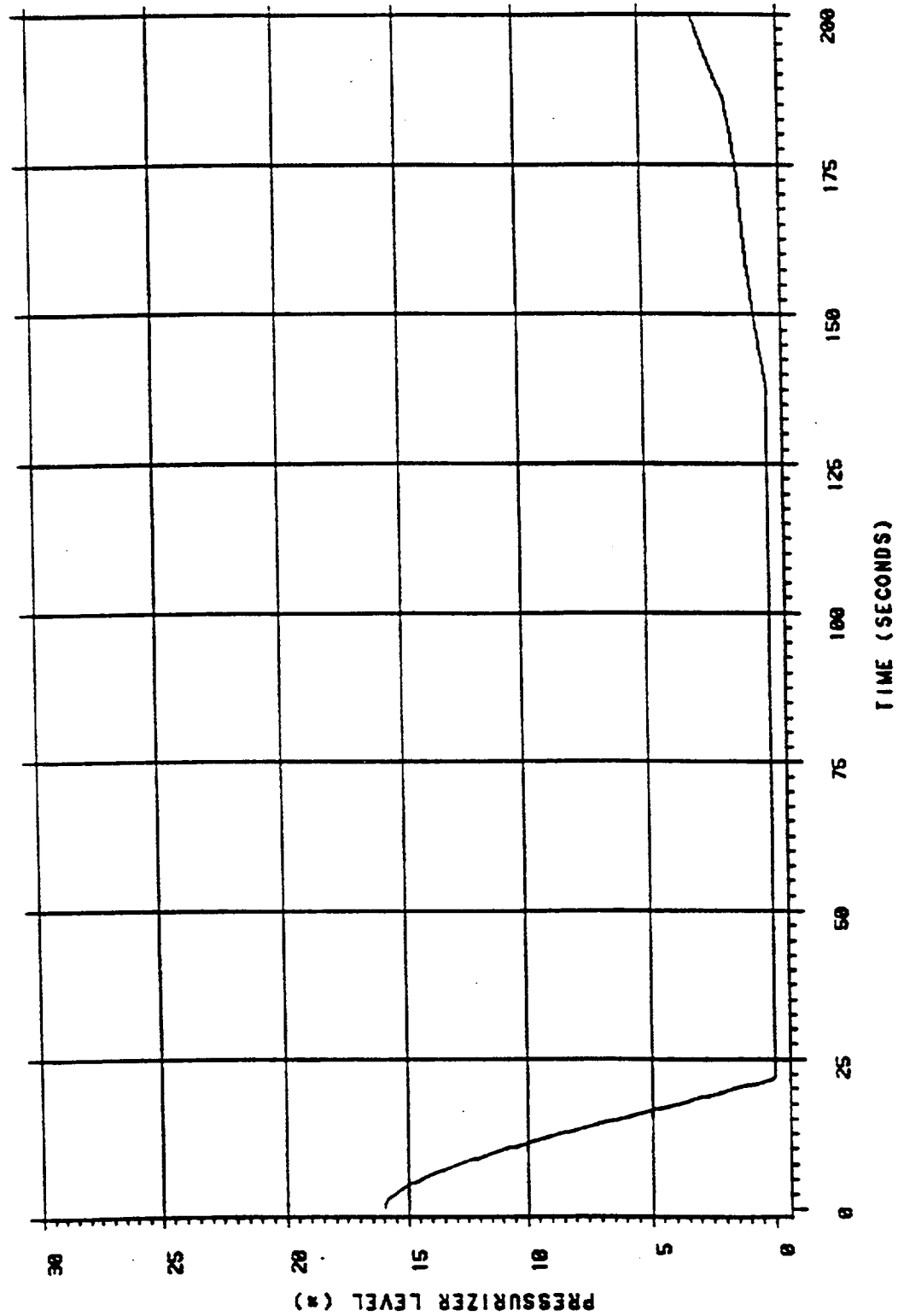


Figure 5-11

# FSAR SECTION 15.1.5 - STEAM LINE BREAK

OFFSITE POWER MAINTAINED

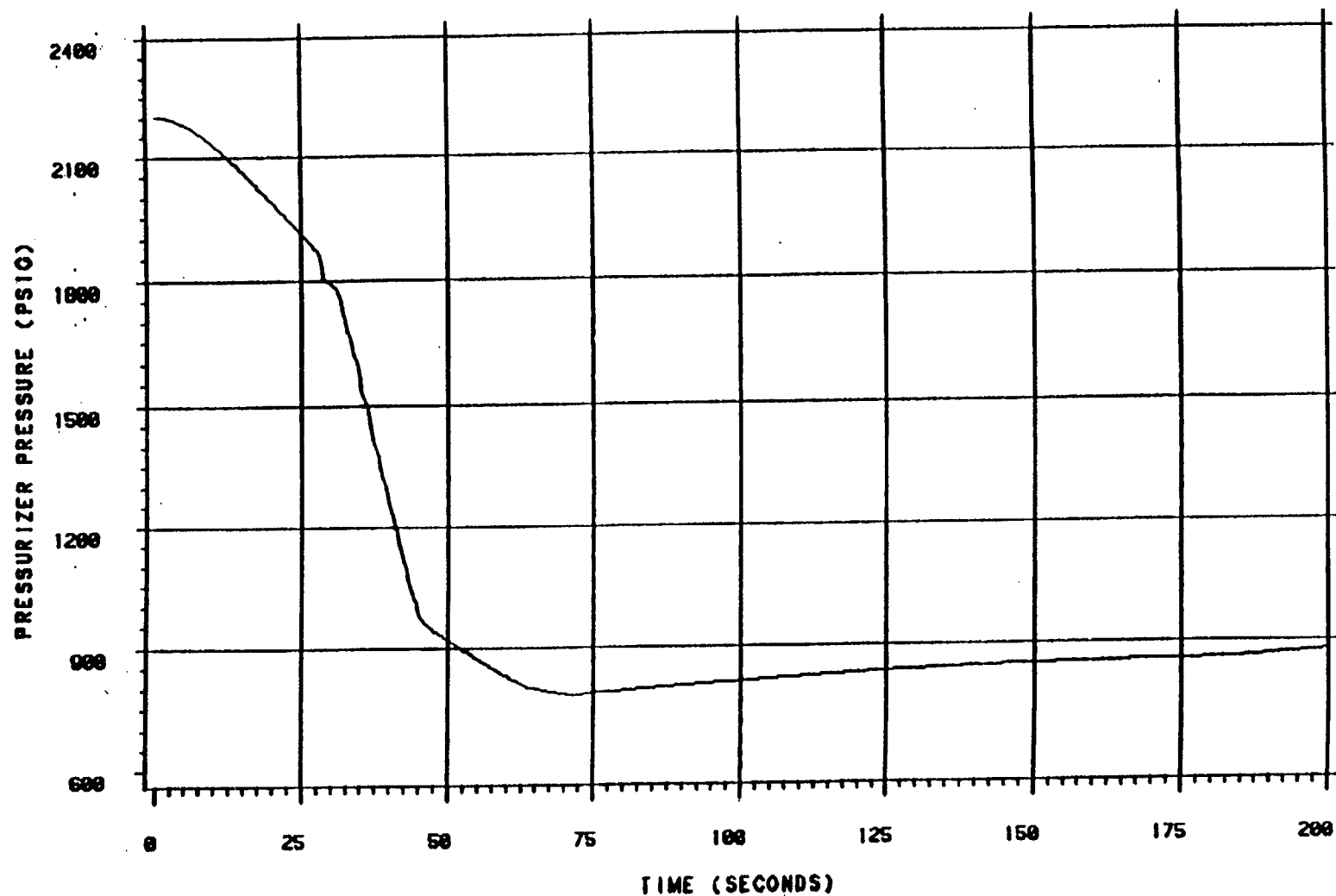


Figure 5-12

# FSAR SECTION 15.1.5 – STEAM LINE BREAK

OFFSITE POWER MAINTAINED

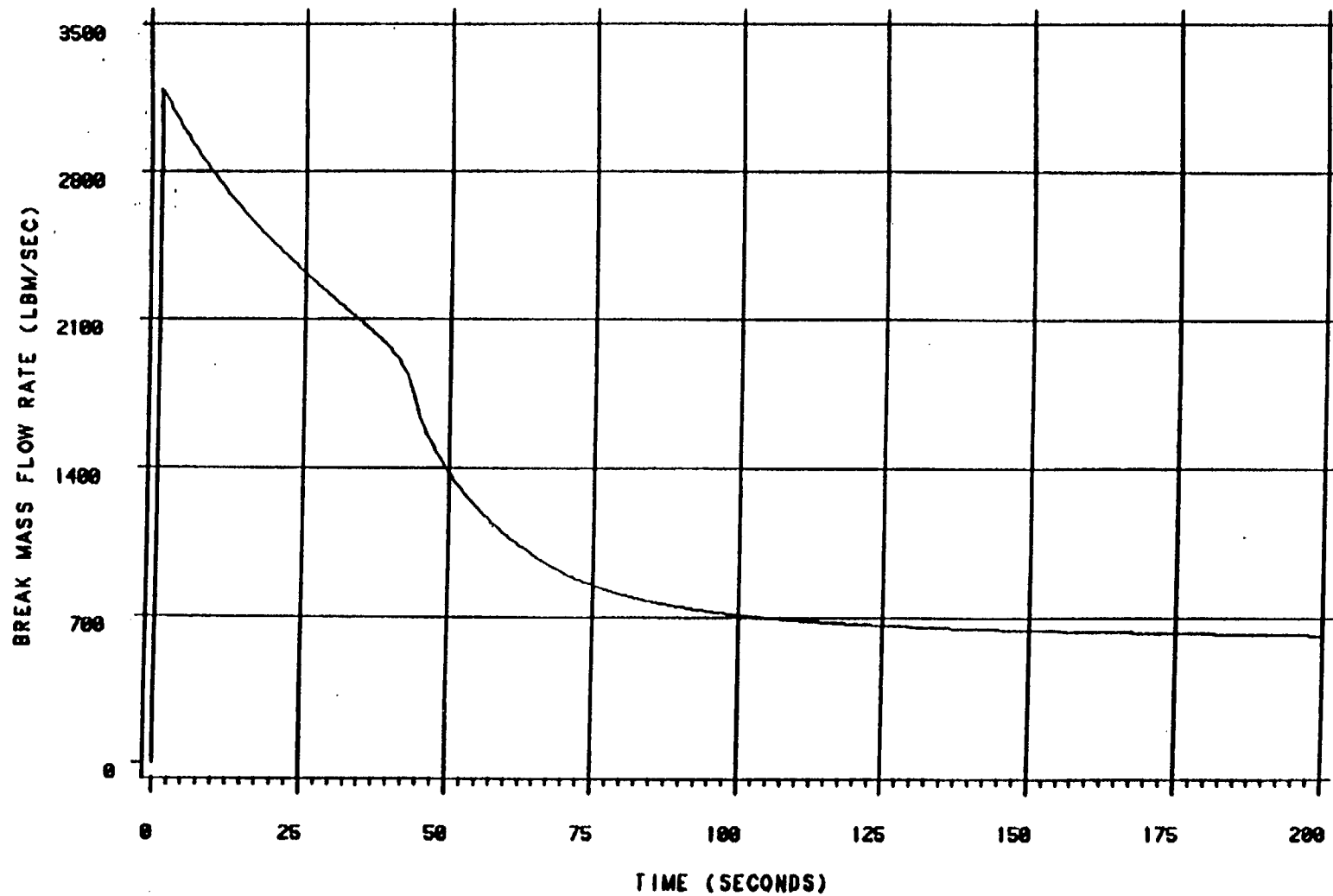


Figure 5-13

# FSAR SECTION 15.1.5 - STEAM LINE BREAK

OFFSITE POWER MAINTAINED

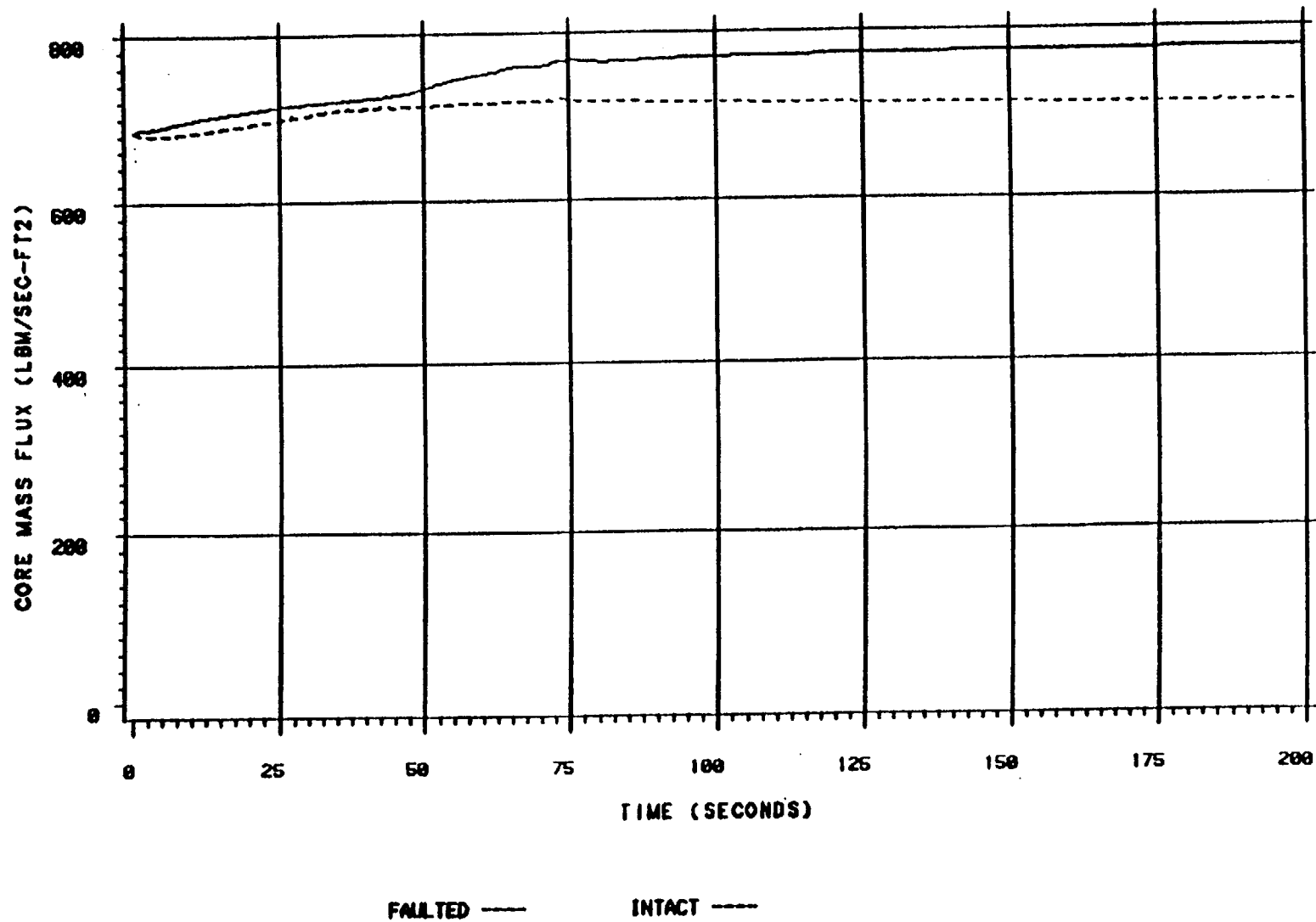
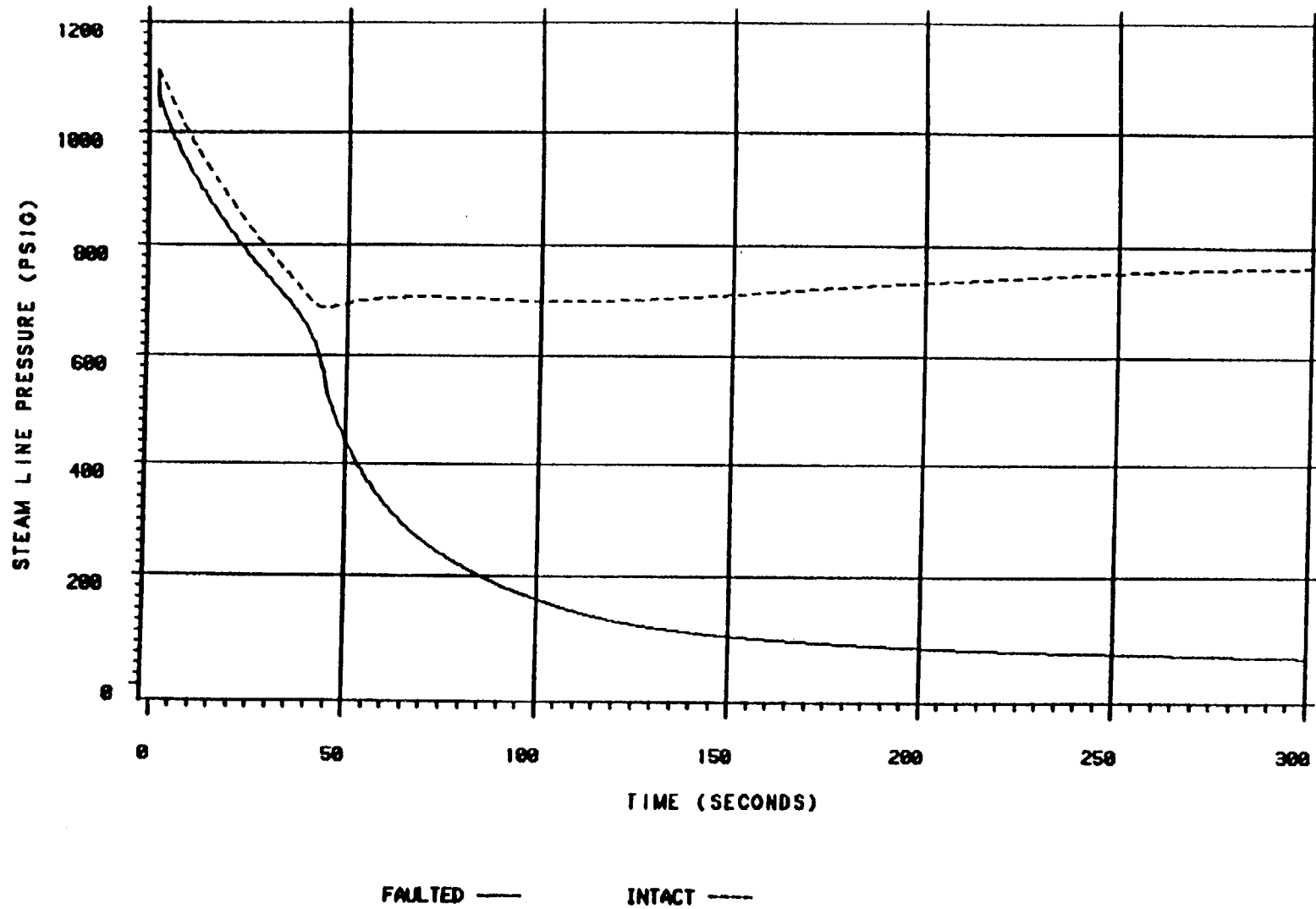


Figure 5-14

# FSAR SECTION 15.1.5 – STEAM LINE BREAK

OFFSITE POWER LOST



# FSAR SECTION 15.1.5 – STEAM LINE BREAK

OFFSITE POWER LOST

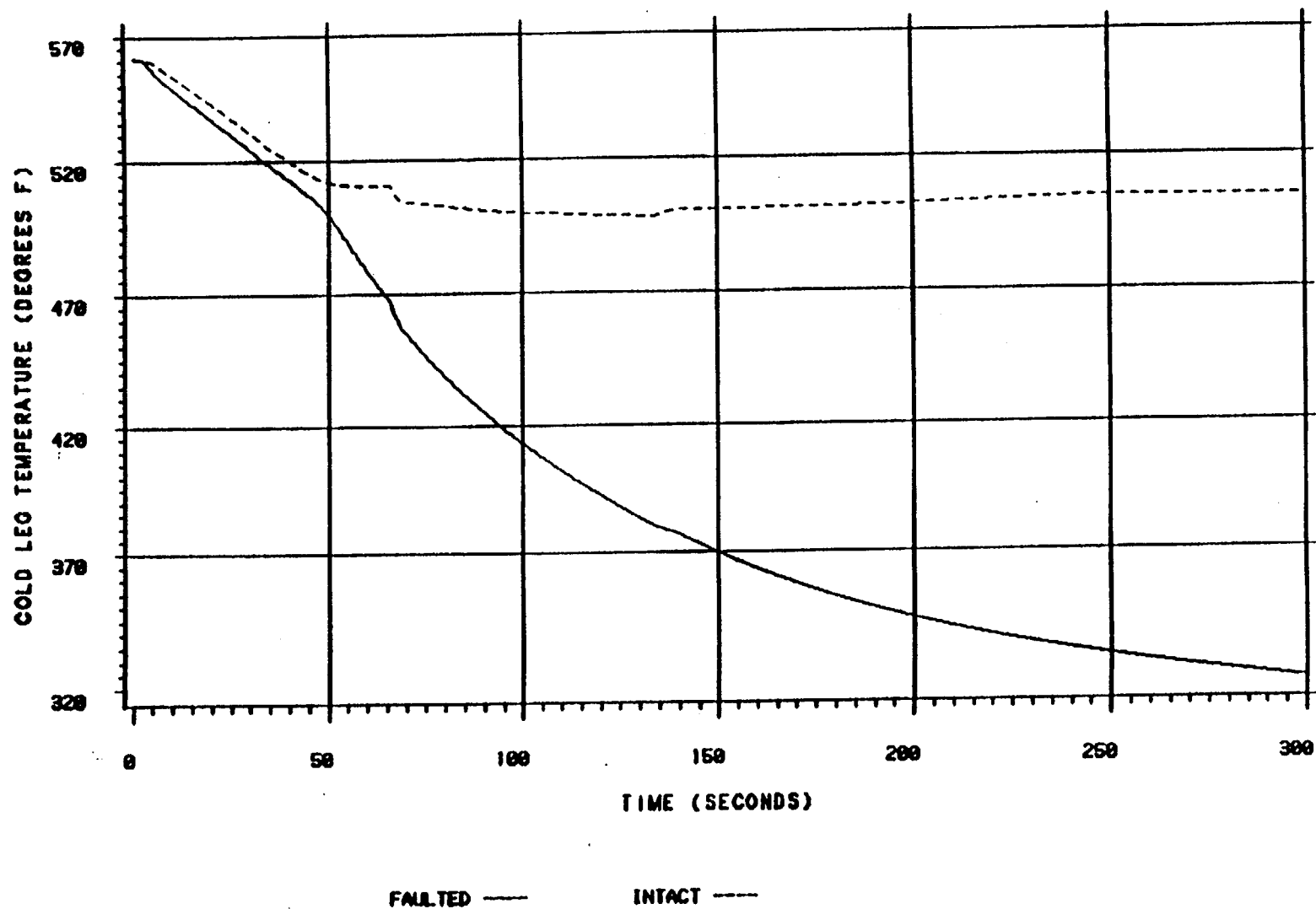


Figure 5-16



# FSAR SECTION 15.1.5 - STEAM LINE BREAK

OFFSITE POWER LOST

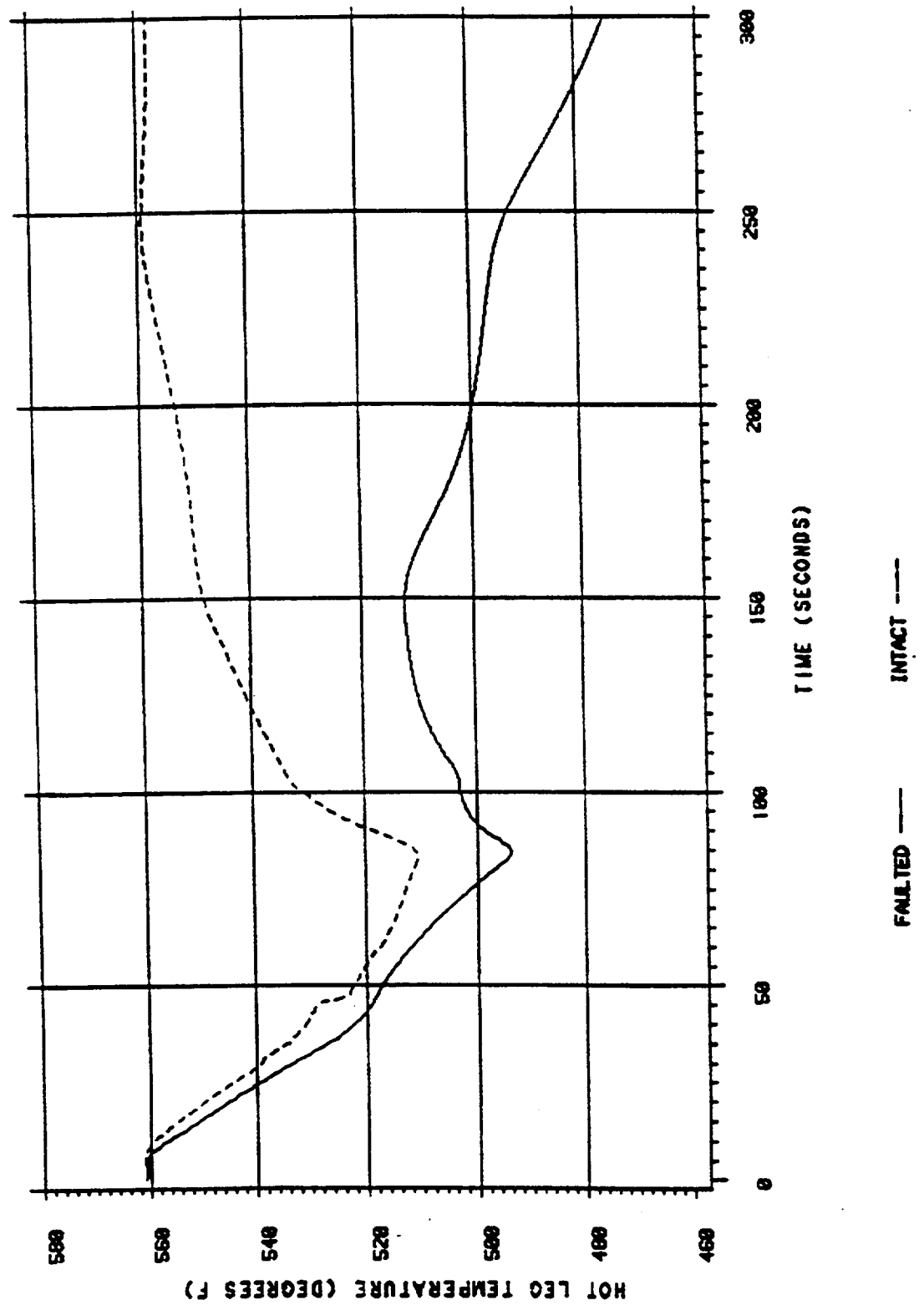


Figure 5-17

# FSAR SECTION 15.1.5 - STEAM LINE BREAK

OFFSITE POWER LOST

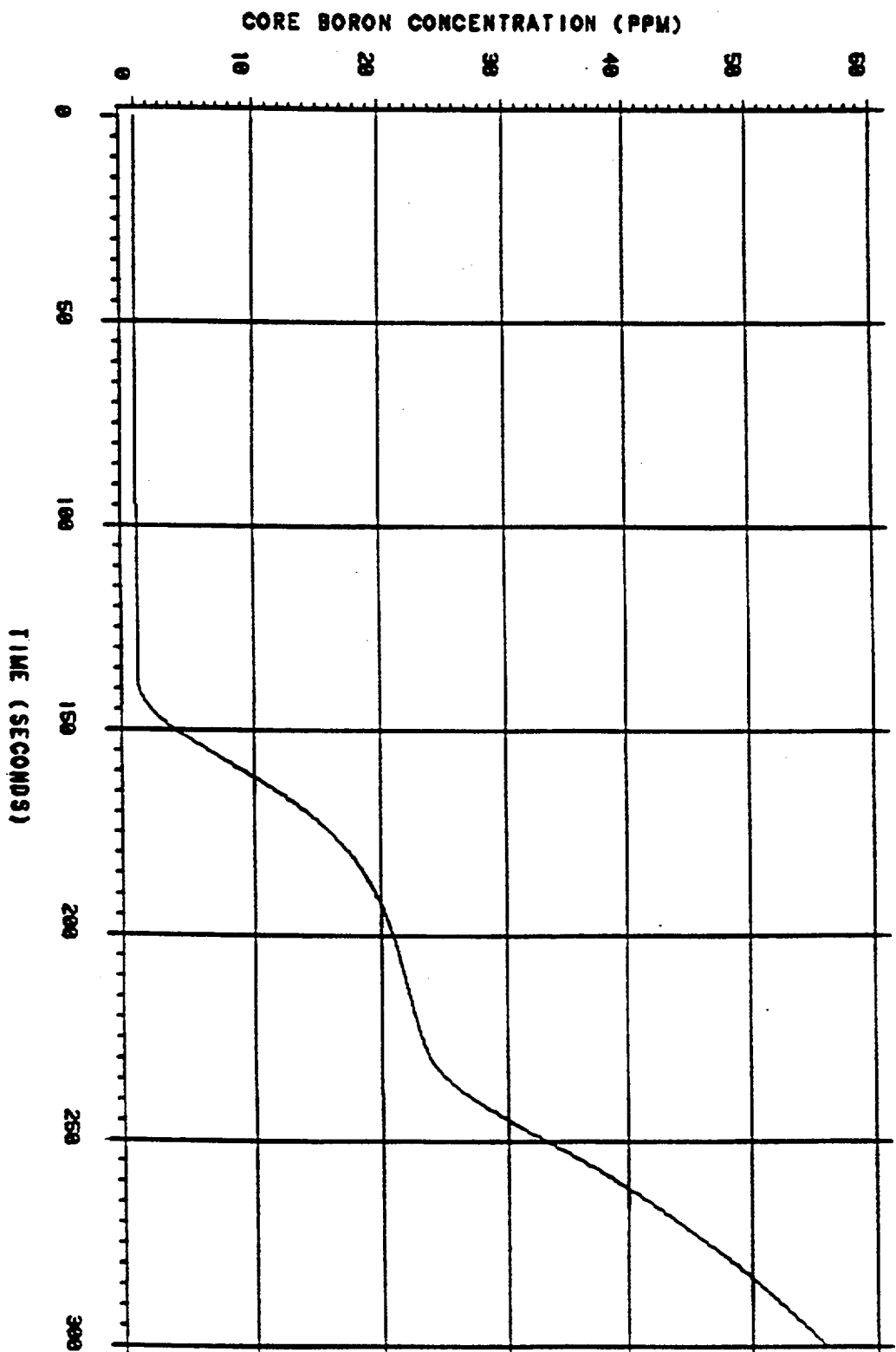


Figure 5-18

# FSAR SECTION 15.1.5 – STEAM LINE BREAK

OFFSITE POWER LOST

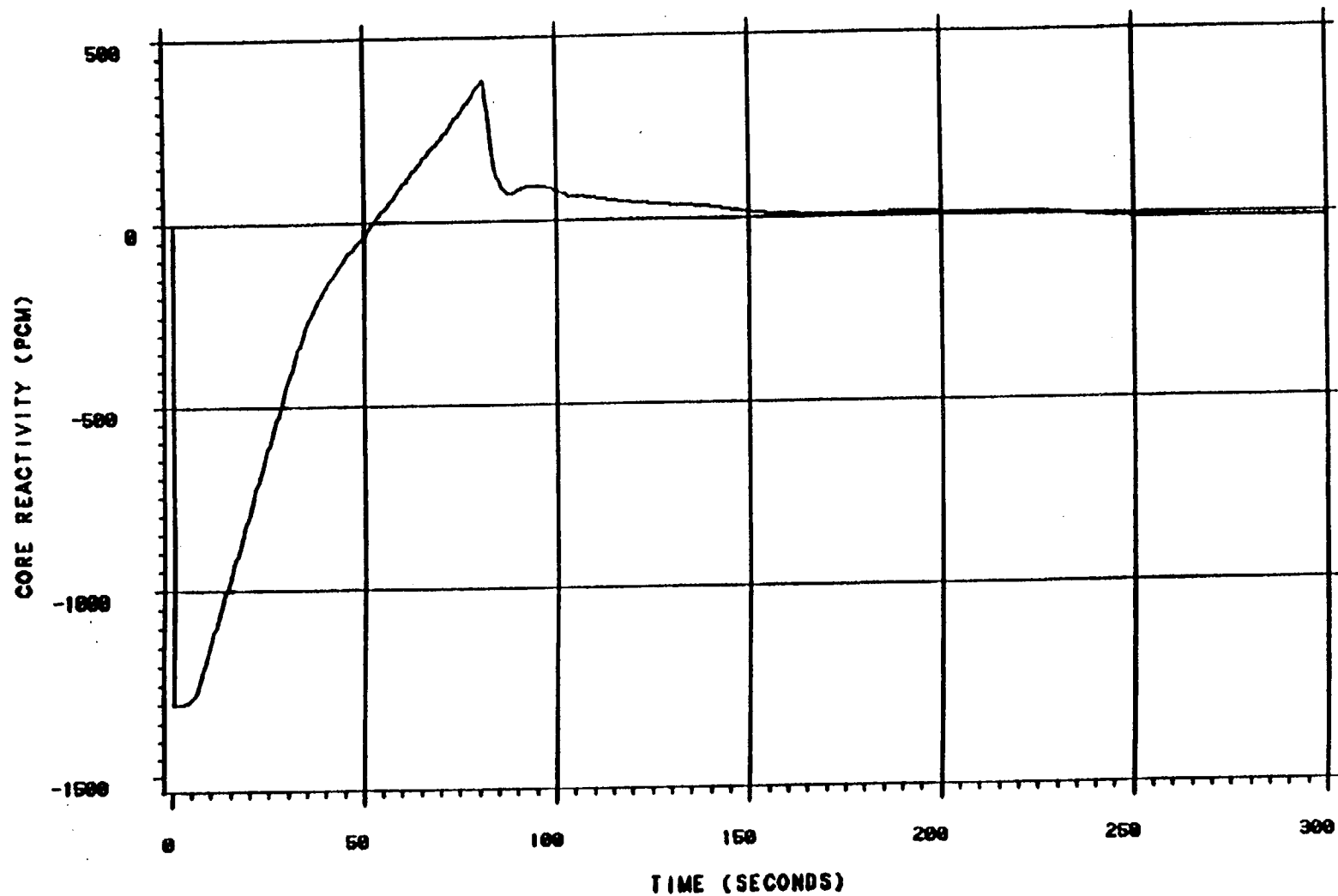


Figure 5-19

# FSAR SECTION 15.1.5 - STEAM LINE BREAK

OFFSITE POWER LOST

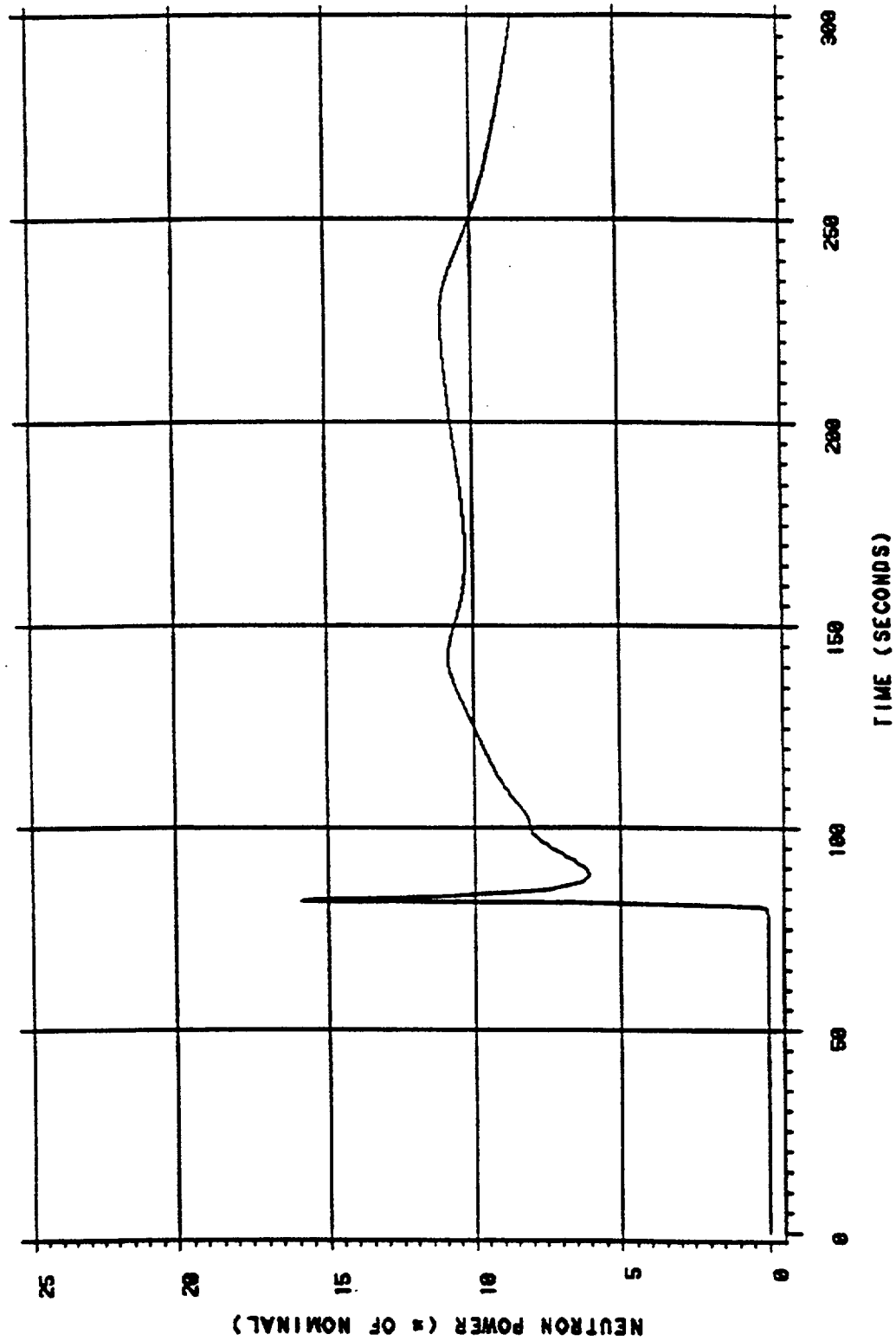


Figure 5-20

# FSAR SECTION 15.1.5 - STEAM LINE BREAK

OFFSITE POWER LOST

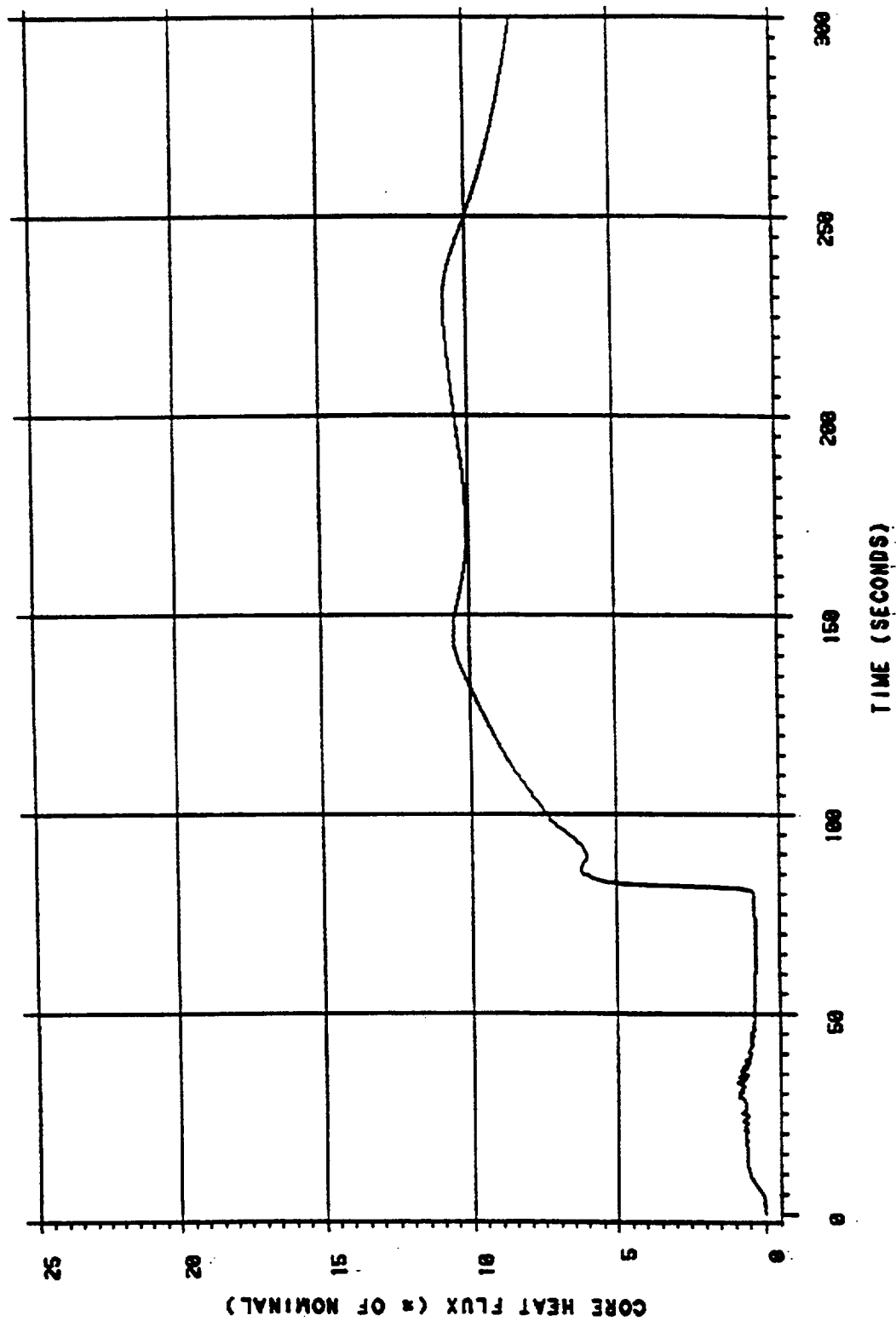


Figure 5-21

# FSAR SECTION 15.1.5 - STEAM LINE BREAK

OFFSITE POWER LOST

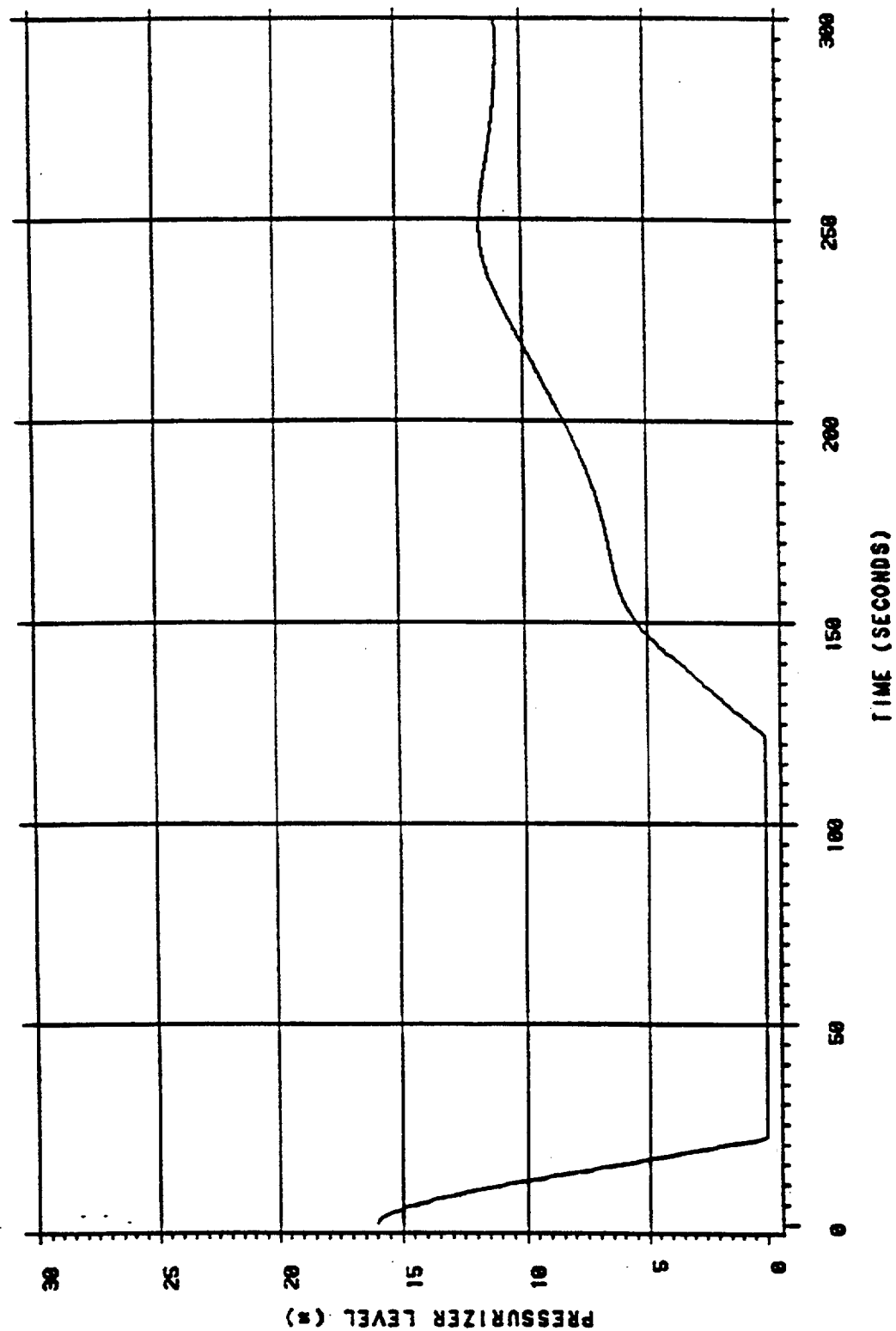


Figure 5-22

# FSAR SECTION 15.1.5 – STEAM LINE BREAK

OFFSITE POWER LOST

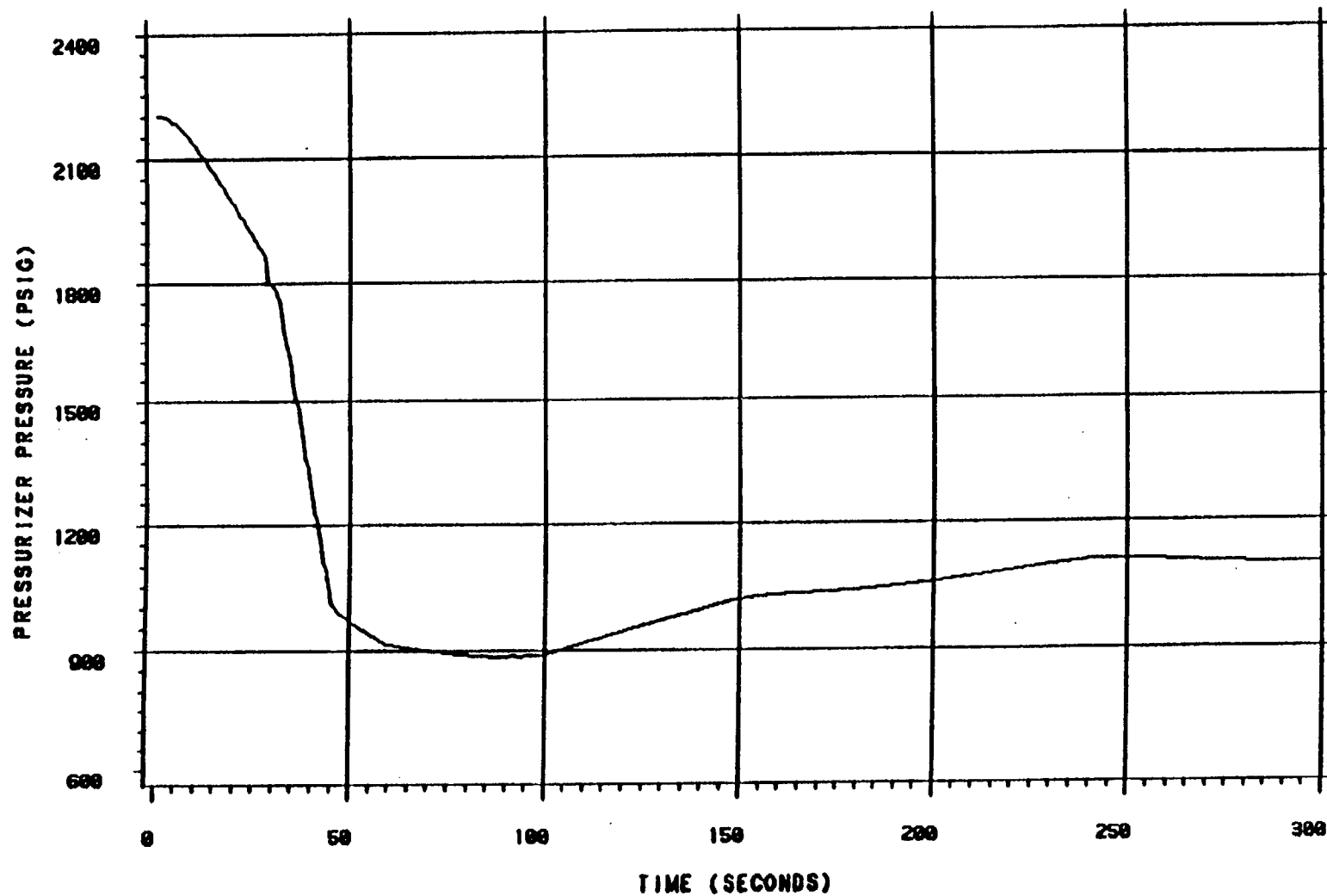


Figure 5-23

# FSAR SECTION 15.1.5 - STEAM LINE BREAK

OFFSITE POWER LOST

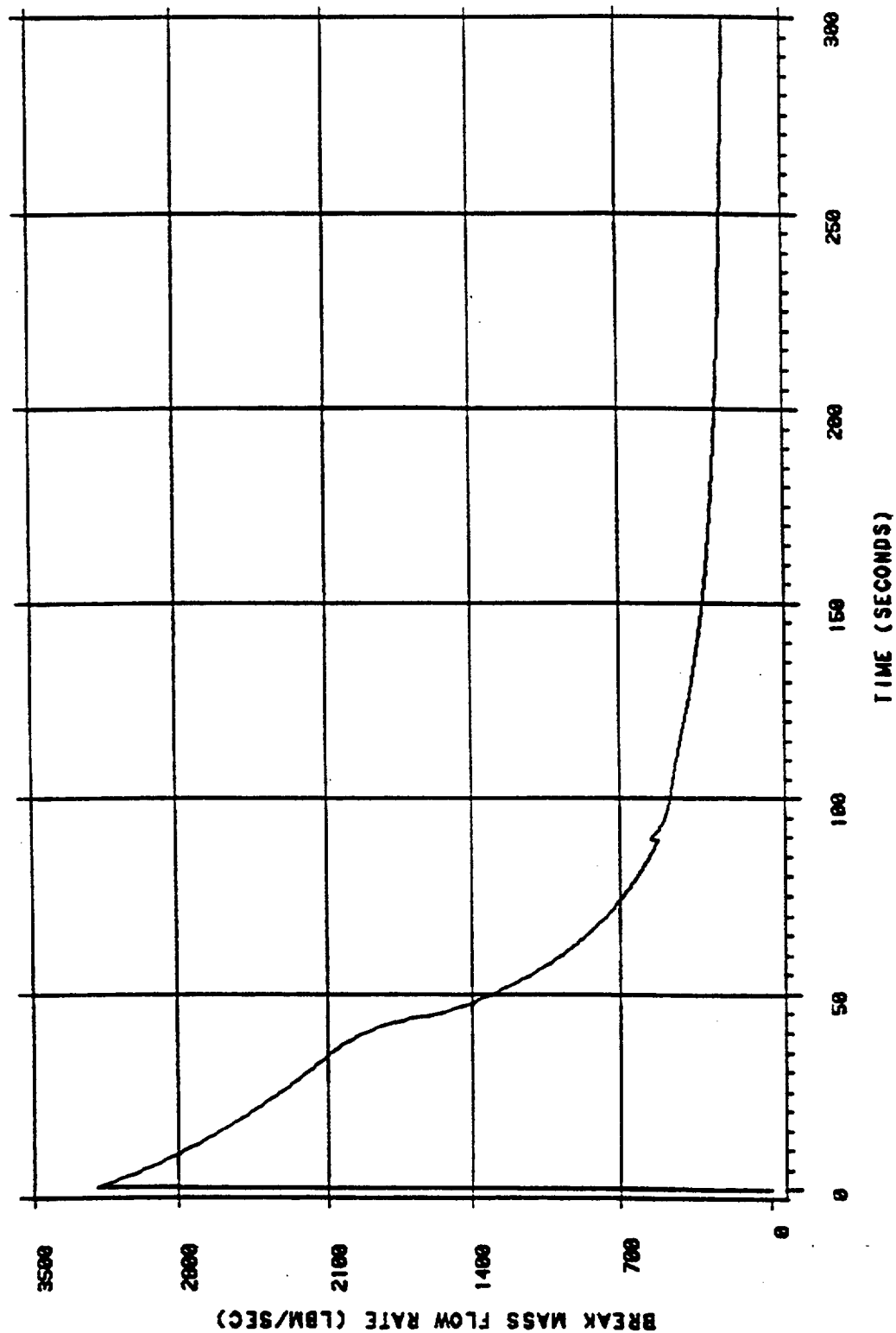


Figure 5-24



# FSAR SECTION 15.1.5 - STEAM LINE BREAK

OFFSITE POWER LOST

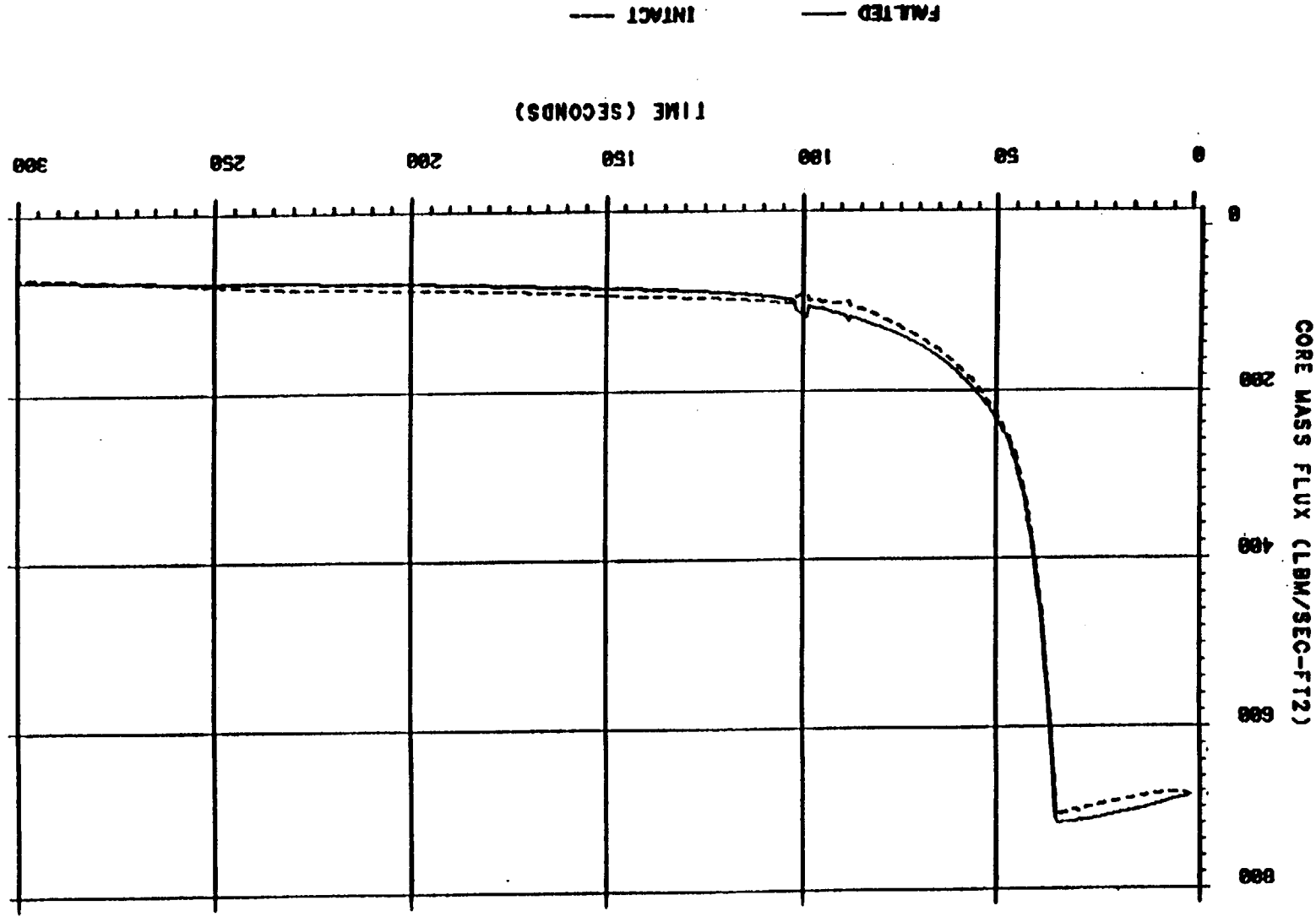


Figure 5-25

Figure 5-26  
Typical Radial Power Distribution  
Offsite Power Available, Peak Heat Flux

|    | R    | P    | N    | M    | L    | K    | J    | H    | G    | F    | E    | D    | C    | B    | A    |
|----|------|------|------|------|------|------|------|------|------|------|------|------|------|------|------|
| 1  |      |      |      |      | 0.11 | 0.17 | 0.17 | 0.20 | 0.20 | 0.21 | 0.15 |      |      |      |      |
| 2  |      |      | 0.11 | 0.07 | 0.16 | 0.10 | 0.19 | 0.12 | 0.22 | 0.13 | 0.24 | 0.11 | 0.20 |      |      |
| 3  |      | 0.11 | 0.26 | 0.18 | 0.14 | 0.31 | 0.15 | 0.19 | 0.19 | 0.46 | 0.23 | 0.31 | 0.48 | 0.21 |      |
| 4  |      | 0.07 | 0.18 | 0.19 | 0.50 | 0.47 | 0.54 | 0.26 | 0.73 | 0.72 | 0.84 | 0.34 | 0.34 | 0.14 |      |
| 5  | 0.11 | 0.16 | 0.14 | 0.50 | 0.55 | 0.73 | 0.60 | 0.77 | 0.80 | 1.17 | 1.02 | 1.00 | 0.30 | 0.41 | 0.32 |
| 6  | 0.17 | 0.10 | 0.31 | 0.47 | 0.73 | 0.37 | 0.64 | 0.41 | 0.91 | 0.68 | 1.58 | 1.07 | 0.74 | 0.28 | 0.57 |
| 7  | 0.17 | 0.19 | 0.15 | 0.54 | 0.60 | 0.64 | 0.87 | 1.24 | 1.32 | 1.33 | 1.57 | 1.44 | 0.43 | 0.68 | 0.69 |
| 8  | 0.20 | 0.12 | 0.19 | 0.26 | 0.77 | 0.41 | 1.24 | 0.81 | 2.36 | 1.22 | 2.83 | 1.01 | 0.78 | 0.56 | 1.03 |
| 9  | 0.20 | 0.22 | 0.19 | 0.73 | 0.80 | 0.91 | 1.32 | 2.36 | 3.03 | 4.21 | 3.91 | 3.74 | 1.00 | 1.32 | 1.23 |
| 10 | 0.21 | 0.13 | 0.46 | 0.72 | 1.17 | 0.68 | 1.33 | 1.22 | 4.21 | 5.98 | 6.90 | 3.90 | 2.59 | 0.80 | 1.43 |
| 11 | 0.15 | 0.24 | 0.23 | 0.84 | 1.02 | 1.58 | 1.57 | 2.83 | 3.91 | 6.90 | 4.88 | 4.33 | 1.22 | 1.52 | 1.00 |
| 12 |      | 0.11 | 0.31 | 0.34 | 1.00 | 1.07 | 1.44 | 1.01 | 3.74 | 3.90 | 4.33 | 1.66 | 1.74 | 0.67 |      |
| 13 |      | 0.20 | 0.48 | 0.34 | 0.30 | 0.74 | 0.43 | 0.78 | 1.00 | 2.59 | 1.22 | 1.74 | 2.75 | 1.23 |      |
| 14 |      |      | 0.21 | 0.14 | 0.41 | 0.28 | 0.68 | 0.56 | 1.32 | 0.80 | 1.52 | 0.67 | 1.23 |      |      |
| 15 |      |      |      |      | 0.32 | 0.57 | 0.69 | 1.03 | 1.23 | 1.43 | 1.00 |      |      |      |      |



- Stuck Rod Location

Figure 5-27  
Typical Radial Power Distribution  
Offsite Power Lost, Peak Heat Flux

|    | R    | P    | N    | M    | L    | K    | J    | H    | G    | F    | E    | D    | C    | B    | A    |
|----|------|------|------|------|------|------|------|------|------|------|------|------|------|------|------|
| 1  |      |      |      |      | 0.26 | 0.43 | 0.41 | 0.40 | 0.42 | 0.45 | 0.27 |      |      |      |      |
| 2  |      |      | 0.20 | 0.18 | 0.40 | 0.29 | 0.45 | 0.25 | 0.47 | 0.30 | 0.43 | 0.20 | 0.22 |      |      |
| 3  |      | 0.20 | 0.47 | 0.52 | 0.35 | 0.68 | 0.35 | 0.39 | 0.36 | 0.73 | 0.39 | 0.57 | 0.52 | 0.22 |      |
| 4  |      | 0.18 | 0.52 | 0.39 | 0.87 | 0.93 | 1.13 | 0.50 | 1.20 | 1.01 | 0.97 | 0.44 | 0.59 | 0.21 |      |
| 5  | 0.26 | 0.40 | 0.35 | 0.87 | 1.06 | 1.45 | 1.30 | 1.36 | 1.39 | 1.61 | 1.23 | 1.03 | 0.43 | 0.50 | 0.34 |
| 6  | 0.43 | 0.29 | 0.68 | 0.93 | 1.45 | 0.70 | 1.43 | 0.71 | 1.60 | 0.85 | 1.82 | 1.18 | 0.86 | 0.38 | 0.59 |
| 7  | 0.41 | 0.45 | 0.35 | 1.13 | 1.30 | 1.43 | 1.32 | 1.36 | 1.59 | 1.88 | 1.83 | 1.56 | 0.49 | 0.66 | 0.62 |
| 8  | 0.40 | 0.25 | 0.39 | 0.50 | 1.36 | 0.71 | 1.36 | 0.98 | 1.98 | 1.27 | 2.44 | 0.93 | 0.73 | 0.47 | 0.74 |
| 9  | 0.42 | 0.47 | 0.36 | 1.20 | 1.39 | 1.60 | 1.59 | 1.98 | 2.82 | 3.82 | 3.22 | 2.74 | 0.84 | 1.06 | 0.94 |
| 10 | 0.45 | 0.30 | 0.73 | 1.01 | 1.61 | 0.85 | 1.88 | 1.27 | 3.82 | 3.63 | 4.25 | 2.51 | 1.78 | 0.74 | 1.08 |
| 11 | 0.27 | 0.43 | 0.39 | 0.97 | 1.23 | 1.82 | 1.83 | 2.44 | 3.22 | 4.25 | 3.01 | 2.36 | 0.96 | 1.07 | 0.69 |
| 12 |      | 0.20 | 0.57 | 0.44 | 1.03 | 1.18 | 1.56 | 0.93 | 2.74 | 2.51 | 2.36 | 1.07 | 1.40 | 0.50 |      |
| 13 |      | 0.22 | 0.52 | 0.59 | 0.43 | 0.86 | 0.49 | 0.73 | 0.84 | 1.78 | 0.96 | 1.40 | 1.27 | 0.55 |      |
| 14 |      |      | 0.22 | 0.21 | 0.50 | 0.38 | 0.66 | 0.47 | 1.06 | 0.74 | 1.07 | 0.50 | 0.55 |      |      |
| 15 |      |      |      |      | 0.34 | 0.59 | 0.62 | 0.74 | 0.94 | 1.08 | 0.69 |      |      |      |      |



- Stuck Rod Location

## 6.0 DROPPED ROD ANALYSIS

### 6.1 Overview

#### 6.1.1 Description of Dropped Rod Accident

The dropped rod accident is described in FSAR Section 15.4.3 (Reference 6-1). The scenarios of concern consist of all single and multiple dropped control rods for rods originating in the same group. Beginning from a full power initial condition (lower power levels are less limiting), one or more rods drop into the core and cause a prompt reduction in reactor power. The Rod Control System, in the automatic control mode, detects a mismatch between reactor and turbine power and responds by withdrawing the controlling rod group, Control Bank D. With the Rod Control System in manual, Control Bank D does not withdraw, and the reactor power decreases to a new equilibrium power level. The power mismatch also results in a reduction in the average core moderator temperature, which typically adds positive reactivity due to the presence of a negative moderator temperature coefficient (MTC). The combination of rod withdrawal and decreasing temperature can cause the reactor to return to full power and even exceed the initial power level. Since the core power peaking is increased by the dropped rod(s), the potential exists for the DNBR limit to be approached.

#### 6.1.2 Acceptance Criteria

The dropped rod accident is classified as an ANS Condition II event, an anticipated transient. Therefore, it must be demonstrated that the DNBR limit is not exceeded. The other Condition II criteria regarding overpressurization or propagation to a Condition III event are not challenged by a dropped rod transient.

#### 6.1.3 Analytical Approach

The dropped rod accident requires a large set of physics parameters to be determined for use as initial and boundary conditions. These parameters are input to a RETRAN-02 (Reference 6-2) McGuire/Catawba model (Reference 6-3) for the system thermal-hydraulic analysis. The RETRAN analysis generates the core statepoint conditions which correspond to the transient

time of minimum DNBR. EPRI-NODE-P (Reference 6-4) or SIMULATE-3P (Reference 6-5) is used to generate power distributions corresponding to the possible dropped rod combinations. The power peaking analysis uses either the pre-drop or the post-drop thermal boundary conditions. The core power distribution along with the core thermal-hydraulic boundary conditions from the RETRAN analysis are then input to a VIPRE-01 (Reference 6-6) McGuire/Catawba model (Reference 6-3) to calculate the minimum DNBR.

## 6.2 Simulation Codes and Models

### 6.2.1 System Thermal-Hydraulic Analysis

The McGuire/Catawba RETRAN model described in Section 3.2 of DPC-NE-3000 (Reference 6-2) is used for the dropped rod analysis. A one-loop model is sufficient since little loop asymmetry develops during this transient. A Catawba Unit 1 model is selected due to the higher primary system T-ave used in the core thermal-hydraulic analysis. There are no differences between the McGuire and Catawba units which are significant in the context of a dropped rod transient. [

]

### 6.2.2 Nuclear Analysis

The dropped rod transient is modeled using EPRI-NODE-P or SIMULATE-3P to predict three-dimensional power distributions and core reactivity. The analysis is based on several cycles at various burnups. Each core analyzed contains 193 Westinghouse optimized fuel assemblies. However, the behavior of the important physics parameters and the bounding values selected for this analysis would not change for cores containing Mk-BW fuel.

### 6.2.3 Core Thermal-Hydraulic Analysis

#### Methodology

The VIPRE-01 code is used for the dropped rod core thermal-hydraulic analyses. VIPRE thermal-hydraulic boundary conditions are obtained from the RETRAN system transient simulation. RETRAN predicts core inlet flow, inlet temperature, outlet pressure, and heat flux for a set of cases based on the dropped rod worth and limiting burnup condition. A core neutronics simulation code provides the axial shape and radial power distributions. The standard [ ] VIPRE model (Reference 6-3) is used to calculate the limiting statepoint local coolant properties and DNBR. One critical heat flux (CHF) correlation used to evaluate DNBR is the B&W BWCMV CHF correlation (Reference 6-7). The VIPRE analysis employs the BWCMV statistical core design DNBR limit of 1.55 (Reference 6-8). The second CHF correlation used to perform DNB analysis is the BWU-Z CHF correlation (Reference 6-9). The BWU-Z correlation was reviewed and approved by the NRC for use in McGuire/Catawba analyses in References 6-10 and 6-11. The BWU-Z statistical core design limit is 1.37 (Reference 6-12).

#### Model Description

## 6.3 Transient Analysis

### 6.3.1 Initial Conditions

The VIPRE evaluation of the minimum DNBR resulting from the dropped rod transient uses the statistical core design (SCD) methodology. Consequently, the following RETRAN initial conditions are specified as nominal values since the uncertainty is factored into the SCD design limit.

- Power level = 100% FP
- RCS flow = 382,000 gpm
- Pressurizer pressure = 2235 psig
- RCS T-ave = 590.8°F
- Core bypass flow = 7.5%

A discussion of the non-SCD parameters and the basis for selecting their initial condition values follows.

#### Pressurizer Level

A low initial pressurizer level reduces the initial core outlet pressure and minimizes the transient pressure response, which is conservative for DNBR. The full power programmed pressurizer level for the Catawba Unit 1 model is 60%. The initial condition uncertainty allowance for reduced pressurizer level is 9%. Therefore, the initial pressurizer level for this analysis is 51%.

#### SG NR Level

A low initial steam generator narrow range level minimizes the initial steam generator inventory. Catawba Unit 1 has model D3 steam generators that have a programmed level that varies with reactor power. A low initial level serves to maximize effects due to changes in feedwater flow. This parameter has no significant impact on the results of the dropped rod transient. The full power programmed steam generator narrow range level is 66.5%. The initial condition

uncertainty allowance is 8%. Therefore, the initial steam generator level for this analysis is 58.5%.

### Average Fuel Temperature

Maximum average fuel temperatures for an equilibrium 390 EFPD fuel cycle with Mark-BW fuel at BOC, MOC and EOC conditions are used. The average fuel temperatures used are [ ] at BOC, MOC and EOC, respectively.

### SG Tube Plugging

Assuming no steam generator tube plugging maximizes the initial steam line pressure and results in a more limiting transient. Therefore, no tube plugging is assumed for this analysis. This parameter has no significant impact on the results of the dropped rod transient.

## 6.3.2 Boundary Conditions

### 6.3.2.1 Physics Parameters

The important physics parameters required by the RETRAN and VIPRE models for the dropped rod analysis are discussed below. These parameters are evaluated for the dropped rod scenarios over a range of conditions to ensure that the selected values bound current and future reload designs. The RETRAN analysis uses values for each of these parameters that are consistent in terms of a beginning, middle, or end-of-cycle condition.

|                                      | <u>RETRAN</u> | <u>VIPRE</u> |
|--------------------------------------|---------------|--------------|
| • Dropped rod worth                  | X             |              |
| • Control Bank D worth               | X             |              |
| • Core tilt following rod drop       | X             |              |
| • Moderator temperature coefficient  | X             |              |
| • Doppler temperature coefficient    | X             |              |
| • Effective delayed neutron fraction | X             |              |
| • Radial peaking factor              |               | X            |
| • Axial peaking factor               |               | X            |



### Dropped Rod Worth

The dropped rod worth ranges up to [ ] pcm. This worth exceeds the worth of all possible combinations of dropped rods from the same rod group.

### Control Bank D Worth

Control Bank D worth ranges from [ ] pcm at the rod insertion limit as a function of burnup.

### FΔH Versus Worth

Power peaking increases in those areas of the core opposite the dropped rod(s) and is generally greatest for those cases in which three rods are dropped. The effect of a dropped rod on FΔH is a function of burnup, dropped rod worth, and the number of dropped rods. Enveloping FΔH responses derived from assembly average power are presented in Figures 6-2 to 6-4.

### Axial Shape

A bounding axial shape at each burnup condition, based on a top peaked power distribution, is chosen for the thermal-hydraulic analysis.

### Core Tilt Following Rod Drop

Fifty-three full-length control rods of two designs, Ag-In-Cd and boron carbide ( $B_4C$ ), are analyzed. All combinations of rods in each group of the control banks and shutdown banks are dropped into the core from the rod insertion limit (RIL) and the all-rods-out (ARO) position to determine which dropped rod cases would result in the worst excore tilts and power peaking. Figure 6-5 illustrates the effect of increasing dropped rod worth on the induced tilt. In general, a set of three dropped rods results in the most severe combination of excore tilts and power peaking. The reactor response to a dropped rod transient depends on the core tilt detected by the excore detectors since the excore detector signal is an input to the Rod Control System. Dropped rods cause the power level to decrease in the vicinity of the dropped rod and to increase in areas

away from the dropped rod. The excore tilt for the four quadrants is modeled by using the assemblies closest to the excore detector to generate a detector response.

#### Moderator Temperature Coefficient

Several fuel cycles were reviewed to determine realistic but conservative moderator temperature coefficients (MTCs) to use in the dropped rod analysis. Conservative slopes were chosen for the MTCs versus moderator temperature at several burnup statepoints and boron concentrations. An MTC was conservatively chosen at the burnup statepoints analyzed for the HFP, nominal condition moderator temperature. The HFP moderator temperature and the slope of the MTC versus moderator temperature curve are used to determine MTCs at various power levels occurring during the dropped rod transient. The MTC assumed is a least-negative or most-positive value depending on the core burnup and moderator temperature. This assumption minimizes the negative reactivity feedback that is available when the post-drop power level increases as Control Bank D is withdrawn.

#### Doppler Temperature Coefficient

The Doppler temperature coefficient is selected as a least-negative value. This assumption minimizes the negative reactivity feedback that is available when the post-drop power level increases as Control Bank D is withdrawn.

#### Effective Delayed Neutron Fraction

The effective delayed neutron fraction is not a very important parameter since the transient response near the DNBR statepoint is slow. A minimum value of beta-effective is used.

#### 6.3.2.2 Reactor Protection System

The RETRAN analysis takes credit for a reactor trip only on low pressurizer pressure. The trip setpoint is reached only for higher dropped rod worth cases at beginning-of-cycle. The overtemperature and overpower DT trip setpoints may be reached for some dropped rod events.

No credit is taken for the negative flux rate trip function, low-low steam generator level trip or main steam isolation on low steam line pressure.

#### 6.3.2.3 Power Range Nuclear Instrumentation

[

]

#### 6.3.2.4 Rod Control System

The Rod Control System is explicitly modeled in the RETRAN analysis. The controller uses a power mismatch signal and a temperature error signal to determine Control Bank D insertion or withdrawal and rod speed. The power mismatch signal is a difference between turbine power (impulse pressure) and the auctioneered-high NI flux indication. The temperature error signal is a difference between a reference temperature based on turbine power and the auctioneered-high primary loop T-ave indication. Due to the importance of Control Bank D withdrawal on the dropped rod analysis, the worst case single failure has been determined to result in the NI flux indication auctioneering low. This failure causes the maximum post-drop power levels by accelerating the onset and increasing the rate of Control Bank D withdrawal.

#### 6.3.2.5 Pressurizer Pressure and Level Control

Since the dropped rod transient is a DNB transient, pressurizer sprays and the pressurizer PORV are assumed to function in order to minimize primary pressure. Pressurizer heaters are assumed not to function. Pressurizer level control is assumed to be in manual, and is not important for this transient.

### 6.3.2.6 Main Feedwater and Turbine Control

## 6.4 Results and Conclusions

### 6.4.1 System Transient Results

The dropped rod event is analyzed at beginning, middle, and end-of-cycle conditions. The typical transient response at beginning and end-of-cycle conditions are discussed in detail below, and the results of the bounding cases are presented.

#### 6.4.1.1 Typical Beginning-of-Cycle Response

##### 100 pcm Case

Reactor power (Figure 6-6) initially decreases rapidly in response to the dropped rod. Then power recovers as the Rod Control System withdraws Control Bank D and power overshoots the initial level. Reactor power reaches a maximum value of 115.3% and starts to decrease again before the Rod Control System terminates rod withdrawal. Also shown on Figure 6-6 is the NI signal that is input to the Rod Control System. While core power reaches a maximum of 115.3%, the NI signal is only about 72%. Control Bank D position is shown in Figure 6-7. Bank D motion results from the combination of power mismatch and temperature error signals. Average loop temperature (T-ave) as shown in Figure 6-8 initially decreases about 2°F and then increases about 7°F. The T-ave response is determined by the balance between core power and the steam load. Pressurizer level, shown in Figure 6-9, responds to the change in T-ave. The pressurizer pressure response (Figure 6-10) is dictated by changes in pressurizer level and by the actuation of pressure mitigation equipment. Pressure initially decreases due to the impact of the dropped rod

on reactor power, and then increases with power. Pressurizer sprays and PORVs actuate to minimize primary pressure, which is conservative with respect to DNBR. The PORVs continue to cycle until T-ave begins to decrease. The limiting statepoint occurs at the time of maximum heat flux.

### Higher Worth Cases

As the dropped rod worth is increased above 100 pcm, the initial reduction in core power is larger, and consequently the initial reductions in T-ave and pressurizer pressure are larger. For beginning-of-cycle (BOC) cases at or above [ ] pcm, a reactor trip occurs on low-low pressurizer pressure and DNB is not a concern. In general, the transient responses to dropped rod worth cases at [ ] pcm have lower statepoint values for core power, pressurizer pressure, and T-ave. The difference in statepoint conditions mainly results from the response of the Rod Control System to the combined power mismatch and temperature error signals.

#### 6.4.1.2 Typical End-of-Cycle Response

##### 400 pcm Case

Reactor power (Figure 6-11) initially decreases rapidly in response to the dropped rod, then increases due to the negative MTC and to the Rod Control System withdrawing Control Bank D. Reactor power recovers, overshoots its initial value reaching a maximum value of 109.8%, and starts to decrease before the Rod Control System terminates rod withdrawal. Also shown on Figure 6-11 is the NI signal input to the Rod Control System. Control Bank D position is shown on Figure 6-12. T-ave (Figure 6-13) initially decreases approximately 7°F, then increases about 3°F to the point of maximum heat flux. T-ave decreases until core power exceeds the steam load. Pressurizer level (Figure 6-14) also follows the trend of T-ave, reaching a minimum of about 42% at 20 seconds. Pressurizer pressure (Figure 6-15) initially decreases with the drop in T-ave and reaches a minimum of approximately 2150 psig before increasing to a maximum of about 2280 psig. Pressurizer spray actuates at approximately 47 seconds and continues for the remainder of the simulation. The limiting statepoint occurs at the time of maximum heat flux.

### Lower Worth Cases

For dropped rod worths lower than 400 pcm, the power overshoot is slightly higher. The initial power reduction is less, and therefore, the reactivity addition due to moderator feedback and Bank D withdrawal has less of a deficit to offset. As in the BOC cases, the most important boundary condition is the response of the Rod Control System.

### Higher Worth Cases

As the dropped rod worth increases above 400 pcm, the power overshoot decreases in magnitude. The most significant change with increasing worth is that pressurizer pressure is significantly lower at the statepoint. The substantial contraction of the primary coolant immediately following the rod drop, and the associated depressurization, have not resulted in pressurizer level and pressure recovering to the initial values at the statepoint time.

#### 6.4.1.3 Limiting Statepoint Selection

### Cases Analyzed

Dropped rod cases are analyzed at beginning, middle, and end-of-cycle (EOC) conditions. The dropped rod worth for cases analyzed at a given time in cycle is in increments of 100 pcm until a reactor trip on low pressurizer pressure occurs. Reactor trips on low pressurizer pressure occur in the [ ] pcm beginning-of-cycle case and [ ] pcm middle-of-cycle (MOC) case. The maximum dropped rod worth analyzed is [ ] pcm.

### Beginning-of-Cycle Cases

The trends of the key results for the spectrum of BOC cases are shown in Figures 6-16 through 6-18. The peak core power (Figure 6-16) decreases with increasing dropped rod worth. T-ave (Figures 6-17) decreases with increasing rod worth. In the [ ] pcm case, pressurizer pressure (Figure 6-18) at the statepoint does not follow the trend of decreasing pressure with increasing dropped rod worth. During this case, reactor power continues to increase for several minutes

after Bank D is fully withdrawn due to the positive MTC applied. During this relatively long transient pressurizer pressure recovers to above its initial value.

#### Middle-of-Cycle Cases

The trends of the key results for the spectrum of MOC cases are shown in Figures 6-19 through 6-21. The peak core power (Figure 6-19) decreases with increasing dropped rod worth. T-ave (Figure 6-20) also decreases with decreasing rod worth. Above [ ] pcm, pressurizer pressure (Figure 6-21) at the peak power statepoint does not recover to the initial value.

#### End-of-Cycle Cases

The trends of the key results for the spectrum of end-of-cycle cases are shown in Figures 6-22 through 6-24. The peak core power (Figure 6-22) decreases with increasing dropped rod worth. T-ave (Figure 6-23) also decreases with decreasing rod worth. Above [ ] pcm, pressurizer pressure (Figure 6-24) at the peak power statepoint does not recover to the initial value.

#### Limiting Cases

For each dropped rod worth the RETRAN analysis results were compared and the limiting burnup condition was determined. The selection of the limiting case is based on the product of the peak core power and the associated radial peaking factor for that dropped rod worth and burnup. The burnup with the largest value of this parameter is then evaluated with respect to the other important DNB parameters (pressure, temperature, flow) to confirm the limiting burnup condition. The limiting burnup condition for each dropped rod worth is then analyzed with VIPRE to determine the minimum DNBR. The limiting cases were determined to be as follows:

| Dropped Rod Worth (pcm) | Burnup Condition |
|-------------------------|------------------|
|                         |                  |

Figures 6-25 through 6-27 show the trends of neutron power, T-ave, and pressurizer pressure for the limiting analyses. In all cases the limiting statepoint occurred at the time of peak core power.

#### 6.4.2 Core Response

##### 6.4.2.1 Statepoint Conditions

RETRAN results yield the following statepoint conditions for the limiting cases analyzed.

| Case | Dropped Rod Worth (pcm) | Heat Flux (MBtu/hr-ft <sup>2</sup> ) | Core Inlet Temperature (°F) | Core Outlet Flow (Mbm/hr-ft <sup>2</sup> ) | Core Pressure (psia) |
|------|-------------------------|--------------------------------------|-----------------------------|--|----------------------|
|      |                         |                                      |                             |  |                      |

##### 6.4.2.2 Thermal-Hydraulic Results for DNBR



The dropped rod event is analyzed utilizing the VIPRE-01 code and a SCD DNBR limit of 1.55. The [ ] VIPRE model DNBR results for the limiting cases with the given axial shapes (Figure 6-28) and radial power peaking (Figures 6-2 through 6-4) are greater than 1.55 for each case.

## 6.5 Cycle Specific Evaluation

The reference dropped rod analysis is verified to be bounding by comparison of several cycle-specific physics parameters against values assumed in the reference analysis. Physics parameters that are checked for each reload core are:

- Initial  $F_{DH}$
- Axial Flux Shape
- Moderator and Doppler Temperature Coefficients
- Maximum Dropped Rod Worth
- Available Control Bank Worth for Withdrawal

Several reload cycles were analyzed in order to determine bounding inputs for the reference dropped rod analysis. The results of these analyses established bounding curves, versus the number and worth of dropped rods, defining both the increase in radial peaking and limiting excore detector responses. These inputs are considered independent of the reload core design and will not be checked on a cycle-specific basis.

While the above physics parameters are not expected to change for a reload core, they are checked to ensure that the reference dropped rod analysis remains valid. For each reload core, the maximum core  $F_{DH}$  for the pre-dropped condition is verified to be less than [ ] for allowed rod insertions. Moderator and Doppler temperature coefficients are also verified to be conservative by comparison against the coefficients used in the reference analysis. The axial shapes assumed in the reference analysis will be checked for all dropped rod combinations. The maximum allowable dropped rod worth is verified to be less than the maximum worth analyzed [ ] pcm). Also, the available control bank worth for withdrawal is verified to be less than the values assumed in the reference analysis.

In conclusion, the reference dropped rod analysis is applicable to the reload core if the cycle-specific physics parameters are determined to conservatively bound the values assumed in the reference analysis. In the unlikely event that any of the reference analysis input physics parameters do not bound a given reload design, there are several recourses. The reload core can be redesigned, the dropped rod analysis can be reevaluated with cycle-specific inputs, or a new reference analysis can be performed with updated limiting values.

### References

- 6-1     Catawba Nuclear Station Final Safety Analysis Report, 1988 Update.
  
- 6-2     RETRAN-02: A Program for Transient Thermal-Hydraulic Analysis of Complex Fluid Flow Systems, EPRI NP-1850-CCM, Revision 4, EPRI, November 1988.
  
- 6-3     Thermal-Hydraulic Transient Analysis Methodology, DPC-NE-3000-PA, Revision 2, Duke Power Company, December 2000.
  
- 6-4     Nuclear Physics Methodology for Reload Design, DPC-NF-2010A, Duke Power Company, June 1985.
  
- 6-5     Nuclear Design Methodology Using CASMO-3/SIMULATE-3P, DPC-NE-1004-A, Revision 1, Duke Power Company, December 1997.
  
- 6-6     VIPRE-01: A Thermal-Hydraulic Code for Reactor Cores, EPRI NP-2511-CCM-A, Revision 3, EPRI, August 1989.
  
- 6-7     BWCMV Correlation of Critical Heat Flux in Mixing Vane Grid Full Assemblies, BAW-10159-P, May 1986.
  
- 6-8     Core Thermal-Hydraulic Methodology Using VIPRE-01, DPC-NE-2004P-A, Revision 1, Duke Power Company, February 1997.

- 6-9 D. A. Farnsworth and G. A. Meyer, The BWU Critical Heat Flux Correlations, BAW-10199P, BWFC, November 1994
- 6-10 Letter , H. N. Berkow (NRC) to M. S. Tuckman (Duke), November 7, 1996
- 6-11 Letter, P. S. Tam (NRC) to M. S. Tuckman (Duke), February 20, 1997
- 6-12 K. R. Epperson and J. L. Abbott, Thermal-Hydraulic Statistical Core Design Methodology, DPC-NE-2005-PA, February 1995

Figure 6-1  
VIPRE [ ] Model

[

]

Figure 6-2  
F-Delta-H versus Dropped Rod Worth  
Beginning of Cycle

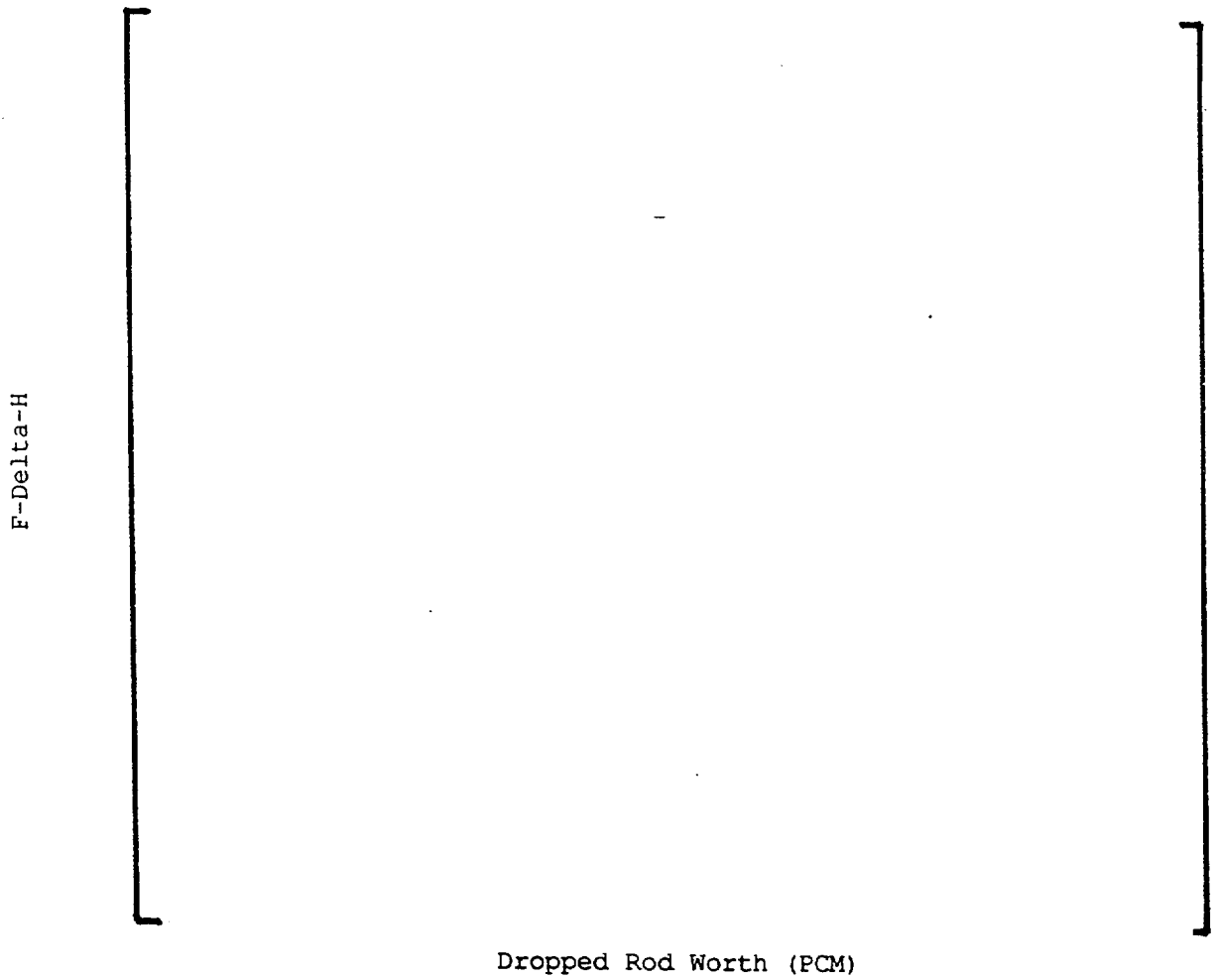


Figure 6-3  
F-Delta-H versus Dropped Rod Worth  
Middle of Cycle

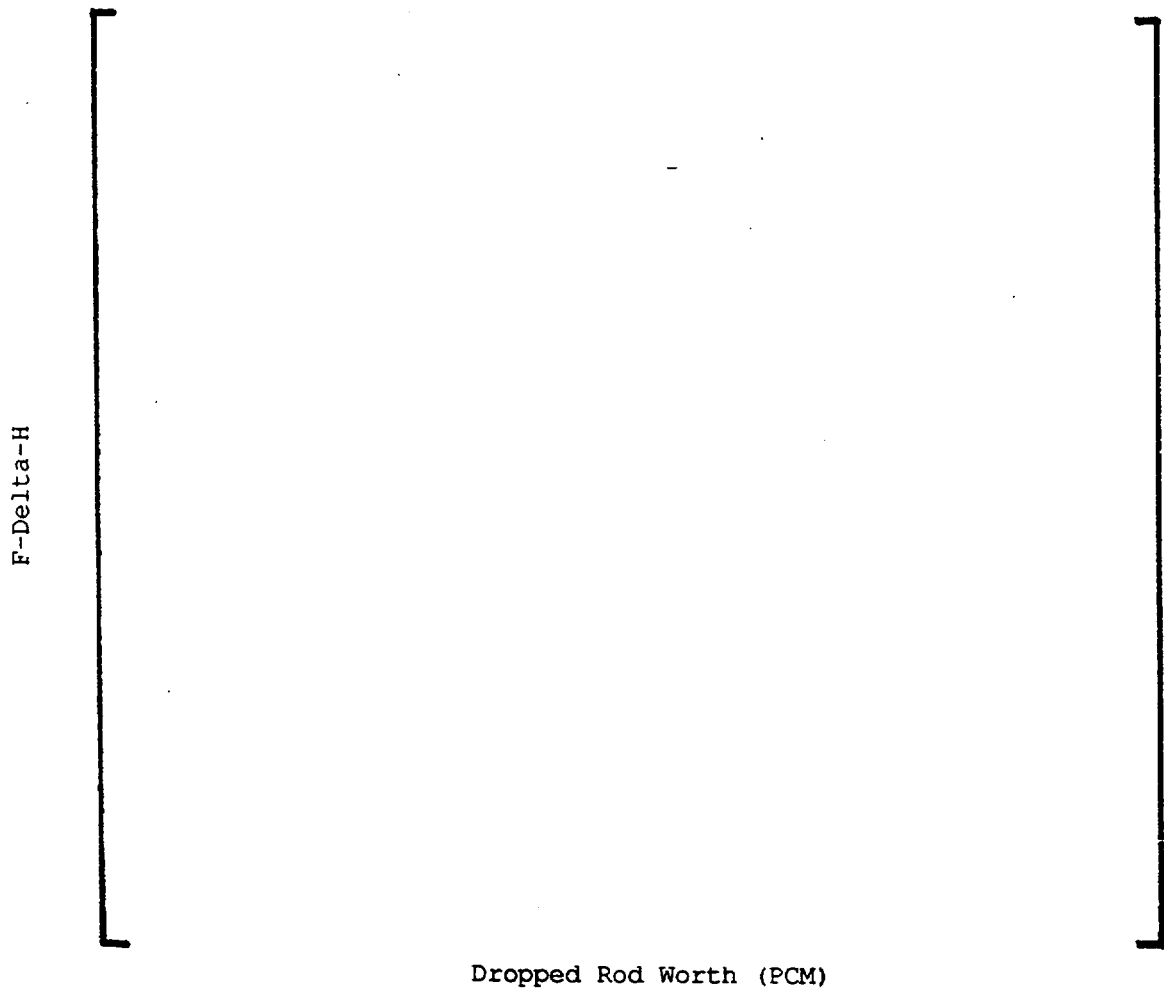


Figure 6-4

F-Delta-H versus Dropped Rod Worth

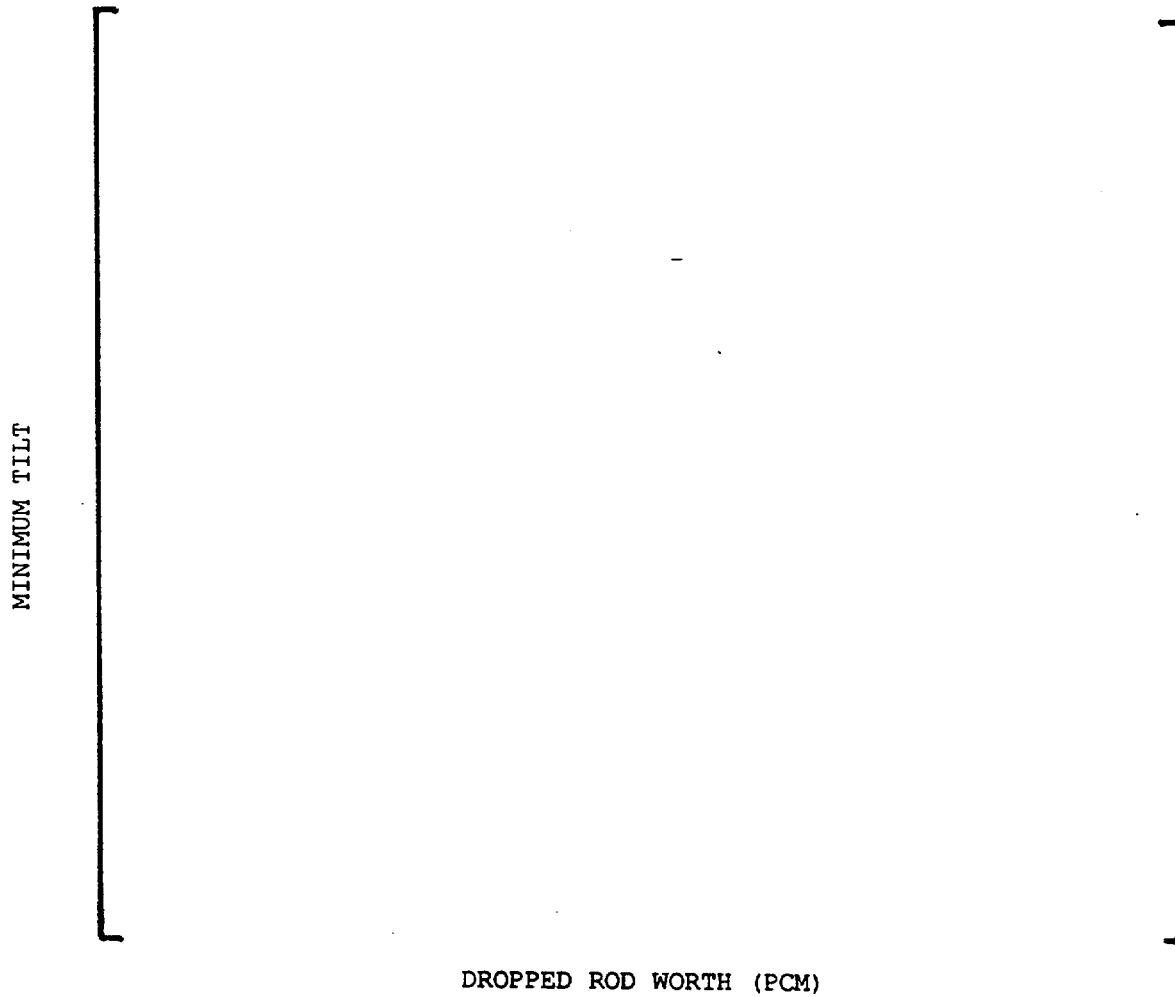
End of Cycle

F-Delta-H

Dropped Rod Worth (PCM)

Figure 6-5

Minimum Tilt vs. Dropped Rod Worth





# FSAR SECTION 15.4.3 – DROPPED ROD

100 PCM - BOC CASE

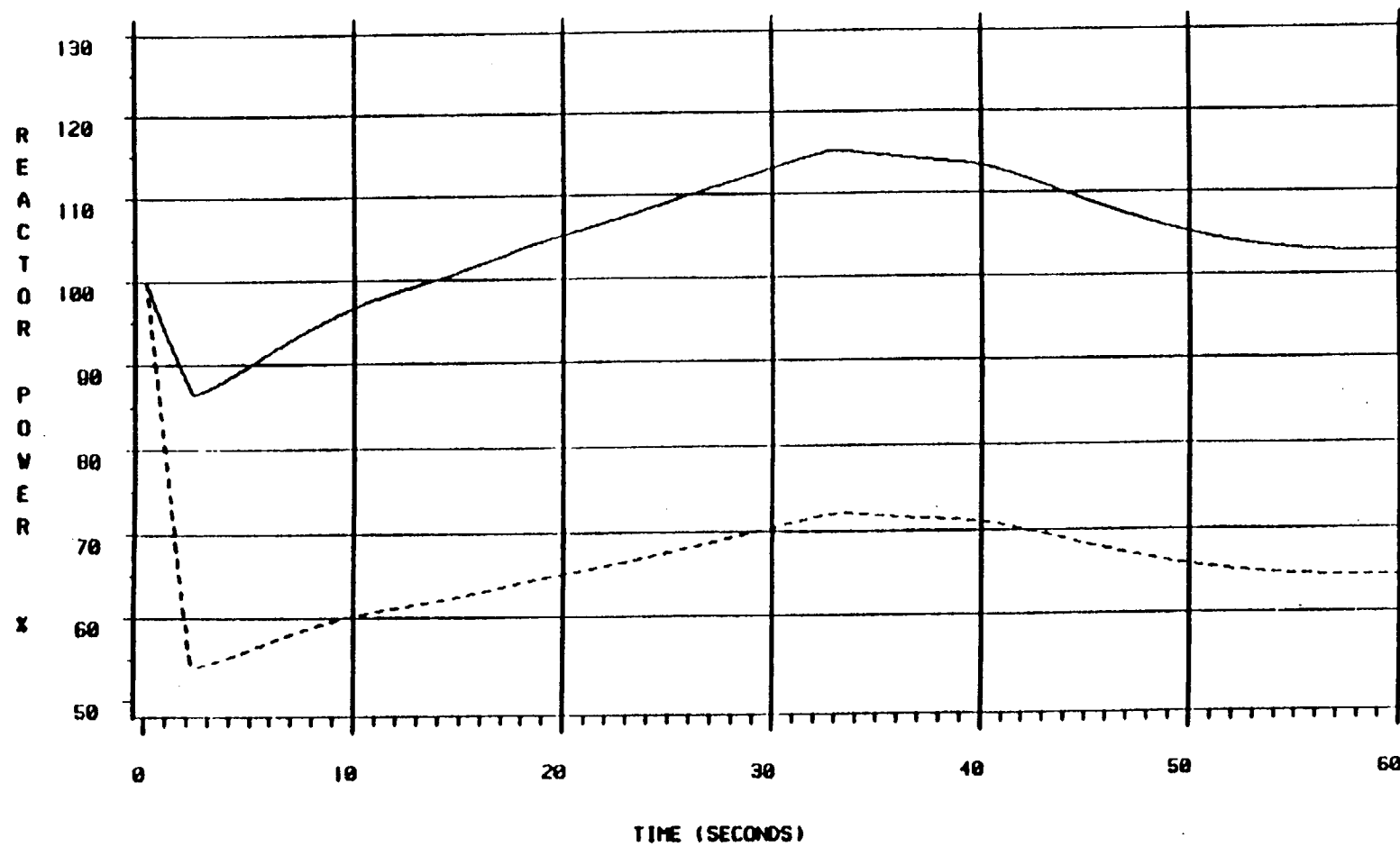


Figure 6-6

# FSAR SECTION 15.4.3 – DROPPED ROD

100 PCH - BOC CASE

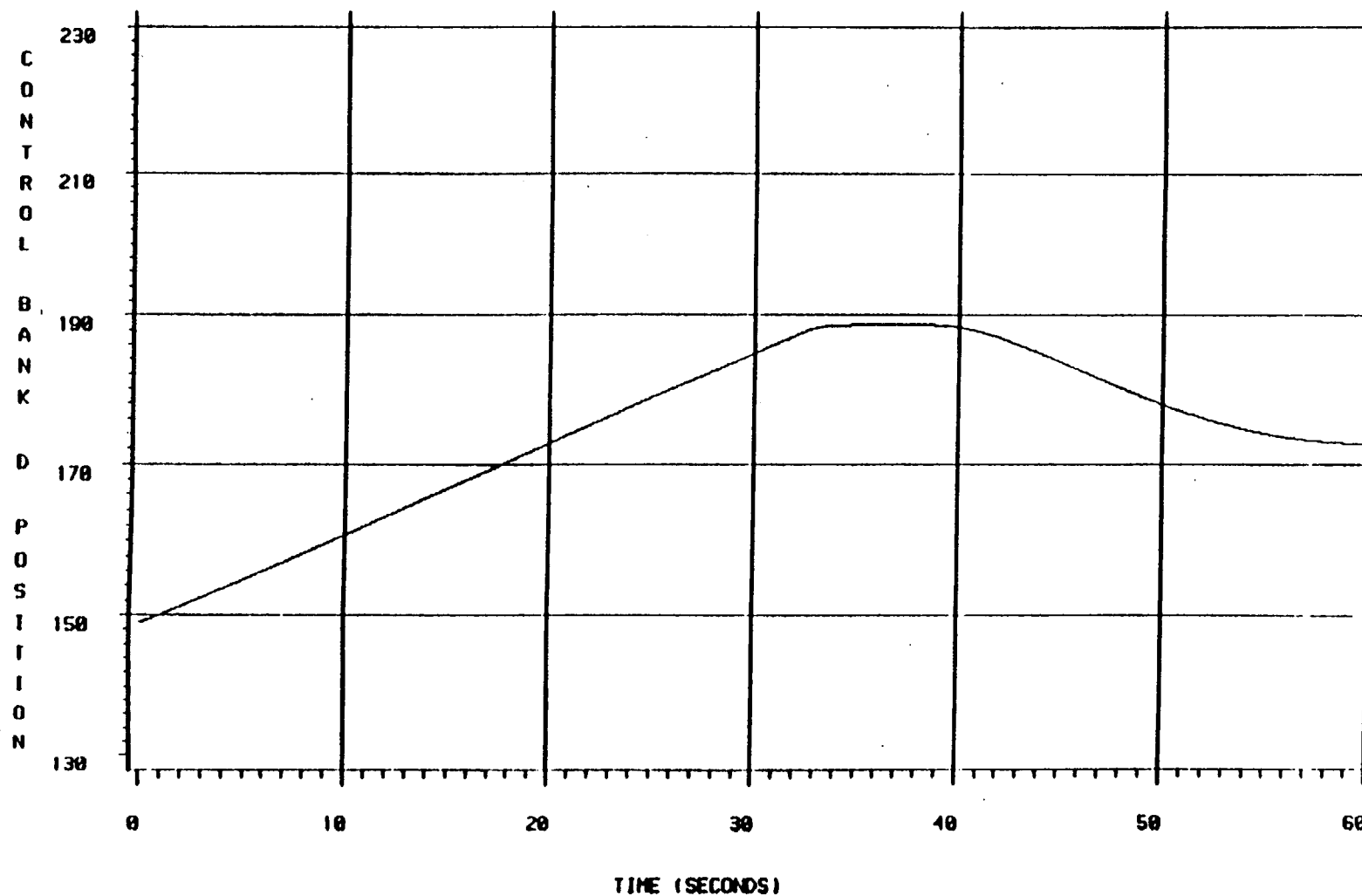


Figure 6-7

# FSAR SECTION 15.4.3 – DROPPED ROD

100 PCH – BOC CASE

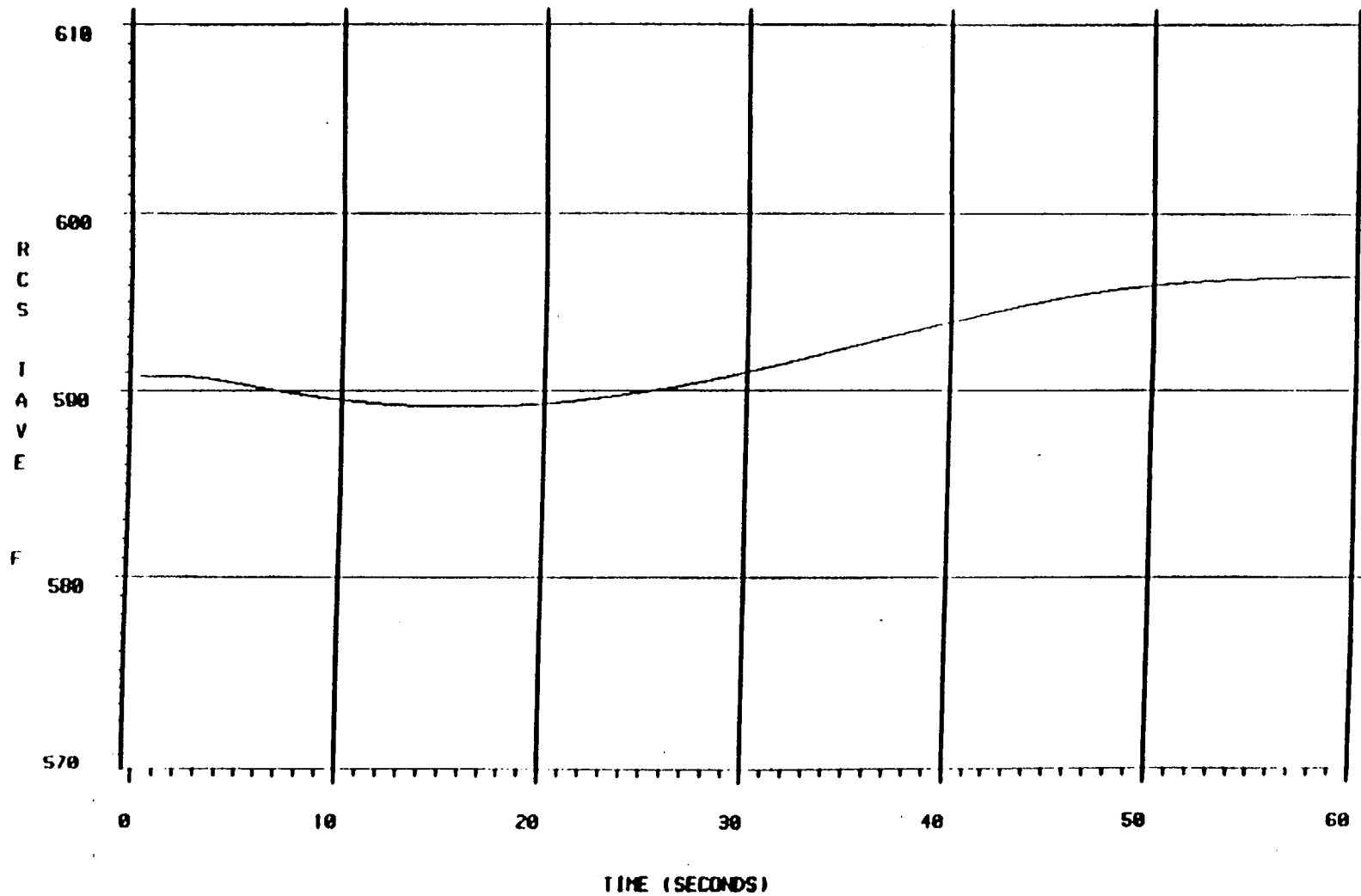


Figure 6-8

# FSAR SECTION 15.4.3 – DROPPED ROD

100 PCM – BOC CASE

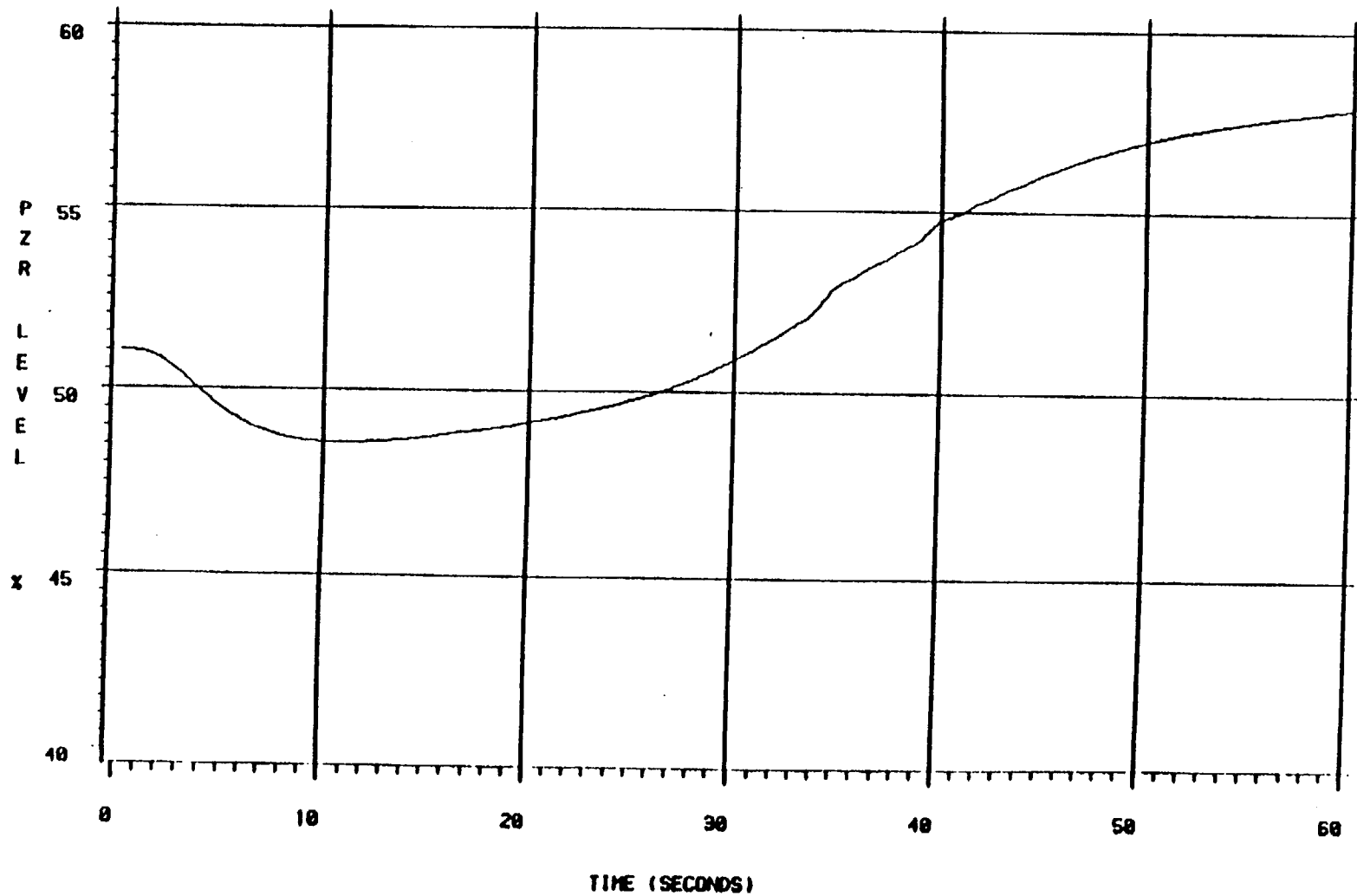


Figure 6-9

# FSAR SECTION 15.4.3 – DROPPED ROD

100 PCM - BOC CASE

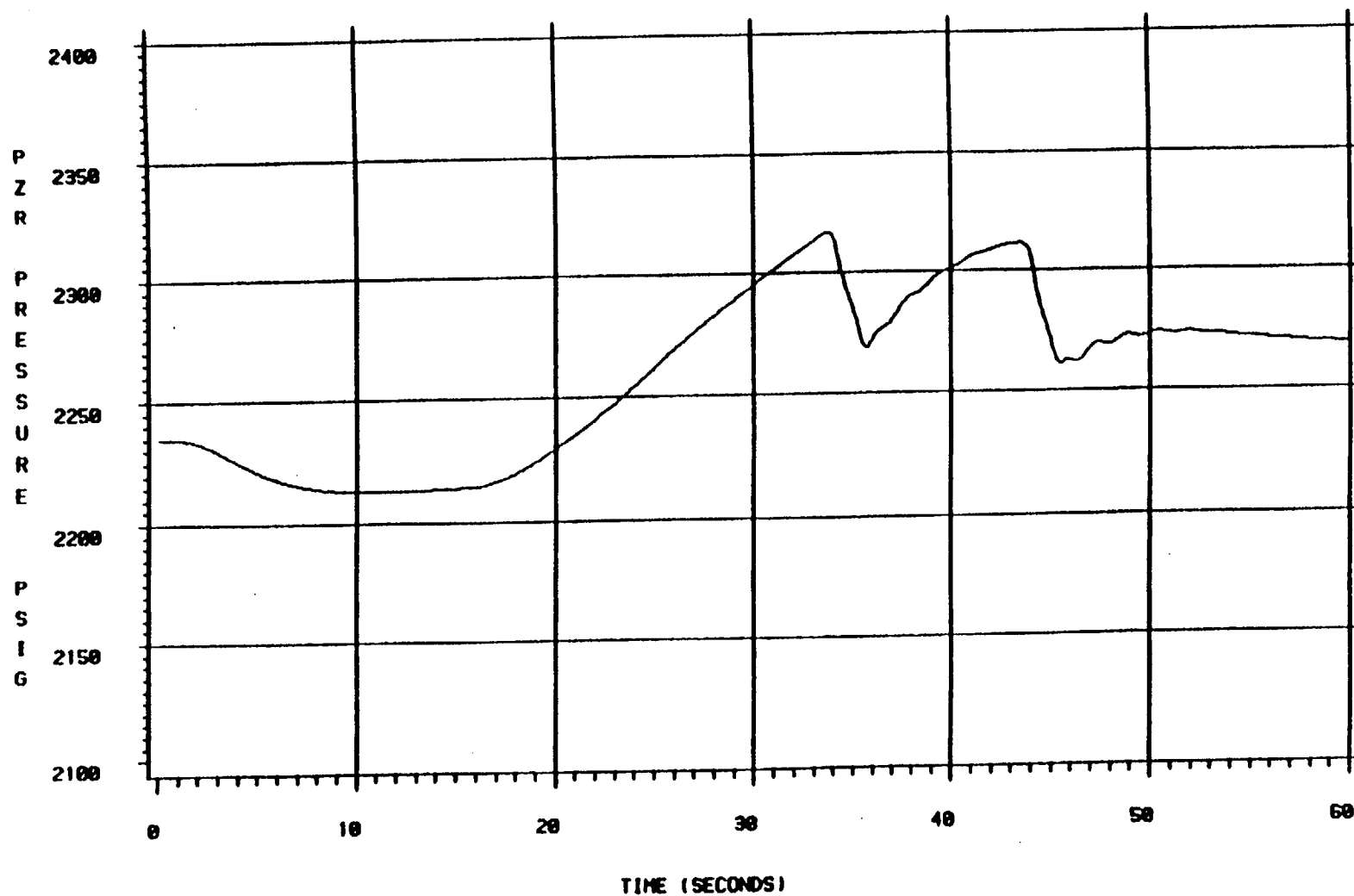


Figure 6-10

# FSAR SECTION 15.4.3 – DROPPED ROD

400 PCM – EOC CASE

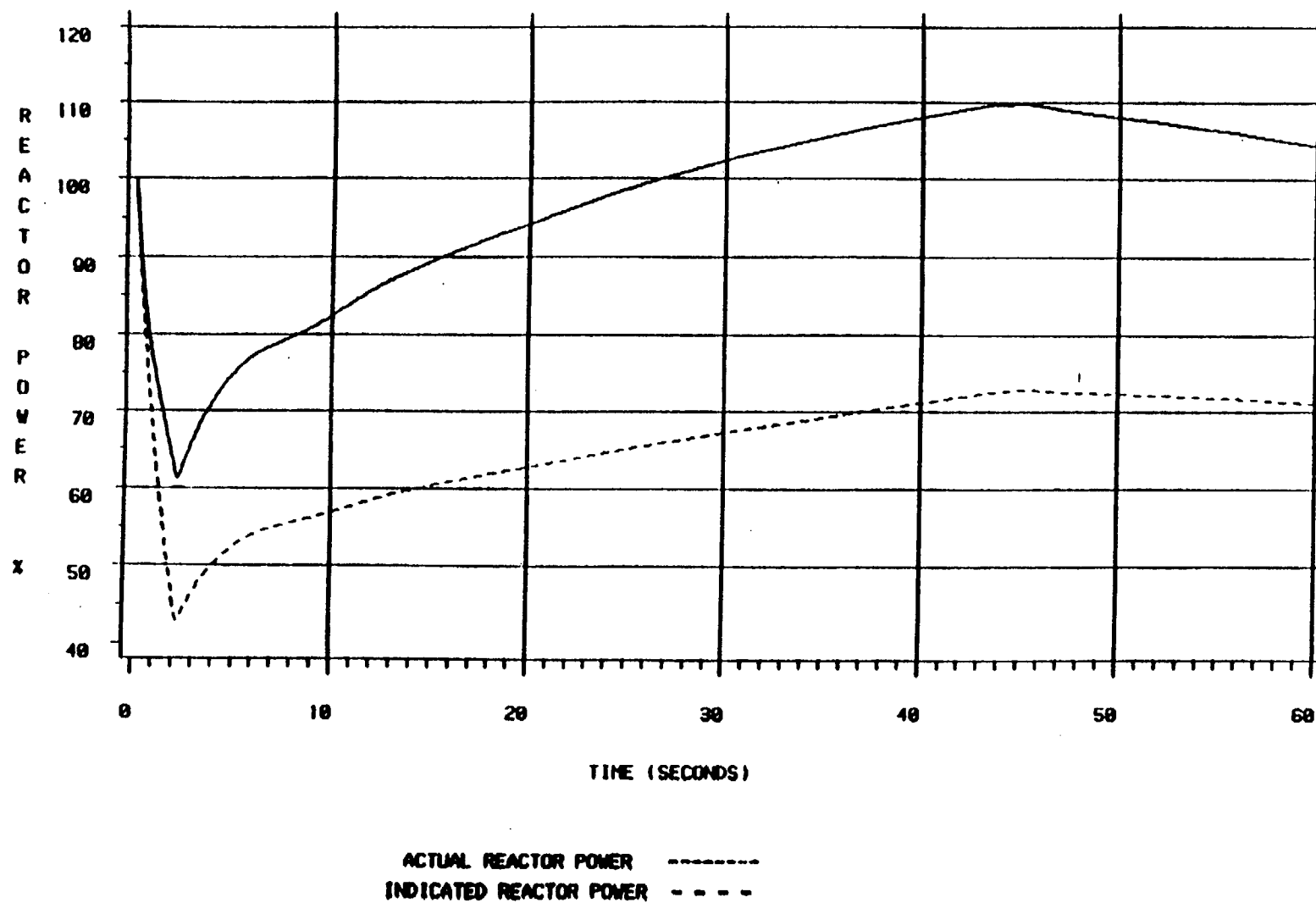


Figure 6-11

# FSAR SECTION 15.4.3 – DROPPED ROD

400 PCM - EOC CASE

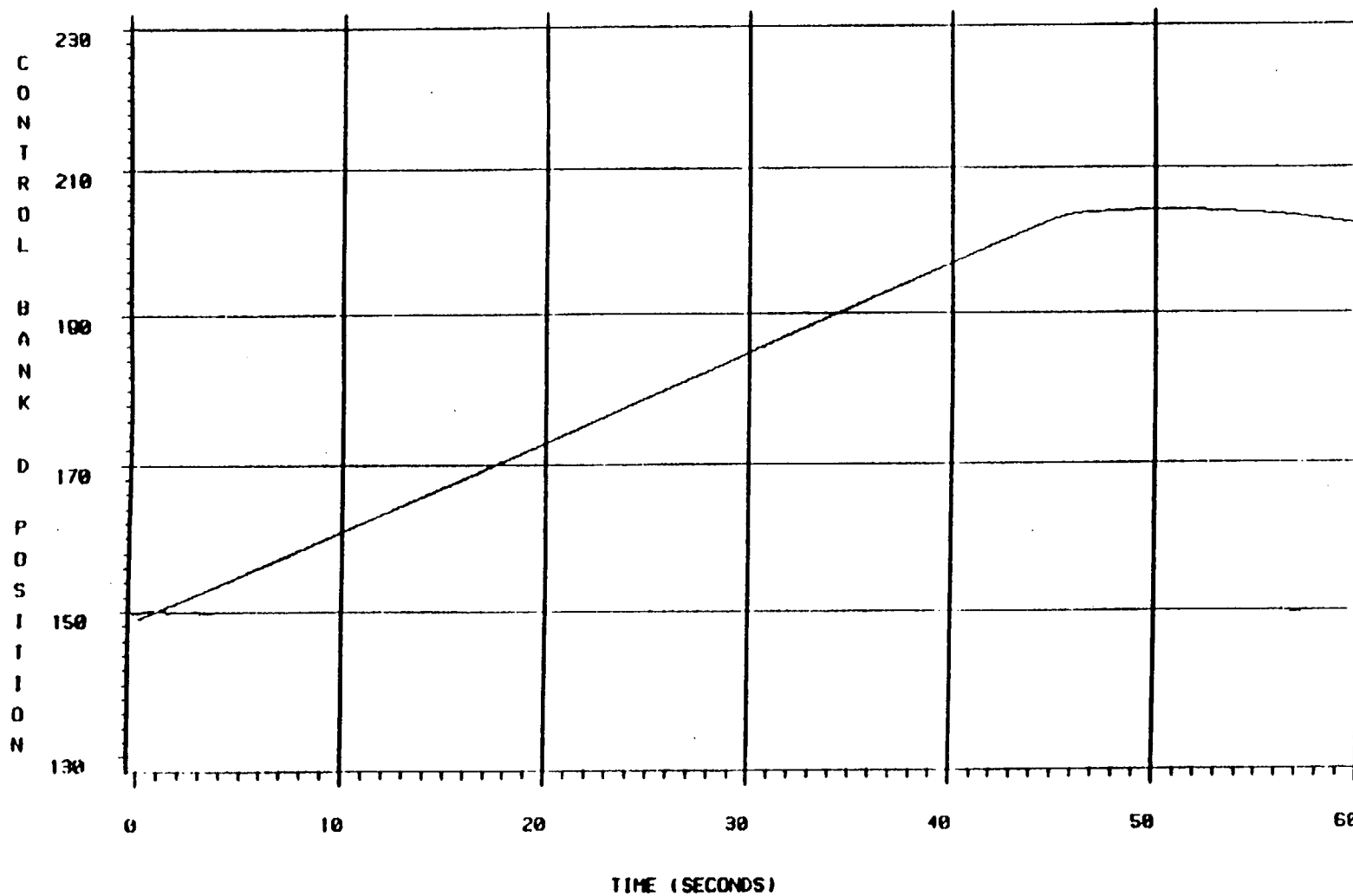


Figure 6-12

# FSAR SECTION 15.4.3 - DROPPED ROD

400 PCH - EOC CASE

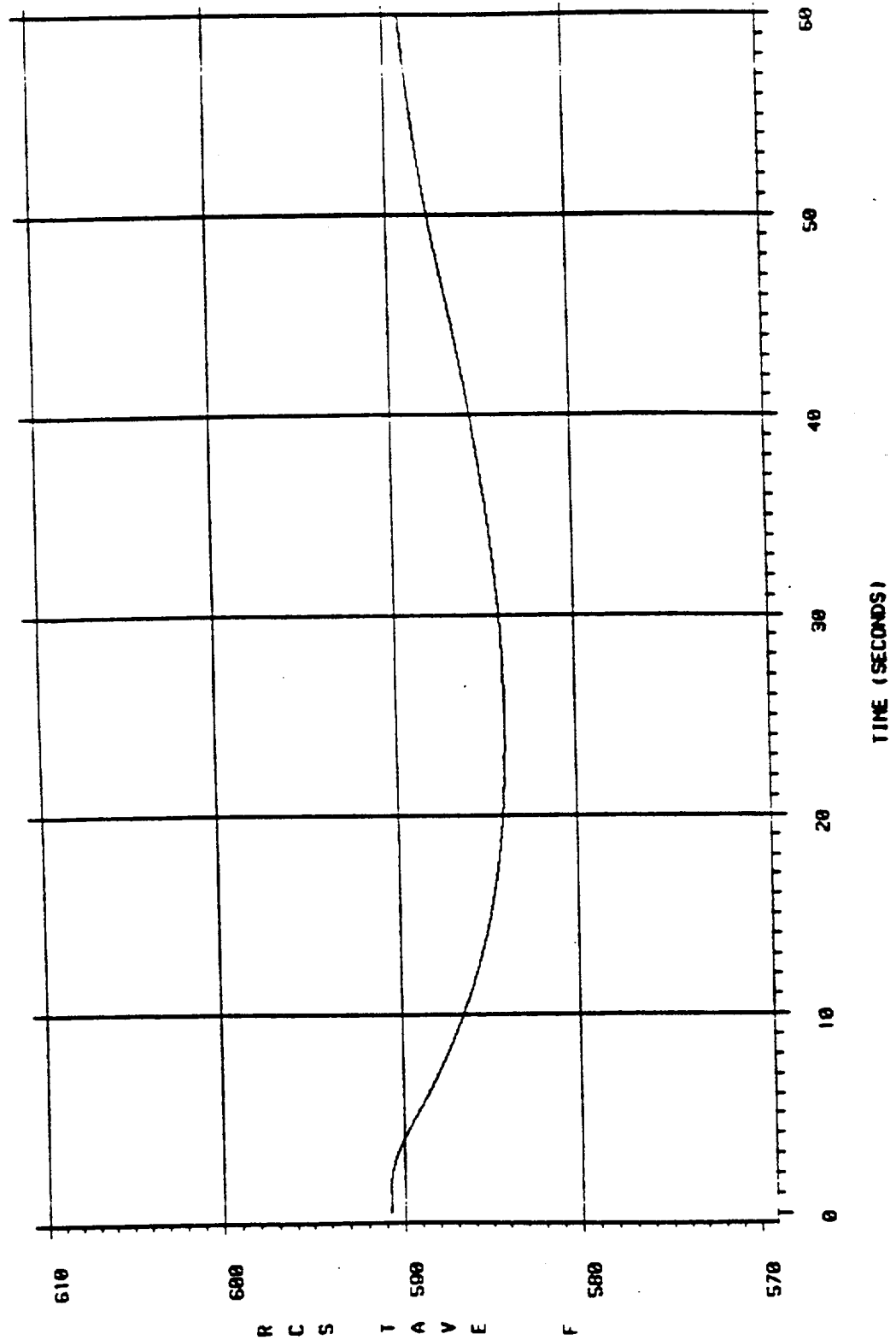


Figure 6-13



# FSAR SECTION 15.4.3 – DROPPED ROD

400 PCM - EOC CASE

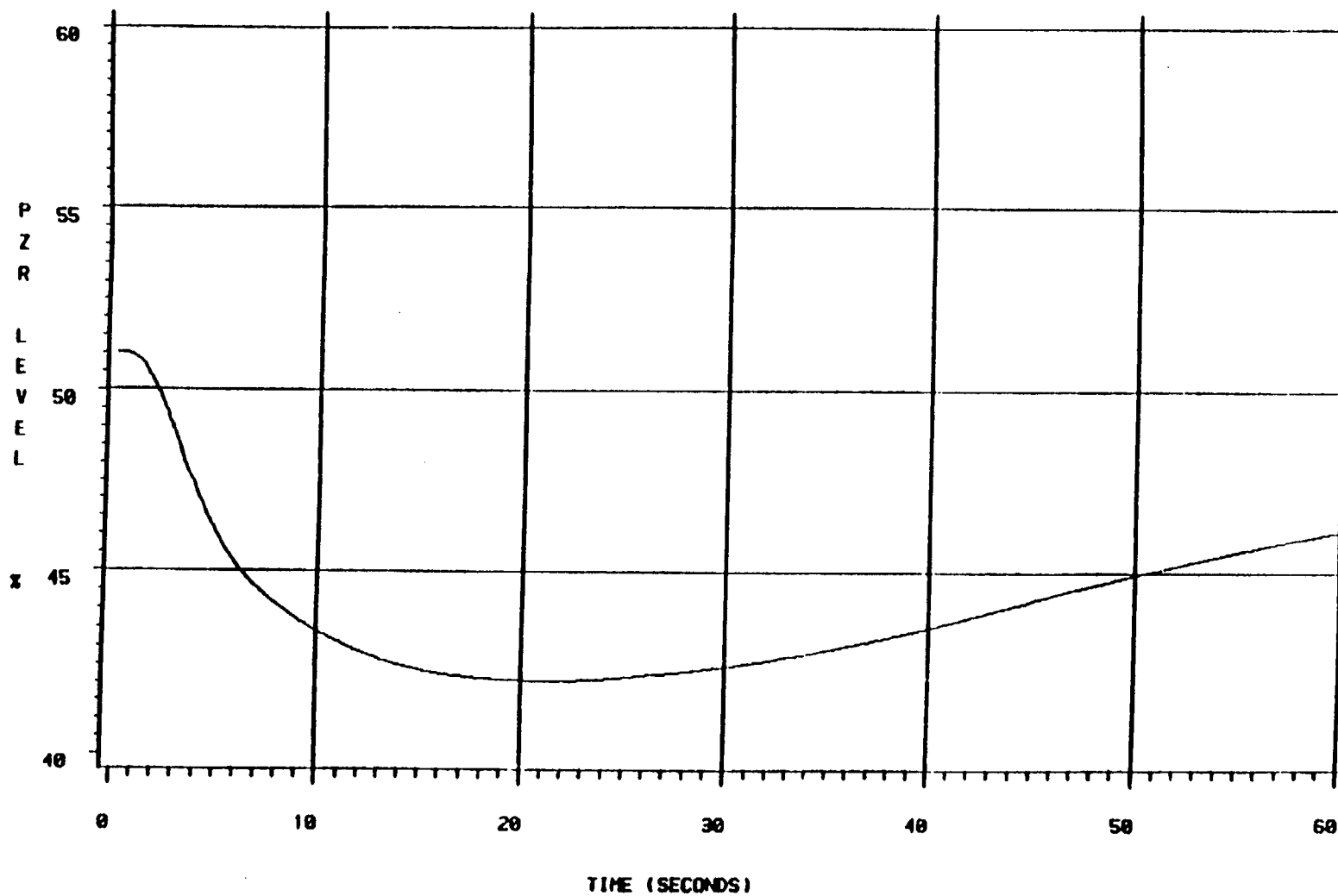


Figure 6-14

# FSAR SECTION 15.4.3 – DROPPED ROD

400 PCM - EOC CASE

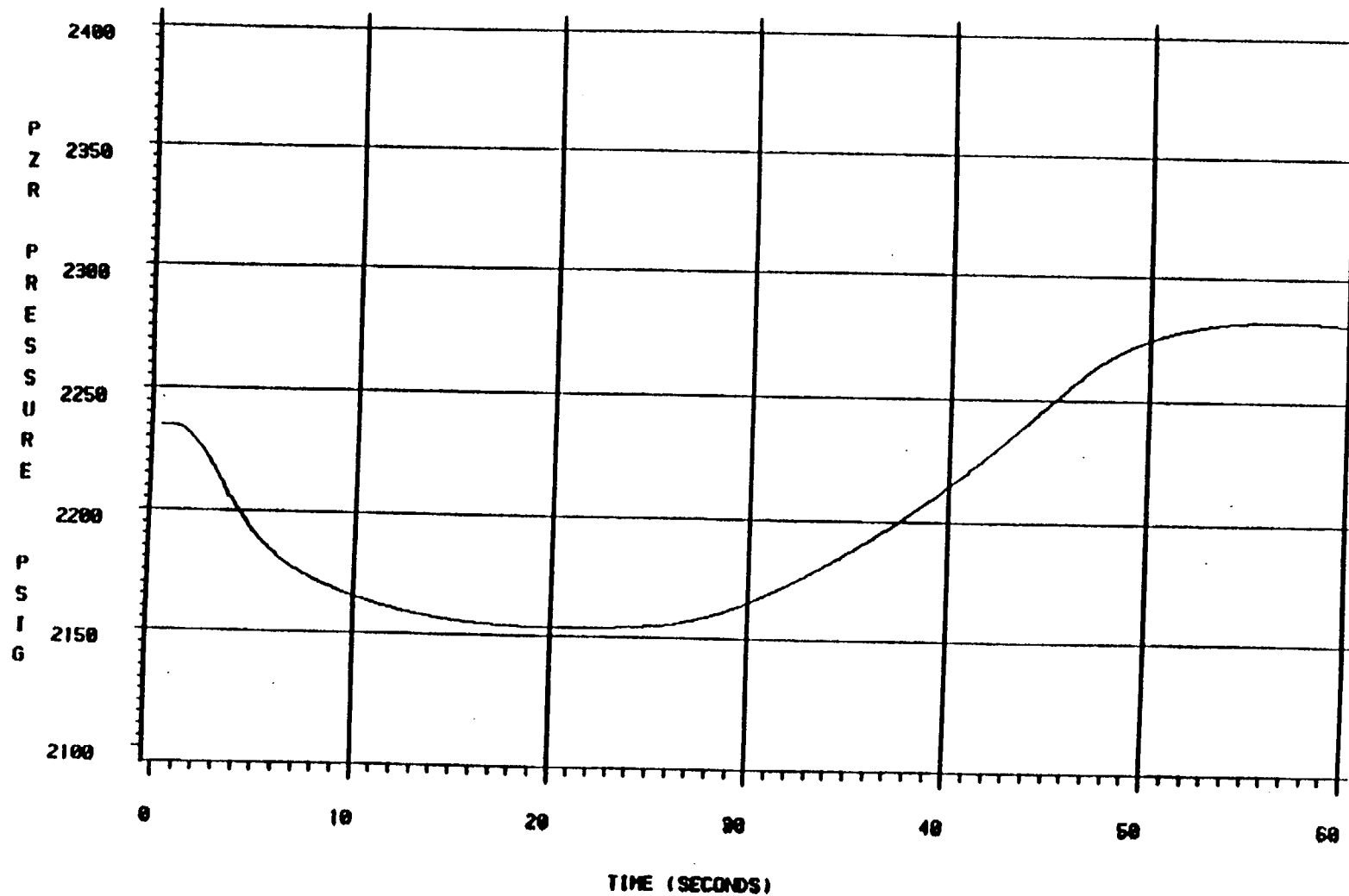


Figure 6-15

Figure 6-16

# FSAR SECTION 15.4.3 - DROPPED ROD

BOC CASES

R E A C T O R   P O W E R   X

Figure 6-17.

# FSAR SECTION 15.4.3 - DROPPED ROD

BDC CASES

R C S T A V E F

# FSAR SECTION 15.4.3 – DROPPED ROD

BOC CASES

Figure 6-18

P  
Z  
R  
  
P  
R  
E  
S  
S  
U  
R  
E

P  
S  
I  
G

# FSAR SECTION 15.4.3 – DROPPED ROD

MOC CASES

R  
E  
A  
C  
T  
O  
R  
  
P  
O  
W  
E  
R

X

Figure 6-19

# FSAR SECTION 15.4.3 – DROPPED ROD

MOC CASES

R  
C  
S  
  
I  
A  
V  
E  
  
F

6-35

Figure 6-20

# FSAR SECTION 15.4.3 – DROPPED ROD

HOC CASES

P  
Z  
R  
  
P  
R  
E  
S  
S  
U  
R  
E  
  
P  
S  
I  
G

Figure 6-21



# FSAR SECTION 15.4.3 – DROPPED ROD

EOC CASES

Figure 6-22

R  
E  
A  
C  
T  
O  
R  
  
P  
O  
W  
E  
R

X

# FSAR SECTION 15.4.3 – DROPPED ROD

EOC CASES

R  
C  
S  
  
I  
A  
V  
E  
  
F

6-38

Figure 6-23

# FSAR SECTION 15.4.3 – DROPPED ROD

EOC CASES

P  
Z  
R

P  
R  
E  
S  
S  
U  
R  
E

P  
S  
I  
G

Figure 6-24

# FSAR SECTION 15.4.3 – DROPPED ROD

LIMITING CASES

R  
E  
A  
C  
T  
O  
R  
  
P  
O  
W  
E  
R

X

Figure 6-25

Figure 6-26

# FSAR SECTION 15.4.3 - DROPPED ROD

LIMITING CASES

R C S I A V E

# FSAR SECTION 15.4.3 – DROPPED ROD

LIMITING CASES

P  
Z  
R  
  
P  
R  
E  
S  
S  
U  
R  
E

P  
S  
I  
G

6-42

Figure 6-27

# FSAR 15.4.3 - AXIAL POWER SHAPES

$\rho$  /  $\rho$   $\rho$   
 0 0 0

6-43

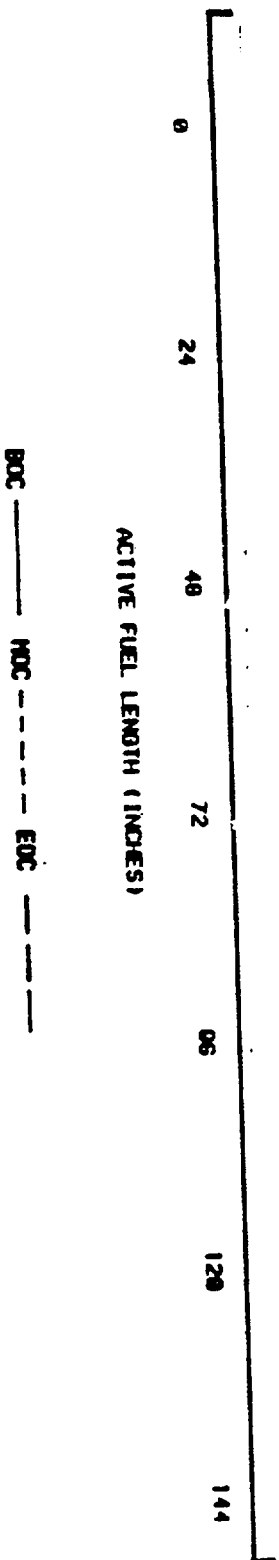


Figure 6-28

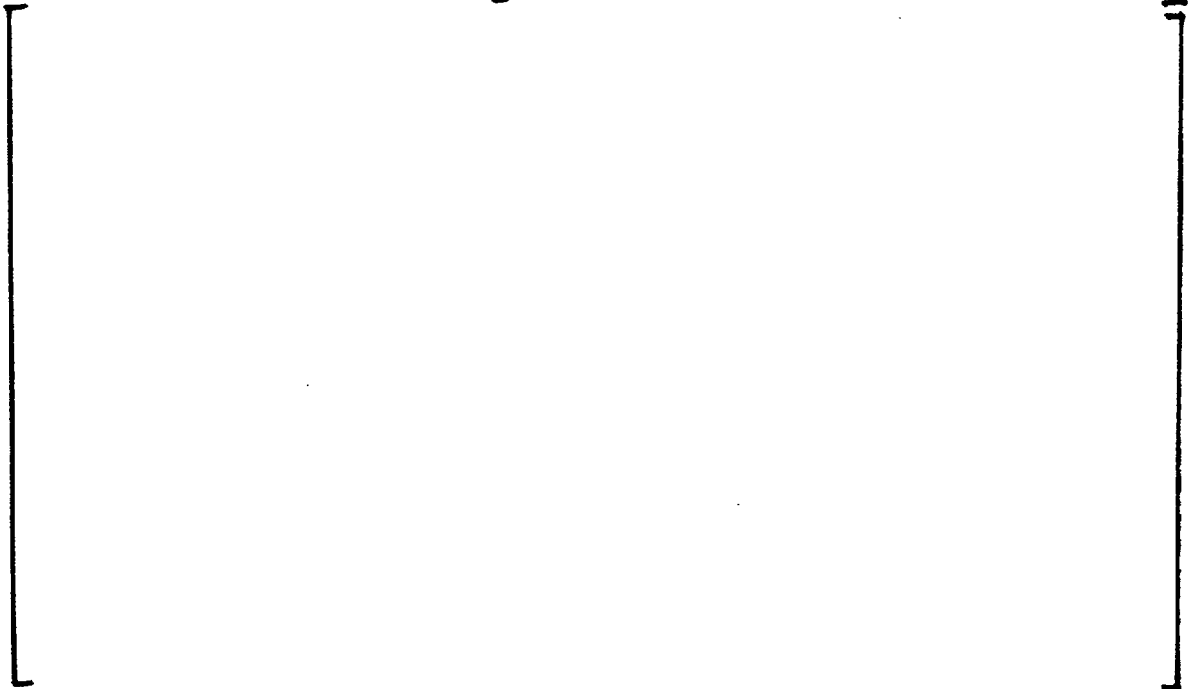
## Appendix A

### REACTOR VESSEL THERMAL MIXING EVALUATION

#### Part A: Forced Circulation Mixing

##### A.1 Background

A thermal mixing test was performed at McGuire Nuclear Station Unit 2 to determine the degree of coolant mixing in the reactor vessel [



##### A.2 Approach





### A.3 Instrumentation/Equipment Configuration

The instrumentation used in the thermal mixing test consisted of the wide range hot and cold leg resistance temperature detectors (RTDs) and selected core exit thermocouples (CETCs). Each hot leg or cold leg is equipped with one wide range, thermowell-mounted RTD. The loop B hot leg thermowell is located upstream of the surge line and the loop A cold leg RTD is located upstream of the normal charging such that pressurizer outsurges and charging do not directly impinge on these RTDs and possibly adversely affect the RTD temperature response. The response time of the wide range RTDs is estimated to be approximately 20 seconds.

A total of 26 CETCs were used during the test to obtain core exit temperature measurements. The CETCs utilized are fairly evenly distributed, with approximately 7 CETCs per core quadrant. The positions of the CETCs with respect to core locations and the orientation of the loops with respect to the core are shown in Figure A-1. The response time of the CETCs is relatively fast; it is less than one second based on available references.

### A.4 Data Acquisition

Wide range hot leg and cold leg RTD data was recorded using the Operator Aid Computer (OAC) transient monitor at a one second frequency and on the OAC general program at a five second frequency. CETC data was recorded using the OAC general program at the five second frequency.

### A.5 Definitions



[

]

A.6

A.7

A.8

A.9 Results

[

]

## Part B: Natural Circulation Mixing

### A.10 Background

The two transients on which the natural circulation reactor vessel thermal mixing estimate is based are the September 1, 1981, McGuire Unit 1 natural circulation startup test and the January 29, 1985, Catawba Unit 1 station blackout startup test.

### A.11 Approach

In order to quantify reactor vessel thermal mixing in the absence of forced circulation, data analysis techniques similar to those in Part A are used, but with the following exceptions:

- Since the natural circulation data is from plant events not designed to measure mixing, there are data limitations including the lack of frequent core exit thermocouple data.
- Since the RCS loop flow rates are relatively low, the flow measurement devices are not useful for determining the magnitude. Therefore, the flow rate can only be estimated. This makes transit times only approximate.

### A.12 Instrumentation/Equipment Configuration

The discussion in Part A is applicable for natural circulation, except as noted above concerning core exit thermocouple data.

### A.13 Acquisition

Wide range hot and cold leg temperature data was recorded using the OAC transient monitor at a one second frequency for the Catawba event and a one minute frequency for the McGuire event.

A.14 Definitions

The discussions in Part A are applicable for natural circulation.

A.15

A.16

A.17

[

]

A.18 Results

[

]



Figure A-1  
Mixing Test Thermocouple Locations

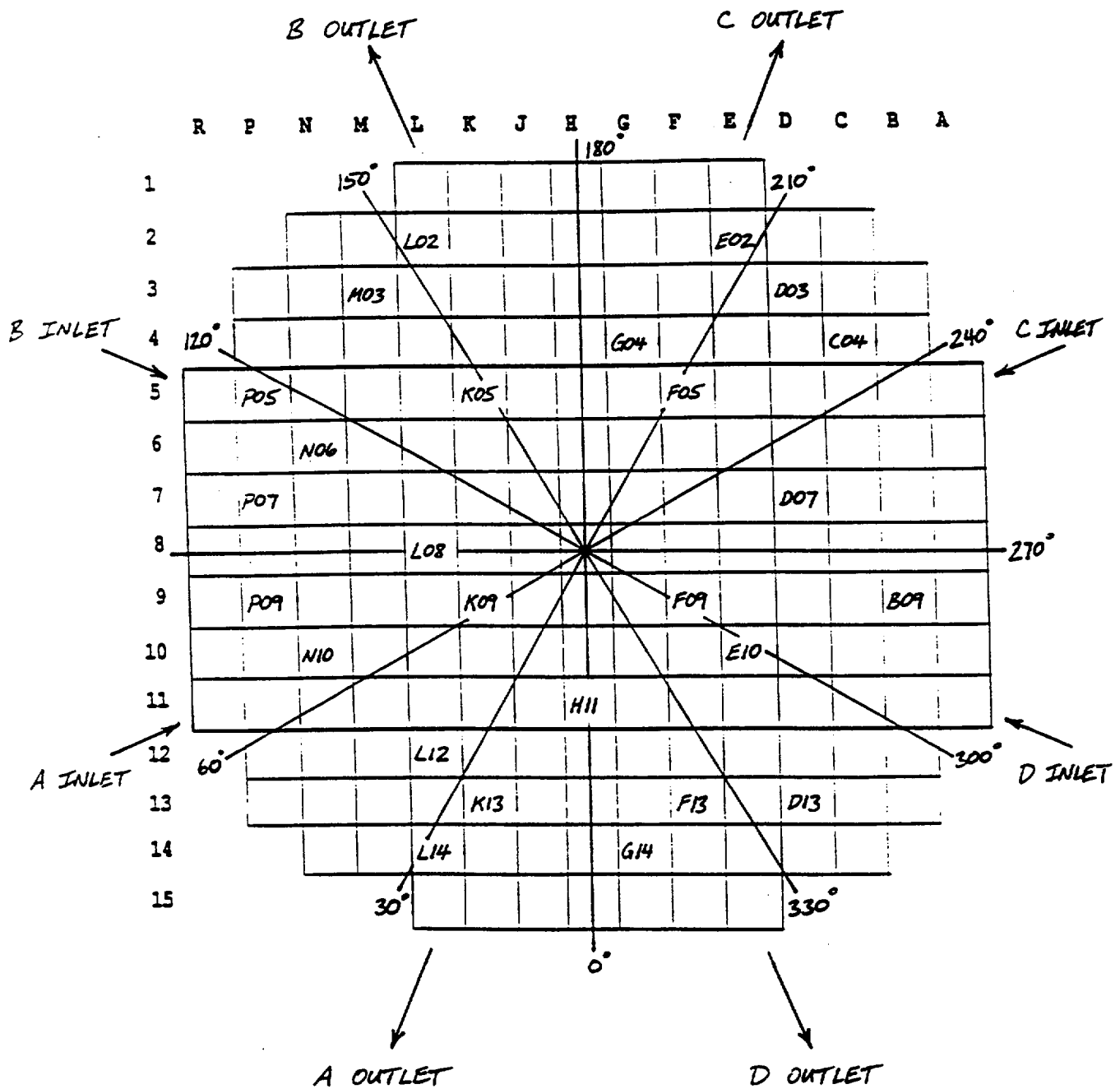
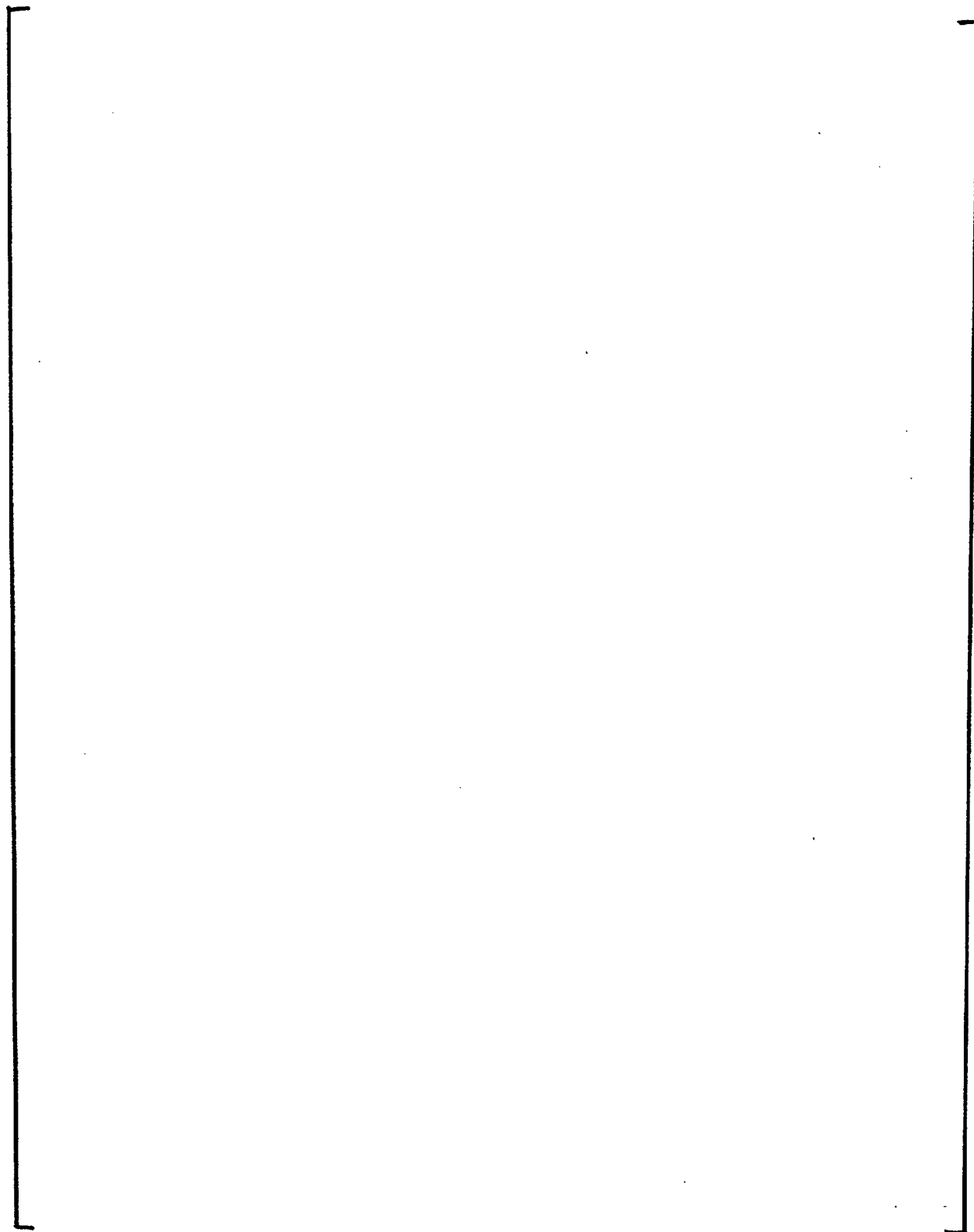


Figure A-2 to A-7



A-12 to A-17

## DPC-NE-3001-A

### List of Changes to the November 1991 Version to Produce the December 2000 Version

The following changes have been incorporated into the republication of DPC-NE-3001-A that is dated December 2000. The November 1991 version, which was the original publication of the approved version, is the previous version. These changes consist of error corrections and enhancements only, and are not significant model or methodology revisions. Since no significant model or methodology changes are included, NRC review and approval of the December 2000 version is not necessary.

1. Cover page updated to specify "Republished December 2000"
2. p. 1-3, Section 1.0: Added a paragraph at the end of Chapter 1.0 to mention that topical report DPC-NE-2009P-A includes NRC-approved revisions to DPC-NE-3001 for the transition to Westinghouse RFA fuel. The DPC-NE-2009 revisions are not included in this republication.
3. p. 1-4, References: Update Reference 1-2 to "-PA" Revision 2, December 2000.
4. p. 1-4, References: Update Reference 1-4 to Revision 3, August 1989
5. p. 1-4, References: Added Reference 1-6, Duke Power Company Westinghouse Fuel Transition Report, DPC-NE-2009P-A, December 1999
6. p. 2-3, Section 2.2, Initial Fuel Temperatures: Added Reference 2-2, the TACO3 fuel pin code topical report BAW-10162P-A. This is an NRC-approved code for calculating fuel rod temperatures and is used by Duke as a replacement for TACO2.
7. p. 2-4, Section 2.3.3: Deleted the last two sentences since this discussion is not significant to the methodology.
8. p. 2-5, Section 2.3.10: Revised the description to indicate that since decay heat is the key parameter, and since it is highest at EOC, an EOC most-negative MTC has been assumed.
9. p. 2-6, Section 2.3.18: Clarify "at maximum speed over the span of rod positions" to "at maximum speed in 100% overlap over the span of rod positions."
10. p. 2-11, References: Added the following: "2-2 D. A. Wesley and K. J. Firth, TACO3 - Fuel Pin Thermal Analysis Code, BAW-10162P-A, Babcock & Wilcox, November 1989
11. p. 2-12, Table 2-1, Effective Delayed Neutron Fraction: Clarified that minimum  $\beta$  is assumed for 15.1.2 and 15.1.3.

List of Changes to the November 1991 Version (cont.)

12. p. 2-12, Table 2-1, 2.3.2 and 2.3.3: Deleted the "Case 1" and "Case 2" designations since this distinction is no longer necessary. The most-negative MTC and the least-negative DTC are conservative for both events.
13. p. 2-12, Table 2-1, 2.3.10: Separated 2.3.10 to indicate most-negative MTC.
14. Section 3.0: Change "assure" to "ensure" throughout
15. p. 3-2, Section 3.1, Shutdown Margin: Insert the words "xenon maldistribution" in the last sentence.
16. p. 3-3, Section 3.1, Maximum Differential Rod Withdrawal From Subcritical: Clarify "assumes that control banks move in 100% overlap" to "assumes the combination of two sequential control banks moving in 100% overlap."
17. p. 3-4, Section 3.1, Dropped Rod Worth: Replace "at both BOC and EOC" with ", which occurs at EOC".
18. p. 3-4, Section 3.1, Dropped Rod Worth: Insert "or RIL" prior to the word "condition" at the end of the paragraph.
19. p. 3-6, References: Update Reference 3-2 to "-A", Revision 1, December 1997
20. p. 3-7, References: Update Reference 3-3 to "-A", March 1990
21. p. 4-3, Section 4.2.1: Revise the axial noding in the ARROTTA model from "twelve equal length" to "a minimum of twelve equal length". Based on phone conversations with NRC Reactor Systems Branch staff, it has been confirmed that increasing the nodalization detail in this manner is not of concern to the NRC.
22. p. 4-6, Section 4.2.2.2: The [ ] VIPRE model has been replaced with the standard [ ] VIPRE model of DPC-NE-3000 through out this chapter. This represents a change to a more detailed model that has already been approved by the NRC.
23. p. 4-7, Section 4.2.2.2, Fuel Conduction Model: Replace "TACO2" with "TACO2 or TACO3 (Reference 4-17)." This change indicates that TACO3 is used as a replacement for TACO2. Both codes are NRC-approved codes.
24. p. 4-8, Section 4.2.2.2, Heat Transfer Correlations: Revised the CHF correlation used to define the peak of the boiling curve to be the same as the correlation used for calculating the DNBR, and its associated limit.
25. p. 4-9, Section 4.2.2.2, Conservative Factors: The word "hot" in inserted to clarify that the flow area reduction factor is used in the hot subchannel.

List of Changes to the November 1991 Version (cont.)

26. p. 4-13, Section 4.2.2.3, Heat Transfer Correlations: Revised the CHF correlation used to define the peak of the boiling curve to be the same as the correlation used for calculating the DNBR, and its associated limit.
27. p. 4-14 and p. 14-15, Section 4.2.2.4: The [ ] VIPRE model has been replaced with the standard [ ] VIPRE model of DPC-NE-3000 throughout this chapter. This represents a change to a more detailed model that has already been approved by the NRC.
28. p. 4-14, Section 4.2.2.4: The BWU-Z CHF correlation and associated references are added. The BWU-Z CHF correlation has been approved by the NRC.
29. p. 4-15, Section 4.2.2.4, Cases Analyzed: A new paragraph has been added to state that DNBR evaluations are no longer performed for the HZP cases based on analysis experience. The DNBR evaluations are performed to determine failed fuel percentages for input to the dose analysis. The key factor in the dose analysis is the duration of steam generator tube bundle uncover, which does not occur for the HZP cases. Even with 100% fuel pin failure, the HZP dose calculations will always be less than the HFP dose calculations. Therefore the HZP cases are no longer analyzed. The methodology and results for the HZP cases are retained.
30. p. 4-15, Section 4.2.2.4, Axial Power Distribution: [ ]
31. p. 4-16, Section 4.2.2.4, Fuel Conduction Model: Replace "TACO2" with "TACO2 or TACO3 (Reference 4-17)." This change indicates that TACO3 may be used as a replacement for TACO2. Both codes are NRC-approved codes
32. p. 4-16, Section 4.2.2.4, Fuel Conduction Model: [ ]
33. p. 4-16, Section 4.2.2.4, Heat Transfer Correlations: Revised the CHF correlation used to define the peak of the boiling curve to be the same as the correlation used for calculating the DNBR, and its associated limit.
34. p. 4-19, Section 4.3.1, top paragraph: [ ]
35. p. 4-19, Section 4.3.1, top paragraph: [ ]

List of Changes to the November 1991 Version (cont.)

36. p. 4-20, Section 4.3.1, top paragraph: Added the following alternate method for specifying an average value for  $\beta_{eff}$ . "... desired limiting value, or by changing the values of  $\beta$  in each composition by a constant multiplicative value to produce a  $\beta$  in each composition at the desired limiting value."
37. p. 4-21, Section 4.3.3, first paragraph: Clarified the time step selection to be "... relaxed to no greater than 0.01 seconds".
38. p. 4-23, Section 4.4.1, second paragraph: The HZP REA analysis results presented assume two-reactor coolant pumps in operation. The technical specifications were subsequently revised to require three pumps in operation at this condition. The text is revised to now credit three pumps, and to indicate that the actual gpm values can change as the technical specification flow changes. The sentence "The core flow remains essentially constant during the HZP transient, and therefore a constant flow is used.", has been deleted to reflect that flow reductions are now considered for all cases.
39. p. 4-27, Section 4.5.3: Change "psig" to "psia".
40. p. 4-28, Section 4.7, second paragraph: Inserted the use of SIMULATE-3P for the pin census. "... as described in Section 4.4.4, with the radial pin information being calculated with SIMULATE-3P."
41. p. 4-29, References: Update Reference 4-5 to Revision 3, August 1989
42. p. 4-29, References: Update Reference 4-8 to "-A" Revision 1, 1997
43. p. 4-30, References: Update Reference 4-15 to "-PA" Revision 2, December 2000
44. p. 4-30, References: Update Reference 4-16 to "-A" March 1990
45. p. 4-30, References: Added the following: 4-17 D. A. Wesley and K. J. Firth, TACO3 - Fuel Pin Thermal Analysis Code, BAW-10162P-A, Babcock & Wilcox, November 1989
46. p. 4-30, References: Added the following: 4-18 D. A. Farnsworth and G. A. Meyer, The BWU Critical Heat Flux Correlations, BAW-10199P, BWFC, November 1994. 4-19, The NRC BWU-Z SER letter dated November 7, 1996, H. N. Berkow to M. S. Tuckman. 4-20 The NRC BWU-Z SER letter dated February 20, 1997, P. S. Tam to M. S. Tuckman
47. p. 4-31, Table 4-2: The HFP and HZP inlet temperatures were reversed. The text is correct.
48. p. 4-32, Table 4-4: The DTC for EOC was incorrectly given as "-1.1". The corrected value of "-1.2" is inserted.
49. p. 4-34, Figure 4-2: The figure is revised due to the [ ] model has been replaced with the standard [ ] model. This represents a change to a more detailed model that has already been approved by the NRC

List of Changes to the November 1991 Version (cont.)

- 50. p. 4-55, Figure 4-23: Replaced with a figure showing a spectrum of assumed axial shapes.
- 51. p. 4-57, Figure 4-25: Replaced with a figure showing a spectrum of assumed axial shapes.
- 52. p. 5-2, Section 5.2.1.1: Revised to address the deletion of the Catawba auxiliary feedwater pump runout protection function.
- 53. p. 5-2, Section 5.2.1.1: Revised to mention the steam generator replacement for McGuire and Catawba Unit 1, and that the Catawba Unit 2 results are presented.
- 54. p. 5-4, Section 5.2.1.3: Revised to state that the break spectrum is varied in increments of  $0.1 \text{ ft}^2$  "or less".
- 55. p. 5-5, Section 5.2.2.1: Replace the phrase "is expected to occur" with "occurs", for clarity. Replace the word "isothermal" with "asymmetric". This revision was previously communicated to the NRC in the response to Question #36, in the letter dated 6/3/91.
- 56. p. 5-5, Section 5.2.2.2: [ 

]
- 57. p. 5-6, Section 5.2.3.2: The MacBeth correlation and reference were deleted from the methodology since it is not in use. The BWU-Z CHF correlation was added and including the following references. 5-9 D. A. Farnsworth and G. A. Meyer, The BWU Critical Heat Flux Correlations, BAW-10199P, BWFC, November 1994. 5-10, The NRC BWU-Z SER letter dated November 7, 1996, H. N. Berkow to M. S. Tuckman. 5-11 The NRC BWU-Z SER letter dated February 20, 1997, P. S. Tam to M. S. Tuckman
- 58. p. 5-8, Section 5.2.3.2, Radial Power Distributions: [ 

]
- 59. p. 5-10, Section 5.3.1, Core Bypass Flow: This value has been changed to 6%.
- 60. p. 5-11, Section 5.3.2.1, Main Feedwater: Added two additional causes for MFW pump trip (condensate booster pump trip and safety injection)
- 61. p. 5-14, Section 5.3.2.4, Safety Injection: Revised to delete SI on low steam line pressure due to a station modification.
- 62. p. 5-14, Section 5.3.2.4, Dynamic Compensation of Steam Line Pressure Signal: Revised to delete all discussion of SI on low steam line pressure due to a station modification.
- 63. p. 5-22, References: Update Reference 5-5 to "-A" Revision 1, December 1997
- 64. p. 5-22, References: Update Reference 5-6 to Revision 3, August 1989

List of Changes to the November 1991 Version (cont.)

65. p. 5-22, References: Update Reference 5-7 to “-PA” Revision 2, December 2000
66. p. 5-22, References: Added the following: 5-9 D. A. Farnsworth and G. A. Meyer, The BWU Critical Heat Flux Correlations, BAW-10199P, BWFC, November 1994. 5-10, The NRC BWU-Z SER letter dated November 7, 1996, H. N. Berkow to M. S. Tuckman. 5-11 The NRC BWU-Z SER letter dated February 20, 1997, P. S. Tam to M. S. Tuckman
67. p. 6-2, Section 6.2.2: Insert the use of SIMULATE-3P as follows. “....is modeled using EPRI NODE-P or SIMULATE-3P to predict ....”
68. p. 6-3, Section 6.2.3, Methodology: A reference to Reference 6-3 was added for the [ ] [ ] VIPRE model. This represents a change to a [ ] model that has already been approved by the NRC
69. p. 6-3, Section 6.2.3, Methodology: Added the BWU-Z CHF correlation and SCD limit and references 6-9, 6-10, 6-11, and 6-12. This correlation and this SCD methodology have been previously approved by the NRC.
70. p. 6-9, Section 6.3.2.6: Revised the first two sentences to state that the steam generator level control and feedwater pump speed control are modeled assuming either manual or automatic control, whichever is limiting.
71. p. 6-14, Section 6.5: The maximum core  $F\Delta h$  value for the pre-dropped condition is corrected
72. p. 6-15, References: Update Reference 6-3 to “-PA” Revision 2, December 2000
73. p. 6-15, References: Update Reference 6-5 to “-A” Revision 1, December 1997
74. p. 6-15, References: Update Reference 6-6 to Revision 3, August 1989
75. p. 6-15, References: Update Reference 6-8 to “P-A” Revision 1, February 1997
76. p. 6-15, References: Added the following: 6-9 D. A. Farnsworth and G. A. Meyer, The BWU Critical Heat Flux Correlations, BAW-10199P, BWFC, November 1994. 6-10, The NRC BWU-Z SER letter dated November 7, 1996, H. N. Berkow to M. S. Tuckman. 6-11 The NRC BWU-Z SER letter dated February 20, 1997, P. S. Tam to M. S. Tuckman, 6-12, K. R. Epperson and J. L. Abbott, Thermal-Hydraulic Statistical Core Design Methodology, DPC-NE-2005P-A, Revision 2, June 1999
77. p. A-9, Section A.15: Replace “the expression of Equation 1” with “the equation” since the equation is not numbered.
78. Included this list of changes in the back
79. Reformatted the list of attached correspondence



DPC-NE-3001-A

List of Attached Docketed Correspondence

1. 1/29/90 original submittal letter, H. B. Tucker to NRC
2. 9/14/90 response to NRC question, H. B. Tucker to NRC
3. 2/13/91 response to NRC questions, M. S. Tuckman to NRC
5. 6/3/91 response to NRC questions, M. S. Tuckman to NRC



**DUKE POWER**

January 29, 1990

U. S. Nuclear Regulatory Commission  
Washington, D.C. 20555

Attention: Document Control Desk

Subject: McGuire Nuclear Station  
Docket Nos. 50-369, 50-370  
Catawba Nuclear Station  
Docket Nos. 50-413, 50-414  
Safety Analysis Physics Parameters  
and Multidimensional Reactor Transients  
Methodology, DPC-NE-3001-P

Gentlemen:

Please find enclosed for your review fifteen copies of the proprietary Topical Report DPC-NE-3001-P. "Safety Analysis Physics Parameters and Multidimensional Reactor Transients Methodology." This report describes the Duke Power Company methodologies for: (i) simulating the FSAR Chapter 15 events characterized by multidimensional reactor transients, and ii) systematically confirming that reload physics parameters important to Chapter 15 transients and accidents are bounded by values assumed in the licensing analyses. The multidimensional reactor transients described are the rod ejection accident, the main steam line break, and the dropped rod transient.

Also, included are four copies of three reports describing the EPRI computer code ARROTTA. This code is used in the analysis of the rod ejection accident. The reports are:

- ARROTTA: Advances Rapid Reactor Operational Transient Analysis Computer Code, Computer Code Documentation Package, Theory Manual.
- ARROTTA Validation and Verification - Standard Benchmark Set, EPRI Research Project 1936-6, July 1989, Prepared by S. Levy, Inc.
- ARROTTA-HERMITE Code Comparison, EPRI NP-6614, December 1989.

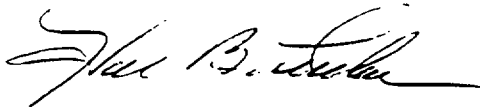
The first report describes the theory incorporated into the computer software. The second provides validation and verification of the computer software to various numerical benchmarks. The third report provides comparison of a rod ejection transient analyzed using ARROTTA to one analyzed using HERMITE which has already been reviewed and approved by the NRC. These reports are included to facilitate review of the rod ejection section.

The objectives of this report are to document the methods to be used to verify that the key physics parameters calculated for a reload core are bounded by values assumed in the Licensing Chapter 15 analyses, and to describe the methods used to analyze three complex FSAR Chapter 15 accidents. Results of the multidimensional reactor transient analyses are presented to demonstrate the methods and to serve as substitute FSAR analyses.

In accordance with 10CFR 2.790, Duke Power Company requests that this report be considered proprietary. Information supporting this request is included in the attached affidavit. A non-proprietary version will be submitted following receipt of the Safety Evaluation Report.

If you have any questions, or require more information, please call Scott Gewehr at (704) 373-7581.

Very truly yours,



Hal B. Tucker

SAG206/lcs

xc: (w/o Attachments)

Mr. Darl S. Hood, Project Manager  
Office of Nuclear Reactor Regulation  
U. S. Nuclear Regulatory Commission  
Washington, D.C. 20555

Dr. Kahtan Jabbour, Project Manager  
Office of Nuclear Reactor Regulation  
U. S. Nuclear Regulatory Commission  
Washington, D.C. 20555

Mr. S. D. Ebnetter, Regional Administrator  
U. S. Nuclear Regulatory Commission  
101 Marietta Street, NW, Suite 2900  
Atlanta, Georgia 30323

Mr. Robert C. Jones, Acting Branch Chief  
Reactor Systems Branch  
Office of Nuclear Reactor Regulation  
U. S. Nuclear Regulatory Commission  
Washington, D.C. 20555

**Duke Power Company**  
P.O. Box 33198  
Charlotte, N.C. 28242

**Hal B. Tucker**  
Vice President  
Nuclear Production  
(704)373-4531



**DUKE POWER**

September 14, 1990

U. S. Nuclear Regulatory Commission  
ATTN: Document Control Desk  
Washington, D.C. 20555

Subject: McGuire Nuclear Station  
Docket Numbers 50-369 and -370  
Catawba Nuclear Station  
Docket Numbers 50-413 and -414  
Topical Report DPC-NE-3001

By letter dated January 29, 1990, Duke submitted the subject Topical Report, "Safety Analysis Physics Parameters and Multidimensional Reactor Transients Methodology" for review.

During a July 23, 1990 meeting between representatives from Duke, NRC Staff, and Brookhaven National Laboratory, a question was raised by the staff regarding the scope of review required. Attached is the response to that question. Please note that a portion of the response is proprietary, and should be withheld from public disclosure. Included with the January 29, 1990 letter is an affidavit which supports the proprietary designation.

If there are any questions, please call Scott Gewehr at (704) 373-7581.

Very truly yours,

Hal B. Tucker

SAG/231/lcs

U. S. Nuclear Regulatory Commission  
September 14, 1990  
Page 2

xc: Mr. Tim Reed, Project Manager  
Office of Nuclear Reactor Regulation  
U. S. Nuclear Regulatory Commission  
Washington, D.C. 20555

Dr. Kahtan Jabbour, Project Manager  
Office of Nuclear Reactor Regulation  
U. S. Nuclear Regulatory Commission  
Washington, D.C. 20555

Mr. S. D. Ebnetter, Regional Administrator  
U. S. Nuclear Regulatory Commission  
101 Marietta Street, NW, Suite 2900  
Atlanta, Georgia 30323

Mr. Robert C. Jones  
Reactor Systems Branch  
Office of Nuclear Reactor Regulation  
U. S. Nuclear Regulatory Commission  
Washington, D.C. 20555

Q. Are there parts of ARROTTA that do not need to be reviewed?

A. Yes. Duke Power uses ARROTTA only for the rod ejection transient which is a very rapid transient. Therefore, the ability to model fission product poisoning (iodine, xenon, promethium and samarium) does not need to be reviewed. Also due to the rapidity of the event moderator feedback effects are not very important. Therefore ARROTTA's ability to model moderator feedback does not need to be reviewed.

ARROTTA's neutronic theory is identical to QUANDRY's, however the numerical solution technique is different. ARROTTA also utilizes the same thermal hydraulics routines found in BEAGL. The material properties have been modified to match those of RETRAN and the steam properties enhanced to allow supercritical properties. Since Doppler feedback terminates the power excursion, the fuel pin thermal model is important, however, the fluid modeling has a secondary effect.

Because the input cross sections have been adjusted in many ways to make the licensing model limiting [

], the source of the cross sections and ARROTTA's ability to match measurements is of minor importance.

Duke Power Company  
Nuclear Production Dept  
P.O. Box 1007  
Charlotte, NC 28201-1007

M.S. Tuckman  
Vice President  
Nuclear Operations  
(704) 758-1851



**DUKE POWER**

DUKE POWER CO.  
NUCLEAR ENGINEERING

February 13, 1991

U. S. Nuclear Regulatory Commission  
ATTN: Document Control Desk  
Washington, D.C. 20555

Subject: McGuire Nuclear Station  
Docket Numbers 50-369 and -370  
Catawba Nuclear Station  
Docket Numbers 50-413 and -414  
Responses to Questions on  
Topical Report DPC-NE-3001

On January 29, 1990, Duke submitted the subject Topical Report, "Safety Analysis Physics Parameters and Multidimensional Reactor Transients." By letter dated December 24, 1990, the NRC staff provided questions regarding the subject Topical Report. Attached are formal responses to the staff's questions.

If there are any further questions, please call Scott Gewehr at (704) 373-7581.

Very truly yours,

*M. S. Tuckman*

M. S. Tuckman

SAG/252/lcs

xc: (W/Attachments)

Mr. T. A. Reed, Project Manager  
Office of Nuclear Reactor Regulation  
U. S. Nuclear Regulatory Commission  
Washington, D.C. 20555

Mr. R. E. Martin, Project Manager  
Office of Nuclear Reactor Regulation  
U. S. Nuclear Regulatory Commission  
Washington, D.C. 20555

Mr. S. D. Ebnetter, Regional Administrator  
U. S. Nuclear Regulatory Commission  
101 Marietta Street, NW, Suite 2900  
Atlanta, Georgia 30323

Mr. Robert C. Jones, Acting Branch Chief  
Reactor Systems Branch  
Office of Nuclear Reactor Regulation  
U. S. Nuclear Regulatory Commission  
Washington, D.C. 20555

1. Will the DPC methods be applied to cores including fuel from multiple fuel vendors? If so, justify the use of VIPRE01, ARROTTA and RETRAN-02 and the selected options/data for this application?

**Response:**

The DPC methods described in DPC-NE-3001 will be applied to reload cores which may include fuel from different fuel vendors. Due to the relative similarity of current PWR fuel designs, it is anticipated that the DPC methods will remain valid. At present, the Westinghouse optimized fuel assembly (OFA) design and the B&W Mark-BW fuel design have been analyzed. The neutronic differences in these fuel designs are accommodated by determining values of safety analysis physics parameters that conservatively bound both fuel types, or by explicitly analyzing a specific reload design. Fuel design data input to the VIPRE-01, ARROTTA, and RETRAN-02 codes are selected to be consistent with one of these approaches. The VIPRE-01 and RETRAN-02 analyses model both fuel types to ensure that the impact of fuel design data is explicitly calculated. In the ARROTTA rod ejection analysis, the relatively small neutronic differences between OFA and Mark-BW fuel designs are insignificant when compared to the conservative adjustments made to the cross sections in order to model a highly peaked core with bounding physics parameters. In addition, the selection of code options is not affected by a different fuel design. The fuel assembly design data employed in the analyses will be consistent with the fuel types comprising the reload core.



1. Discuss the conclusion that a VIPRE-01 uniform pellet power profile is conservative for fuel temperature calculations and non-conservative for DNBR calculations (at both BOL and EOL).

**Response:**

[ ]

**Fuel Pellet Radial Power Profiles  
Used for Rod Ejection Analyses**

$P/P_0$

$R/R_0$

3. What is the effect of neglecting the time-dependence of the assembly-wise flow distribution and assembly cross flow in ARROTTA?

**Response:**

The effect of neglecting the time dependence of the assembly-wise flow distributions and assembly cross flow in ARROTTA is negligible. In the HZP cases, the water is not significantly heated until after the transient power level peaks and starts to decrease. Bulk boiling does not occur until well after VIPRE predicts DNB to occur. For the HFP cases, bulk boiling never occurs in the ARROTTA model. Thus, the reactivity effects of the rod ejection transient are relatively unaffected by the changes to the water properties, which means that cross flow or changes in the flow distribution have little effect upon the transient results.

4. Are all the key safety parameters calculated with approved codes and methods?

**Response:**

Yes, Section 3.0 states that for generation of key safety parameters for reload cores approved codes and methods will be used. The currently approved codes and methods are described in DPC-NE-2010A. As the NRC approves other Duke Power Topical Reports, those methods and codes may be substituted for the ones described in DPC-NE-2010A.

5. What ARROTTA version and options are being used in the DPC reference analyses? If these are not the same version/options used in the code benchmarking, justify the applicability of the benchmarking comparisons for licensing calculations.

**Response:**

The DPC reference analysis used version 1.02 of ARROTTA. The same version was used for the HERMITE comparison. A comparison of the options used by DPC and the options used for the HERMITE comparison is given below. The differences shown are negligible.

| <u>Parameter</u> | <u>DPC-NE-3001</u> | <u>ARROTTA-HERMITE<br/>Comparison</u> | <u>Comments</u> |
|------------------|--------------------|---------------------------------------|-----------------|
|------------------|--------------------|---------------------------------------|-----------------|

6. Provide the appendices to the ARROTTA code description report (Volume-1). The code description provided is a draft report. Has this code description received final approval? Please provide the final code description report.

**Response:**

See revised response in June 3, 1991 letter

7. The six key safety parameters of Table 4-4 do not provide a complete characterization of the three-dimensional ARROTTA reference calculation. For example, two cores having identical key safety parameters but, due to core loading, fuel burnup, rod insertion or xenon distribution, can have different axial and radial power distributions which affect both the reactivity insertion and the feedback and scram reactivities. Discuss the ability of these selected key safety parameters to completely characterize the three-dimensional rod ejection event. What uncertainty is introduced by this specific selection and definition of the key safety parameters.

**Response:**

The six key safety parameters of Table 4-4 are very similar to the current list of parameters described in the McGuire and Catawba FSARs for the rod ejection transient. In addition to these parameters, Technical Specifications establish limits on shutdown margin, core power level, reactor system pressure, core flow, and control rod insertion. Values for these parameters were set conservatively in the rod ejection analyses.

Other parameters are established conservatively to assist in providing limits on initial conditions for the rod ejection transient. These include the Power-Axial Flux Difference (AFD) operating limits and  $F_{AH}$ . The Power-AFD limits restrict the initial axial power shapes and xenon distributions that must be considered. The  $F_{AH}$  limit restricts the initial pin peaking allowed in a reload core. Both of these limits are established through Technical Specifications and are monitored through Technical Specification surveillance requirements.

Cycle-specific analyses are performed to verify the bounding nature of the parameters assumed in the reference analyses. The DNB and  $F_q$  checks performed account for cycle-specific radial and axial power distributions and rod worths. The DNB and  $F_q$  checks are based on static post-ejected power distributions which are conservatively calculated by neglecting both moderator and Doppler feedbacks. For additional details concerning the calculation of the key safety parameters, refer to the answer of Question 13.

Radial and axial power distributions also impact reactivity insertions and trip reactivities. Technical Specifications govern the amount rods can be inserted as a function of reactor power and therefore limits the amount of reactivity that can be inserted from a rod ejection event. The amount of excess shutdown reactivity available for insertion (shutdown margin) is set by Technical Specifications at 1300 pcm. For the rod ejection analysis, the shutdown margin was pessimistically reduced below 1300 pcm (to 250 pcm) by assuming the simultaneous occurrence of a stuck rod coincident with an ejected rod. The rate in which reactivity is inserted to the core is governed by the trip reactivity curve, Figure 4-7. The trip reactivity curve is calculated assuming a bottom peaked power distribution to delay reactivity insertion for as long as possible. This curve is verified for each reload core.

The combination of checks on the six key parameters and Technical Specification limits, and the cycle specific calculations serve to define an acceptable envelope of reload core characteristics. Changes to Technical Specifications by requirement are submitted to and reviewed by the NRC. Changes in the six key parameters outside of the range used in this analysis would require an evaluation, reanalysis of the transient, or a redesign of the reload core.



8. Provide a description of the code used to prepare the composition-dependent cross sections for ARROTTA. Since the capability of this code has not been exercised in the benchmarking comparisons, provide the appropriate code validation for the rod ejection application.

**Response:**

All cross sections were calculated by the CASMO-3 program. A series of auxiliary programs transform the fuel cross sections into a database suitable for the SIGTRAN program. For each point in core life, SIGTRAN prepares the cross section data for ARROTTA by transforming the cross sections from the database into the ARROTTA composition dependent functions. An ARROTTA composition may be applied to different nodes in the core that have identical enrichment and burnable poison content but with slightly different fuel exposure. The nodes are combined into compositions by scanning through the core to find the nodes that match within some criteria and averaging those nodes into a single composition. Nodes are averaged only if the enrichment and BP content are identical. If the number of compositions is too high, more sweeps are made with incrementally less restrictive criteria until the number of compositions is acceptable.

      ] SIGTRAN also creates the ARROTTA geometry input to correctly place each composition into the core.

The entire cross section process was verified at DPC by forcing SIGTRAN to create cross sections for selected CASMO-3 exposure points. ARROTTA was then forced to evaluate these cross section sets at the CASMO-3 state points (fuel and moderator temperature, boron concentration, etc.). Finally, the cross sections produced by ARROTTA were compared back to the original CASMO-3 cross sections. The ability to prepare a model of a reactor core was tested as described in Question 9.

SIGTRAN has been validated and certified in accordance with Duke Power Design Engineering Quality Assurance procedures.

9. How is the number of ARROTTA fuel cross section compositions determined to be adequate for modeling the three-dimensional fuel burnup distribution?

**Response:**

In the development of the BOC model for the reference analysis, several preliminary ARROTTA models were created. Comparison of

10. The ejected rod location D-12 is near the core boundary and tends to maximize leakage and to minimize the spatial region approaching limits. For the same key safety parameters, what is the increase in the number of rods in DNB for a centrally located ejected rod?

**Response:**

The Technical Specifications allow only bank D to be inserted at full power and allow bank D to be inserted the furthest at hot zero power. Bank D consists of 5 rods: the center (H-08) location and the four locations symmetric to D-12. Because of core loading considerations, the D-12 location typically has a higher worth than the H-08 location. Thus, location D-12 will almost always be the location of the highest worth ejected rod.

Because of these adjustments, the calculations show DNB occurring in the two quadrants adjacent to the quadrant with the ejected rod. If H-08 were chosen as the ejected rod location, the power distribution adjustments would have been made only in the center of the core, which would eliminate this effect. Because of these power distribution adjustments, the DNB response from ejecting D-12 is conservative with respect to H-08.

Reload check cases will be executed using approved codes and methods to evaluate the ejection of control rods from H-08, D-12, and from the control rod banks that are not fully inserted at HZP. These cases will evaluate ejected control rod worths and post-ejected power distributions to determine the number of pins in DNB. These values, as well as the other key safety parameters, will be calculated and compared to the reference analysis. If the parameters for a given reload cycle exceed those used in the safety analysis, then either an evaluation, a new safety analysis, or a core redesign is performed.

11. Provide the rod ejection analysis sensitivity studies of Reference 4.1 of EPRI-NP-6614.

**Response:**

The report titled "PWR Rod Ejection Accident: ARROTTA Sensitivity Studies", Research Project 2941-2, January 1991, is enclosed.

12. Discuss the selection of the VIPRE-01 fuel thermal conductivity and gap conductance used to insure conservative calculations of both the fuel temperature and the DNBR/pressure increase calculations.

Response:

#### REFERENCES

1. C. W. Stewart, et al. VIPRE-01: A Thermal Hydraulic Code for Reactor Cores, Volume 1: Mathematical Modeling, EPRI, NP-2511-CCM-1, Rev. 3, August 1989.

13. How are the rod ejection worth, MTC, DTC,  $\beta$ ,  $F_q$ , and pin census key safety parameters determined? Are these calculated for the state with the rod inserted or ejected? Are the MTC and DTC calculated isothermally? Is the rod worth calculated with feedback? Are these parameters calculated for the state in which the cross sections have been adjusted?

**Response:**

Ejected rod worths for the reference calculation are determined using the computer code ARROTTA. Static eigenvalue calculations are performed for the initial condition and post ejected statepoints. The initial condition for the ejected rod worth calculation is established by positioning control banks at their rod insertion limit and performing an eigenvalue calculation. Next, a second eigenvalue calculation is performed with the ejected rod fully withdrawn. For the full power cases, fuel and moderator temperature feedbacks are held constant at their initial condition values.

Moderator and Doppler temperature coefficients (MTCs and DTCs) are typically calculated by isothermally perturbing the moderator temperature or fuel temperature from an initial value and then calculating the resulting change in core reactivity.

The effective delayed neutron fraction,  $\beta$ , is calculated in ARROTTA for each composition using 6 group delayed neutron data.  $\beta$  is set at its respective limit for each rod ejection transient by modifying the 6 group delayed neutron data. The value of  $\beta$  used in each transient is shown in Table 4.4.

A description of the pin census performed to determine the number of fuel pins in DNB is described on pages 4-14 and 4-15 in DPC-NE-3001-P.

14. Are the checklist parameters calculated in exactly the same manner for both the reference analysis and the cycle-specific analysis? If not, justify this inconsistency.

**Response:**

Checklist parameters will be calculated using approved steady state physics codes and methods. For all transients other than rod ejection, checklist parameters will be calculated in a similar manner to the reference analyses.

The rod ejection reference analyses used ARROTTA to calculate the key parameters and to set them at the appropriate bounding values. The calculation of Doppler and moderator coefficients using ARROTTA is performed slightly differently from that using the steady state physics codes due to the ARROTTA coding. In the steady state codes, the coefficients are calculated by individually perturbing the fuel or moderator temperature and calculating the resulting reactivity change. In ARROTTA, the moderator and Doppler coefficients are calculated as described in the response to Question 13. Calculations of DTCs and MTCs by either method yield similar results. Other key parameters are calculated in a similar manner in both the reference analyses and the cycle-specific checks.



15. Is the cycle-specific pin census compared to a static pin census for the reference core? If not, justify this inconsistency.

**Response:**

The dose analysis was conservatively performed assuming 50% of the fuel pins fail as a result of DNB. Static pin censuses for the reload cycle will be compared against the 50% criteria. Static pin censuses for the BOC reference analyses were performed and found to be more conservative than the reference transient cases with Doppler feedback and are also bounded by the 50% failed pin value used in the dose analysis.

16. Provide the details of the dose calculations of Section 4.6.

**Response:**

The dose analysis for the rod ejection accident was performed using the data and assumptions given in FSAR Chapter 15 for McGuire and Catawba except as noted in the topical report. In this analysis the dose contribution from the containment release was mathematically modeled assuming the rod ejection accident was similar to the design basis LOCA, except that the source term was limited to the gap activity of the fraction of the assemblies experiencing DNB. This source was instantaneously released to containment. All fuel noble gas release was assumed to be released into containment and iodines were deposited in the sump water and containment atmosphere as proportioned in the LOCA analysis. A 95% filtration efficiency for the Annulus Ventilation System was assumed. A 7% unfiltered bypass leakage fraction was also assumed. The containment leakrate was assumed to be the Technical Specification maximum the first day and half this amount for the remainder of the 30 days. Inside containment, conservative credit was taken for iodine removal by the ice condenser and containment spray based on assumptions given in Standard Review Plan Sections 6.5.2 and 6.5.4. Emergency Core Cooling System (ECCS) leakage and the Hydrogen Purge System were considered as release paths.

The secondary side dose contribution was calculated by assuming maximum Technical Specification primary-to-secondary leakage for the steam release. A 0.10 iodine partition factor and a 1.0 noble gas partition factor were assumed in the steam generators. The entire source released from the fuel was assumed to be mixed with the reactor coolant volume for the secondary side dose contribution. The primary and secondary coolant were assumed to be at Technical Specification limit activity levels at the start of the accident.

The dose calculation performed for the topical report has been revised for the Catawba 1 Cycle 6 reload report to incorporate changes which more accurately represent station response to the accident. The revised results continue to meet the applicable acceptance criteria. Assumptions and methodology provided by the Standard Review Plan (NUREG-0800) and Reg. Guide 1.77 are incorporated into the revised analysis. The source term is based on DPC-NE-3001 Chapter 4 DNB calculations, and no fuel melting is assumed. Gap releases are determined as before. No ECCS leakage or hydrogen purge release from containment was considered. Technical Specification containment leakage was assumed and the source term was released into the containment instantaneously. Credit for ice condenser and containment spray removal of iodine was taken as before. The secondary side steam release was extended to 8 hours with releases comparable to other secondary side release accident assumptions. The steam generator partition factor was set at 0.01 for iodine and 1.0 for noble gas in accordance with the Standard Review Plan. Technical Specification limit concentrations of iodine were assumed in the coolant at the beginning of the accident as before.

17. The xenon-induced top-peaked axial power distribution used in the cycle-specific analysis is not conservative in general (e.g., for a deeply inserted rod). Justify this assumption for all applications.

Response:

A top-peaked axial power distribution is conservative for the

18. The present VIPRE-01/ARROTTA model assumes Mark-BW design data including dimensions and loss coefficients. How will this model be validated for new fuel designs?

**Response:**

The rod ejection analysis results presented in DPC-NE-3001 are based on the Mark-BW fuel design for the thermal analysis, and on the OFA design for the neutronic analysis. As stated in the response to Question 1, the neutronic differences between OFA and Mark-BW are minor. Since the cross sections were significantly modified to obtain a highly-peaked power distribution with bounding physics parameters, the ARROTTA analysis is conservative for either fuel type. The VIPRE-01 thermal-hydraulic analysis was explicitly analyzed for both fuel types. The Mark-BW results are presented in DPC-NE-3001 since this fuel type is the new one. The results for the OFA fuel type are slightly worse but meet all acceptance criteria. It is expected that future fuel designs will be sufficiently similar to Mark-BW so that the model will remain valid. For any fuel design change the impact on all analyses will be evaluated and a reanalysis performed as necessary.

19. Provide the uncertainty estimates and basis for each key safety parameter. What additional uncertainty estimates will be used to account for the uncertainties introduced by (1) the VIPRE-01, RETRAN-02 and ARROTTA codes, modeling and assumptions and (2) the selection and definition of the checklist parameters? How will these uncertainties be incorporated in the fuel temperature, DNB, and licensing predictions of the rod ejection, steamline break and dropped rod events?

**Response:**

See revised response in June 3, 1991 letter

20. Has the fuel temperature calculation in ARROTTA been conservatively modeled to minimize the Doppler feedback?

Response:

|  |
|--|
|  |
|--|

21. Regulatory Guide 1.77 recommends a low-powered calculation as well as the hot-zero-power rod ejection calculations. What reference analysis will be performed for the low-powered case? How will the possibility of a positive MTC be evaluated?

**Response:**

Regulatory Guide 1.77, Section B, recommends analysis of the rod ejection accident for at least the following three initial conditions:

- o Hot standby
- o Low power
- o Full power

The analyses documented in DPC-NE-3001 do not cover the hot standby case from the Regulatory Guide. Hot standby at McGuire and Catawba is defined as the core being subcritical by at least  $1\Delta k/k$ . The reactivity inserted to the core in excess of 1% at hot standby conditions is considerably less than the ejected rod worth assumed in the low power case. Therefore, there are no severe consequences from a rod ejection transient from hot standby conditions.

The DPC-NE-3001 low power case initial condition is critical at  $10^{-9}$  times nominal power. The choices of core power initial conditions for the DPC-NE-3001 rod ejection cases are consistent with the McGuire and Catawba FSAR Chapter 15 analyses. The SERs for McGuire and Catawba, NUREGs-0422 and -0954, both conclude that this approach is "in accordance with, or more conservative than, those recommended in Regulatory Guide 1.77". Therefore, the DPC-NE-3001 choice of initial power levels is consistent with the approved licensing bases of the McGuire and Catawba Stations. In addition, it would be expected that a full power case would bound results from positive, but lower, power levels for at least two reasons. First, the fuel temperature coefficient becomes more negative as core power decreases, even though no credit was taken for this in DPC-NE-3001, i.e., the same coefficient was used for the full and low power cases. Second, four reactor coolant pumps are always required to be operable per the McGuire and Catawba Technical Specifications while the reactor is at power. The ratio of core heat flux to required core flow is therefore highest at full power, where a high value of this ratio minimizes the margin to DNB. The analysis was performed at the Technical Specification limits on MTC: 0.0 pcm/F at HFP to +7.0 pcm/F at HZP. Thus, the effects of a positive MTC are already included in the analysis.

22. Provide the basis for the assumed rod ejection velocity and scram delay time?

Response:

The assumed rod ejection velocity is constant based on the active core length divided by a rod ejection time of 0.1 second. The 0.1 second value is the current FSAR assumption. The scram delay time is 0.5 seconds. This is also an FSAR value and a Technical Specification surveillance.



23. Is any credit taken for the assumed rupture of the control rod housing in the rod ejection pressure calculation?

**Response:**

No. No loss of coolant and depressurization are modeled due to the ejected rod.

24. What modifications will be made to the reference analyses in the case that future reloads include new fuel designs involving changes to parameters not included in the key safety parameter checklist which makes the reference analysis less bounding?

**Response:**

Before any fuel assemblies with significant design differences from the current designs would be included in a reload, a complete safety evaluation would be performed. This evaluation would determine whether the reference analyses remained valid or whether reanalysis would be necessary. The intent of the key safety parameter checklist is to identify whether reanalysis is necessary. The reference analyses include a set of conservative assumptions that are expected to remain bounding for the foreseeable future. The reload safety evaluation process described in DPC-NE-3001 will identify any such situations and appropriate action will be taken. For parameters not included in the key safety parameter checklist, it is concluded that their collective impact on the safety analysis as a result of the expected minor differences between reloads will be insignificant.

25. Do the initial conditions (core power, flow, pressure, temperature, etc.) and core protection setpoints used in the transient analyses include an allowance for uncertainty? If not, how will this uncertainty be accommodated?

**Response:**

This question was partially answered in the response to Question 19, which stated that all of the initial conditions have included an appropriate allowance for uncertainty. The uncertainty associated with the Reactor Protection System setpoints is explicitly required and is documented in the Catawba Technical Specifications. The McGuire Technical Specifications do not include this information, however the same analyses are applicable to both stations. A total uncertainty allowance plus some margin has been factored into the analysis values.

Duke Power Company  
Attn: Document Control Desk  
P.O. Box 107  
Charlotte, NC 28201-0107

M.S. Tuckman  
Vice President  
Nuclear Operations  
(704) 373-7581



**DUKE POWER**

June 3, 1991

U. S. Nuclear Regulatory Commission  
ATTN: Document Control Desk  
Washington, D. C. 20555

Subject: McGuire Nuclear Station  
Docket Numbers 50-369 and -370  
Catawba Nuclear Station  
Docket Numbers 50-413 and -414  
Response to Request for Additional  
Information Relative to Topical Report DPC-NE-3001

By letter dated February 13, 1991, Duke Power Company submitted responses to NRC Staff questions relative to Duke-proprietary Topical Report DPC-NE-3001. As a result of telephone conversations among the report reviewer, NRC staff, and Duke, revisions to two of the responses (6 and 19) have been prepared and are attached. Also attached are responses to a second set of questions which have been received. Note that the second set of 21 questions has been renumbered (26-46) consecutive to the original 25 questions to avoid confusion. Please find also (Attachment 2) marked-up revision pages to the Topical Report. The report will be reprinted in its entirety upon receipt of the Safety Evaluation Report.

Please note that both the question responses and the revision contain proprietary information and should be withheld from public disclosure. An affidavit supporting this designation was contained in the original submittal of the report, dated January 29, 1990.

If there are any questions, please call Scott Gewehr at (704) 373-7581.

Very truly yours,

*M. S. Tuckman*

M. S. Tuckman

resp3001/sag

Nuclear Regulatory Commission  
June 3, 1991  
Page 2

cc: Mr. T. A. Reed, Project Manager  
Office of Nuclear Reactor Regulation  
U. S. Nuclear Regulatory Commission  
Mail Stop 9H3, OWFN  
Washington, D. C. 20555

Mr. R.E. Martin, Project Manager  
Office of Nuclear Reactor Regulation  
U. S. Nuclear Regulatory Commission  
Mail Stop 9H3, OWFN  
Washington, D. C. 20555

Mr. S. D. Ebnetter, Regional Administrator  
U.S. Nuclear Regulatory Commission - Region II  
101 Marietta Street, NW - Suite 2900  
Atlanta, Georgia 30323

Mr. R. C. Jones  
Reactor Systems Branch  
Office of Nuclear Reactor Regulation  
U. S. Nuclear Regulatory Commission  
Washington, D. C. 20555

- (6) Provide the appendices to the ARROTTA code description report (Volume-1). The code description provided is a draft report. Has this code description received final approval? Please provide the final code description report.

Response:

The appendix describing the ARROTTA code theory was transmitted to the NRC Document Control Desk in a letter from H. B. Tucker dated March 20, 1990. Appendices A-1 and A-2 were omitted in that transmittal. Enclosed are appendices A-1, A-2, and A-3 from Kord S. Smith's Master's Thesis at the Massachusetts Institute of Technology: "An Analytic Nodal Method for Solving the Two-Group, Multidimensional, Static and Transient Neutron Diffusion Equations," dated March 1979. These three appendices will be incorporated into Appendix A of the ARROTTA theory manual.

The final ARROTTA Volume-1 code report is currently expected to go to the printer near the end of May and be released in the middle of June. EPRI has indicated that there are no substantive changes from the draft version provided with the Duke Power submittal.

- (19) Provide the uncertainty estimates and basis for each key safety parameter. What additional uncertainty estimates will be used to account for the uncertainties introduced by (1) the VIPRE-01, RETRAN-02 and ARROTTA codes, modeling and assumptions and (2) the selection and definition of the checklist parameters? How will these uncertainties be incorporated in the fuel temperature, DNB, and licensing predictions of the rod ejection, steamline break and dropped rod events?

Response:

The methodology of DPC-NE-3001 addresses the issue of uncertainty in models and input by applying explicitly determined uncertainty allowances and by adding conservative margins to reload-typical values. This approach is applied to both key parameters and to many other parameters, and ensures sufficiently conservative results. Uncertainty modeling and allowances for the steam line break, rod ejection, and dropped rod analyses are listed in Tables 1-3 and are based on the following approach.

**Initial Conditions:** The initial conditions in the analytical models include appropriate allowances for uncertainty. These are summarized below and include allowances on power level, temperature, pressure, flow, pressurizer level, etc. For analyses using the statistical core design (SCD) core thermal-hydraulic design approach, the uncertainties in the DNB-related parameters are incorporated in the DNBR limit and are not repeated in the simulations.

**Boundary Conditions:** Boundary conditions are modeled with attention to the impact on the transient response and the end result. These include parameters such as control rod drop time, ECCS flowrate, Reactor Protection System setpoints and delays, etc. Each parameter value is conservatively selected and many include an explicit uncertainty allowance.

Code Options: Each of the codes in the methodology includes different modeling options, the use of which is determined by the user. The selection process is analysis-specific. Examples are the models for the fuel-cladding gap, core thermal feedback, and time step selection. These options are selected based on sensitivity studies, comparisons to data or reference analyses, or based on user experience. For those options which impact a given analysis, attention is paid in the selection process to ensure a conservative result. The selected modeling options are described in the report.

Core Thermal-Hydraulic Models: Uncertainty in predicting local fluid conditions and critical heat flux is addressed by the statistically-based DNBR limit. Specific uncertainties in fuel assembly design and manufacturing variances are accounted for in the SCD DNBR limit or in the hot channel factors if the SCD approach is not used. The SCD limit also includes an uncertainty allowance for the VIPRE-01 code.

Core Physics Models: The core power distributions include 95/95 reliability factors which are documented in DPC-NE-2010A and have been approved by the NRC. Axial flux difference, scram worth, and rod position values all include explicit uncertainty allowances. Key safety analysis physics parameters, such as moderator and Doppler temperature coefficients, effective delayed neutron fraction, and ejected rod worth (refer to Table 2-1 of DPC-NE-3001) are determined using the bounding parameter approach. Based on current reload designs and expectations for future reloads, values which should not be exceeded are selected for key parameters. Margin exists between cycle-specific values and the values assumed in the transient analyses. Due to cycle-to-cycle variations in these parameters, the margin may vary. However, the integral effect of margins in all parameters ensures a conservative result. Additional margin exists between the analysis results and the acceptance criteria.

The above approach for introducing sufficient conservatism into the analyses is consistent with the current licensing basis. Uncertainties are determined for some but not for every key safety parameter. For all important parameters margin exists between the values assumed in the analysis and calculated values for current cores and those expected for future reload cores. Code uncertainties are not determined (note VIPRE-01 code and nuclear reliability factor exceptions). Each code has been validated to benchmark data as part of the code development and model development processes. Based on these efforts it has been concluded that each code is suited for the applications in DPC-NE-3001.

In the event that any key safety analysis physics parameter associated with a given reload exceeds the value assumed in the transient analyses, a 50.59 evaluation will be performed to determine whether an unreviewed safety question exists. If this evaluation has a positive finding, then a reanalysis will be performed and submitted for NRC review. Alternatively, the reload core can be redesigned.

Table 1

Steam Line Break Analysis Uncertainty Allowances

RETRAN Analysis

Initial Conditions:

- Pressurizer pressure: -30 psig
- Pressurizer level: -9%
- RCS temperature: +4 F
- RCS flow: -2.2%
- SG level: +8%
- Core bypass flow: +1.5%

Boundary Conditions:

- Maximum auxiliary feedwater flow
- Maximum credible main feedwater flow
- Maximum safety injection flow when unborated
- Minimum safety injection flow when borated
- Bounding long time for feedwater isolation
- Bounding long time for main steam isolation
- Bounding large purge volume for safety injection piping
- \*\*\* ● Boron concentration in safety injection water: -1%
- \*\*\* ● Bounding moderator density reactivity feedback
- \*\*\* ● Bounding fuel temperature reactivity feedback
- Minimum Tech Spec shutdown margin
- \*\*\* ● Minimum boron worth: -10%
- Minimum credit for reactor vessel thermal mixing
- Maximum delays in engineered safeguards actuation

Core Power Peaking Analysis

- \*\*\* ● Axial peak uncertainty: [   ]
- \*\*\* ● Radial peak uncertainty: [   ]
- \*\*\* ● Radial peak uncertainty due to tilt: [   ]
- Shutdown margin calculation
  - -10% rod worth uncertainty
  - worst stuck rod

Core Thermal-Hydraulic Analysis

- Enthalpy rise hot channel factor to account for manufacturing tolerances: +3%
- Subchannel flow area reduction: -2%
- Hot assembly flow reduction: -5%

NOTE: "\*\*\*\*" indicates key physics parameters



Table 2

## Rod Ejection Analysis Uncertainty Allowances

ARROTTA Analysis

| ● Parameter |                              | Value Assumed | Typical<br>Reload Value |
|-------------|------------------------------|---------------|-------------------------|
| ***         | Ejected rod worth: HFP/BOC   | 200 pcm       | 58 pcm                  |
|             | HFP/EOC                      | 200 pcm       | 79 pcm                  |
|             | HZP/BOC                      | 720 pcm       | 327 pcm                 |
|             | HZP/EOC                      | 900 pcm       | 411 pcm                 |
| ***         | Beta-effective: HFP/BOC      | 0.0055        | 0.0061                  |
|             | HFP/EOC                      | 0.0040        | 0.0052                  |
|             | HZP/BOC                      | 0.00551       | 0.0061                  |
|             | HZP/EOC                      | 0.0040        | 0.0052                  |
| ***         | DTC: HFP/BOC                 | -0.9 pcm/F    | -1.18 pcm/F             |
|             | HFP/EOC                      | -1.1 pcm/F    | -1.45 pcm/F             |
|             | HZP/BOC                      | -0.9 pcm/F    | -1.51 pcm/F             |
|             | HZP/EOC                      | -1.1 pcm/F    | -1.85 pcm/F             |
| ***         | MTC: HFP/BOC                 | 0.0 pcm/F     | -12.1 pcm/F             |
|             | HFP/EOC                      | -10.0 pcm/F   | -32.3 pcm/F             |
|             | HZP/BOC                      | +7.0 pcm/F    | -2.8 pcm/F              |
|             | HZP/EOC                      | -10.0 pcm/F   | -17.5 pcm/F             |
| ***         | F-Q (total pin peak) HFP/BOC | 4.12          | 3.00                    |
|             | HFP/EOC                      | 4.88          | 3.40                    |
|             | HZP/BOC                      | 16.62         | 6.30                    |
|             | HZP/EOC                      | 23.55         | 9.50                    |

Pin Census

- Radial peak uncertainty: [ ]
- Axial peak uncertainty: [ ]

Core Thermal-Hydraulic Analyses

- Enthalpy rise hot channel factor to account for manufacturing tolerances: +3%
- Subchannel flow area reduction: -2%
- Hot assembly flow reduction: -2%

### RETRAN Analysis

- Pressurizer pressure: +60 psi
- Pressurizer level: +9%
- Pressurizer safety valve modeling
  - +3% drift in lift setpoint
  - 3% accumulation

[

]

NOTE: "\*\*\*\*" indicates key physics parameters

Table 3

Dropped Rod Analysis Uncertainty Allowances

RETRAN Analysis

- Uncertainties in power level, flow, bypass flow, pressure, and temperature and factored into the SCD DNBR approach
- Pressurizer level: -9%
- SG level: -8%

Core Physics and Power Peaking Analyses

- \*\*\* ● Bounding dropped rod worth
- \*\*\* ● Bounding available rod worth for withdrawal
- \*\*\* ● Bounding core tilt
- \*\*\* ● Bounding MTC
- \*\*\* ● Bounding DTC
- Bounding beta-effective
- \*\*\* ● Bounding radial peak
- \*\*\* ● Bounding axial peak
- Power peaking uncertainties are factored into the SCD DNBR approach

Core Thermal-Hydraulic Analysis

- Hot assembly flow reduction: -5%
- Other uncertainties covered by the SCD DNBR approach

NOTE: "\*\*\*\*" indicates key physics parameters

- (26) Is a recriticality analysis performed for the RCP startup event (Section 2.3.22)? If so, isn't the minimum shutdown margin considered a key physics safety parameter for this event?

Response:

No, because McGuire and Catawba Technical Specifications 3.4.1.1 require that during power operation and startup all four reactor coolant pumps be operating. Therefore, reactor coolant pump start is procedurally allowed only under two conditions:

- a. An isothermal, i.e., zero core power, situation in which 1) all reactor coolant loops are at the same temperature condition as each other and as the core and 2) backwards forced circulation is provided in the inactive loops by a portion of the flow from the operating pumps. In such a situation there is essentially no temperature difference in the RCS and there can be no reactivity transient initiated by a pump restart.
- b. Because three loop operation at McGuire and Catawba is not licensed, the "nominal N-1 loop operation values," referred to in Section 15.4.4.2, Item 1 of each plant's FSAR, do not exist. The trip of any single pump above 48% power (the Technical Specification P-8 interlock) would cause a reactor trip. Three pump operation at power is therefore an unlikely phenomenon since the permissible initial condition, a single pump trip from less than 48% power so that the reactor does not trip, is very rare. Three pump operation is therefore a transient condition prior to restart of the fourth pump to satisfy the Technical Specification requirements. Since the plant begins such a transient at power, there is no recriticality analysis.

- (27) Why isn't the prompt neutron lifetime a key safety parameter for the uncontrolled RCCA withdrawal?

Response:

- a. Uncontrolled Bank Withdrawal at Power, FSAR Section 15.4.2.  
The core kinetics response in the Uncontrolled Bank Withdrawal at Power (UCBW) transient is dominated by the moderator temperature and fuel temperature feedback. For a given set of feedback parameters, a withdrawal rate sensitivity is performed over the spectrum of rates from very slow to the maximum possible. A change in the prompt neutron lifetime causes a small change in the kinetics response, which manifests itself as a small change in the rod withdrawal rate at which the MDNBR occurs, but the value of the MDNBR is unaffected.
- b. Single Uncontrolled Rod Withdrawal at Power, FSAR Section 15.4.3d.  
Since the reactivity insertion during the transient is limited to the worth of a single rod, the limiting statepoint occurs after the rod has been fully withdrawn. At the limiting statepoint, the net reactivity due to rod withdrawal and feedback effects is nearly

zero, and the time interval during which the prompt neutron lifetime is significant has passed.

- c. Uncontrolled Bank Withdrawal at Subcritical, FSAR Section 15.4.1. A sensitivity study has been performed to demonstrate that the prompt neutron lifetime is not a key safety parameter for the uncontrolled bank withdrawal at subcritical transient. The study showed that a sensitivity factor of [ ] exists for this parameter (a [ ] change in the parameter results in a [ ] change in the transient result). A sensitivity factor of this small magnitude confirms that the prompt neutron is not a key safety parameter for the uncontrolled bank withdrawal at subcritical transient.

- (28) Why isn't the decay heat a key safety parameter for the loss-of-feed-water/loss of offsite power and LOCA events?

Response:

Decay heat is a key safety parameter for these transients as well as other transients where post-trip overheating of the RCS or the fuel is of concern. In Duke Power terminology decay heat is considered to be a boundary condition rather than a physics parameter. It is for that reason that decay heat is not included in Table 2-1 of DPC-NE-3001. A conservative decay heat boundary condition will be assumed in those analyses for which it is important.

- (29) Is the application of VIPRE-01 and RETRAN-02 in the rod ejection, steamline break and dropped rod analysis consistent with the limitations of their approval (e.g., Reference 4-11 in the case of VIPRE-01)?

Response:

The limitations on the approval of RETRAN-02 are given for the MOD002 code version in Reference 1. Although the code changes resulting from the MOD003 and MOD004 versions of the code were recognized in Reference 2, that document left the limitations of Reference 1 essentially unchanged. The approval of RETRAN-02 MOD005 has not been issued. The limitations in Reference 1 were reviewed with respect to the analyses in DPC-NE-3001. The conclusions regarding the pertinent limitations are given below. The letters correspond to those in the original list:

- a. The neutronic space/time effects of rod ejection are not simulated with RETRAN-02. For the steam line break and dropped rod transients the multidimensional space/time effects are conservatively treated as explained in DPC-NE-3001.
- b. The neutronics model is not started from subcritical or zero fission power. For steam line break, the initial condition is critical at 10<sup>9</sup> times nominal power. Shutdown margin is simulated by an immediate reactor trip of an amount of negative reactivity equal to that shutdown margin.
- c. The generalized transport model included in MOD005 version has been used for boron transport modeling in the steam line break transient

only. The conservative application of this model with respect to purge volumes and assumed boron concentrations is discussed in Section 5.3.2.5 of DPC-NE-3001.

- f. The nonequilibrium pressurizer model is used in all transients in DPC-NE-3001.
- m. The core heat transfer in the steam line break and dropped rod transients is restricted to situations in which single phase or pre-CHF regimes dominate. The transient core heat transfer in the RETRAN-02 analysis of rod ejection, as described in Section 4.5 of DPC-NE-3001, is not simulated.
- o. The steam line break transient was analyzed both with and without wall heat conductors in the pressurizer. The analysis without these conductors produced the lower core exit pressure at the DNB statepoint and this analysis is therefore presented in DPC-NE-3001. The dropped rod analyses used the [ ] to simulate wall heat conduction in the pressurizer as described in Section 6.2.1 of DPC-NE-3001. The RETRAN-02 rod ejection analysis used the [ ] modeling as the dropped rod analysis.
- q. The suitability of the default Westinghouse single phase homologous pump curves for the McGuire and Catawba reactor coolant pumps is demonstrated in Reference 3.
- u. The dropped rod and RETRAN-02 rod ejection analyses use no applications of the bubble rise model which were not already justified in Reference 3. The use of the [ ] steam generator secondary model presented in Reference 3. The other aspects of a [ ] are discussed in the response to Question 32.
- v. A dominant flow direction is provided by sustained forced or natural circulation in all loops in all transients analyzed in DPC-NE-3001.
- x. The steam generator model used for the dropped rod and the RETRAN-02 rod ejection analyses is the [ ] model described in Reference 3, which has the phase separation in the [ ]

- ]
- y. Application of the RETRAN local conditions heat transfer model in DPC-NE-3001 is [ ]

] The local conditions model provides a more

realistic approach than the standard homogenous model, and is applied for that reason.

- z. As part of the pre-execution review of the initialization for a particular transient, the analyst ensures that the feedwater flow is adjusted so that the RETRAN-02 fill enthalpy bias correction results in a negligible change to the user input enthalpy. Similarly, when there is a change in the conditions under which primary-to-secondary heat transfer occurs, e.g., due to steam generator tube plugging or a change in power level, the [ ] until the RETRAN-02 heat transfer area adjustment correction results in a negligible change to the user input area.
- i) Validation of the secondary-side transient modeling including two-phase effects is addressed by the benchmarking performed and documented in Reference 3. [

] HEM modeling is adequate for these conditions.

- ii) The pressurizer does not fill for any of the transients analyzed in DPC-NE-3001. The rod ejection transient is simulated for only a few seconds. Although the pressurizer level is still rising at the end of this time, the sharp decrease in energy deposition into the RCS which accompanies rod insertion, the increase in energy removal from the RCS which accompanies steam line safety valve lift, and the loss of RCS inventory out the break, will reverse the level trend prior to filling the pressurizer. The rod ejection accident resembles a SBLOCA following reactor trip. The qualification of the McGuire/Catawba RETRAN-02 pressurizer model for pressurizer emptying was presented in Reference 3.

The limitations on the approval of VIPRE-01 are given in Reference 4. The limitations in Reference 4 were reviewed with respect to the VIPRE-01 analysis in DPC-NE-3001. The conclusions regarding the pertinent limitations are given below. The numbers correspond to those in the original list (Page 28 of Reference 4):

- (1) In the rod ejection analysis, the transient VIPRE-01 fuel pin conduction model is utilized. In the fuel temperature/enthalpy calculations, the heat transfer can reach the film boiling regime. On Page 4-13 of the report, heat transfer correlations used for the four major segments of the boiling curve are shown. The use of these heat transfer correlations was determined by sensitivity study to assure acceptable and conservative fuel temperature results. In Reference 4, it states on Page 28: "The application of VIPRE-01 is limited to PWR licensing calculations with heat transfer regime up to CHF. Any use of VIPRE-01 in BWR calculations or post CHF calculations will require prior NRC review and approval." Thus, Duke Power Company requests NRC's review and approval for use of VIPRE-01 in post CHF calculations in the rod ejection analysis.

In the steam line break and dropped rod analyses, the RETRAN-02 heat flux boundary condition is used and the VIPRE-01 fuel conduction model is not employed. This means that heat is added directly from the cladding surface to the fluid as a boundary condition in the calculation. Consequently, the heat transfer solution is not required.

- (2) In the rod ejection analysis, the W-3S critical heat flux (CHF) correlation is used to define the peak of the boiling curve, and the minimum DNBR value for which transition boiling occurs is set to be 1.30 (Page 4-13 of the report). The historical W-3S CHF correlation limit is 1.30, which was determined using closed channel core thermal-hydraulic methods. The W-3S CHF correlation limit utilizing VIPRE-01 has not been determined. Since VIPRE-01 is an open channel core thermal-hydraulic code, it is obvious that a lower DNBR limit value could be obtained if VIPRE-01 were to be used to determine the correlation limit. Therefore, a limit of 1.30 is conservatively assumed in the analysis.

In the DNBR evaluation of the rod ejection analysis, the BCCMV CHF correlation is utilized to generate the maximum allowable radial peaking (MARF). The correlation limit utilizing VIPRE-01 has been determined to be 1.21 (Reference 5). The NRC is currently reviewing Reference 5. The DNBR limit utilized in the rod ejection analysis is 1.331 ( $1.331 = 1.10 \times 1.21$  where the 1.10 factor adds 10% margin).

In the steam line break VIPRE-01 analysis, the W-3S CHF correlation is utilized for the DNBR calculation. As described above, the W-3S CHF correlation limit utilizing VIPRE-01 has not been determined. However, a DNBR limit of 1.45 ( $1.30 \times 1.115$  where the 1.115 factor adds margin) is utilized in the analysis (Page 5-21 of the report).

In the dropped rod VIPRE-01 analysis, the BCCMV CHF correlation is utilized for the DNBR calculation. The BCCMV Statistical Core Design (SCD) limit of 1.55 (Page 6-3 of the report) is employed in the analysis. This SCD limit of 1.55 has been determined utilizing the VIPRE-01 code (Reference 5).

- (3) For the rod ejection analysis, the specific modeling assumptions, choice of two-phase flow models and correlations, heat transfer correlations, thermal-hydraulic correlations, and conservative factors, etc. are described in Sections 4.2.2.2, 4.2.2.3, and 4.2.2.4 of the report.

For the steam line break and dropped rod analyses, the core thermal-hydraulic models utilized are described in Sections 5.2.3.2 and 6.2.3 of the report. The choice of two-phase flow models and correlations, thermal-hydraulic correlations, and conservative factors, etc. are described in Reference 3. The NRC is currently reviewing Reference 3.

- (4) In the rod ejection analysis, the VIPRE-01 transient mode is employed in the fuel temperature, DNBR, and coolant expansion rate



calculations. The profile fit subcooled void model (such as Levy and EPRI models) is not utilized in the analysis. [ ]

Models are used as described on Page 4-8 of the report. Thus, the transient time step size is not a concern.

In both the steam line break and dropped rod analyses, the VIPRE-01 steady-state mode is employed in the DNBR calculation. Thus, the transient time step size is again not a concern.

(5) Duke Power Company has abided by the quality assurance procedures described in Section 2.6 of Reference 4.

(30) Does Catawba-2 have a larger steam generator inventory than McGuire. If not, how is this nonconservatism in the steamline break analysis accounted for?

Response:

Yes. At zero power, which is the initial condition for the steam line break analysis presented in DPC-NE-3001, Catawba Unit 2 does have a larger steam generator liquid mass than either McGuire unit. This is because the programmed level at Catawba Unit 2 remains constant, at the full power value, as power level decreases, while programmed level at the other three units decreases as power level decreases.

(31) What are the modeling differences between the DPC and Westinghouse analyses of the steamline break and dropped rod events?

Response:

The relevant non-proprietary Westinghouse topical reports, WCAP-9227 and WCAP-11395, along with the McGuire/Catawba FSAR descriptions, were reviewed to determine the modeling differences between the Duke Power and Westinghouse analyses of the steam line break and dropped rod events. The following list is incomplete for two main reasons: 1) the Westinghouse methodology is presented in insufficient detail to determine all differences and 2) some differences which are discussed by Westinghouse are deleted from the non-proprietary versions of the reports.

As Duke understands them, the differences for steam line break are:

- 1) Westinghouse takes credit for a reduction in the primary-to-secondary heat transfer after the steam generator U-tubes uncover.
- 2) Westinghouse takes no penalty for cold, possibly unborated flow from the intermediate head safety injection pump(s) discharge piping.
- 3) Westinghouse takes a penalty for immediate auxiliary feedwater flow delivery, while Duke Power assumes immediate delivery after the earliest actuation signal, in this case safety injection.

- 4) Westinghouse used the Technical Specification limit on refueling water storage tank boron concentration without taking a penalty for concentration measurement error.
- 5) Westinghouse assumes delays of 30 and 40 seconds, for offsite power maintained and lost, respectively, between the generation of a safety injection signal and the point at which the ECCS valves reach their final positions and the high head safety injection pump is at full speed. The Duke Power corresponding assumptions are specified in Section 5.3.2.2 of DPC-NE-3001. In Revision 1 the following sentence will be added to the end of the relevant paragraph of this section:

For the case in which offsite power is maintained, the corresponding delay is 19 seconds.

- 6) Westinghouse assumes that the loss of offsite power occurs simultaneous with the steam line break and the initiation of the safety signal. Although this is an approximate statement since the former event causes the latter, the two events are in close succession in the Westinghouse analysis. As shown in Table 5-2 of DPC-NE-3001, there is a 35 second difference between the times of the two events in the Duke Power analysis. Therefore, as explained in Section 5.3.2.1 of DPC-NE-3001, Duke Power conservatively assumes that the loss of offsite power is concurrent with safety injection.
- 7) Westinghouse assumes equilibrium xenon conditions when calculating the available shutdown margin. Duke Power calculations assume transient xenon conditions which typically result in a reduction in the available shutdown margin by as much as [       ] pcm.
- 8) The Westinghouse k-effective versus temperature curve includes the effects of pressure, temperature and a rodged core with the most reactive rod at its fully withdrawn position. The Duke Power k-effective versus temperature curve was conservatively generated with respect to the above mentioned conditions in addition to including the reactivity penalty [

]

As Duke understands them, the differences for dropped rod are:

- 1) Westinghouse assumes a linear variation of Control Bank D worth versus burnup to obtain the middle-of-cycle value. Duke Power explicitly evaluates the worth at this condition.
- 2) The Westinghouse analysis assumes cycle-specific values for the control rod worth available for withdrawal and for the moderator temperature coefficient (MTC). The Duke Power analysis assumes bounding values for both the control rod worth available for withdrawal and MTC.
- 3) The control rod worth available for withdrawal is calculated assuming a [       ] from the HFP rod insertion limit in

the Duke Power analysis. The Westinghouse analysis calculates the control rod worth available for withdrawal from the HFP rod insertion limit.

- (32) What error is introduced by the steam generator modeling used in the steam line break analysis?

Response:

The [ ] McGuire/Catawba steam generator secondary model described in DPC-NE-3000 is generally used by Duke Power Company in system transient analyses because it has two main advantages over a simpler model:

- i) Multiple nodes allow a more realistic mass and energy distribution within the steam generator, making it easier to accurately predict physically significant quantities such as total steam generator liquid and vapor masses, U-tube bundle region void fraction, and preheater subcooling.
- ii) Having separate, geometrically accurate nodes inside and outside the U-tube bundle/wrapper boundary enables a meaningful calculation of the steam generator level indications at the plants, which are based on differential pressure.

These effects are not important for a steam line break at zero power:

- i) Because of the very low steaming rates prior to the accident, the steam generator inventory below the mixture level is much more nearly saturated single phase liquid. With much more uniform mixture thermodynamic conditions and a negligible U-tube bundle void fraction, a [ ] secondary model is much more accurate at predicting the above parameters. At zero power, the feedwater flow is not introduced into the preheater region, but rather into the upper downcomer. This gives this flow a chance to mix with the fluid already in the steam generator before entering the preheater. As a result, the preheater, at zero power, is not significantly subcooled compared to the remainder of the steam generator.
  - ii) The steam generator level indications are not used as inputs for either automatic or manual actions in the mitigation of the limiting steam line break at zero power. Therefore it is not necessary that the steam generator secondary nodalization used for this analysis be capable of modeling the level indications.
- (33) Discuss the cause of the observed mixing during the McGuire forced circulation tests, and the applicability of these results to steamline breaks in the other three loops as well as the the Catawba units.

Response:

[ ]

(34) The flow behavior observed in the McGuire tests, and used to determine the thermal mixing, involves mixing between the loops. Discuss the adequacy of the RETRAN-02 model to calculate the observed mixing.

Response:

(35) Discuss in detail the method used to convert the observed limiting thermal mixing (LM) of Appendix-A into a flow representation.

Response:

It should be noted that this relation is valid only for a four loop plant.

(36) In the steamline break analysis the assumed isothermal cooldown reactivity is less than the actual distributed temperature cooldown

reactivity due to spatial weighting. How is this nonconservatism accounted for?

Response:

The reactivity insertion from a distributed temperature cooldown is more limiting than the reactivity insertion from an isothermal cooldown due to spacial weighting. However, conservatisms employed in the reactivity weighting used in the RETRAN-02 temperature feedback model, and in the development of the isothermal k-effective versus temperature curve, more than compensate for the non-conservatisms introduced by not explicitly modeling the cooldown asymmetrically. The reactivity versus temperature curve was generated assuming virtually [

] This assumption results in an overprediction of the reactivity insertion. The RETRAN-02 temperature feedback model [

] The combination of these conservatisms ensures a conservative reactivity insertion during the cooldown.

- (37) Locating the stuck rod close to the faulted loop results in increased power peaking, but also results in a reduced inlet temperature. Since these effects have an opposite impact on DNBR margin, what is the effect of assuming the stuck rod is located away from the faulted loop?

Response:

[

] The combination of increased power peaking and low flow ensures a conservative DNBR evaluation even though the inlet temperature in the faulted loop is lower than the inlet temperature in the intact loop.

[

]

- (38) In view of the large axial peaking that occurs in the steamline break, what error is introduced in the axial heat flux by the number of axial zones in RETRAN-02?

Response:

The error introduced in the axial heat flux from using[ ]  
in the RETRAN-02 core model is judged to be relatively small for the  
following reasons: .

- (39) The thermal mixing approach results in a less bottom peaked power distribution, which is nonconservative for the steamline break with the loss of offsite power. How is this nonconservatism accounted for?

Response:

- (40) In the cycle-specific steamline break analysis describe the evaluation of the return to criticality which will be performed if the reload core is not subcritical at the limiting conditions.

Response:

The cycle-specific reactivity check will reveal whether the reload core will be subcritical with respect to the core previously analyzed. If the reload core is determined not to be subcritical, it will be redesigned or the transient will be reanalyzed. Therefore, in Revision 1 of DPC-NE-3001 the last paragraph of Section 5.5 has been revised to read:

If the cycle-specific reactivity check shows the reactor to be subcritical with respect to the core assumed in the existing licensing basis analysis, including a stuck rod, then the response predicted by the system analysis bounds the reload core. If the reload core is not subcritical at these conditions, two approaches are available to obtain acceptable steam line break analysis results: redesign the reload core or reanalyze the transient.

- (41) In the dropped rod analysis, the most negative temperature coefficients provide the maximum positive reactivity insertion from the cooldown but also provide the greatest negative feedback during the power excursion. What are the bounding temperature coefficients (most positive/negative) for the dropped-rod analysis at BOC and EOC?

Response:

As stated on p. 6-7 of DPC-NE-3001, the least negative (most positive) value of MTC is assumed for BOC, MOC, and EOC. The least negative DTC is also assumed. These values were selected following sensitivity studies which clearly showed that minimizing the negative feedback during the power excursion produced the limiting results. This effect is more significant than the positive reactivity insertion from the cooldown, since surplus positive reactivity remains available from the withdrawal of Bank D. It is the withdrawal of Bank D that causes the power overshoot.

- (42) In the dropped rod analysis, has the effect of a worst case power tilt on the excore detector response been accounted for?

Response:

Yes. As stated on pp. 6-6 and 6-8 of DPC-NE-3001, and as shown in Figure 6-5, the effect of power tilt on the dropped rod analysis has been conservatively modeled. Due to the importance of Bank D withdrawal on this event, the condition analyzed was a failure in the Rod Control System. This postulated failure results in the minimum excore flux signal (lowest power quadrant) appearing to be the core average power in the Rod Control System. Since the indicated power is low, Bank D withdrawal is maximized and worsens the power overshoot. Figure 6-5 shows that the tilt factor input to the analysis bounds predicted tilts. It is noted that for large summed dropped rod worths, there is no tilt



since a symmetric pattern of rods must be dropped to obtain worths of that magnitude.

- (43) The control system response has a major effect on the consequences of a dropped rod. How are conservative control system parameters selected which bound all Duke Power plants and cycles including uncertainties?

Response:

There are no significant differences between the control systems in the four Duke Power units in the context of dropped rod transients. The control systems are modeled assuming nominal setpoints. Two major conservative assumptions are made which dominate the effects of control systems. The Rod Control System is assumed to fail in a manner which results in the lowest excore flux signal (rather than the highest) being used as an indication of core power level. The limiting power tilt is assumed. This assumption maximizes withdrawal of Bank D and worsens the power overshoot. The Rod Control System rod withdrawal stops are also assumed to be inoperative. These rod stops terminate rod withdrawal whenever any of the following conditions exist:

- Auctioneered high NI power greater than 103%
- Bank D at 223 steps withdrawn
- Urgent failure alarm for Bank D (prevents Bank D withdrawal if a Bank D rod drops)

This assumption allows the power overshoot to continue above 103% power. It is noted that this failure mode can be related to the failure that inputs the lowest excore power signal to the Rod Control System.

Many other process parameters are used in the control logic. However, the impact of the two major assumptions discussed above is so dominant as to relegate other considerations to insignificance.

- (44) When are the pre-drop and post-drop thermal boundary conditions used in the dropped rod power peaking analysis?

Response:



- (45) Is a full-core neutronics calculation performed for the dropped-rod event? If not, discuss the effects of this approximation.

Response:

Yes. Full-core three-dimensional calculations were performed to calculate dropped rod worths, radial peaking factors, excor detector responses and axial shapes for the reference dropped rod analysis.

- (46) How are the effects of crossflow between adjacent channels treated in the VIPRE-01 model used in the dropped-rod event?

The [ ] channel model shown in Figure 6-1 of DPC-NE-3001 is utilized in the dropped-rod DNBR analysis. This [ ] channel model is identical to that described in Reference 3. In Reference 3, model development, model justification, code options, and input selection have been described in detail. The modeling of crossflow between adjacent channels in the dropped-rod analysis is identical to that in Reference 3.

#### REFERENCES:

1. September 2, 1984 letter from C. O. Thomas (NRC) to T. W. Schnatz (UGRA), "Acceptance for Referencing of EPRI NP-1850-CCM, 'RETRAN-02 A Program for Transient Thermal-Hydraulic Analysis of Complex Fluid Flow Systems,'" Enclosure 2 to the attached SER.
2. Enclosure to October 19, 1988 letter from A. C. Thadani (NRC) to R. Furia (UGRA), "Acceptance for Referencing Topical Report EPRI NP-1850-CCM-A, Revisions 2 and 3 Regarding RETRAN-02 MOD003 and MOD004."
3. "Thermal Hydraulic Transient Analysis Methodology," DPC-NE-3000, Duke Power Company, Revision 1, February 20, 1990.
4. Letter from C. E. Rossi (NRC) to J. A. Blaisdell (UGRA), "Acceptance for Referencing of Licensing Topical Report, VIPRE-01: A Thermal-Hydraulic Analysis Code for Reactor Cores, EPRI-NP-2511-CCM, Vol. 1-5, May 1986."
5. "Duke Power Company McGuire and Catawba Nuclear Stations Core Thermal-Hydraulic Methodology Using VIPRE-01," DPC-NE-2004, December 1988.